To the Graduate Council:

I am submitting herewith a dissertation written by Donna Rice Quillen entitled "Synthesis and Characterization of Polymer-Supported Bifunctional Reagents with Enhanced Ionic Recognition." I have examined the final copy of this dissertation for form and content and recommend that it be accepted in partial fulfillment of the requirements for the degree of Doctor of Philosophy, with a major in Chemistry.

Spiro D. Alexandratos, Major Professor

We have read this dissertation
and recommend its acceptance:

Accepted for the Council:

Vice Provost
and Dean of The Graduate School

SYNTHESIS AND CHARACTERIZATION OF POLYMER-SUPPORTED BIFUNCTIONAL REAGENTS WITH ENHANCED IONIC RECOGNITION

A Dissertation

Presented for the

Doctor of Philosophy

Degree

The University of Tennessee, Knoxville

Donna Rice Quillen

December 1989

To my husband Jeff and my parents, Tom and Alpha Rice

ACKNOWLEDGEMENTS

I am grateful to Professor Spiro D. Alexandratos for his expert guidance during the course of this work. I also thank W. Jack McDowell, Gerry Case and Dr. Bruce Moyer of the Chemistry Division at the Oak Ridge National Laboratory for generously providing the technical assistance and facilities for the radiotracer experiments. Finally, I gratefully acknowledge the Department of Energy, Office of Basic Energy Sciences for financial support.

ABSTRACT

Ion-exchange/redox and ion-exchange/coordination resins have been developed as highly selective metal ion complexing agents. The resins belong to a new category of polymers termed dual mechanism bifunctional polymers (DMBP's) which contain two groups on the same support network each of which operates by a different mechanism. Ion-exchange/redox resins, which form the first class of DMBP's, were prepared containing phosphinic acid ligands covalently bound to a polystyrene matrix. The phosphinic acid moiety is capable of ion exchange with a metal ion allowing for its entry into the polymer network and of reduction of metal ions with reduction potentials greater than approximately 0.3 V thus providing specificity in metal ion complexation. The second class of DMBP's, ion-exchange/coordination resins, combine an ion-exchange reaction to allow for metal ion accessibility with a coordinative component to give enhanced selectivity through metal ion complexation. These polymers were synthesized to contain a phosphonic acid group for ion exchange and either phosphonate ester or tertiary amine ligands for coordination.

The complexing ability of the ion-exchange/redox and ion-exchange/coordination resins was determined with selected lanthanide and actinide series ions (Am^{3+}, Eu^{3+}, Th^{4+}, UO_2^{2+} and Pu^{4+}) and transition metal ions (Fe^{3+}, Hg^{2+}, Mn^{2+}, Co^{2+}, Cu^{2+}, Zn^{2+} and Ag^{+}). The performance of the bifunctional resins was compared to that of the purely ion exchanging sulfonic acid resin both in the presence and absence of excess sodium ions. The affinities of the DMBP's for the target metal

ions were determined over a wide variety of conditions in order to elucidate their mechanisms of complexation. Extractions were performed both in the presence and absence of excess sodium ions under a variety of pH conditions (-0.6 to 2.5). Metal complexation was also investigated for a broad range of metal ion concentrations. The results for the polymer-supported extractants were compared to some liquid extractant analogues.

TABLE OF CONTENTS

LIST OF TABLES

LIST OF FIGURES

INTRODUCTION

A need exists for the development of new separating agents and technologies. Areas of importance to separations research have been addressed recently in a report by the National Research Council.[1] This report targets the areas which will benefit from advances in separation science and makes recommendations as to the direction of future research in the area. Among the targeted areas are new uses of separating agents in biotechnology and strategic metal recovery, in protecting and improving the environment, in the production of ultrapure materials, and in the development of new energy sources and feedstocks.

In the area of biotechnology, new systems and reagents must be developed which will facilitate separation of fragile biologically-active molecules from very dilute synthesis broths of complex composition.[1] The cost of the bioproduct is directly correlated to the concentration of the synthesis broth so that new reagents and processes must be developed to provide economical recovery of these molecules from very dilute solutions. Additionally, in many cases, the separating agents must be able to distinguish between different optical isomers of the bioproduct.

The United States is increasingly dependent on foreign sources for a number of strategic metals.[1] For example, in 1978 over 90 percent of niobium, tantalum, cobalt, strontium, manganese, and platinum group metals were imported from foreign countries. New and advanced separation technologies and reagents are needed to lessen foreign dependence for these and other metals. These technologies could be

applied to obtain metals from currently available sources such as low grade ores, process waste materials, and spent nuclear fuels. New extractants with high selectivities are required to more efficiently and effectively utilize these sources of strategic metals.

In addition to uses in biotechnology and metal recovery, better separation agents must be developed to reduce the release of potentially hazardous substances into the environment.[1] Advances in separation science can also benefit industries which rely upon the production of materials of extremely high purity, such as silicon, germanium, and pharmaceutical products. Separations research will play a major role in the preparation and purification of new fuels as alternate energy sources as the depletion of current fuel reserves continues.

The future of research in the area of separation science is clear: through an understanding of the nature of interactions on the molecular level between separating agent and substrate, strategies will be developed with an emphasis on the selective recovery of substances from very dilute solutions. Solvent extraction (or liquid-liquid extraction) is the first example of a well-defined process used to separate the components of a solution by transferring one component from one liquid phase into another liquid phase. Since the 1940's, solvent extraction has been used for the separation and recovery of radioactive materials[2] and metal recovery in metallurgical processing. For example, solvent extraction has been utilized in the metallurgical industry for the recovery of copper, nickel, cobalt, zinc, chromium, uranium, vanadium, molybdenum, tungsten, gold, niobium, tantalum, zirconium, hafnium, and the platinum metals.[3]

Solvent extraction systems consist of two immiscible phases: an aqueous phase which initially contains the targeted metal ion, and a solvent phase which is capable of concentrating the metal ion.[4] The solvent phase consists of an extractant, which is usually dissolved in a organic diluent, and sometimes also contains a modifier, such as an alcohol, which suppresses emulsion formation and increases the solubility of the extractant in the solvent phase. The extractant is a substance which can react with the metal ion in some manner (chelation, solvation, ion-exchange, ion association, etc.) in order to transfer it from the aqueous phase into the organic phase. To be commercially successful, an extractant must:[2,3]

1. be capable of extracting the desired metal at the required pH
2. be selective for the targeted metal ion
3. exhibit acceptable rates of extraction, scrubbing, and stripping
4. possess high solubility in the organic diluent and low solubility in the aqueous phase
5. be chemically stable during the entire extraction process
6. not form stable emulsions with the aqueous phase when mixed
7. be relatively inexpensive
8. be non-volatile, non-flammable, and non-toxic

The extraction process itself generally consists of three main stages: extraction, scrubbing, and stripping.[2] In the extraction stage the solvent phase is mixed with a metal-containing aqueous feed. The

metal is "loaded" onto the solvent phase by virtue of its reaction with the extractant either by solvation, chelation, ion-exchange, or ion association. After the two phases are allowed to separate, the metal-barren aqueous phase (raffinate) is removed and either discarded or further processed. Scrubbing of any unwanted co-extracted species in the loaded solvent is the next stage in many extraction processes.[2] The scrubbing technique is important for many less selective extraction systems because it can greatly improve the quality of the metal-loaded solvent phase before it is stripped to recover the metal ion of interest. Scrubbing may be accomplished by contacting the metal-loaded solvent phase with an aqueous solution at a pH just sufficient to strip the unwanted co-extracted metal. An alternate method of scrubbing is to contact the loaded solvent with a solution of a salt of the metal ion of interest which replaces the unwanted metal by the desired metal. The conditions to affect stripping depend on the mechanism by which the metal was extracted. All extractants which operate by chelation or ion-exchange reactions generate hydrogen ions upon the extraction of the metal:

$$M^{n+} + n\overline{HA} \rightleftharpoons \overline{MA}_n + nH^+ \qquad (1)$$

According to equation (1), stripping requires use of an acid solution of sufficiently low pH to shift the equilibrium far to the left, driving the metal into the aqueous phase. The stripping process thus allows for the recovery of a concentrated solution of the metal ion of interest. In the case of metals extracted by solvating or ion association

mechanisms where high salt or acid concentrations are required for extraction, stripping can be achieved by contact of the metal-loaded solvent with water which usually results a shift of the equilibrium to the left.

The nature of the extraction reaction can serve as a basis for the classification of the various types of extractants. Extractants can be broadly categorized into three classes:[2]

1. those which involve compound formation
2. those which involve ion association
3. those which involve solvation of the metal ion

Extractants involving compound formation can be further subdivided into two sub-classes: acidic extractants and chelating extractants. Examples of acidic extractants (sometimes called liquid cation exchangers) are organic derivatives of carboxylic acids, phosphoric acids, phosphonic acids, phosphinic acids and sulfonic acids. In general, these acidic extractants extract metal ions by the cation-exchange reaction represented by equation (1), in which the acidic hydrogens of the extractant are exchanged for metal ions. One of the most versatile and commercially successful of the acidic extractants is di-2-ethylhexyl phosphoric acid (DEHP) which has been used commercially for the extraction of uranium[5], cobalt and nickel[6], vanadium[7,8], and the rare earths[9,10] and owes much of its popularity to its good chemical stability, rapid kinetics of extraction, low aqueous phase solubility, versatility in the metal ions which it extracts and availability in commercial quantities.[2] Chelating extractants are a special type of acidic extractant in which the exchanged metal also forms a strong

chelate bond with the extractant. For instance, acetylacetone and its derivatives form coordination complexes containing a stable six-membered ring with metal ions through the two oxygen atoms as shown below:[11]

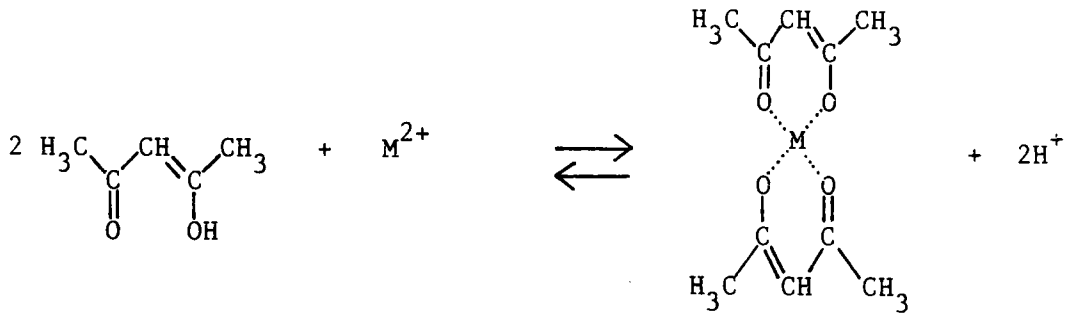

Some examples of chelating extractants are β-diketones, 8-hydroxyquinoline and its derivatives, oximes, hydroxamic acids, thiocarbazone, dithiocarbamates, and dithiols. A series of substituted 2-hydroxybenzophenone oximes (LIX reagents) have been successfully used in the solvent extraction processing of copper-containing leach liquors.[12,13] These reagents are capable of selective extraction of copper at quite low pH values and today play an important role in the copper processing industry.

The second class of extractants, those involving ion association, are comprised of high molecular weight amines and quaternary ammonium halides. These basic extractants (or liquid anion exchangers) extract metal ions existing in solution in anionic form, such as $Au(CN)_2^-$, by an anion exchange reaction. The amine must be converted to its amine salt which is present in the organic solvent as an ion-association complex as

shown in equation (2). The associated anion can exchange with the targeted anionic metal species in the aqueous phase, MY^-, as shown in equation (3):

$$\overline{R_3N} + HX \leftrightarrows \overline{R_3NH^+X^-} \qquad (2)$$

$$\overline{R_3NH^+X^-} + MY^- \leftrightarrows \overline{R_3NH^+MY^-} + X^- \qquad (3)$$

Amine extractants have been utilized in the recovery of uranium[14], hafnium and zirconium[15] from sulfate media, and for the extraction of gold from alkaline cyanide solution[16].

The third class of extractants are those which extract neutral inorganic complexes by solvation. These neutral extractants contain electron-donating groups of two types: carbon-oxygen bonds and phosphorus-oxygen or sulfur bonds.[2] The role which water plays in the extraction process differs for the two types of extractants. In the case of the phosphorus extractants, the strongly polar phosphorus-oxygen or phosphorus-sulfur bond is able to replace the water molecules in the primary coordination sphere of the metal ions. Extractants containing phosphorus-oxygen bonds are generally derivatives of phosphorus acids, such as trialkyl phosphates, dialkyl alkylphosphates, alkyl dialkylphosphinates, and trialkyl phosphine oxides. The most extensively used and studied neutral phosphorus extractant is tri-*n*-butyl phosphate (TBP). Today TBP is used by almost all nuclear plants for the reprocessing of spent nuclear fuel to separate uranium and plutonium from fission products.[17] It is also used extensively in the

hydrometallurgical industry for the separation of rare earths[10,18]; for the removal of iron from chloride liquors containing cobalt, nickel, and copper[19]; and for the separation of zirconium from hafnium[20]. The extractants containing carbon-oxygen bonds require that water molecules be transferred into the organic phase with the metal ion so that they can form bridges between the metal and the electron-donating group of the complex through hydrogen bonding.[2] Commonly used extractants containing carbon-oxygen bonds are ethers, ketones, esters, and alcohols. Quantitative extraction of Mo(VI), Fe(III), Au(III), Ga(III), In(III), Tl(III), and As(III) has been obtained using aliphatic ketone extractants.[21]

The widespread use of solvent extraction for the recovery of metals from both metallurgical processing and nuclear fuel recycling has been due in large part to the many advantages the process provides over many other recovery processes such as precipitation, electrolysis, evaporation, cementation, electrodialysis, reverse osmosis, carbon adsorption, and ion-exchange. First, a very large number of extractants have been developed and commercialized for extraction of a wide range of metals. The extractive ability of these reagents has been studied quite extensively for many metal ions, and numerous reviews have been published which describe these results.[11,22,23] Improvements in extractant structure are constantly being sought to improve the selectivity and kinetics of metal uptake and to lessen the solubility of the extractant in the aqueous phase. Additionally, mixed extractant systems can be used in some cases to improve extraction by synergism.[24] Second, the solvent extraction process provides flexibility in adjusting

the aqueous and organic feeds. For instance, the ratio of aqueous to organic phases can be easily adapted so that high concentration factors of the recovered metal can be obtained.[25] The extractant feed can also be easily changed depending on the nature of the aqueous stream. Third, due to the ability of the extractant to form a specific compound with the metal ion of interest, considerable selectivity in the extraction can generally be achieved with high levels of purity of recovered metal. Fourth, in most solvent extraction systems, metal ion uptake is very rapid, usually only a few seconds or minutes. In cases where metal ion uptake is too slow, accelerators can sometimes be added to improve the kinetics of extraction.[26] Solvent extraction, therefore, is often the preferred method of metal recovery because it can be used for the selective and rapid recovery of a wide range of metal ions and can also offer a high degree of flexibility in the operating conditions of the system, depending on the demands of the aqueous stream.

Solvent extraction, while possessing many advantages as a metal recovery process, does have some serious disadvantages which can limit its usefulness. One of the major problems is the loss of the solvent phase into the aqueous phase through either solubility or entrainment. This not only leads to economic losses, but also pollutes the aqueous environment. Entrainment of solvent may thus necessitate further treatment of the aqueous phase after metal ion removal. Solubility losses can best be obviated by the judicious choice of diluent and extractant while entrainment losses can be minimized by proper mixing of the phases and allowing for adequate disengagement periods. Addition of a modifier to prevent emulsion formation is also beneficial to avoid

entrainment losses. The solvent phase may also be lost through the formation of crud, a solid material which forms at the interface of the aqueous and organic phases as a result of agitation of the two phases with fine solid particles.[2] In fact, solvent extraction is economically unfeasible when the aqueous feed contains more than about 1000 ppm suspended solids (e.g., pulp systems).[25] Another problem with solvent extraction is the large volumes of liquids involved in the process which precludes it from use for metal ion recovery from very dilute solutions, such as from mine waste streams and effluents from various industrial processes.[27] These systems require a very large plant area and the use of large volumes of organic diluents. Thus, in considering use of a solvent extraction system, both economic and environmental concerns must be considered. The value of the recovered metal must be weighed against the cost of solvent, and the replacement of an undesirable metal with an undesirable organic material must be considered.[28]

The use of polymer-supported ion-exchange systems can solve many of the problems associated with solvent extraction. In this process, an ion-exchange resin is loaded with the metal ion of interest by passage of the metal-containing aqueous stream through a resin-packed column. After loading, the resin is eluted with an appropriate solution to strip the loaded metal from the resin, yielding a regenerated resin which can be recycled and a concentrated aqueous solution of the desired metal. Use of ion-exchange systems have both economic and environmental advantages over solvent extraction systems. Application of ion-exchange resins is economically advantageous when the metal to be recovered is present in very dilute solution, making use of solvent extraction

prohibitive due to the large volumes of solvent required. Although the initial costs of the ion-exchange system may be greater due to the high expense of the resins, the ion-exchangers can be used and regenerated thousands of times with little or no decrease in ion-exchange capacity.[26] In polymer-supported systems the polymer backbone itself acts as the organic diluent of the system with the extractant covalently bound to the polymer support. Thus, problems with loss of the organic diluent and extractant into the aqueous phase as in solvent extraction are obviated by the use of a polymer-supported system allowing for the discharge of organic-free raffinates. The ion-exchange process itself presents advantages over solvent extraction in several respects. By packing the beads into a column, long-term continuous operations are possible. The ion-exchange process is simpler in equipment and operation than solvent extraction because no mixing and settling stages are required.[26] The development of countercurrent processes for the loading and stripping of resin has permitted the use of less regenerant in the ion-exchange system.[29] Another significant advantage of resin ion-exchange over solvent extraction is for systems containing high levels of suspended solids.[30] Whereas crud formation prohibits uses of solvent extraction in this case, the resin-in-pulp process makes use of ion-exchange resins possible. In this procedure the resin is placed in baskets which are then dipped into the metal solution which also contains a high level of suspended solids. The solid material passes through the fluidized body of the resin into the ion-exchange effluent. The use of a conventional packed column in the presence of large amounts

of suspended solids would result in high pressure drops, bed packing, and crushing of the resin.

Although resin ion-exchange can suffer from slow kinetics due to diffusional limitations into the polymer network and bead attrition due to limited mechanical stability, these problems can usually be overcome by proper control of the degree of crosslinking and macroporosity of the polymer network. Despite the disadvantages of higher initial cost, slower kinetics, and polymer attrition, use of ion-exchange for metal ion recovery can have economic, environmental, and processing advantages over solvent extraction in many applications.

The first synthetic ion-exchange resins were prepared by Adams and Holmes in 1935.[31] Sulfonic acid cation exchangers were synthesized either by direct polycondensation of phenolsulfonic acid with formaldehyde or by post-sulfonation of a phenol-formaldehyde polymer. The next major advance in the development of ion-exchange resins was the use of free radical polymerization of vinyl monomers to form the polymer. This was an improvement over condensation polymerization because polymers of a well-defined structure could be prepared by radical polymerization, and a controlled level of crosslinking could be achieved by copolymerization of the vinyl monomer with a divinyl crosslinking agent. The first successful ion-exchange polymer synthesized by vinyl polymerization was prepared by d'Alelio in 1944.[32] He first synthesized a carboxylic acid ion-exchanger by copolymerization of acrylic acid and ethylene dimethacrylate. He then prepared a sulfonic acid cation exchanger by sulfonating a copolymer of styrene and divinylbenzene.[33] The sulfonated polystyrene resin was the first to be

synthesized in bead form by suspension (or pearl) polymerization, which produces polymer in the form of spherical particles. In this process, droplets containing a mixture of monomer and initiator are suspended in an aqueous solution containing various stabilizers which prevent the agglomeration of the monomer droplets. The temperature is then raised to affect polymerization, producing the polymer in the form of spherical gel beads ranging from 1 micron to 2 millimeters in diameter.[34] By slight variation of the suspension polymerization technique, highly porous macroreticular ion-exchange resins can be prepared. Use of a highly porous resin is desired, for example, when the resin is used in a nonpolar solvent in which it does not swell. Macroreticular resins are prepared by the addition of an organic solvent to the polymerization mixture which is a good solvent for the monomer but not for the polymer. As the polymerization proceeds, solvent is squeezed out of the growing polymer, giving spherical beads with pores of several hundred angstroms.[34] The enormous success of the sulfonic acid resins prepared by suspension polymerization of vinyl monomers is largely due to their good chemical stability, high acid capacity, and convenient physical form.

Following the successful development of the sulfonic acid resin, the synthesis of strongly basic anion exchange resins was carried out in 1948 at the Rohm and Haas Company.[35] These polymers were produced in two steps from crosslinked polystyrene resins. First, the polystyrene resin was chloromethylated to introduce a $-CH_2Cl$ group onto the benzene ring by reaction with chloromethyl methyl ether in the presence of a Friedel-Crafts catalyst such as aluminum chloride. The second step was

the quaternization reaction of the chloromethylated polymer with a tertiary amine such as trimethylamine to yield the quaternary ammonium chloride group. The amination of chloromethylated polystyrene with primary or secondary amines can also be used to prepare weakly basic anion exchangers.

The conventional ion-exchange resins -- the sulfonic, carboxylic, and anion exchange resins -- represent over 90 percent of all ion-exchange resin use in traditional applications.[36] These resins have a wide variety of applications, including water treatment, pharmaceuticals processing, sugar processing, chromatographic separations, metal ion recovery, use as medicinal agents, and use as catalysts. In the area of water treatment, ion-exchange resins are used for both the softening and deionization of water.[37] A sulfonic acid cation exchange resin can be used to soften water by removing calcium and magnesium ions while total deionization can be achieved by passage of water through both cation and anion exchange resins. In the sugar processing industry, both cation and anion exchange resins are used to deionize beet sugar extracts to improve the white sugar yield over molasses.[38] In pharmaceutical processing, use of weak acid cation exchange resins was instrumental in the successful production of streptomycin.[29] In addition to streptomycin, other biologically active substances have been purified using ion-exchange resins including penicillin, vitamin B12, insulin, and certain viruses. Some interesting medical applications of ion-exchange resins have been explored. For example, the use of ion-exchange resins has been examined as a means of removing sodium for the treatment of various edemas and hypertension, in the removal of stomach

acid for treatment of gastrointestinal disorders, and as a means for removal of calcium in blood processing.[37] Much attention has also been focused on the use of ion-exchange resins as catalysts, mainly due to the ease of recovery of the solid catalyst from the reaction products. For example, cation exchange resins have been used to catalyze ester hydrolysis, esterification, inversion, dehydration, acetal formation and condensation reactions.[39] The largest industrial application at present is use of a sulfonic acid cation exchanger to catalyze the addition of methanol to isobutylene to form methyl *tert*-butyl ether.[40,41]

The use of ion-exchange resins in chromatographic separations includes two main techniques: ion-exchange chromatography and ligand exchange chromatography. In a broad sense, ion-exchange chromatography encompasses the separation of both ionic and nonionic substances using and ion-exchange material as the stationary phase.[42] Ion-exchange chromatography has been successfully used for the separation of metal ions, amino acids, proteins, and neutral organic compounds. Ligand exchange chromatography is a highly selective technique for the separation of compounds which form complexes with metal ions.[43] The stationary phase is a cation exchanger loaded with a metal ion which is capable of complex formation with the ligands to be separated. Ligands can thus be separated based on the strength of their interaction with the complexing metal ion. This technique has been used to separate many substrates, including amino acids, polyhydric alcohols, carbohydrates, and nucleic acids.

Use of ion-exchange resins for metal ion recovery from hydrometallurgical and wastewater streams is of growing importance owing

to both economic and environmental considerations. Since many strategic metals must now be obtained from leaching of low grade ores, use of ion-exchange resins in hydrometallurgical operations is instrumental in the economic recovery of these metals from very dilute leach liquors. For example, ion-exchange resins are used for the recovery, purification, and concentration of uranium from low grade ores.[36] Use of ion-exchange resins in this process is economically advantageous over solvent extraction since the concentration of uranium in the leach liquors is very low (less than 300 ppm).[30] The uranium is recovered as a uranium sulfate complex on an anion exchange resin. Ion-exchange resins have also found increasing use in metal ion recovery from industrial waste streams due to heightened concern over the release of metals into rivers and streams. For instance, strong acid cation exchangers and strong base anion exchangers have been used for the removal, recovery and recycle of chromium pollutants from plating rinse waters.[44] One of the first commercially accepted applications for metals recovery by ion-exchange was in the recovery of copper from rayon spinning wastes.[45] The use of ion-exchange resins for metals recovery has also extended to the nuclear industry because they offer an economic means to remove radionuclides from reactor effluents.[46] Although the sulfonic and carboxylic resins are at present the most commonly used cation exchangers, they have some important limitations which can restrict their usefulness. The most serious disadvantage of the strongly acidic sulfonic resin is its lack of selectivity in the cations which it absorbs. In general, the selectivity of an ion-exchanger is for the counterion of higher valence, smaller hydrated volume, and greater

polarizibility.[34] Additional factors such as the possibility of interactions of the polymer matrix with the targeted counterion, the strength of the interaction between the counterion and its associated anion, the level of crosslinking in the ion-exchanger, and the concentration of the counterion in solution also influence the observed selectivity of the ion-exchanger.[47] Boyd and coworkers determined by calorimetric measurements the changes in free energy for various ion-exchange equilibria using the sulfonic resin. The range of reaction free energy values using a variety of alkali metal cations were within one to two kilocalories per mole.[48] As a result of the narrow range of free energies, the sulfonic resin becomes ineffective for metal ion recovery when the targeted metal ion is present in low concentrations in the presence of a large excess of background metal ions. For example, attempts to recover uranium using the sulfonic resin have been unsuccessful because iron, aluminum, and other heavy metals present in the leach liquor are extracted along with the uranyl ion, UO_2^{2+}.[29] Much greater selectivities can be obtained using the weakly acidic carboxylic acid resin, especially for divalent over monovalent ions.[49] The weak acidity of the carboxylic resin (dissociation constant of between 10^{-5} and 10^{-7})[29], however, severely limits the pH range that can be used with the resin. The high affinity of the carboxylic acid resin for protons can be a problem, for instance, when the metal ion to be recovered is present in a highly acidic leaching solution.

Due to the limitations of selectivity and pH presented by the sulfonic and carboxylic resins, recent synthetic efforts have been directed toward the development of highly ion-specific polymer-supported

extractants which can operate over a wide range of experimental conditions. Through the understanding of the ligand to metal interactions, a wide variety of polymers have been synthesized containing ligands which are highly selective for certain metal ions. Numerous reviews on this subject have been published.[50,51,52,53] Polymer-supported picolylamines (Figure 1) exhibit selectivity for copper especially over the ferric ion.[54] Polymers containing both nitrogen and oxygen donors comprise the largest group of chelating ion-exchange resins.[52] The iminodiacetic acid resin (Figure 2) is probably the most extensively studied chelating resin and is commercially available as Dowex A-1 and Chelex 100. This versatile resin has been effective in the separation and preconcentration of transition metals from seawater in the pH range 6 to 8.[55] Polymer-supported extractants containing 8-hydroxyquinoline (Figure 3)[56] and hydroxyoxime groups (Figure 4)[57] have been developed for the selective recovery of copper based on the high copper selectivity of the liquid extractant analogues.[58] Sulfur-containing resins were developed for recovery of both noble and heavy metals.[50] A thioglycolate chelating resin (Figure 5) was found to retain Ag(I), Bi(III), Sn(IV), Sb(III), Hg(II) and Au(III) from 0.1 M mineral acid.[59] The isothiouronium resin (Figure 6) is selective for platinum metals and Au(III), while the thiol resin (Figure 7) takes up Hg(II) quantitatively.[52] Chelating ion-exchange resins have also been prepared which contain macrocycle ligands. Polymeric crown ethers (Figure 8) have been synthesized for the selective complexation of alkali metal cations depending on the size of the crown ether cavity used.[60] These highly specialized polymer-supported extractants can have

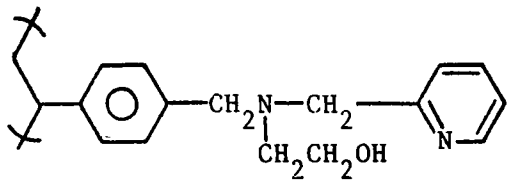

Figure 1. Polymer-supported picolyamine.

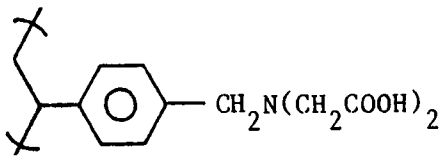

Figure 2. Iminodiacetic acid resin.

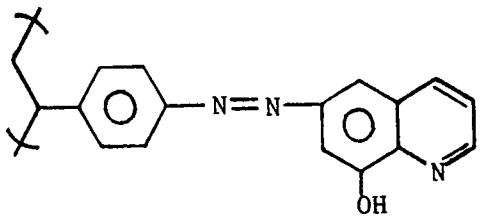

Figure 3. Polymer-supported 8-hydroxyquinoline.

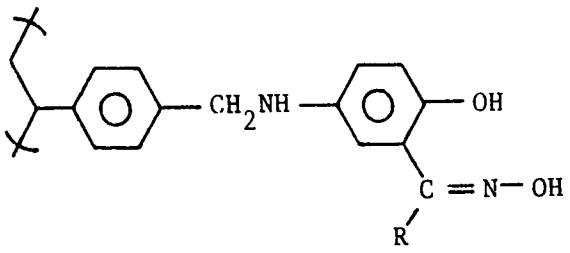

Figure 4. Polymer-supported hydroxyoxime.

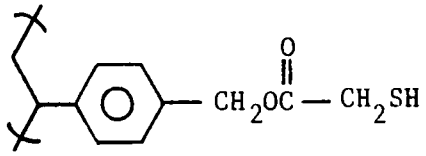

Figure 5. Thioglycolate chelating resin.

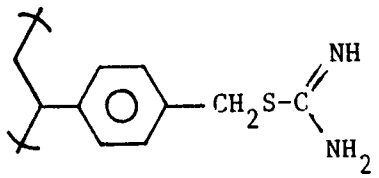

Figure 6. Isothiouronium resin.

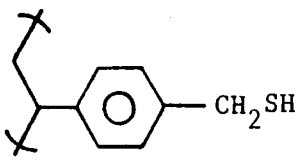

Figure 7. Thiol resin.

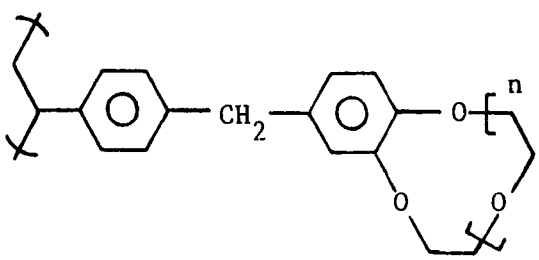

Figure 8. Polymer-supported crown ether.

a number of disadvantages. The synthesis of many of the extractants is difficult and costly. Additionally, many of these systems have highly restrictive operating conditions and pH requirements. For instance, if the polymer contains hydroxylic or carboxylic groups a relatively high pH must be maintained for the extractant to be effective. The isothiouronium resin, however, must be used in acidic media because hydrolysis of the amine groups occurs in alkaline environments.[61] Finally, the purely coordinating extractants which do not contain ionic substituents suffer from low ionic accessibility due to the lack of hydrophilicity within their matrices. In fact, a major drawback to the thiol resin is its low apparent capacity due to the hydrophobic nature of its polymer matrix.[52]

The use of phosphorus-based polymer-supported extractants provides many advantages over the sulfonic, carboxylic, and highly ion-specific chelating and coordinating extractants. Because phosphorus acids are less acidic than sulfonic acids, the phosphorus-based ion-exchange resins are more selective ion-exchangers than the sulfonic.[62] The phosphorus acid ligand is more acidic than the carboxylic acid, thus allowing a wider pH range to be used with the phosphorus acid resin. Phosphorus acid resins, consequently, can be highly selective metal ion extractants even in low pH solutions. Additionally, the presence of ionic groups on the polymer backbone increase its hydrophilicity giving the resin high ionic accessibility. Finally, phosphorus-based resins can, in general, be easily and cheaply prepared to high capacities.

Phosphorus acid ion-exchange resins have been synthesized by polymerization of phosphorus containing monomers, either by vinyl

polymerization or polycondensation reactions, or by post-phosphorylation of polymers. Kennedy and coworkers prepared phosphorylated polymers by polymerization of triallyl phosphate followed by hydrolysis of the resulting polymer to form monobasic polymeric esters.[63] These polymers were found to exhibit considerable selectivity for UO_2^{2+} and to be substantially more selective than the sulfonic resin for beryllium.[64,65] Phosphonic acid ion-exchange resins have been synthesized from a polycondensation reaction between phenoxymethylphosphonic acid and formaldehyde.[66] A variety of polymers, including polyethylene, polystyrene, and chloromethylated polystyrene, have been phosphorylated to form phosphonic acid resins. Oxidative chlorophosphorylation of polyethylene was carried out by Bartulin and coworkers using oxygen and phosphorus trichloride.[67] Reaction of the resulting intermediate polyphosphonic dichloride with a bifunctional nucleophile such as ethylene diamine gave a crosslinked polymer. Hydrolysis of the crosslinked polymer then produced a polyphosphonic acid. This polymer was found to exhibit a high selectivity for uranium with no significant interference from either copper or iron at pH 2. Phosphorylation of styrene and chloromethylstyrene are the most commonly utilized methods to synthesize phosphonic acid resins. Marhol and coworkers describe the synthesis of phosphonic acid resin from polystyrene by Friedel-Crafts reaction of crosslinked polystyrene with phosphorus trichloride in the presence of aluminum trichloride catalyst.[68] The resulting $-P(OH)_2$ groups are then oxidized with nitric acid to form $-PO(OH)_2$ groups. Phosphonic and phosphinic acid resins (Figures 9 and 10) have been commercially available under the tradenames Duolite C-63 and Duolite C-

62 respectively.[69] Phosphorylation of chloromethylated polystyrene is carried out in the same manner as for polystyrene to yield methylenephosphonic acid groups bound to the polystyrene backbone.[70] Recently, phosphonic acid ester cation exchange resins have been prepared from chloromethylated polystyrene.[71] The chloromethyl groups are converted to 2-hydroxyethyl groups which are then phosphorylated with monoethylphosphate to yield the phosphate monoester resin.

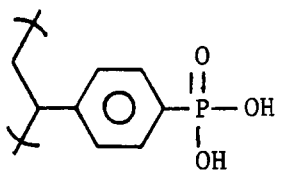

Figure 9. Doulite C-63 (phosphonic acid resin).

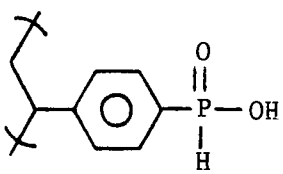

Figure 10. Duolite C-62 (phosphinic acid resin).

Helfferich introduced[72] and Janauer extended[73] the concept of reactive ion-exchange (RIEX) as a method to increase selectivity in the isolation, concentration, or removal of a targeted species from a complex mixture. RIEX is defined as any process in which the ion-exchange reaction is directly coupled with another chemical reaction such as reduction, precipitation, chelation, neutralization, ion complex

formation, ligand exchange, and so on. An example of RIEX is the titration of a strong acid cation exchange resin with sodium hydroxide which involves an ion-exchange reaction (exchange of the resin proton with the sodium ion) accompanied by a neutralization reaction (water formed by the consumption of hydroxide ions from solution and protons from the resin). The RIEX process exploits favorable free energy changes of these chemical reaction to affect a quantitative separation of species which would be difficult to separate by ion-exchange alone. The ion-exchange process is merely a redistribution of counterions in which the exchanging ion retains its identity. As previously mentioned, the free energy changes associated with this process are too small (only one to two kilocalories per mole) to impart selectivity to the separation. Coupling of the ion-exchange reaction, however, with another suitable reaction having a favorable free energy change for a spontaneous chemical reaction will yield an overall negative free energy change of sufficient magnitude for the desired separation. Because of the very large number of suitable reactions to couple with ion-exchange, RIEX is a powerful tool for the design of new extractants for selective metal ion recovery.

A new category of polymers, termed dual mechanism bifunctional polymers (DMBP's) has been developed by Alexandratos and coworkers for the selective complexation and recovery of metal ions.[74] These polymers are unique in that they operate through two different groups by two different mechanisms. The access mechanism allows for metal ion entry into and mobility within the polymer network and is provided by an ion-exchange group. The recognition mechanism allows for metal ion

specificity through either a reduction, coordination, or precipitation group on the same polymer. The ion-exchange group, a phosphorus-based acid, serves to bring the metal ion in close enough proximity to the recognition group for a highly specific reaction to occur between the metal ion and the group, thus leading to the selective complexation of the targeted metal ion.

DMBP's are divided into three classes based upon the type of recognition group present on the polymer. The Class I DMBP, the ion-exchange/redox resin, combines the ion-exchange group with a recognition group capable of reducing certain metal ions. The ion-exchange/redox resin is represented by the phosphinic acid resin (Figure 11). This resin contains both primary and secondary acid sites which are capable of ion-exchange with a metal ion through the acidic hydrogen. The primary acid site, however, is also capable of reduction of certain metal ions through its phosphorus-hydrogen bond. Reduction of both Ag(I) and Hg(II) to the zerovalent state is possible using the Class I resin.[75]

The significance of coordination of a metal ion with the phosphoryl oxygen of the Class I resin was indicated in extraction studies of this resin with some non-reducible metal ions in highly acidic solutions where ion-exchange is not expected to occur.[76] The observation of the importance of coordination as an extraction mechanism in Class I polymers led to the development of the Class II DMBP's, the ion-exchange/coordination resins (Figure 12). Neutral coordinating phosphorus extractants are widely used in solvent extraction. Furthermore, a synergistic enhancement in metal extraction by adduct

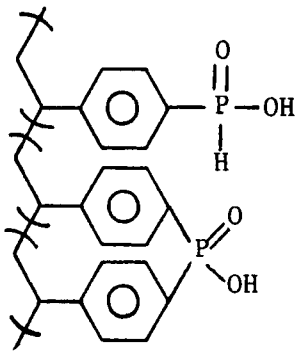

1° acid site

2° acid site

Figure 11. Class I resin.

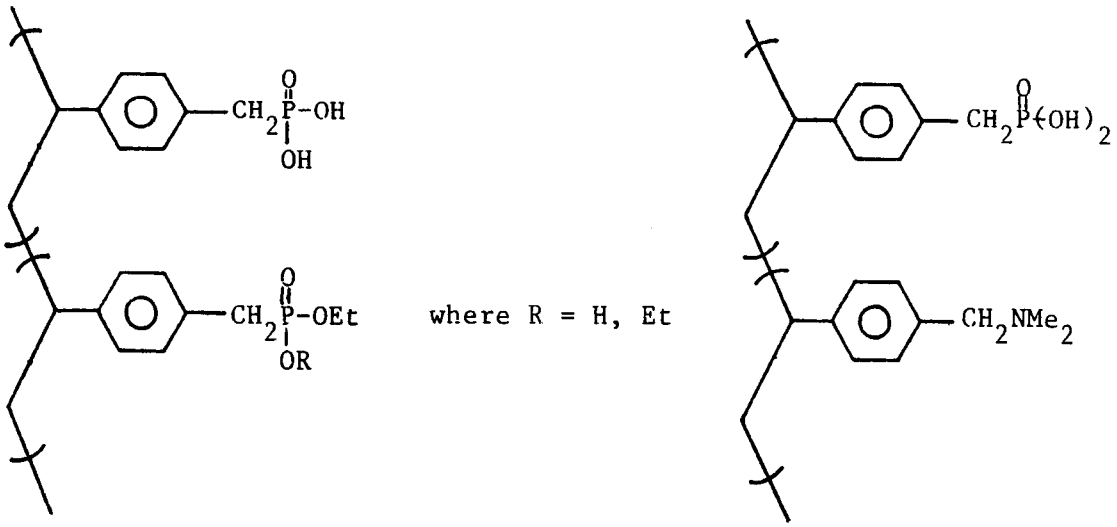

Figure 12. Class II resin.

formation is observed in solvent extraction when a neutral coordinating extractant is added to the extraction system with an acidic extractant.[12] The Class II resins consist of phosphorus acid derivatives to provide ionic accessibility through ion exchange and either a phosphoryl oxygen or tertiary amine group as the coordinating ligand for enhanced ionic recognition.[77] The basicity of the phosphoryl oxygen was varied by changing the substituents attached to phosphorus in order to produce resins of differing coordinative abilities and hence different metal ion selectivities. The principles of hard-soft-acid-base theory[78] were utilized to predict the affinity of the phosphoryl oxygen for the targeted metal ion. HSAB theory states that hard acids prefer to bind to hard bases and soft acids prefer to bind to soft bases. Pearson classified Lewis acids into categories of hard, borderline or soft based upon physical properties such as polarizability, electronegativity and oxidation potential.[79] Hard metal ions generally have one or more of the following characteristics: small size, high positive charge, no easily distorted valence electrons, high electronegativity and low polarizability. In contrast, soft metals tend to be large in size, have low positive charge and contain unshared electrons in their valence shell. These characteristics lead to high polarizability and low electronegativity. The borderline ions represent intermediate cases between the hard and soft categories. In addition to the physical properties described above, Pearson used equilibrium constant data in the classification of Lewis acids as hard or soft. For example, a Lewis acid, M^+, can be classified as hard or soft by measuring the equilibrium constant of the following reaction:

$$MF + I^- \rightleftharpoons MI + F^-$$

A large equilibrium constant indicates that M^+ is a soft Lewis acid because it prefers to bind the soft, polarizable base I^-. Conversely, a small equilibrium constant for the reaction indicates that M^+ is a hard metal ion because it prefers to coordinate the hard, nonpolarizable base F^-.

The aim of the present research is to design a series of Class II dual mechanism bifunctional polymers containing coordinating ligands with a wide range of polarizabilities to allow for the selective complexation of metal ions with varying hard/soft character. The degree of polarizability of the phosphoryl oxygen coordinating ligand was varied by changing the electronic nature of the groups attached to phosphorus. Electron-withdrawing groups attached to phosphorus remove electron density from the phosphoryl oxygen thus decreasing the ligand's polarizability and increasing its preference to bind hard cations. Conversely, attachment of electron releasing groups to phosphorus increases the electron density of the phosphoryl oxygen rendering it more polarizable and hence more likely to preferentially bind soft metal ions.

Ion-exchange/precipitation resins represent the third class of DMBP's (Figure 13). These polymers combine a phosphonic acid access group along with a quaternary amine moiety whose associated anion can selectively precipitate certain metal cations, thus leading to the recovery of an insoluble metal salt from solution.[80] Class III resins

are particularly useful for the recovery of metal ions such as barium which readily form precipitates with certain anions and have reduction potentials too low to be reduced by the Class I resins and do not readily coordinate with the phosphoryl ligands of the Class II resins.

This dissertation describes the synthesis and characterization of some Class I and Class II DMBP's. Metal ion complexation studies have been carried out using lanthanide, actinide, and transition metal ions over a wide range of experimental conditions. The results are interpreted in terms of both the coordinative ability of the extracting ligand and the hard/soft acid-base character of the metal ion. The mechanism of the extraction process for these new polymers has been studied over a wide range of solution acidities and metal ion concentrations. Additionally, results for resins are compared to those for some liquid extractant analogues.

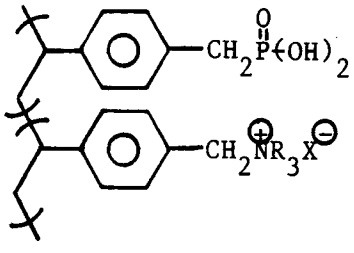

Figure 13. Class III resin.

CHAPTER I

CLASS I DUAL MECHANISM BIFUNCTIONAL POLYMERS

Introduction

The phosphinic resin represents the first class of DMBP's, the ion-exchange/redox polymers. When these polymers are synthesized at high temperatures and catalyst levels, a fully functionalized phosphinic resin is obtained which consists of both primary and secondary acid sites as shown in Figure 11 (page 26). Both primary and secondary acid sites have acidic hydrogens which can ion-exchange with a metal ion, giving the polymer a hydrophilic matrix and therefore high ionic accessibilty. Even in solutions too acidic for ion-exchange to occur, coordination of the metal ion to the phosphoryl oxygen can provide an access mechanism for metal entry into the polymer network. In addition to the ion-exchange group, the primary acid also contains a P-H bond which is capable of reducing metal ions having favorable reduction potentials, thus leading to a high observed selectivity of the resin for these metal ions. Numerous variables in the synthesis of these resins have been studied. The effect of the phosphorylation reaction temperature on the primary and secondary acid capacities and metal ion complexing abilities of the resulting phosphinic resins has been determined. Oxidation of the phosphinic resin to form a phosphonic resin has been studied using a variety of metal ions and hydrogen peroxide as oxidizing agents over a wide range of experimental conditions. Additionally, phosphinic resins of varying levels of

divinylbenzene (DVB) cross-linking and macroporositites have been synthesized and characterized. The metal ion complexation studies of this resin with lanthanide, actinide, and transition metal ions are discussed in Chapter III and Chapter IV.

Synthesis of the Phosphinic Resin

The high capacity phosphinic resin was prepared by Friedel-Crafts reaction of PCl_3 with polystyrene gel beads (cross-linked with two weight percent of DVB unless noted otherwise) using 0.77 mole $AlCl_3$ catalyst (per mole of copolymer) for 4 h at 76 °C. Following hydrolysis of the intermediate phosphinated polymer and subsequent oxidation with 1M NaOH, a bifunctional phosphinic acid resin was obtained as shown in Figure 14.[81] Phosphination of polystyrene first leads to the formation of dichloromonoarylphosphine ligands, which upon further heating undergo a disproportionation reaction resulting in the formation of monochlorodiarylphosphine ligands. Ample experimental precedent exists in aromatic systems for this reaction sequence. For example, Kosolapoff and Huber found that refluxing benzene with PCl_3 in the presence of $AlCl_3$ led to the formation of both dichlorophenylphosphine and monochlorodiphenylphosphine.[82] Additionally, a precipitate of crosslinked polymer was formed during the phosphorylation of linear polystyrene with PCl_3 and $AlCl_3$, indicating that a secondary cross-linking reaction occurred between polymer chains to form monochlorodiarylphosphine ligands.[81] Evidence for the presence of the phosphine oxide intermediate in the reaction sequence is provided by the work of Frank who found that hydrolysis of monochlorodiarylphosphine containing bulky

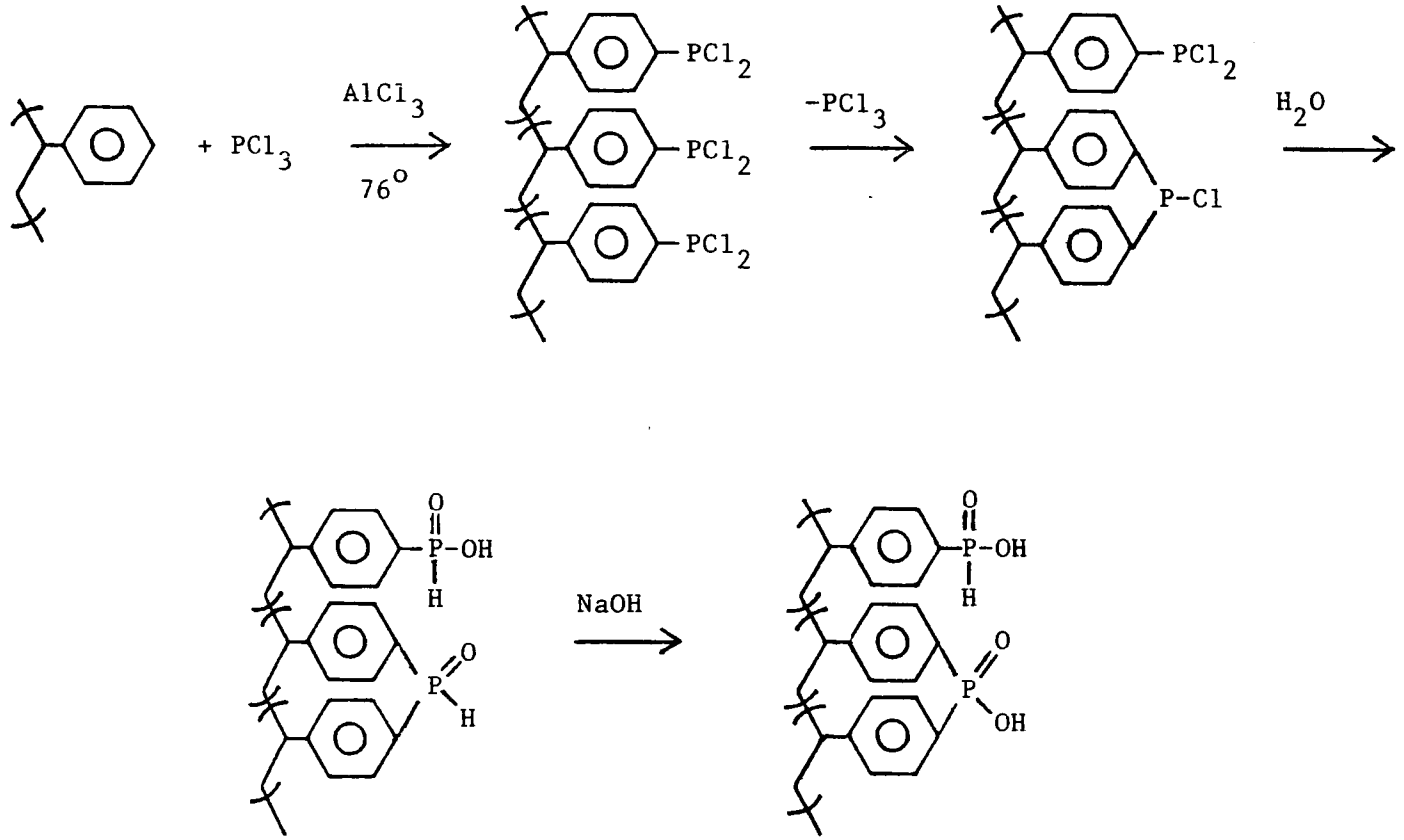

Figure 14. Phosphinic resin synthesis.

groups on the aromatic ring resulted in the formation of phosphine oxide groups.[83] Further evidence to support the formation of phosphine oxide groups on the polymers comes from total acidity determinations on the phosphorylated resins before and after contact with 1M NaOH.[81] These results show the uncontacted resin to have a lower total acid capacity than the contacted resin. Furthermore, when the uncontacted resin was then treated with 1M NaOH, its total acidity increased to the same value as the resin previously contacted with NaOH, indicating that oxidation of the phosphine oxide to a secondary phosphinic acid group occurred upon treatment with 1M NaOH.

Characterization of the Phosphinic Resin

The phosphinic acid resin was characterized in terms of its total acid capacity (tot(OH)), total phosphorus capacity (tot(P)), apparent primary acid capacity and percentage of solids (%S). Characterization results are summarized in Table 1 for 2% DVB crosslinked phosphinic resins synthesized at 76 °C with 0.77 mole $AlCl_3$. The good agreement between the tot(OH) determined by titration of whole beads and the tot(P) determined by elemental analysis on solubilized beads indicates good reagent accessibility within the resin was achieved in the NaOH titration. The results also demonstrate that consistent values of tot(OH) and tot(P) can be obtained between different batches of resins but that some variation in the apparent primary acid capacity occurred among batches. The %S values indicate that the suction-dried phosphinic resin consists of approximately equal amounts of water and polymer, thus demonstrating that the resin has good hydrophilicity. The theoretical

Table 1

Characterization of Phosphinic Resins Synthesized at 76 °C with 0.77 Mole $AlCl_3$

Resin Code	Capacity (mequiv/g dry resin)			
	tot(OH)[a]	tot(P)[b]	primary acid[c]	% Solids[d]
DQ-02-015D	4.73	5.16	2.23	49.90
DQ-02-035D	4.79	4.55	2.20	52.30
DQ-02-059D	4.82	4.88	1.97	51.59
DQ-01-092D	5.25	4.78	1.56	50.85
DQ-01-127D	4.60	4.72	3.05	49.24
DQ-02-109	4.96	4.96	2.92	52.94
DQ-02-109 (Na Salt)			2.42	23.44

[a] Average of all values is 4.86 mequiv/g with standard deviation of 0.22 mequiv/g.

[b] Average of all values is 4.84 mequiv/g with standard deviation of 0.21 mequiv/g.

[c] Apparent primary acid capacity determined by iodine oxidation at room temperature. Average of all values is 2.32 mequiv/g with standard deviation of 0.57 mequiv/g.

[d] Average of all values is 51.14% with standard deviation of 1.42%.

total acid capacity of the phosphinic resin can be calculated by assuming complete substitution of sytrene rings and the experimental value for the amount of primary acid (average value of 2.32 mequiv/g from Table 1). Because the DVB monomer solution used in the copolymerization contains only 55.4% DVB (the remaining 44.6% is primarily ethylvinylbenzene), 100 g of a 2% DVB crosslinked copolymer actually contains only 96.32 g of styrene rings.[34] Assuming that only the aromatic rings from styrene are substituted leads to a theoretical maximum acid capacity of 4.44 mequiv/g. Comparing this value to the average tot(OH) of 4.86 mequiv/g in Table 1 shows that a capacity greater than the theoretical maximum is actually obtained. If, however, substitution of all aromatic rings present on the polymer is assumed, a theoretical maximum capacity of 4.58 mequiv/g is obtained, in better agreement with the experimental value.

The total acid capacity of the resin was determined by stirring a weighed amount of resin with an excess amount of NaOH whereby a neutralization reaction occurs between the resin and the base. After a prescribed equilibration period, a portion of the supernatant NaOH solution was removed and titrated with H_2SO_4, thus giving a measure of the number of acidic groups present on the polymer. An important variable in this experiment is the length of the equilibration period between the resin and the base. If the equilibration period is not sufficient for the neutralization reaction to occur, erroneously low capacities will be obtained. On the other hand, if the equilibration period is too long, reaction of the NaOH with the atmosphere or glass surfaces could lead to an erroneously high capacity. The results of the

study of the equilibration period on the total acid capacity of the phosphinic resin are shown in Table 2. Equilibrium is reached with the phosphinic resin after a 4-h contact time. Furthermore, no increase in capacity is observed at very long equilibration times. The optimum contact period was determined to be 17 h, which should allow sufficient time for equilibration when less hydrophilic resins than the phosphinic are used.

Another method of determining the total acidity of the resin is through a titration curve. Titration curves for a 2% DVB crosslinked phosphinic resin are shown in Figure 15. In this procedure, the resin was titrated by hourly additions of 0.1 M NaOH. The hour equilibration period is required for full exchange to occur per addition of NaOH. The neutralization reaction between the resin and NaOH was followed with a pH meter. Titration of the resin was carried out in the presence of water alone (curve A) and with the addition of dissolved NaCl (curve B). Comparing the initial pH values of the two curves shows that when the resin is placed in a solution of NaCl, ion exchange begins even before NaOH is added, causing the pH of the solution to decrease. The solution pH at this point depends on the amount of NaCl added, the amount of resin used, the volume of solution, and on the nature and capacity of the resin.[34] The pK_a determined from Curve A is 4.0, whereas the apparent pK_a determined in the presence of added salt is 3.0. Comparison of the apparent pK_a value to those of other cation exchangers shows that the phosphinic resin is of intermediate acidity compared to the sulfonic resin (apparent pK_a < 1) and the carboxylic resin (apparent pK_a 4-6).[34] The pK_a for the phosphinic resin obtained without

Table 2

Equilibration Time Study on Total Acidity Determination[a]

Time (h)	tot(OH) capacity (mequiv/g)
4	4.90
8	4.93
12	4.93
17	4.91
24	4.92
48	4.97

[a]Phosphinic acid resin used; tot(P) = 4.79 mequiv/g.

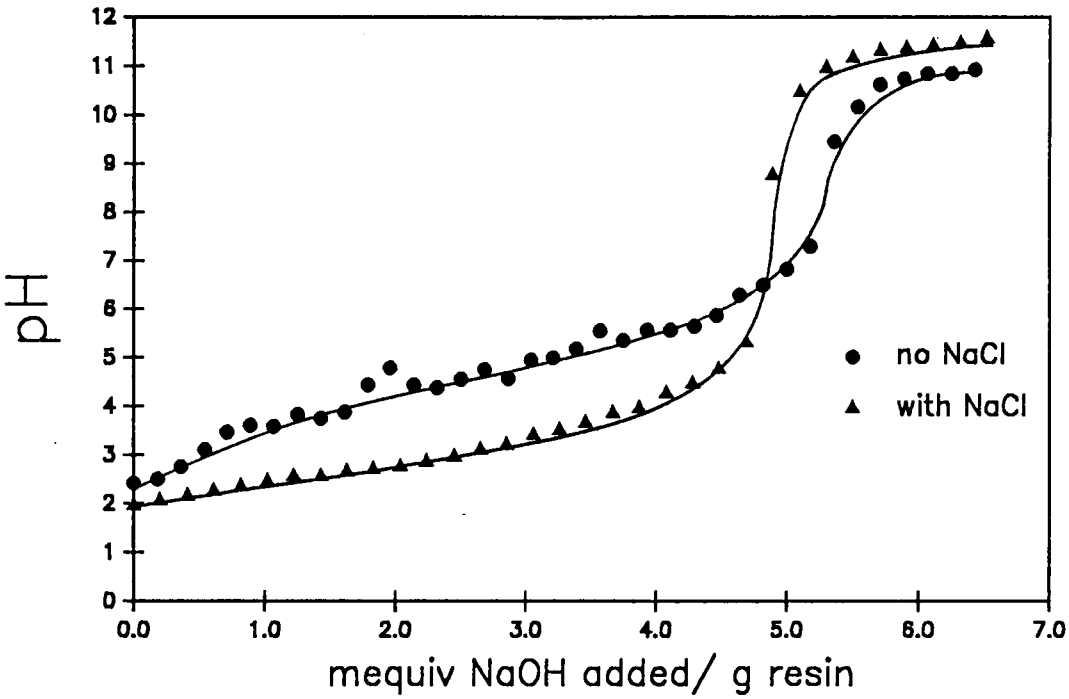

Figure 15. Titration curves of the phosphinic resin in the presence and absence of added NaCl.

added NaCl is consistent with the pK_a of 3.49 for phenylphosphinic acid, suggesting that pH curves can be applied to determine the pK_a's of these resins.[81] Both titration curves show only one endpoint as expected for the monoprotic primary and secondary phosphinic acid groups. The difference in pK_a values for the primary and secondary acid groups is far too small for separate endpoints to be detected for the two groups. The endpoint of the titration reflects the total acid capacity of the resin which is determined to be 5.29 mequiv/g from titration curve A and 4.79 mequiv/g from titration curve B, both in good agreement with the value of 4.82 mequiv/g obtained from the excess NaOH method.

The total phosphorus capacity of the resin was determined by phosphorus elemental analysis. This technique is of particular importance in the characterization of the resin because it is carried out using solubilized polymers. Thus, this technique is especially valuable when analyzing partially functionalized resins in which problems with reagent accessibility may limit the usefulness of titrimetric methods. In this procedure, the polymer beads were first digested using hot perchloric and nitric acids; the phosphorus content of the resulting solution was then determined spectrophotometrically using Beer's Law.

The apparent primary acid capacity is a measure of the number of oxidizable P-H bonds present on the polymer and may be determined by either an iodine oxidation analysis or by metal ion oxidation methods carried out at room temperature. Since the phosphinic acid ligand on the polymer should have an oxidation potential similar to that of phosphonous acid, H_3PO_2, (E°_{ox} = +0.50 V), then Hg^{2+} (E°_{red} = +0.85 V), Ag^+

(E°_{red} = +0.80 V), and I_3^- (E°_{red} = +0.53 V) are all capable of oxidation of the phosphinic ligand.[84] Iodine oxidation analysis involved the reaction of the phosphinic resin with an excess amount of iodine reagent, KI_3. The phosphinic acid group was thus oxidized to form a phosphonic acid group with the concomitant reduction of iodine reagent to iodide ion as shown in Figure 16. An excess amount of standard sodium thiosulfate solution was then added to reduce the remaining iodine reagent, and after an appropriate reaction time, the remaining thiosulfate solution was titrated with standard iodine reagent. The amount of iodine originally consumed in the oxidation of the P-H bonds of the phosphinic resin can thus be determined and used to calculate the apparent primary acid capacity of the resin. An alternate method for the determination of apparent primary acid capacity is through metal ion oxidation of the P-H bond using either Hg^{2+} or Ag^+. In this technique the resin was contacted with an excess amount of either $Hg(NO_3)_2$ or $AgNO_3$ which are both capable of oxidation of the phosphinic acid group to a phosphonic acid. The equations for reduction of Hg^{2+} and Ag^+ are represented in Figures 17 and 18, respectively. Elution of the resulting phosphonic resin with 4-8 M HNO_3 stripped any extracted metal from the resin which was then titrated using the excess NaOH procedure to determine the increase in acid capacity over that of the original phosphinic resin. Apparent primary acid capacity values obtained by metal ion oxidation using Hg^{2+}, Ag^+, and iodine oxidation analyses at room temperature are shown in Table 3. Generally good agreement in apparent primary acid capacity was obtained using the three different methods. Results are also included in Table 3 for contact of the

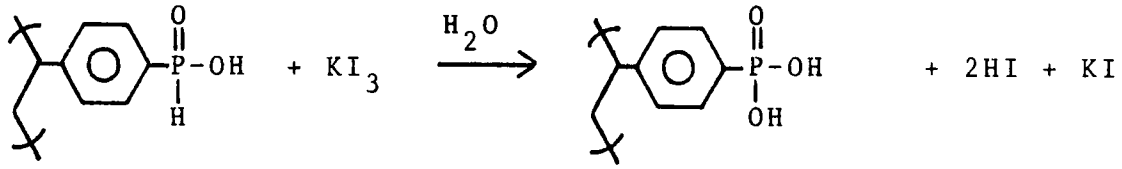

Figure 16. Iodine oxidation of the phosphinic resin.

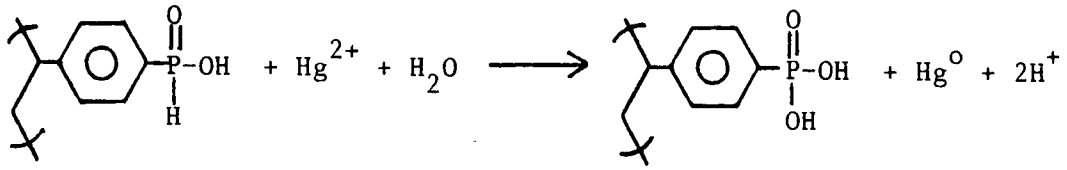

Figure 17. Hg^{2+} oxidation of the phosphinic resin.

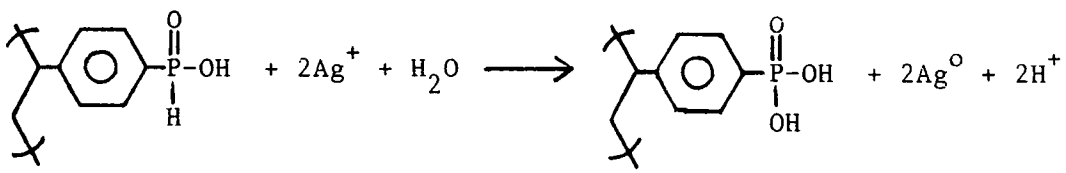

Figure 18. Ag^{+} oxidation of the phosphinic resin.

Table 3

Metal Ion Oxidation of Phosphinics[a]

Resin	Metal	total acid capacity[b]		primary acid capacity[b]	
		$tot(OH)_i$[c]	$tot(OH)_f$[d]	$\Delta tot(OH)$[e]	I_2 oxid.[f]
DQ-02-109	Ag	4.96	7.82	2.86	2.92
DQ-02-109[g]	Ag	4.96	7.15	2.19	2.42
DW-01-142B	Ag	5.08	7.73	2.65	1.82
DQ-02-059B	Hg	3.04	5.44	2.40	2.07
DQ-02-059C	Hg	3.79	6.33	2.54	2.14
DQ-02-059D	Hg	4.82	8.09	3.27	1.97
DQ-02-059B	Zn	3.04	3.05	0.01[g]	2.07
DQ-02-059C	Zn	3.79	3.59	-0.20[g]	2.14
DQ-02-059D	Zn	4.82	4.82	0.00[g]	1.97

[a]17 h contact time; measured at room temperature.
[b]Measured in mequiv/g.
[c]Measured by excess NaOH technique before oxidation.
[d]Measured by excess NaOH technique after oxidation and stripping.
[e]$\Delta tot(OH) = tot(OH)_{final} - tot(OH)_{initial}$.
[f]Apparent primary acid capacity measured at room temperature.
[g]Sodium salt form of the resin.

phosphinic resin with Zn^{2+} which, as expected by its low reduction potential (E°_{red} = -0.76 V)[84], was not capable of oxidizing the phosphinic ligand. The apparent primary acid capacities presented in Tables 1 and 3 (pages 34 and 42, respectively) were determined at room temperature. The effect of changing the temperature of the oxidation reaction on the observed primary acid capacity was determined using both iodine and metal ion oxidation techniques. The data is summarized in plots of Δtot(OH) versus temperature shown in Figures 19 and 20. The results for Ag^{+} show that the Δtot(OH) values increased with increasing temperature to a maximum value of 4.0 mequiv/g obtained at temperatures greater than 65 °C. These results suggest that more primary acid sites were present on the polymer than indicated by the apparent primary acid capacity obtained at 25 °C. The data for Hg^{2+}, however, show a levelling off of the Δtot(OH) values at approximately 2.7 mequiv/g, indicating that the apparent primary acid capacity obtained by Hg^{2+} oxidation was indeed a valid measure of the total primary acid ligands on the polymer. Results using $NaNO_3$ as a possible oxidant show that the nitrate ion itself is not capable of oxidation of the resin over a temperature range of 15-70 °C. Iodine oxidation reactions also show a strong dependence on temperature (Figure 20). Iodine oxidation reactions were carried out using initial amounts of 50 and 100 meq of iodine reagent at temperatures from 0 to 80 °C. The results indicate that the iodine reagent was decomposed at elevated temperatures, thus giving artificially high primary acid capacities. Indeed, changes in the normality of the iodine reagent can result from the heat-catalyzed oxidation of the iodide present in solution.[85] When

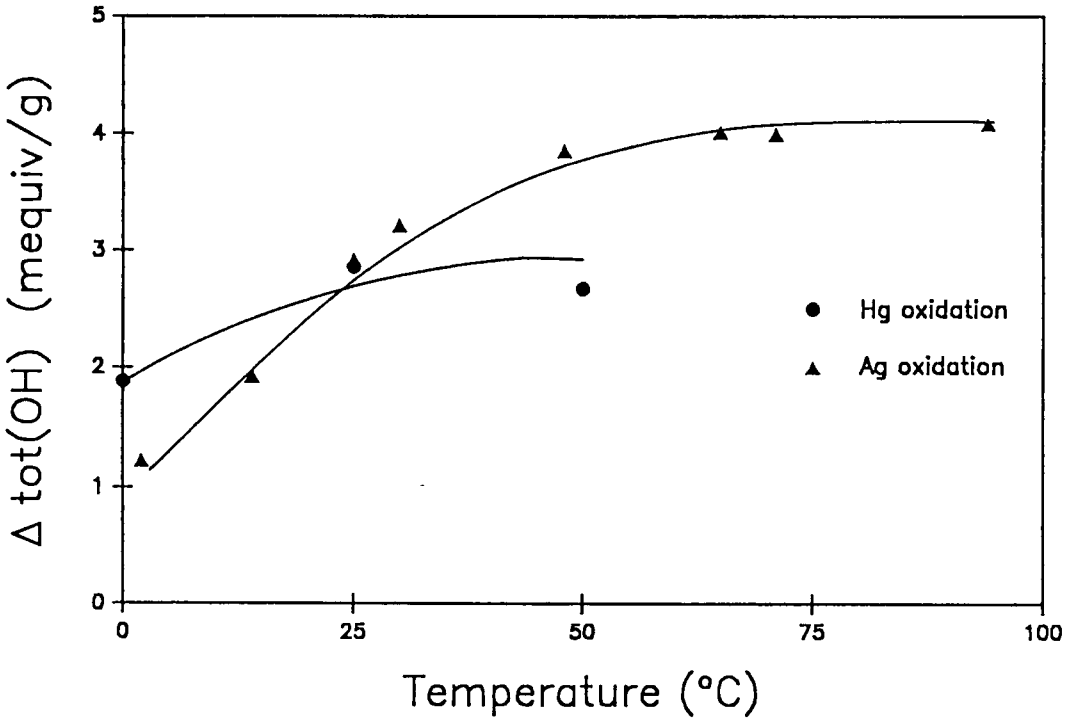

Figure 19. Primary acid capacity of the phosphinic resin measured at various temperatures by the Hg^{2+} and Ag^{+} oxidation techniques.

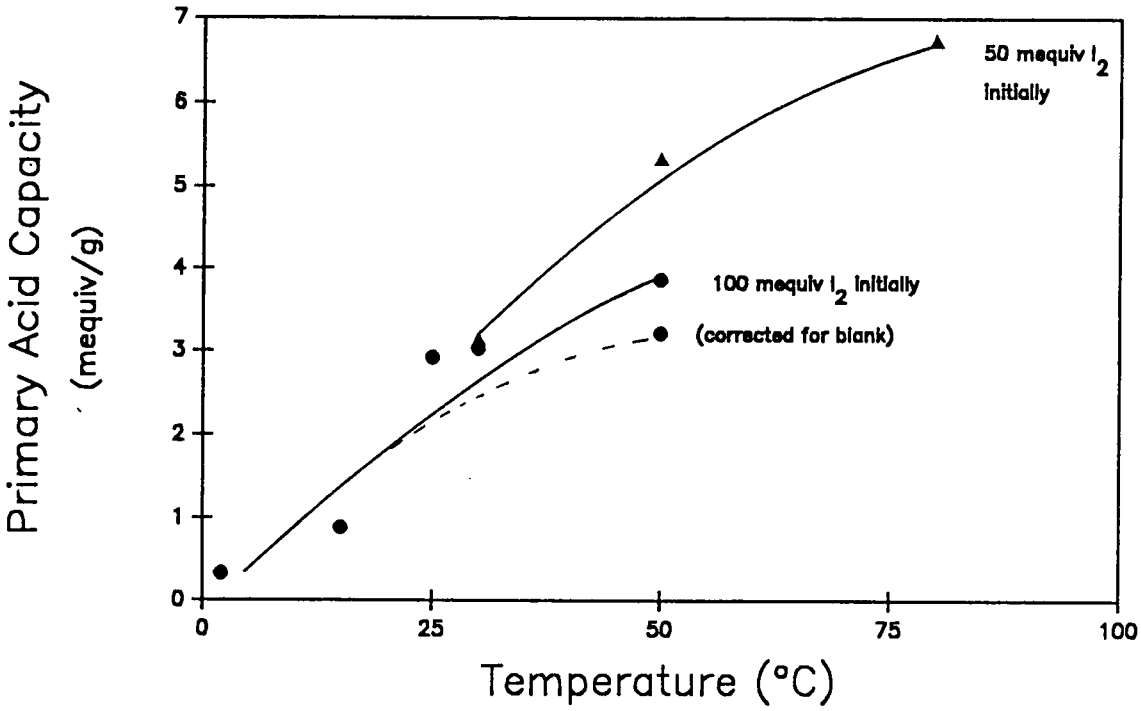

Figure 20. Primary acid capacity of the phosphinic resin measured at various temperatures by the iodine oxidation technique.

the primary acid capacity obtained at 50 °C was corrected by a blank, the value for the resin agreed with the results obtained at 25 °C (Figure 20). Dependence of the results on the initial amounts of iodine present also suggests that decomposition of iodine reagent occurs at elevated temperatures because much larger primary acid capacity values are obtained when a greater initial amount of iodine reagent is present.

The apparent primary acid capacities were determined by both iodine and metal ion oxidation techniques using the sodium salt form of the phosphinic resin to increase the ionic accessibility of the resin. The hydrophilicity of the resin was greatly increased in the sodium salt form as evidenced by the decrease in %S from 50% in the protonated form to 23% in the sodium form. The primary acid capacity of the sodium form of the resin was determined by iodine oxidation to be 2.42 mequiv/g, in close agreement with the value of 2.22 mequiv/g for the resin in the protonated form (Table 1, page 34). As shown in Table 3, the Δtot(OH) value for Ag^+ oxidation of phosphinic resin in the sodium form (2.86 mequiv/g) was also consistent with that of the protonated resin (2.19 mequiv/g). Both sets of results indicate that reagent accessibility was not a problem in the iodine or Ag^+ oxidation analyses of these highly functionalized polymers.

A kinetic study on the oxidation of the phosphinic resin by Hg^{2+} was carried out to establish the time required for equilibrium to be reached. According to the results shown in Table 4, equilibrium was attained by a 5-h contact period. In order to ensure that adequate equilibration time was allowed for less functionalized (and therefore less hydrophilic resins), a standard 17-h contact time was established.

Table 4

Kinetic Study of Hg^{2+} Oxidation of the Phosphinic Resin

Contact Time (h)	Primary Acid Capacity (mequiv/g) $\Delta tot(OH)^a$
5	2.76
7	3.00
9	3.13
12	2.78
17	2.86

[a]$\Delta tot(OH)$ = tot(OH) after oxidation - tot(OH) before oxidation.

In addition to Hg^{2+}, Ag^{+}, and I_3^{-}, the phosphinic resin may also be oxidized by the dichromate ion, $Cr_2O_7^{2-}$ ($E°_{red}$ = +1.33 V).[84] This reaction (Figure 21) was the basis for another technique used to determine the apparent primary acid capacity. After the phosphinic acid resin was contacted with an excess of potassium dichromate solution for a suitable reaction period at room temperature, the amount of dichromate remaining after reaction was quantified by potentiometric titration with standard iron(II) ammonium sulfate solution. The primary acid capacity of the resin was then related to the amount of dichromate which had reacted per gram of resin. The results of dichromate oxidation analysis and apparent primary acid capacities for a series of phosphinic resins are summarized in Table 5. The primary acid capacities obtained by dichromate oxidation were much greater and showed more scatter than those obtained by iodine oxidation analysis. Apparently the dichromate ion is too powerful an oxidizing agent to be selective for oxidation of only the primary acid site. Furthermore, because this technique uses a strong oxidizing agent, the results may also be affected by the oxidation of the pendent ethyl groups in the resin.

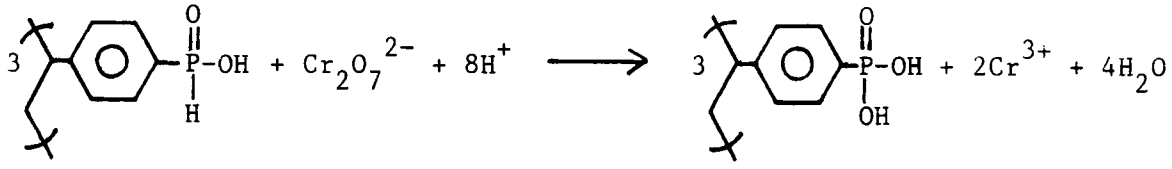

Figure 21. Chromic acid oxidation of the phosphinic resin.

Table 5

Apparent Primary Acid Capacities of Phosphinic Resins Determined by Dichromate and Iodine Oxidation Techniques[a]

Resin	Apparent Primary Acid Capacity (mequiv/g)	
	dichromate oxidation[b]	iodine oxidation
DQ-01-092A	5.00	1.74
DQ-01-092B	6.79	1.82
DQ-01-092C	5.75	1.66
DQ-01-092D	5.57	1.56
DQ-01-127A	4.08/8.28[c]	1.78
DQ-01-127B	3.21/4.38[c]	2.11
DQ-01-127C	1.23/1.74[c]	1.56
DQ-01-127D	4.35/4.08[c]	3.05
DQ-01-127A (Na salt)	5.25	
DQ-01-127B (Na salt)	11.19	
DQ-01-127C (Na salt)	10.03	

[a]All reactions carried out at room temperature.
[b]12 h reaction time, unless noted otherwise.
[c]36 h reaction time.

The presence of impurities remaining in the resin pores, such as catalyst from the phosphorylation reaction, can greatly affect the analysis of the resin, especially in trace-level metal ions extraction. Because these impurities may only be partially removed by the resin conditioning process (successive 1 h elutions of H_2O, NaOH, H_2O, HCl and H_2O), the resins were soxhleted in water to effect complete purification of the resin pores. The pores of the resin collapsed upon soxhleting, requiring that the resin be reswelled by NaOH through a complete reconditioning process. Water was excluded from the polymer matrix as the pores collapse, as evidenced by the increase in %S values from 50% to 70% after soxhleting. After it was reconditioned to allow for reswelling of the pores, however, the resin was rehydrated, regaining its original %S value of 50%. The resin was also reswelled upon contact with 0.1 M NaOH used in the tot(OH) determination, because the same acid capacity was obtained before and after soxhleting. Extraction studies using $Ni(NO_3)_2$, however, showed that accessibility of the metal ion into the polymer network of the soxhleted polymer was greatly decreased. For example, approximately 20% of Ni^{2+} in a 0.1M solution was absorbed by both the unsoxhleted resin and the resin which had been soxhleted and reconditioned. By contrast, only 4% of Ni^{2+} was extracted using the soxhleted, unconditioned resin. The same tot(P) values were obtained by phosphorus elemental analysis on soxhleted and unsoxhleted resins, indicating that phosphorylated linear polymers were not present as impurities in the polymer matrix.

Another method to remove any remaining catalyst from the resin pores is washing the intermediate phosphinated polymer with a suitable

solvent before hydrolysis. Phosphinic resins were thus synthesized using a dioxane wash prior to hydrolysis in 70% dioxane. The resins were then characterized before and after soxhleting in dioxane (followed by complete reconditioning). No difference in tot(OH), tot(P), or %S was observed for resins before and after soxhleting. Additionally, the characterization results for resin washed in dioxane and hydrolyzed in an aqueous dioxane solution were the same as those for unwashed resins quenched in pure water. This indicates that the dioxane wash did not change the resin capacities, but may have produced a resin having lower levels of catalyst impurities. The dioxane-wash technique is of great importance when functionalizing poly(vinylbenzyl chloride) beads, as will be seen in Chapter III, because a higher level of catalyst is incorporated into the polymer network using these polymers than with polystyrene.

Effect of Functionalization Temperature on Resin Acid Capacity

Fully functionalized phosphinic acid resins were obtained by reaction of PCl_3 and polystyrene at a temperature of 76 °C. These hydrophilic resins, while allowing for good reagent accessibility, exhibit a high degree of swelling in ionic solutions which can weaken the polymer matrix and thus lead to bead attrition. Consequently, the degree of functionalization is an important variable in allowing for good reagent accessibility with a minimum of swelling. In order to vary the degree of functionalization, phosphinic acid resins were synthesized over a temperature range of -78 to 76 °C. The effect of reaction temperature on the relative amounts of primary and secondary acid groups

formed on the polymer was then determined. In addition, the influence of the degree of resin functionalization on its metal ion complexing ability was examined.

Results of the functionalization temperature study for the phosphinic resin are summarized in Table 6. The data for duplicate reactions are presented as average values with the standard deviations given. For resins functionalized at temperatures less than 20 °C, the lack of hydrophilic groups on the polymer limited the accessibility of NaOH so that the total phosphorus capacity was a better measure of the degree of functionalization than the tot(OH). In an effort to increase reagent accessibility into less functionalized resins, titration curves and tot(OH) determinations were carried out on resins which had been dried and then powdered. Powdering the resins, however, did not increase the acid capacity obtained by the excess NaOH procedure. In fact, the acid capacities obtained by titration curve decreased using powdered samples because the dried resins were not fully rehydrated during the titration process.

The relationship of the primary acid capacity, secondary acid capacity, and total acid capacity to the functionalization temperature is illustrated in Figure 22. The data show that as the reaction temperature increased, the extent of reaction to form acidic groups also increased. At temperatures below 25 °C, only primary acid groups were formed, indicating that phosphination to form dichloromonoarylphosphine ligands is a lower energy process than disproportionation. The disproportionation reaction between dichloromonoarylphosphine groups, which subsequently leads to the formation of secondary acid sites as

Table 6

Effect of Functionalization Temperature on Phosphinic Resin Acid Capacity[a]

Functionalization Temperature (°C)	Capacity (mequiv/g)					% reaction
	primary[b] acid	secondary acid	tot(OH)	tot(P)	theoretical tot(OH)[g]	
-78	1.33	0	c	1.12	5.73	19.5
0	1.45	0	1.22[c]	1.30	5.73	22.7
15	1.79	0	1.01[c]	1.84	5.73	32.1
20	2.07	0	2.18	2.69	5.73	38.0
23	2.08	0	2.01	2.69	5.73	35.1
25[d]	2.27	0.85	3.12	3.79	4.42	70.6
30[d]	2.03	0.95	2.98	3.31	4.33	68.8
35	1.89	1.83	3.72	4.20	4.28	86.9
40[e]	2.50	1.41	3.91	4.18	4.51	86.7
50[f]	2.02	1.83	3.85	3.81	4.33	89.0
76[f]	2.32	2.47	4.79	4.78	4.44	100

[a] 0.77 mole $AlCl_3$/mole copolymer; 4 h. reaction period.
[b] Apparent primary acid capacity measured by iodine oxidation at 25°C.
[c] Tot(OH) value limited by low OH^- accessibility. Tot(P) is a better measure of degree of functionalization.
[d] The capacities listed are averaged from five functionalizations. The standard deviations are 0.12, 0.19, 0.23,
[e] and 0.32 for primary acid, secondary acid, tot(OH), and tot(P), respectively.
The capacities listed are averaged from six functionalizations. The standard deviations are 0.34, 0.53, 0.30,
[f] and 0.29 for primary acid, secondary acid, tot(OH), and tot(P), respectively.
The capacities listed are averaged from eight functionalizations. The standard deviations are 0.48,0.63, 0.25,
[g] and 0.21 for primary acid, secondary acid, tot(OH), and tot(P), respectively.
Assuming complete substitution of styrene rings and the experimental value for primary acid capacity.

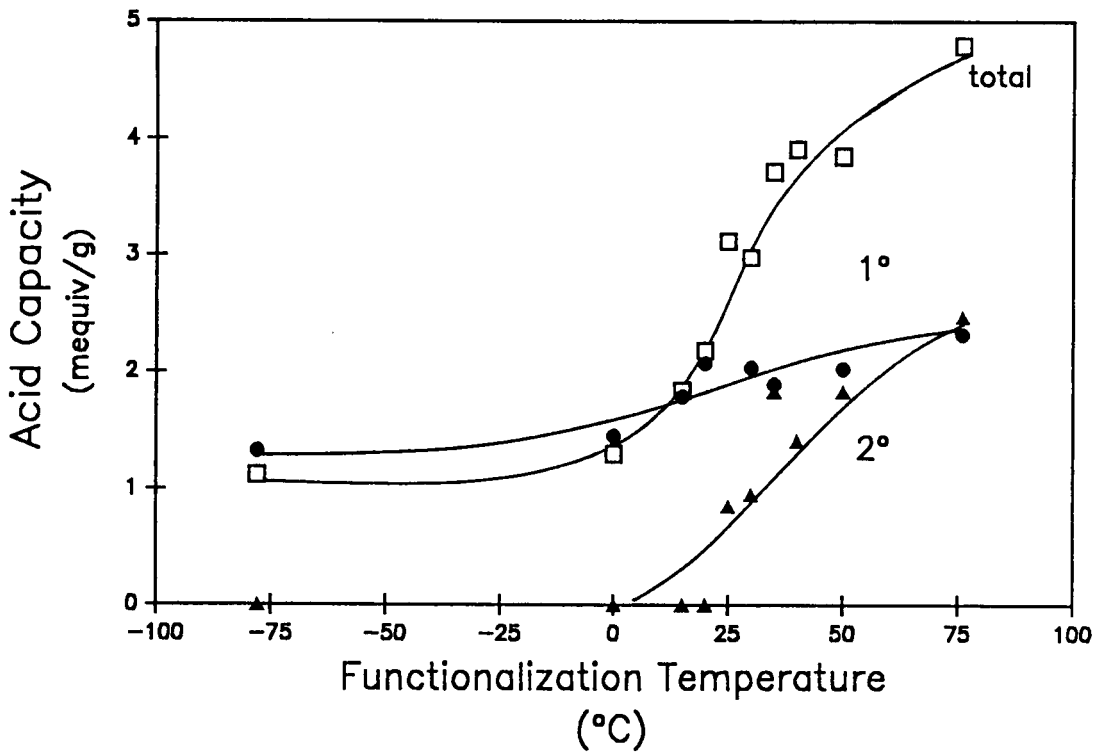

Figure 22. Relationship of the primary acid, secondary and total acid capacities of the phosphinic resin to the functionalization temperature.

shown in Figure 14 (page 32), began only after 20-25 °C. The increase in total acid capacity after 25 °C was the result of formation of secondary acid sites because the primary acid capacity remained constant at approximately 2 mequiv/g over the temperature range of 25-76 °C. These temperature study results also indicate that a temperature of 76 °C was required for complete functionalization of the polymer to form a phosphinic resin which contains approximately equal amounts of primary and secondary acid groups.

Effect of Acid Capacity on Metal Ion Complexation

The influence of resin acid capacity on the extraction of both reducible (Hg^{2+}) and non-reducible (Zn^{2+}) metal ions was investigated using the phosphinic resin. Phosphinic resins with four different acid capacities prepared by functionalization at different temperatures were used: 1.08 mequiv/g (15 °C), 3.25 mequiv/g (30 °C), 3.90 mequiv/g (50 °C), and 4.79 mequiv/g (76 °C). The amount of metal absorbed by the resin from solution was determined by following the loss of a radioactive tracer from solution into the resin. In this set of experiments, enough resin to give one milliequivalent of acid sites was contacted with initial amounts of $Zn(NO_3)_2$ or $Hg(NO_3)_2$ of 0.1, 1.0, or 1.5 milliequivalents. Hereafter, the initial ratios of the milliequivalents of metal ions to the milliequivalents of resin active sites (in this case acid sites) is referred to as the R_i. The acid capacity determined from the excess NaOH procedure was used to quantify the number of acid sites even though this value is limited by inaccessibility of NaOH when incompletely functionalized resins are

used. It is expected, however, that the same accessibility problems would be encountered for zinc and mercury ions as for sodium ions, so that in this situation, use of the acid capacity is a more accurate reflection of the resin's total capacity than its phosphorus content. In addition to $Zn(NO_3)_2$ or $Hg(NO_3)_2$, the solution also contained enough added $NaNO_3$ to maintain a constant 4M NO_3^- background, and a trace level of radioactive ^{65}Zn or ^{203}Hg. After a 17-h equilibration period, a portion of the solution was removed and counted using a gamma scintillation counter; comparison of the sample counts to those of a blank quantified the amount of metal absorbed from solution by the resin. The results for the different resins were compared in terms of the % loading values which were calculated to be the milliequivalents of metal ions absorbed by the resin per milliequivalent of acid sites available from the resin.

The % Zn^{2+} and Hg^{2+} loading results for R_i values of 0.1, 1.0, and 1.5 are summarized in Table 7 for the four phosphinic resins of varying capacities. The data for both Hg^{2+} and Zn^{2+} show that % loading was relatively independent of the resin acid capacity, except for a small decrease in the % Zn^{2+} loading using the lowest capacity resin at an R_i of 1.5. Overall, the % loading data indicate that metal ion accessibility was not significantly diminished with decreasing acid capacity, even when using a resin functionalized to the extent of only 1.08 mequiv/g.

In addition to equilibrium % loadings, another important consideration of partially functionalized resins is their kinetic behavior. Even if lower capacity resins can be loaded to comparable

Table 7

Effect of Phosphinic Resin Acid Capacity on
% Zn^{2+} and Hg^{2+} Loading

Metal	R_i	Resin Acid capacity, mequiv/g) A (1.08)	B (3.25)	C (3.90)	D (4.79)
Zn^{2+}	0.1	5.6	5.1	5.1	5.6
	1.0	27.3	27.1	22.4	24.0
	1.5	23.8	32.0	30.9	30.3
Hg^{2+}	0.1	9.1	8.9	9.2	9.7
	1.0	79.0	72.5	71.3	67.3
	1.5	90.0	98.0	87.3	85.3

levels as the high capacity resins, they may not be useful if their kinetics are significantly slower. Kinetic studies were thus carried out using four phosphinic resins prepared in the same manner as those studied previously under equilibrium loading conditions. The kinetic experiments were accomplished using a radiotracer analysis as for the equilibrium studies described above. The % Zn^{2+} loaded onto the resin at an R_i of 1.0 was measured at contact times from 1 min to 17 h. The % Zn^{2+} loading results for the four phosphinic resins at various equilibration times are shown in Table 8. Comparison of the kinetic behavior of the four resins shows that the least functionalized resin (resin A, tot(OH) = 1.00 mequiv/g) exhibited the fastest kinetics. Apparently this resin can absorb no more of the zinc ions after 17 h than it can after 5 min. This indicates that all the loading may occur on the surface of the resin and that the metal ions do not diffuse into the resin pores. The results also show that as the capacity increased in resins B,C, and D, the time required to attain equilibrium slightly increased: resin B (2.94 mequiv/g) reached equilibrium after approximately 5-10 min, resin C (3.79 mequiv/g) after 15-30 min, and resin D (4.88 mequiv/g) after 30 min. In comparing the equilibrium % Zn^{2+} loading values obtained in the kinetic study with those from the equilibrium study using similar resins, it can be seen that good reproducibility of the experimental values was obtained for different batches of resins.

Table 8

Percent Zn^{2+} Loading as a Function of Equilibration Time Using Phosphinic Resins of Varying Capacities

contact time	% Zn^{2+} Loading			
	DQ-02-059A[a]	DQ-02-059B[b]	DQ-02-059C[c]	DQ-02-059D[d]
1 min	21.6	9.4	10.5	2.8
5 min	27.8	21.5	19.1	13.6
15 min	23.6	23.9	20.7	19.0
30 min	33.5	25.8	32.2	22.5
45 min	28.0	34.4	33.1	36.5
1 h	24.9	30.9	27.3	29.0
1.5 h	22.7	25.8	24.2	26.5
2 h	21.2	23.8	30.7	23.6
6 h	24.0	24.8	27.3	26.1
17 h	27.3	29.1	31.3	26.6
24 h	24.9	26.7		

[a]tot(OH) = 1.00 mequiv/g.
[b]tot(OH) = 2.94 mequiv/g.
[c]tot(OH) = 3.79 mequiv/g.
[d]tot(OH) = 4.88 mequiv/g.

Oxidation of Phosphinic Resins by Hydrogen Peroxide

Phosphonic resins were synthesized by hydrogen peroxide oxidation of phosphinic resins of varying acid capacities. Presented in Table 9 are the primary and secondary acid capacities for the starting phosphinic resins and the %S, tot(OH) and tot(P) values for the phosphonic resins resulting from their oxidation. The theoretical tot(OH) and tot(P) capacities reported in this table can be calculated for each phosphonic resin in the following manner. For resins which contain only primary acid groups (i.e. those functionalized at temperatures below 20-25 °C), oxidation leads to the formation of a phosphonic resin as shown in Figure 23. The theoretical tot(OH) for the

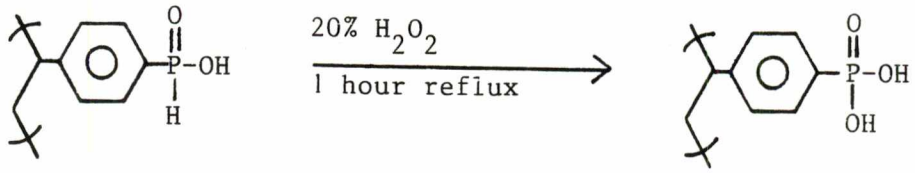

Figure 23. Oxidation of the primary acid site of the phosphinic resin by hydrogen peroxide.

phosphonic resin may be calculated from the primary acid capacity of the starting phosphinic resin and the weight change factor which corrects for the weight increase of the resin after oxidation:

$$\text{tot(OH)} = 2(\text{primary cap})(168/184)$$

Table 9

Results of Hydrogen Peroxide Oxidation of Phosphinic Resins

Phosphonic Resin Code	Phosphinic Resin Oxidized	Oxidation Conditions	Characterization Results (mequiv/g)						
			Phosphinic		Phosphonic				
			primary[c] acid	secondary acid	%S	tot(OH)	theoretical tot(OH)	tot(P)	theoretical tot(P)
DQ-02-033A	DQ-02-015A	a	1.64	0	50	2.77	2.99	1.79	1.50
DQ-02-033B	DQ-02-015B	a	2.08	0.86	37	6.29	5.33	3.45	2.66
DQ-02-033C	DQ-02-015C	a	2.45	1.42	29	7.66	7.00	3.68	3.50
DQ-02-033D	DQ-02-015D	a	2.23	2.50	7	10.08	8.51	4.26	4.26
DQ-02-050A	DQ-02-035A	a	2.06	0	50	1.46	3.76		
DQ-02-050B	DQ-02-035B	a	2.07	1.18	25	5.49	5.88		
DQ-02-050C	DQ-02-015C	a	2.45	1.42	8	7.53	7.00		
DQ-02-050D	DQ-02-035D	a	2.20	2.59	10	8.21	8.62		
DQ-02-065A	DQ-02-059A	a	1.68	0	51	1.59	3.07	1.62	1.53
DQ-02-065B	DQ-02-059B	a	2.07	0.97	41	5.33	5.50	2.93	2.75
DQ-02-065C	DQ-02-059C	a	2.14	1.65	33	6.90	6.84	3.48	3.42
DQ-02-065D	DQ-02-059D	a	1.97	2.85	13	9.53	8.66	4.29	4.33
DQ-02-067A	DQ-02-059A	b	1.68	0	52	0.97[d]	3.07		
DQ-02-067B	DQ-02-059B	b	2.07	0.97	47	1.81[d]	5.50		
DQ-02-067C	DQ-02-059C	b	2.14	1.65	41	3.15[d]	6.84		
DQ-02-067D	DQ-02-059D	b	1.97	2.85	13	7.28[d]	8.66		

a 20% H_2O_2/4 hr heat up/ 1 hr reflux (100 °C)

b 20% H_2O_2/1 hr heat up/ 4 hr reflux (100 °C)

c Apparent primary acid capacity measured by iodine oxidation at 25 °C

d Results affected by solubilization of beads during oxidation

Similarly, the theoretical tot(P) may be obtained:

$$\text{tot(P)} = (\text{primary cap})(168/184)$$

When the phosphinic resin contains both primary and secondary acid groups, oxidation of both groups is expected to occur as shown in Figure 24. The predicted total acid capacity for the resulting phosphonic resin is calculated by the following equation which assumes that the weakly acidic phenol group does not contribute to the measured acidity:

$$\text{tot(OH)} = 2(\text{primary cap})(168/184) + 2(\text{secondary cap})(270/304)$$

Likewise, the theoretical phosphorus capacity is obtained:

$$\text{tot(P)} = (\text{primary cap})(168/184) + (\text{secondary cap})(270/304)$$

Examination of the results in Table 9 shows that some of the total acid capacities obtained after oxidation of phosphinic resins containing only primary acid groups were significantly lower than the predicted values. Incomplete oxidation of the resin may be the result of limited reagent accessibility into these partially functionalized resins under the reaction conditions studied. For the phosphinic resins containing both primary and secondary acid groups, the observed tot(OH) values were consistent with the values predicted by the reaction in Figure 24.

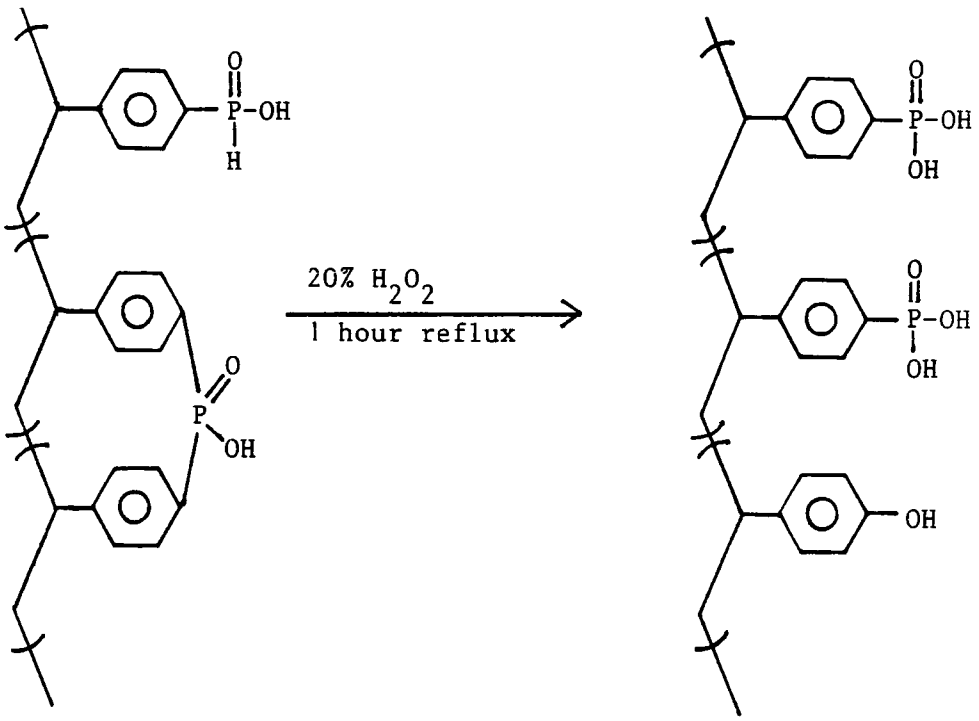

Figure 24. Proposed oxidation products of the primary and secondary acid sites of the phosphinic resin by hydrogen peroxide.

Furthermore, the observed tot(P) values were in very good agreement with the theoretical values, indicating that no loss of phosphorus occurred when the resin was refluxed for 1 h in hydrogen peroxide. However, some beads were solubilized during a 4-h reflux period in hydrogen peroxide which resulted in loss of phosphorus and led to the low observed tot(OH) values reported in Table 9. The titration curves for phosphonic resins DQ-02-065C and DQ-02-065D (Figure 25) both show only one endpoint leading to capacities of 3.61 mequiv/g and 4.35 mequiv/g, respectively. Apparently the pK_a for the second proton of the phosphonic acid is too weak to be detected when titrating with NaOH. However, when the phosphonic resin DQ-02-065D was titrated with sodium ethoxide

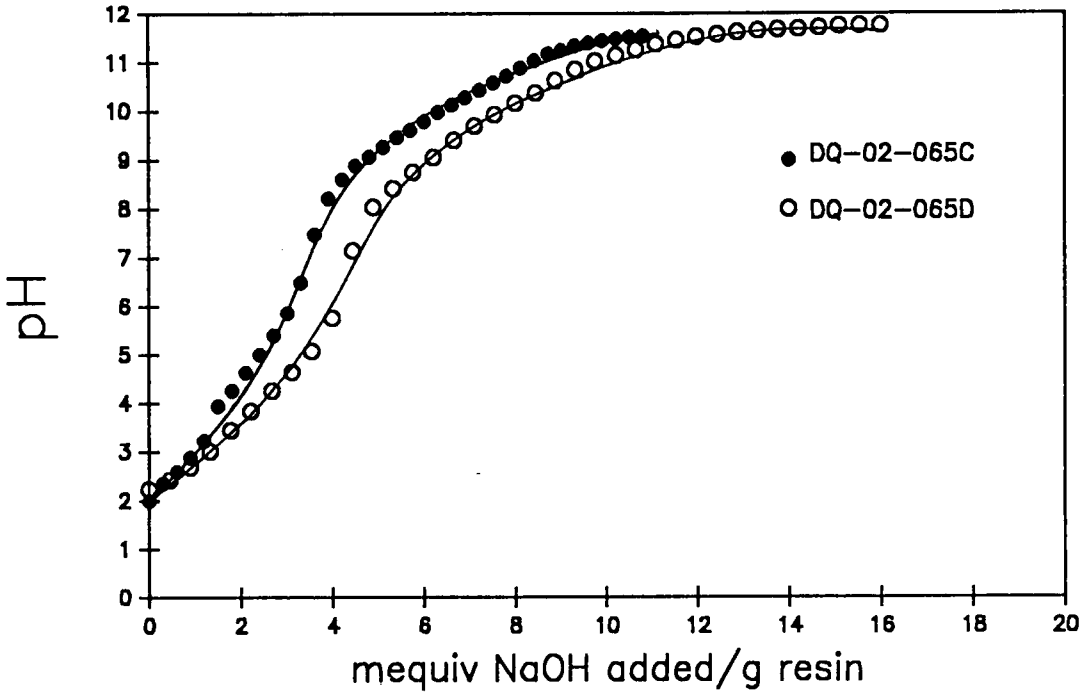

Figure 25. Titration curves for phosphonic resins using sodium hydroxide as the titrant.

(Figure 26), a weak second endpoint was observed corresponding to an acid capacity of approximately 9.25 mequiv/g, consistent with the tot(OH) value from Table 9. None of the curves however showed any evidence of a phenol group on the resin. Furthermore, qualitative tests for phenol using ferric chloride and potassium dichromate on the solubilized polymers from the 4 h oxidation reaction were inconclusive for the existence of phenol as a reaction product. Even though formation of phenol was not proven by these methods, the excellent agreement of the observed tot(OH) and tot(P) capacities with the predicted values suggests that the oxidation reaction proceeds as indicated in Figure 24.

The metal ion complexing abilities of some phosphinic and phosphonic resins were investigated using Hg^{2+} and Zn^{2+} ions. This study was carried out in order to determine the relative strengths of the two extractants and to investigate the influence of the redox component of the phosphinic resin in the extraction of Hg^{2+}. The phosphinic resins used (DQ-02-059A,B,C,D) were functionalized to different capacities at temperatures of 15-76 °C, and the phosphonic resins (DQ-02-065A,B,C,D) were obtained by hydrogen peroxide oxidation of the phosphinics (see Table 9. The extraction experiments were carried out by radiotracer analysis as previously described at R_i levels of 0.1, 1.0, and 1.5. The % Zn^{2+} and Hg^{2+} loading results are presented for both sets of resins in Table 10. Because some of the highly functionalized phosphonic resins had a very high water content in the suction-dried form (i.e. low %S), correction was made in the % loading values for dilution of the metal ions by the water present in the resin pores. The % loading values for

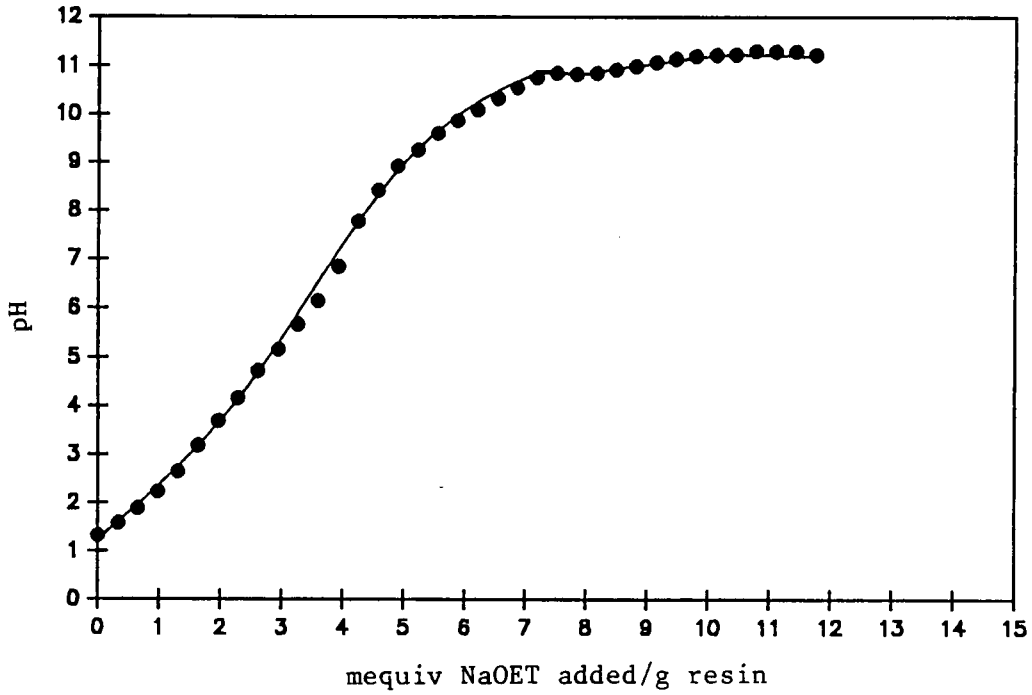

Figure 26. Titration curve for the phosphonic resin using sodium ethoxide as the titrant.

Table 10

Comparison of % Zn^{2+} and Hg^{2+} Loading
Using Phosphinic and Phosphonic Resins

Metal	Ri	% Loading							
		Phosphinic Resins				Phosphonic Resins			
		DQ-02-059A	DQ-02-059B	DQ-02-059C	DQ-02-059D	DQ-02-065A	DQ-02-065B[a]	DQ-02-065C[a]	DQ-02-065D[a]
Zn^{2+}	0.1	5.6	5.1	5.1	5.6	1.8	1.8	2.7	1.5
	1.0	27.3	27.1	22.4	24.0	14.6	18.5	11.8	11.7
	1.5	23.8	32.0	30.9	30.3	18.5	23.3	17.6	12.7
Hg^{2+}	0.1	9.1	8.9	9.2	9.7	4.9	7.8	8.3	8.6
	1.0	79.0	72.5	71.3	67.3	44.4	43.0	41.8	40.1
	1.5	90.0	98.0	87.3	85.3	61.6	56.6	53.8	47.7

[a] % Loading values corrected by macrodilution factor.

the phosphonic resins DQ-02-065B,C,D were corrected by a macroporosity dilution factor (MDF) as previously described for macroporous resins.[86] Examination of the % loading results for both metal ions studied shows the phosphinic resin to be an overall better extractant than the phosphonic resin at all the R_i levels studied. Furthermore, the phosphinic resin showed even larger increases in % loading over the phosphonic for Hg^{2+} than for Zn^{2+}, pointing to the importance of the reduction component of this resin in the extraction of reducible metals such as Hg^{2+}.

Effect of Cross-Link Level and Porosity on Phosphinic Resin Capacity

In order to study the influence of cross-link level and polymer porosity on resin capacity, phosphinic resins were synthesized containing levels of DVB cross-linking from 2-30%, either without macroporosity (gel beads) or with 50 vol % macroporosity (MR beads). A summary of the data is presented in Table 11 for 2,10,15, and 30% cross-linked gel resins and 2 and 10% cross-linked MR resins synthesized at 76 °C using 0.77 mole $AlCl_3$. Average results are reported in the case of replicate syntheses. Comparison of the theoretical and observed capacities reported in this table indicates that complete functionalization was achieved using copolymers containing 2-10% DVB. At the higher cross-link levels of 15 and 30% however, the extent of functionalization decreased due to reduced reagent accessibility into the tight polymer matrix. The accessibility of OH^- was also limited in these highly cross-linked gel resins as indicated by the decreased tot(OH) capacity in comparison to the tot(P). These results for the 15

Table 11

Effect of Cross-Link Level on Phosphinic Resin Acidity[a]

DVB %	type	Capacity					
		acid			tot(p)	theory[c]	primary / secondary
		primary[b]	secondary	total			
2	gel	2.32	2.54	4.86	4.44	4.44	0.91
2	MR	2.31	2.28	4.75	4.59	4.44	1.01
10	gel	1.98	1.56	3.54	3.55	3.78	1.27
10	MR	2.06	2.46	4.32	4.25	3.81	0.84
15	gel	1.13	0.26	1.39	2.45	3.12	4.35
30	gel			0.18[d]	0.71	0.96[e]	

[a] Synthesized using 0.77 mole $AlCl_3$ at 76 °C.

[b] Apparent primary acid capacity measured by iodine oxidation at room temperature.

[c] Assuming complete substitution of styrene rings and the experimental value for the amount of primary acid.

[d] Capacity limited by OH^- accessibility.

[e] Calculated using primary acid capacity = 0.71 mequiv/g.

and 30% cross-linked gel beads suggest that when increased levels of DVB cross-linking are required, use of a macroporous rather than gel support is desirable for increased resin capacity and reagent accessibility. The data in Table 11 also indicate that the ratio of primary to secondary acid sites increased as the level of cross-linking increased from 10 to 15%. This decrease in secondary acid capacity is due to the increased rigidity of the polymer matrix at higher cross-link levels which decreases the likelihood of a disproportionation reaction between polymer chains.

CHAPTER II

CLASS II DUAL MECHANISM BIFUNCTIONAL POLYMERS

Introduction

The second class of dual mechanism bifunctional polymers, the ion-exchange/coordination polymers, combines an ion-exchange reaction to allow for metal ion accessibility into the polymer network with a coordinative component to provide for enhanced selectivity through metal ion complexation. These polymers consist of a phosphonic acid group for ion exchange and either phosphonate ester or tertiary amine ligands for coordination. Results from mixed solvent extraction systems suggest that polymer-supported extractants which are composed of both an ion-exchange group and a neutral coordinating ligand may exhibit synergistic extraction in which both groups acting together remove more metal from solution than either one could alone. For example, synergism has been observed in mixed solvent extraction systems containing an acidic extractant such as DEHP and a neutral coordinating extractant such as TBP.[23] The source of the synergistic enhancement is ascribed to the displacement of any residual coordinated water from the neutral metal complex by the coordinating extractant thus decreasing its hydrophilicity and rendering it more compatible with the organic phase. Alternately, in some systems, the synergistic interaction can be attributed to the expansion of the coordination sphere of the metal ion by the adduct molecules.

It is expected that different metal ion selectivities can be achieved based upon the strength of the interaction between the coordinating ligand and metal ion. The principles of hard-soft acid-base (HSAB) theory can be utilized to predict the strength of the ligand-to-metal interactions using the ion-exchange/coordination resins. Based on HSAB principles, extractants containing the relatively soft phosphoryl oxygen as the coordinating ligand should exhibit a preference for soft metal cations over those which are hard or borderline. This chapter details the synthesis of ion-exchange/coordination polymers of differing coordinative abilities depending on the nature of the alkyl groups attached to the phosphoryl oxygen. As described in Chapters III and IV, the resulting effect on the complexing abilities of these polymers was studied using a broad range of hard to soft metal ions.

Initial Synthetic Approaches to Phosphonate Esters

Given the importance of phosphorus esters such as TBP in solvent extraction systems, considerable effort was focused on the synthesis of polymer-supported phosphonate esters for use as metal ion extractants. Numerous examples of phosphonate ester resins can be found in the literature including two types of fully esterified phosphorylated polymers prepared by Kennedy and coworkers. First, cross-linked triallyl phosphate polymer was prepared by bulk polymerization of triallyl phosphate.[63] The resulting polymer structure, however, was not well defined due to the degradative chain transfer reactions involved with the allyl monomers, and the degree of cross-linking obtained was difficult to control. In order to prepare a phosphonate ester resin

with a more defined structure, an Arbuzov reaction was carried out on cross-linked chloromethylated polystyrene using triethyl phosphite.[87] This reaction is described by Kennedy and coworkers to lead to the preparation of a high capacity diethyl polystyrene methylenephosphonate resin as shown below:

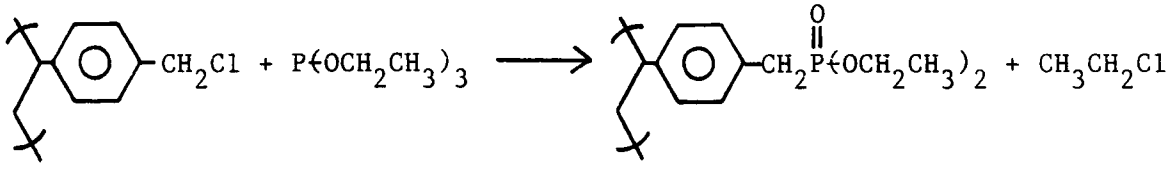

More recently, resins containing phosphoric acid ester functional groups have been prepared from cross-linked chloromethylated polystyrene as illustrated in the following reaction scheme:[71]

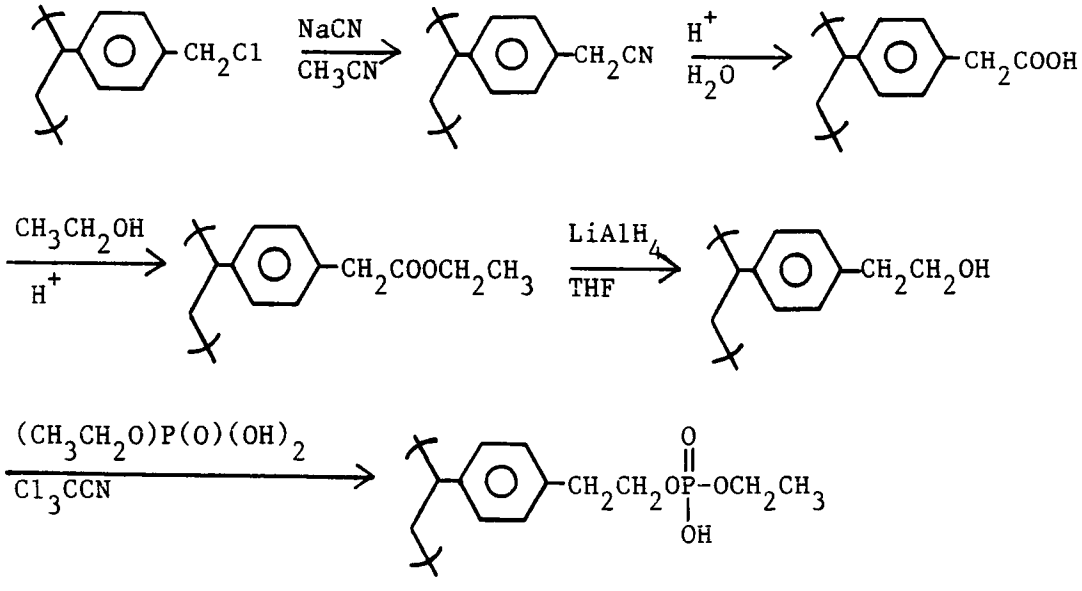

Complete functionalization to phosphoric acid ester groups, however, was not achieved using this lengthy synthetic procedure.

In the present work, three initial approaches to the synthesis of high capacity phosphonate ester resins were attempted as shown in Figure 27. Cross-linked polystyrene or poly(vinylbenzyl chloride) (poly(VBC)) beads were chosen as the polymer support in all the reactions due to the high chemical and thermal stability of these polymers. In addition, a wide variety of reactions can be performed on the aromatic ring of polystyrene and the benzyl carbon of poly(VBC) to produce high capacity resins. The first synthetic attempt (Scheme 1) involved the chlorination of a phosphinic acid resin using thionyl chloride followed by ethanolysis of the resulting arylphosphonyl dichloride to form the ester. In the second synthesis (Scheme 2), polystyrene was phosphorylated by a Friedel-Crafts reaction using PCl_3 and $AlCl_3$ to yield a dichloromonoarylphosphine intermediate. Reaction of this intermediate with ethanol in the presence of pyridine (to neutralize the HCl formed) and toluene (to aid in heat dissipation from the exothermic reaction and maintain reaction fluidity) followed by oxidation with an aqueous solution of iodine should yield the diethyl ester. The third synthetic endeavor (Scheme 3) involved the functionalization of poly(VBC) with PCl_3 and $AlCl_3$ to form a tetrachlorophosphonium intermediate which was subsequently quenched in a solution of ethanol, pyridine and toluene to yield the phosphonate ester. The reaction of small molecule alkyl chlorides with PCl_3 in the presence of $AlCl_3$ to give intermediate phosphonium salts was first reported by Clay[88] and then by Kinnear and Perren.[89] The three resins were analyzed for their

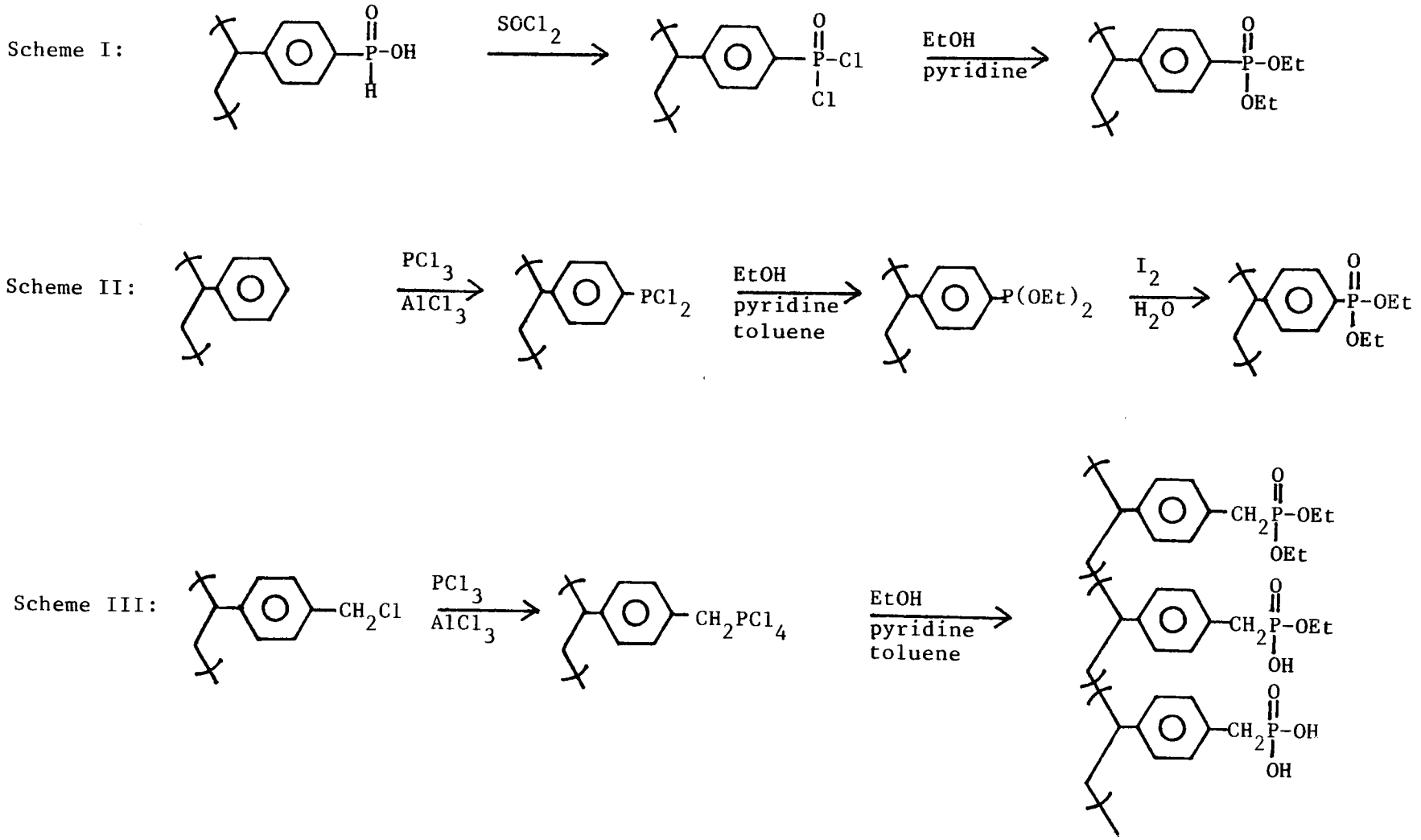

Figure 27. Three approaches to the synthesis of phosphonate ester resins.

total acidity in order to determine the extent of esterification achieved for each reaction scheme. The first and second reactions produced resins with acid capacities of 3.08 mequiv/g and 5.64 mequiv/g, respectively, suggesting very little, if any, esterification of these resins. The third synthetic approach produced a resin with a much lower acid capacity of 0.74 mequiv/g. In order to determine the extent of esterification of this resin, the ester groups were hydrolyzed in concentrated HCl and the total acid capacity of the resin was then redetermined. The acid capacity was found to be 3.11 mequiv/g after hydrolysis corresponding to an ester content of 76%. This resin is termed a mixed ester because it contains of a mix of diacid, monoester and diester groups to give a value of 76% esterification. Because of the relatively high level of esterification obtained with this resin, future synthetic efforts were focused on determining the optimum conditions required to achieve higher degrees of esterification using Scheme 3. The effect of several variables on the extent of esterification was studied including: catalyst level, nature of the solvolysis reaction, and the levels of cross-linking and macroporosity of the polymer support. Efforts were made to determine the solvolytic conditions required to obtain mixed ester resins with a specific ratio of functional groups. In addition, the reaction intermediates were characterized in order to verify the synthetic scheme proposed in Figure 27. Finally, esterification of the monoester and diacid groups on the mixed ester resin was attempted in order to further increase the amount of diester groups on the resin.

Synthesis of Mixed Ester Resins

The influence of catalyst level on the extent of functionalization was the first variable studied in the synthesis of mixed ester resins. Catalyst levels of 0.77 and 1.2 mole $AlCl_3$ (per mole of $-CH_2Cl$ groups) were employed for the functionalization of 2% cross-linked gel and 5% cross-linked MR poly(VBC) beads. The intermediate polymer containing tetrachlorophosphonium groups was first washed in toluene to remove excess PCl_3 and was then esterified by reaction with ethanol in the presence of pyridine and toluene to form the mixed ester resin as shown in Scheme 3 of Figure 27. The quench solution consisted of equimolar amounts of ethanol and pyridine (1.12 mole/10 g polymer) and 20 wt% toluene. The solvolysis reaction was carried out by dropwise addition of the quench solution to the intermediate polymer over a period of 2-3 h. To control the temperature of the exothermic solvolysis reaction, the addition was carried out at 0-5 °C in an ice bath. A rapid addition of the quench solution led to a buildup of heat from the exothermic solvolysis reaction. This allowed some of the liberated HCl to react with the ethoxy groups to produce monoacid or diacid groups on the resin and ethyl chloride. Therefore, careful control of the reaction temperature was critical to achieve high levels of esterification. During the quench reaction, a large amount of pyridinium hydrochloride salt was formed. In this and all subsequent esterification reactions, the quench solution was removed after stirring with the resin for one hour and a fresh quench solution was added and allowed to stir overnight. This procedure was carried out to remove pyridinium hydrochloride salt which was formed in the first quench reaction and to

ensure a sufficient amount of ethanol was added to react with the resin. To remove any pyridinium hydrochloride and remaining catalyst from the resin pores, the resin was washed with aqueous ethanol, 0.01 M NaOH, and water. The mixed ester resins synthesized in this manner (DQ-02-152A,B,C,D) were characterized for their total phosphorus and chlorine content by elemental analysis and for their total acidity before and after ester hydrolysis (Table 12). The phosphorus results indicate that lower levels of functionalization were obtained using 0.77 mole $AlCl_3$ for both polymer supports. The chlorine content suggests that practically all of the benzyl chloride groups were substituted with phosphorus when 1.2 mole $AlCl_3$ was used. Slightly higher levels of phosphorylation were achieved for both levels of catalyst using macroreticular polymers. Unreliable results were obtained in the NaOH analysis of these resins, most likely due to catalyst remaining in the resin pores. The formation of a precipitate of aluminum hydroxide during the titration consumed additional NaOH in the neutralization reaction and resulted in the erroneously high and scattered tot(OH) values reported in Table 12. Apparently, the 0.01M NaOH wash was not of sufficient strength to remove the catalyst from the resin matrix. Hydrolysis of the ester groups was carried out by refluxing the resin in concentrated HCl for 16 h. After complete conditioning of the resin, its total acidity was determined; comparison of the ester resin acidity to that of the completely hydrolyzed resin quantified the degree of esterification. The $tot(OH)_{hyd}$ results from Table 12 indicate that the hydrolysis reaction did not proceed completely to the formation of diacid groups. In fact, the close agreement between the phosphorus

Table 12

Capacities of 2% and 5% Cross-Linked Mixed Ester Resins as a Function of Catalyst Level

Resin Code	Starting Copolymer	$AlCl_3$ level[a]	Capacity (mequiv/g) tot(P)	tot(Cl)	tot(OH)[b]	$tot(OH)_{hyd}$[d]
DQ-02-152A	2% gel	0.77	2.70	1.91	1.82/3.43[c]	2.26
DQ-02-152B	2% gel	1.20	4.28	0.71	3.14/4.64	4.84
DQ-02-152C	5% MR	0.77	3.06	1.59	2.33/3.95	2.92
DQ-02-152D	5% MR	1.20	4.60	0.32	5.15	5.00

[a] Moles of $AlCl_3$ per mole of $-CH_2Cl$ groups.
[b] Results unreliable due to $Al(OH)_3$ formation during analysis.
[c] Repeat run after washing resin in 95% ethanol.
[d] Tot(OH) determined after ester hydrolysis in HCl.

capacities and the tot$(OH)_{hyd}$ values suggests that hydrolysis of the diester groups occurred only to form monoester groups.

In the following set of esterification reactions, 5% cross-linked MR poly(VBC) beads were functionalized with 1.2 mole $AlCl_3$ at 76 °C to form fully phosphorylated resins and with 0.77 mole $AlCl_3$ at 40 °C to give partially functionalized polymers containing unreacted benzyl chloride groups. A 1M NaOH wash was used in order to completely remove the catalyst from the resin matrix. The esterification reaction was accomplished by quenching the intermediate phosphorylated resins with solutions containing equal amounts of ethanol and pyridine (0.70 mole/10 g polymer) and 50 wt% toluene. Following their synthesis, the mixed ester resins were washed in the following manner: 95% ethanol (four times, 15 min each); 50% ethanol (eight times, five min each); water (four times, five min each); 4 wt% NaOH (two times, 15 min each); water (seven times, five min each); 4 wt% HCl (two times, 15 min each, in ice bath); water (until neutral). Because ester stability in acid and base solutions had not yet been investigated, minimal contact of the resin with these solutions was desired. The characterization results for these resins (DQ-02-195A,B) are summarized in Table 13. The low tot(OH) values for these ester resins indicate that washing in 1M NaOH and HCl did not lead to hydrolysis of the ester groups. Additionally, no aluminum hydroxide precipitate was formed during the titration with NaOH. The results from Table 13 also show that a higher level of functionalization was achieved using 1.2 mole $AlCl_3$ at 76 °C; a lower degree of esterification, however, was obtained with this resin. Evidently, a less exothermic quench reaction can be carried out on the

Table 13

Capacities of 5% Cross-Linked MR Mixed Ester Resins as a Function of Catalyst Level, Temperature and Base Used in Quench

Resin Code	Catalyst Level[a]	Temp (°C)	Base Used	Capacity (mequiv/g) tot(P)	tot(Cl)	tot(OH)	$tot(OH)_{hyd}$	% ester[b]
DQ-02-195A	1.2	76	Pyr[c]	3.51	0.49	1.70	7.79	75.8
DQ-02-195B	0.77	40	Pyr	2.41	0.81	0.65	3.38	86.5
DQ-02-207A	0.77	40	Pyr	1.85	0.66	0.72	3.53	80.5
DQ-02-207A	0.77	40	DMA[d]	2.00	0.56	0.92	4.07	77.0

[a] Moles $AlCl_3$ per mole $-CH_2Cl$ groups.
[b] % esterification = [2tot(P) - tot(OH)/2tot(P)][100%]
[c] Pyr = Pyridine.
[d] DMA = *N*,*N*-dimethyl aniline.

partially substituted resin leading to a higher level of esterification. As with the previous synthesis, hydrolysis of the ester groups on resin DQ-02-195B in refluxing concentrated HCl was not complete as indicated by the tot$(OH)_{hyd}$ results in Table 13.

From Table 13 it can be seen that the chlorine content for the resin functionalized under mild conditions was much lower than expected. As shown in the reactions below, the loss of chlorine without a concomitant increase in phosphorus capacity may be explained by $AlCl_3$ catalyzed reaction of the benzyl chloride group with ethanol to form poly(benzyl ethyl ether), with water to form poly(benzyl alcohol) groups or with neighboring aromatic rings to form methylene bridges between polymer chains. Model studies were carried out on small molecule analogues by reacting benzyl chloride with ethanol and pyridine at room temperature and 55 °C for 17 h. The results of these reactions were inconclusive for the formation of benzyl ethyl ether or benzyl alcohol; however, $AlCl_3$ catalyst should have been added to the reaction to more accurately model the resin reaction. To test for benzyl alcohol formation, a mixed ester resin was treated with PCl_5 in order to rechlorinate both the benzyl alcohol and phosphonate ester groups. Because no $AlCl_3$ catalyst was present in the resin at this point, ethanolysis should not result in formation of benzyl alcohol and an increase in the chlorine content of the resin should be observed. In fact, no increase in chlorine capacity was observed after this series of reactions suggesting that benzyl alcohol groups were not originally present on the polymer. The most likely cause of chlorine loss is through methylene bridge formation. This reaction was found to occur

during the chloromethylation of polystyrene using chloromethyl methyl ether and a catalyst of zinc, stannous, or aluminum chloride.[90] Cross-linking on the resin could readily occur before the solvolysis reaction while the partially phosphorylated polymer is being washed in toluene to remove unreacted PCl_3.

In order to determine the effect of the base used in the quench solution on the level of esterification, mixed ester resins were synthesized at 40 °C with 0.77 mole $AlCl_3$ using *N*,*N*-dimethyl aniline and pyridine in the quench solutions (resins DQ-02-207A,B). The two bases are of similar strength (pK_b of pyridine = 8.75, pK_b *N*,*N*- dimethyl aniline = 8.85)[91], but *N*,*N*-dimethyl aniline is a more sterically hindered base than pyridine. The results presented in Table 13 for the two resins show that the same levels of esterification and chlorine content were obtained regardless of the base used.

A study of the solvolysis reaction was carried out by functionalization of a 5% cross-linked MR VBC polymer with 1.2 mole $AlCl_3$ at 76 °C to yield the DQ-02-165 series mixed esters. The solvolytic conditions and characterization results for these resins are summarized in Table 14. Ethanol to pyridine molar ratios of 1:1 and 1:2 were used to synthesize resins DQ-02-165A and DQ-02-165B, respectively. One mole of ethanol was used for every 10 g of starting polymer. The excess amount of pyridine in the quench solution was not found to influence the level of esterification as evidenced by the results in Table 14. Resin DQ-02-165D was prepared by rapidly quenching the phosphorylated intermediate into a cooled solution of ethanol, pyridine, and toluene rather than in a dropwise manner as for DQ-02-165A.

Table 14

Solvolysis Reaction Study on Mixed Ester Resins[a]

Resin Code	Quench Solution	NaOH Wash	Capacity (mequiv/g) tot(P)	tot(Cl)	tot(OH)	$tot(OH)_{hyd}$	% ester
DQ-02-165A	1:1 EtOH/Pyr[c]	0.1M	3.41	0.52	2.34[d]	6.54	65.7
DQ-02-165B	1:2 EtOH/Pyr	0.1M	3.47	0.75	1.99[d]	6.87	71.3
DQ-02-165C	1:1 EtOH/Pyr	1.0M	4.04	0.52	1.15	6.91	85.8
DQ-02-165D	1:1 EtOH/Pyr[e]	0.1M	3.47	0.49	2.34[d]	6.72	66.3

[a] 5% cross-linked MR resins; synthesized with 1.2 moles $AlCl_3$ at 76 °C.
[b] All quench solutions also contained 50 wt% toluene.
[c] 1 mole ethanol(pyridine)/10 g polymer.
[d] Results unreliable due to $Al(OH)_3$ formation during analysis.
[e] 2 moles ethanol(pyridine)/10 g polymer.

Comparison of the two resins shows that the same results were obtained regardless of the quench method. Apparently, no buildup of heat occurred in the rapidly quenched reaction to cause an increase in the acid capacity. However, the slow quench technique is preferred for future syntheses because a rapid solvolysis may result in fracturing of the resin. In order to further study the effect of the NaOH wash on the measured acid capacity, resin DQ-02-165C was washed with 1M NaOH in comparison to DQ-02-165A which was washed with 0.10 M NaOH. A lower acid capacity was obtained for resin C, and no aluminum hydroxide precipitate was observed during the titration. None of this series of resins was neutralized with HCl after the NaOH wash; therefore, the acid capacities reported in Table 14 may be erroneously low. The ester hydrolysis was carried out on these resins as previously described. For this series of resins, the hydrolysis of the ester groups appears to be complete.

In order to determine the effect of toluene and pyridine in the quench solution on the degree of esterification, the DQ-02-224 series of mixed ester resins was synthesized: resin A was quenched in ethanol alone, resin B in a 1:1 molar ratio of ethanol and pyridine, and resin C in a 1:1 molar ratio of ethanol and pyridine in 50 wt% toluene. The results of this study are shown in Table 15. The % esterification for DQ-02-224A was significantly lower than for the two resins prepared with pyridine. The addition of toluene to the quench solution had no effect on the degree of esterification achieved (cf DQ-02-224B and DQ-02-224C). However, toluene was important in maintaining fluidity in the reaction, especially when large amounts of pyridinium hydrochloride were formed.

Table 15

Effect of Toluene and Pyridine in Quench Solution in the Synthesis of Mixed Ester Resins[a]

Resin Code	Quench Conditions[b]	Capacity (mequiv/g)				% ester
		tot(P)	tot(Cl)	tot(OH)	$tot(OH)_{hyd}$	
DQ-02-224A	EtOH	3.47	0.39	2.97	8.27	57.2
DQ-02-224B	1:1 EtOH/Pyr	3.36	0.40	2.12	7.33	68.5
DQ-02-224C	1:1 EtOH/Pyr/ 50 wt% Toluene	3.57	0.47	2.33	8.26	8.26

[a] 5% cross-linked MR resins; synthesized with 1.2 mole $AlCl_3$ at 76 °C.

[b] 0.7 mole ethanol(pyridine)/10 g polymer.

The production of HCl from the solvolysis reaction may lead to lower levels of esterification by its reaction with ethoxy groups to yield mono- and diacid ligands. Additionally, the formation of pyridinium hydrochloride salt greatly reduced the fluidity of the reaction. In an attempt to circumvent these problems caused by HCl production, the tetrachlorophosphonium intermediate was quenched in sodium ethoxide rather than ethanol. Functionalization of 5% cross-linked MR poly(VBC) beads was carried out using 1.2 mole $AlCl_3$ at 76 °C. After washing in toluene to remove unreacted PCl_3, resin A was quenched in a *tert*-butyl alcohol solution of sodium ethoxide and resin B was quenched in a solution of sodium ethoxide in equimolar amounts of ethanol and pyridine. The total acidity of the two resins was measured to be 4.98 mequiv/g and 2.53 mequiv/g, respectively. These results indicate that solvolysis in sodium ethoxide did not lead to high levels of esterification. The ester groups formed in resin B probably resulted from reaction with ethanol, not sodium ethoxide.

Characterization of the intermediates in the esterification reaction was carried out in an attempt to verify the proposed reaction scheme (Scheme 3, Figure 27, page 75). Samples of the resins were removed and analyzed at each step in the synthesis as shown below for the DQ-02-180 series of resins:

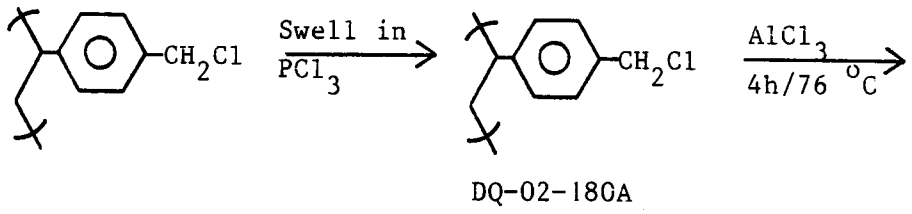

DQ-02-180A

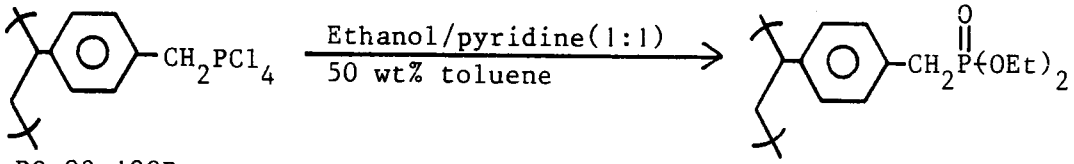

DQ-02-180B DQ-02-180C

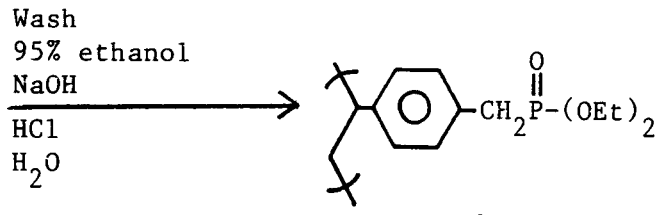

DQ-02-180D

Intermediates DQ-02-180A and DQ-02-180B were washed and gently heated in toluene in order to remove excess PCl_3. After quenching in a solution of ethanol, pyridine, and toluene, intermediate DQ-02-180C was removed and washed in toluene to remove pyridinium hydrochloride salt from the resin pores. The final product, resin DQ-02-180D, was obtained after washing in aqueous ethanol, 4 wt% NaOH, 4 wt% HCl and water. The resins were dried under vacuum at room temperature and then for 1 h at 55 °C before analysis. The characterization results for this series of resins are presented in Table 16. Also included in this table are the theoretical phosphorus and chlorine capacities for the predicted products assuming 100% reaction at each step. For intermediate

Table 16

Characterization of Intermediates
in Mixed Ester Synthesis[a]

Resin Code	Observed capacity[b]			theoretical capacity[b,c]	
	tot(P)	tot(Cl)	tot(OH)	tot(P)	tot(Cl)
DQ-02-180A	6.74	2.93		0.0	5.96
DQ-02-180B	2.15	5.02		3.14	12.56
DQ-02-180C	3.55	1.45		3.58	0.0
DQ-02-180D	3.44	0.49	1.21	3.58	0.0
DQ-02-230A	1.33	5.44		0.0	5.96
DQ-02-230B	2.14	5.99		3.14	12.56
DQ-02-230C	3.14	3.24		3.58	0.0
DQ-02-230D	3.49	0.72	2.19	3.58	0.0
DQ-02-237A	0.78	5.84		0.0	5.96
DQ-02-237B	2.31	5.21		3.14	12.56
DQ-02-237C	3.28	2.04		3.58	0.0
DQ-02-237D	3.19	1.74		3.58	0.0
DQ-02-237E	3.41	0.51	1.37	3.58	0.0

[a] Synthesis Conditions : 5% cross-linked MR poly(VBC) support functionalized with PCl_3 and 1.2 moles $AlCl_3$. Quenched in 1:1 molar ratio ethanol/pyridine in 50 wt% toluene.

[b] units of mequiv/g.

[c] Assuming 100% reaction at each step.

DQ-02-180A, the phosphorus capacity was much higher than the predicted value, whereas the chlorine capacity was much lower than expected. The elevated phosphorus value may be due to phosphoric acid from hydrolysis of PCl_3 remaining in the resin even after washing in toluene; the low chlorine capacity may the result of incomplete sample drying which would lead to inaccurate weights. Intermediate DQ-02-180B had phosphorus and chlorine capacities which were both much lower than the theoretical values. The decreased chlorine content may be the result of hydrolysis of the reactive tetrachlorophosphonium groups upon contact with traces of moisture. Due to the unreliable phosphorus and chlorine capacities obtained on DQ-02-180A and DQ-02-180B, the experiment described above was repeated using a more thorough procedure for drying the resin. In the DQ-02-230 series, the resins were dried under vacuum for 8 h at 60 °C. Examination of the results presented in Table 16 shows that better agreement of the observed and expected capacities was obtained for resin DQ-02-230A than for DQ-02-180A. The results for DQ-02-230B, however, were very similar to those obtained for DQ-02-180B.

Although intermediates DQ-02-180C and DQ-02-230C should have no chlorine remaining after the ethanolysis reaction, they were found to have chlorine capacities of 1.45 mequiv/g and 3.24 mequiv/g, respectively. The chlorine content of these resins may be attributed to the formation of the following phosphonyl chloride resulting from the incomplete ethanolysis of the $-CH_2PCl_4$ intermediate:

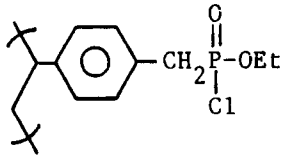

This group may be stable until contact with water, leading to the production of a monoethyl ester.

To determine if the phosphonyl chloride group was an intermediate in the esterification reaction, another series of resins was synthesized in which the quench reaction was heated to 60 °C in an attempt to drive the ethanolysis reaction to completion. The DQ-02-237 series of resins was prepared by the following reaction sequence:

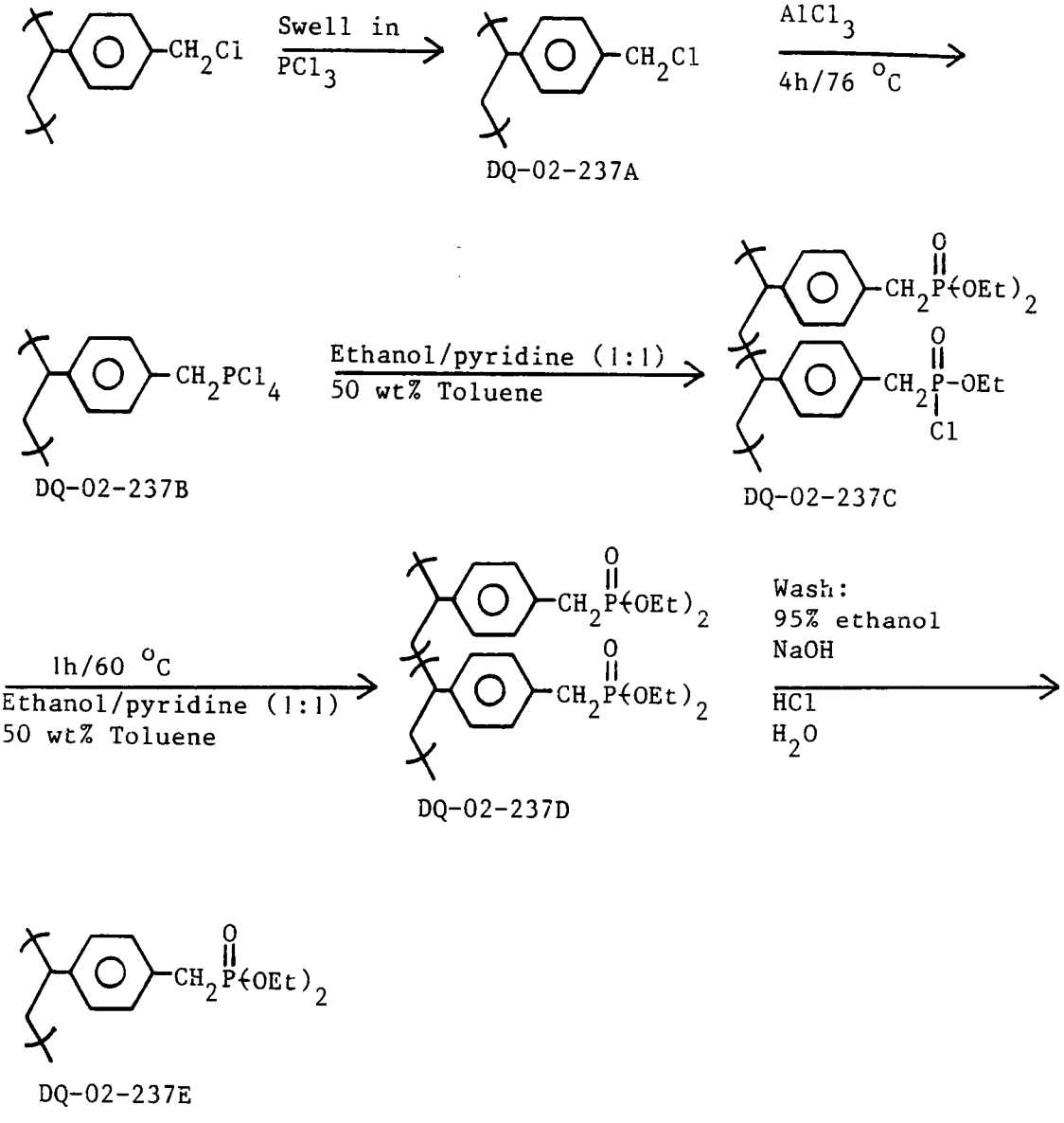

The resins were washed in toluene and diethyl ether and then dried under vacuum at room temperature. The capacities for DQ-02-237C and DQ-02-237D from Table 16 show no loss of chlorine after heating to 60 °C. These results indicate that the phosphonyl chloride was not an intermediate in the esterification reaction. A possible explanation for the presence of chlorine on these resins is due to pyridinium hydrochloride salt remaining within the resin pores until the final washing with NaOH.

The influence of polymer cross-linking and macroporosity on the degree of esterification was examined in the synthesis of mixed ester resins from 2% cross-linked gel and 5% cross-linked MR poly(VBC) supports. The resins DQ-02-245A and DQ-02-245B, respectively, were functionalized using PCl_3 and 1.2 mole $AlCl_3$ catalyst and were quenched in a solution of ethanol and pyridine in a 1:1 molar ratio (0.70 mole/10 g polymer) and 50 wt% toluene. The table below presents the characterization results for these resins:

Characterization of 2 and 5% Cross-Linked Mixed Esters

Resin	Type	Capacity (mequiv/g)			% Ester.
		tot(OH)	tot(P)	tot(Cl)	
DQ-02-245A	2% gel	1.90	3.68	0.47	74.2
DQ-02-245B	5% MR	1.12	2.71	1.17	79.3

The degrees of esterification achieved for the two resins were very similar; the phosphorus capacity for the MR resin, however, was approximately 1 mequiv/g lower than for the gel resin without an accompanying increase in chlorine capacity. Although the phosphorus

capacity was slightly lower for this resin than those of other 5% cross-linked MR resins prepared under the same conditions (DQ-02-180D, DQ-02-230D, and DQ-02-237E; see Table 16), the results for the other 5% cross-linked MR mixed ester resins were in close agreement with those for the 2% cross-linked gel resin. This demonstrates that good reagent accessibility into the higher cross-linked polymer was achieved in both the functionalization and esterification reactions.

The effect of the degree of esterification on the extraction of Hg^{2+} from $Hg(NO_3)_2$ solution was studied using mixed ester resins DQ-02-180D (82.4% esterification) and DQ-02-165A (65.7% esterification) at R_i levels of 1.0 and 2.0 (based on the phosphorus content of the resin). The results of this study are summarized in Table 17. A higher % Hg^{2+} loading was obtained for the resin having a lower degree of esterification. Apparently, the acidic monoester and diacid groups have a higher affinity for Hg^{2+} than does the diester group. The results of this study suggest that control of the resin functionality in mixed ester resins can be used to achieve different metal ion selectivities.

With the goal of preparing mixed ester resins of varying diester/monoester/diacid ratios, the solvolysis reaction was carried out by the addition of ethanol/water solutions in various mole ratios. Mixed ester resins were synthesized by solvolysis in solutions containing 0.70 mole pyridine (per 10 g polymer) and a total of 0.70 mole of ethanol and water in the following molar ratios of ethanol to water: 8:1, 7:1, 4:1, 2:1, 1:2, and 1:0. The amount of diacid, monoester and diester groups on each mixed ester resin was quantified through a titration curve. The titration curve for mixed ester resin

Table 17

Hg^{2+} Extraction Using Mixed Ester Resins

Resin	% Esterification	R_i[a]	% Loading
DQ-02-180A	82.4	1.0	14.5
DQ-02-180A	82.4	2.0	15.0
DQ-02-165A	65.7	1.0	30.6
DQ-02-165A	65.7	2.0	53.2

[a] Based on phosphorus capacity.

DQ-02-245A is represented in Figure 28 and shows one endpoint corresponding to a capacity of diacid and monoester groups of 1.03 mequiv/g. The difference in pK_a values for the two acidic groups is too small for two distinct endpoints to be observed. The percentage of each group on the resin is obtained in the following manner. The amount of diacid groups is given by the difference of the total acid capacity and the acid capacity measured at the breakpoint of the titration curve. The monoester content is then obtained by the difference of the acid capacity at the breakpoint and the diacid capacity. The amount of diester groups is given by the difference of the total phosphorus capacity and the breakpoint acid capacity. The calculation of the percentage of each functional group on the mixed ester resin DQ-02-245A (tot(OH) = 1.90 mequiv/g, tot(P) = 3.68 mequiv/g, acid capacity at breakpoint = 1.03 mequiv/g) is illustrated below:

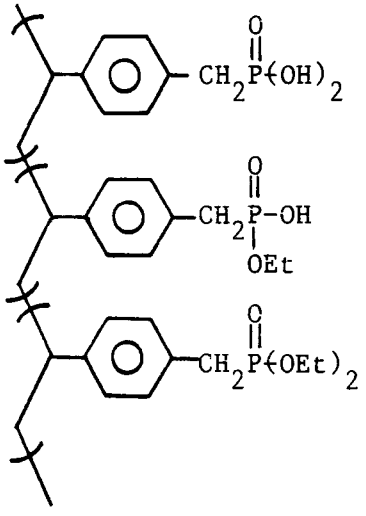

1.90 - 1.03 = 0.87 mequiv/g ; 23.6 %

1.03 - 0.87 = 0.16 mequiv/g ; 4.4%

3.68 - 1.03 = 2.65 mequiv/g ; 72.0%

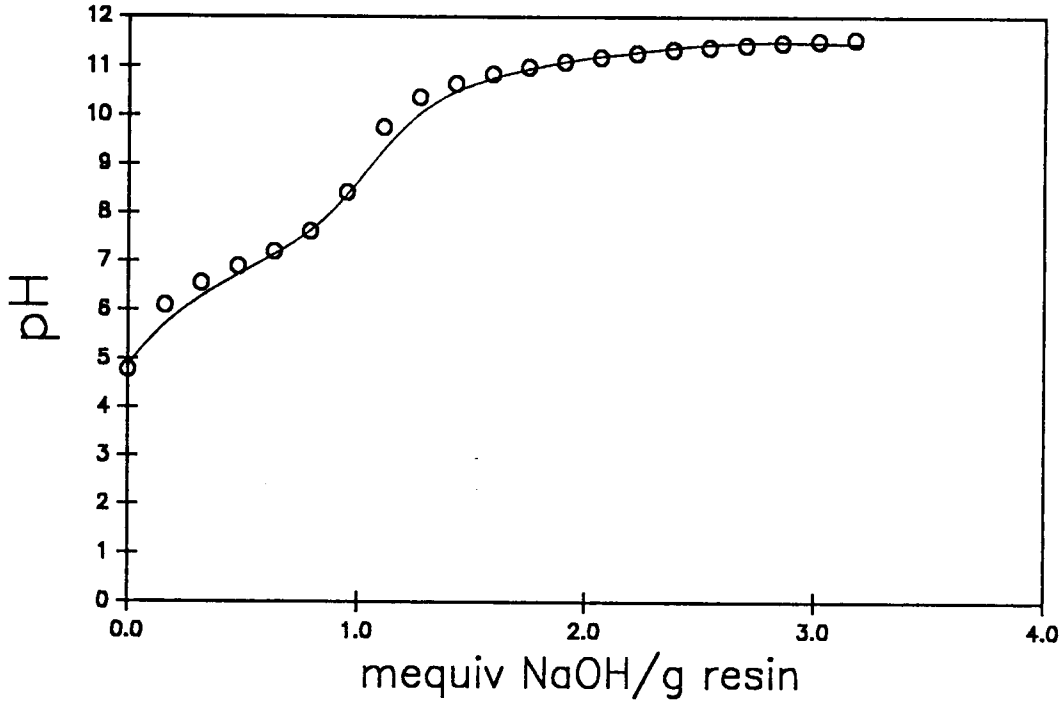

Figure 28. Titration curve for mixed ester resin.

Table 18 summarizes the properties of the mixed ester resins quenched in various ethanol/water solutions. The scattered results obtained for replicate syntheses (e.g. 8:1 and 4:1 ethanol/water ratios) indicate that a controlled solvolysis reaction leading to a specific ratio of diester/monoester/diacid groups is difficult to achieve. A general trend of increased diacid and monoester groups over diester groups, however, was observed as the amount of water in the quench solution was increased.

Table 18 also reports the results of a study of the effect of solvolysis reaction temperature on the degree of esterification. The solvolysis reactions were carried out at lower temperatures using a dry ice/acetone bath in an attempt to obtain higher levels of esterification. For comparison, the quench reaction was also carried out in the usual manner in an ice bath. Examination of the results in Table 18 shows that higher levels of esterification did not result from the lower temperature solvolysis reaction.

The preparation of a large batch (100 g) of mixed ester resin was attempted. This synthesis represents a five-fold scale-up of previous esterification reactions and was carried out by solvolysis of the intermediate phosphorylated polymer in a 4:1 molar ratio of ethanol to water. A mixed ester resin having a tot(OH) = 2.31 mequiv/g and tot(P) = 3.80 mequiv/g (69.65% esterification) was obtained from this reaction. Problems were encountered, however, in this large-scale synthesis. First, because the temperature of the highly exothermic solvolysis reaction was difficult to control for the large scale reaction, many of the beads fractured during the quench. Second,

Table 18

Characterization of Mixed Ester Resins
Quenched in Ethanol/Water [a,b]

Resin Code	Ethanol/H_2O	tot(P) (mequiv/g)	tot(OH) (mequiv/g)	Percentage			
				total ester.	diester	monoester	diacid
DQ-02-259A	8:1	3.49	1.06	84.7	76.8	16.0	7.2
DQ-03-197C	8:1	2.69	1.96	63.6	58.4	10.4	31.2
DQ-03-122A[c]	8:1	3.26	2.94	54.9			
DQ-02-284C	7:1	3.65	3.23	55.7	30.1	51.2	18.6
DQ-02-259B	4:1	3.51	4.56	35.0	15.5	39.0	45.4
DQ-03-197B	4:1	3.22	2.30	64.3	50.3	28.0	21.7
DQ-02-259C	2:1	3.82	5.71	25.3	6.7	37.2	56.2
DQ-02-284B	2:1	3.85	4.78	37.9			
DQ-03-002C	2:1	3.98	4.97	37.6	15.3	44.5	40.2
DQ-03-197A	2:1	3.84	6.24	18.8	3.4	30.7	65.9
DQ-03-002B	1:2	3.95	5.75	27.2	12.3	29.9	57.9
DQ-02-284A	1:1	3.81	4.25	44.2			
DQ-03-002A[d]	0:1	3.87	6.25				100.0
DQ-02-284D[e]	1:0	3.43	1.11	83.8	67.6	32.4	0.0
DQ-02-245A	1:0	3.68	1.90	74.2	72.0	4.4	23.6
DQ-03-002D	1:0	3.56	0.65	90.9	81.7	18.3	0.0

[a] All 2% cross-linked gel copolymers unless noted otherwise.
[b] All resins were functionalized with PCl_3 using 1.2 mole $AlCl_3$.
[c] 5% cross-linked MR copolymer used.
[d] Quenched in dry ice/acetone bath.
[e] Quenched in ice bath.

stirring of the reaction was difficult due to the large amount of pyridinium hydrochloride salt formed. Because of the poor mixing, the solvolysis reaction was not uniform for all of the beads. Thus, beads of different compositions were produced within the same batch of resin, as evidenced by variations in bead colors.

The problem of mixed colors of beads was also encountered in the synthesis of a 20 g batch of mixed ester resins using a 4:1 molar ratio of ethanol to water in the quench solution. After the beads were allowed to separate into two layers, the top fraction of smaller, yellow beads (DQ-04-072B1) was removed from the bottom layer of larger, red beads (DQ-04-072B2). The two fractions were analyzed for phosphorus capacity (measured in mequiv/g), distribution of functional groups, and % Ni^{2+} loading. These results are summarized below:

Characterization of Different Bead Size Fractions of Mixed Ester Resins

Resin	tot(P)	% diester	% monoester	% diacid	%Ni^{2+} loading
DQ-04-072B1	3.79	32.4	54.1	13.5	8.6
DQ-02-072B2	3.65	6.6	64.7	28.8	9.9

The phosphorus capacities were the same for the two fractions, indicating that homogeneous phosphorylation of the beads was achieved. Although nearly the same % Ni^{2+} loadings were obtained, the functional group distribution varied greatly for the two fractions. These results suggest a difference in reactivity with ethanol and water based on bead size; apparently, the smaller beads were more reactive with ethanol leading to a higher percentage of diester groups while the larger beads

were more water reactive, producing mixed ester resins with a higher diacid and monoester content. This problem may be obviated by the use of smaller polymer beads. The increased rate of diffusion of the quench solution into the polymer matrix should lead to a more uniform solvolysis reaction and produce a homogeneous batch of mixed ester resins.

Esterification of the diacid and monoester groups on the mixed ester resin was attempted in order to increase the resin's diester content. In the first attempt at esterification, mixed ester resin DQ-02-165D (tot(OH) = 2.34 mequiv/g) was washed with absolute ethanol and was then refluxed in ethanol in the presence of sulfuric acid catalyst. The acid capacity of this resin was found to be 2.92 mequiv/g, indicating that no further esterification of the resin was achieved. Although the resin was rinsed with absolute ethanol to dehydrate it, enough water may have remained in the pores to prevent esterification. The second attempt at esterification involved azeotropic removal of water to drive the esterification reaction to completion. The mixed ester resin DQ-02-284A (tot(OH) = 4.25 mequiv/g) was first azeotroped in toluene to completely remove all water from the resin pores. The esterification was carried out by azeotroping the resin in toluene for 136 h in the presence of ethanol and methanesulfonic acid catalyst. The water produced by the reaction was collected in a Dean-Stark trap and measured the extent of the esterification reaction. The resin produced from this reaction (tot(OH) = 4.25 mequiv/g) showed no increase in esterification over the original mixed ester resin. Most likely the resin was not completely dried by azeotroping in toluene and the water

formed during the reaction was actually from the resin pores rather than a product of the esterification reaction.

Synthesis of the Phosphonate Monoester Resin

A controlled heatup of the quench solution to 89 °C led to the formation of a resin which was predominately composed of monoester benzylethyl phosphonic acid groups. The monoester groups were formed by the attack of HCl liberated from the esterification reaction on the ethoxy group of the diester. This resulted in the production of monoester groups and ethyl chloride. The synthesis of the phosphonate monoester resin is outlined in Figure 29.

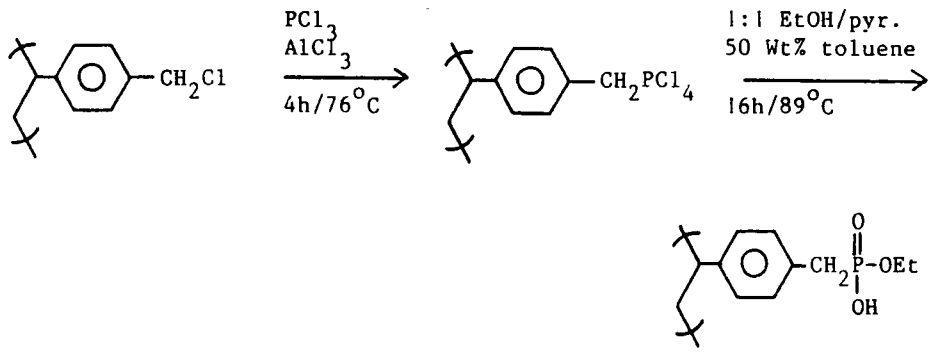

Figure 29. Synthesis of phosphonate monoester resin.

The copolymer was first functionalized with PCl_3 and $AlCl_3$ to yield the phosphorylated intermediate. After removing the excess PCl_3 and washing the resin in toluene, a quench solution consisting of a 1:1 molar ratio of ethanol and pyridine (0.70 mole/10 g polymer) was added at 0-5 °C to the phosphorylated intermediate to produce a resin consisting primarily of diester groups. After the quench solution

stirred with the resin for 1 h, it was removed and a fresh solution was added. This process allowed for the removal of some of the pyridinium hydrochloride salt formed in the esterification thus improving the reaction fluidity. The second quench solution was heated to reflux (89 °C) for 16 h to produce monoester groups. The resulting monoester resin was washed with aqueous ethanol (95 and 50%) followed by complete conditioning with successive 1 h elutions of 1 L of water, 4 wt% NaOH, water, 4 wt% HCl, and water.

The characterization results for monoester resins prepared from 2% cross-linked gel poly(VBC) beads are presented in Table 19. The resins were characterized in terms of their total acidity (measured by the excess NaOH procedure), total phosphorus (measured by elemental analysis), and the distribution of functional groups (measured by titration curve). The results show that each monoester resin contained greater than 75% monoester groups. The diester capacity varied from 7 to 22% and the diacid capacity ranged from 0 to 9%. Comparison of the distribution of functional groups for the monoester resins to those for mixed ester resins DQ-02-284D, DQ-02-245A and DQ-03-002A (Table 18) shows that a much higher percentage of monoester groups was obtained when the resin was refluxed in the second quench solution.

The stability of the monoester resin to the conditioning process was investigated. The results for a resin washed in a batch process were compared to those for a resin washed using a continuous conditioning process. Monoester resin DQ-02-259D was washed with 95% ethanol, 50% ethanol, water, 4 wt% NaOH for 15 min, water, 4 wt% HCl for 15 min (in ice), and water until a neutral pH was obtained. In

Table 19

Characterization of Phosphonate Monoester Resins[a]

Resin Code	capacity (mequiv/g) tot(OH)	tot(P)	% monoester	diester	diacid
DQ-02-259D	3.42	3.44	82.6	17.4	0.0
DQ-03-197D	2.91	3.42	81.0	17.0	2.0
DQ-04-072A[b]	3.77	3.71	83.5	7.4	9.0
DQ-04-173[b]	3.30	3.46	84.4	10.1	5.5
DQ-05-018A	2.94	3.65	75.6	21.9	2.5
DQ-05-018B	2.87	3.84	80.0	20.0	0.0
DQ-05-242B	3.48	3.86	80.8	14.5	4.7
DQ-06-146A	3.60	4.05	81.5	14.8	3.7
DQ-06-146B	3.45	4.00	79.7	17.0	3.3
DQ-07-031A	3.61	4.00	91.7	8.3	0.0
DQ-07-031B	3.91	4.03	81.1	10.9	7.9
Average	3.39	3.77	82.0	14.5	3.5
Stand. Dev.	0.35	0.25	4.0	4.8	3.1

[a] Synthesized from 2% cross-linked gel poly(VBC) beads.
[b] Average results for two different size fractions of beads.

contrast, monoester resin DQ-03-197D was washed with 95 and 50% ethanol and was then conditioned with successive 1 h elutions of 1 L each of water, 4 wt% NaOH, water, 4 wt% HCl, and water. As indicated by the nearly identical characterization results for these two resins in Table 19, the monoester resin was stable to the continuous conditioning process. The ester stability in highly acidic solutions was also determined because the metal ion complexing ability of the monoester resin was carried out using metal solutions in a background of 4 M HNO_3. After monoester resin DQ-05-018B resin was shaken for 17.5 h with a solution of $1X10^{-4}$ N $Hg(NO_3)_2$ in 4 M HNO_3, the resin's acid capacity was measured to be 3.02 mequiv/g. This value closely agreed with the original acidity of 2.87 mequiv/g, demonstrating that the monoester groups were not hydrolyzed in 4 M HNO_3.

A large batch (100 g) synthesis of 2% cross-linked gel monoester resin was attempted (DQ-03-273A). As with the large-scale synthesis of mixed ester resins, the temperature of the exothermic solvolysis reaction was difficult to maintain at 0-5 °C. In addition, the large amounts of pyridinium hydrochloride formed made stirring of the reaction mixture difficult. As a result of these problems, the beads produced by the reaction were fractured and of mixed colors. Additionally, the monoester capacity of the resin was very low (46% monoester, 47.2% diester, 6.8% diacid, tot(OH) = 2.61 mequiv/g, tot(P) = 4.11 mequiv/g) compared to those produced on a 20 g scale. Because of the difficulties encountered in the large-scale synthesis, all future monoester syntheses were carried out using no more than 20 g of polymer.

Even in small scale monoester syntheses, however, the beads can fracture, most likely due to the harsh reflux conditions in the second quench solution. For example, a sample of copolymer beads which were sized with a U.S. Standard Screen Series of sieves to have particle radii ranging from 0.042 to 0.021 cm (-20+40 mesh cut) varied in size from 0.042 cm to 0.0037 cm (-20+200 mesh cut) after the esterification reaction. Additionally, the monoester resin formed was composed of both yellow and orange beads. In general, the amount of orange beads decreased as the particle size decreased. To determine if the variation in bead color corresponded to a difference in chemical composition, the monoester resin was sieved into different size fractions and analyzed. Monoester resin DQ-04-072 was prepared from -20+40 mesh cut polymer beads. After its synthesis, the monoester resin was sieved into mesh cuts of -20+40, -40+60 (0.021-0.013 cm radius) and -60 (<0.013 cm radius). The results of the analysis for the three mesh cuts shown below suggest that the composition of the beads is the same regardless of size. The phosphorus value of 3.67 mequiv/g for all sizes was used in the calculation of the functional group distribution for the -20+40 mesh cut.

Characterization of Different Size Fractions of Monoester Resin

Mesh Cut	Capacity (mequiv/g)		Functional Group Distribution (%)		
	tot(OH)	tot(P)	monoester	diester	diacid
-20+40	3.65		79.8	10.1	10.1
-40+60	3.87	3.75	87.2	4.8	8.0
-60	3.60				
all sizes	3.67	3.67			

The same conclusion can be drawn from the study of monoester DQ-04-173 which was also divided into two size fractions. The beads in fraction A were larger and had a greater amount of red beads than fraction B. The characterization results of the two fractions presented below again indicate resin homogeneity.

Characterization of Two Size Fractions of Monoester Resin

Fraction	tot(OH) (mequiv/g)	% monoester	% diester	% diacid
DQ-04-173A	3.27	88.9	7.9	3.2
DQ-04-173B	3.33	79.9	12.3	7.7

To further verify the uniformity of composition of different sizes of monoester beads, IR spectra were taken of +60 (>0.013 cm radius) and -100+200 (0.0075-0.0037 cm radius) mesh cuts of monoester resin DQ-06-146A. The spectra presented in Figures 30 and 31 indicate no differences between the two size fractions, a further demonstration of monoester resin homogeneity.

In order to investigate the influence of the cross-link level on resin capacity, monoester resins were prepared from 5, 10, and 15% cross-linked gel poly(VBC) beads. In the synthesis of the 5% cross-linked monoester, the solvolysis reaction with ethanol appeared to be slower than for the 2% cross-linked resin. This may occur as a result of slower diffusion of the quench solution into the more tightly cross-linked polymer network. In contrast to the 2% cross-linked resin which showed an increase in temperature shortly after the addition of the quench solution, the reaction temperature of the 5% cross-linked resin

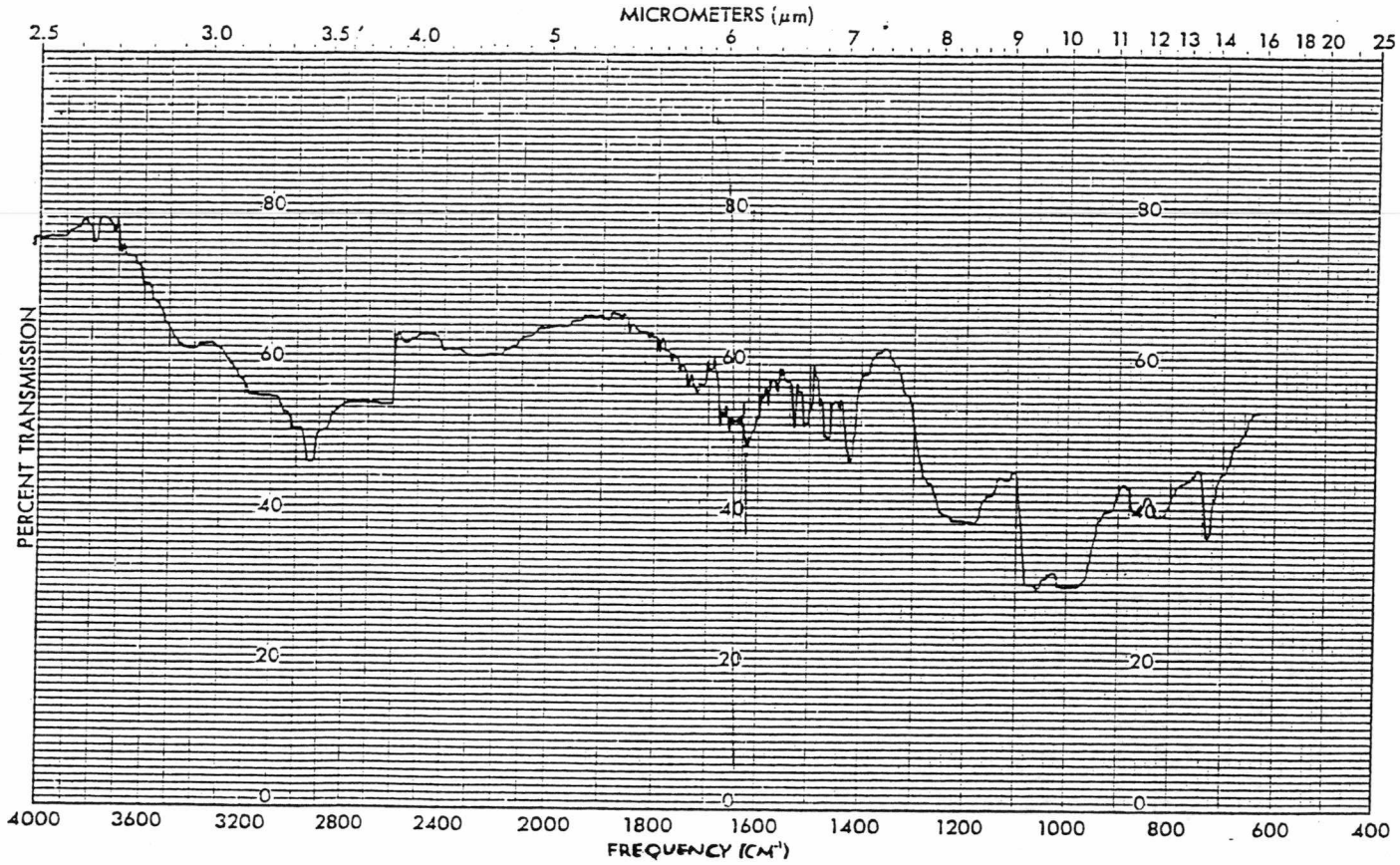

Figure 30. IR spectrum of +60 mesh monoester resin.

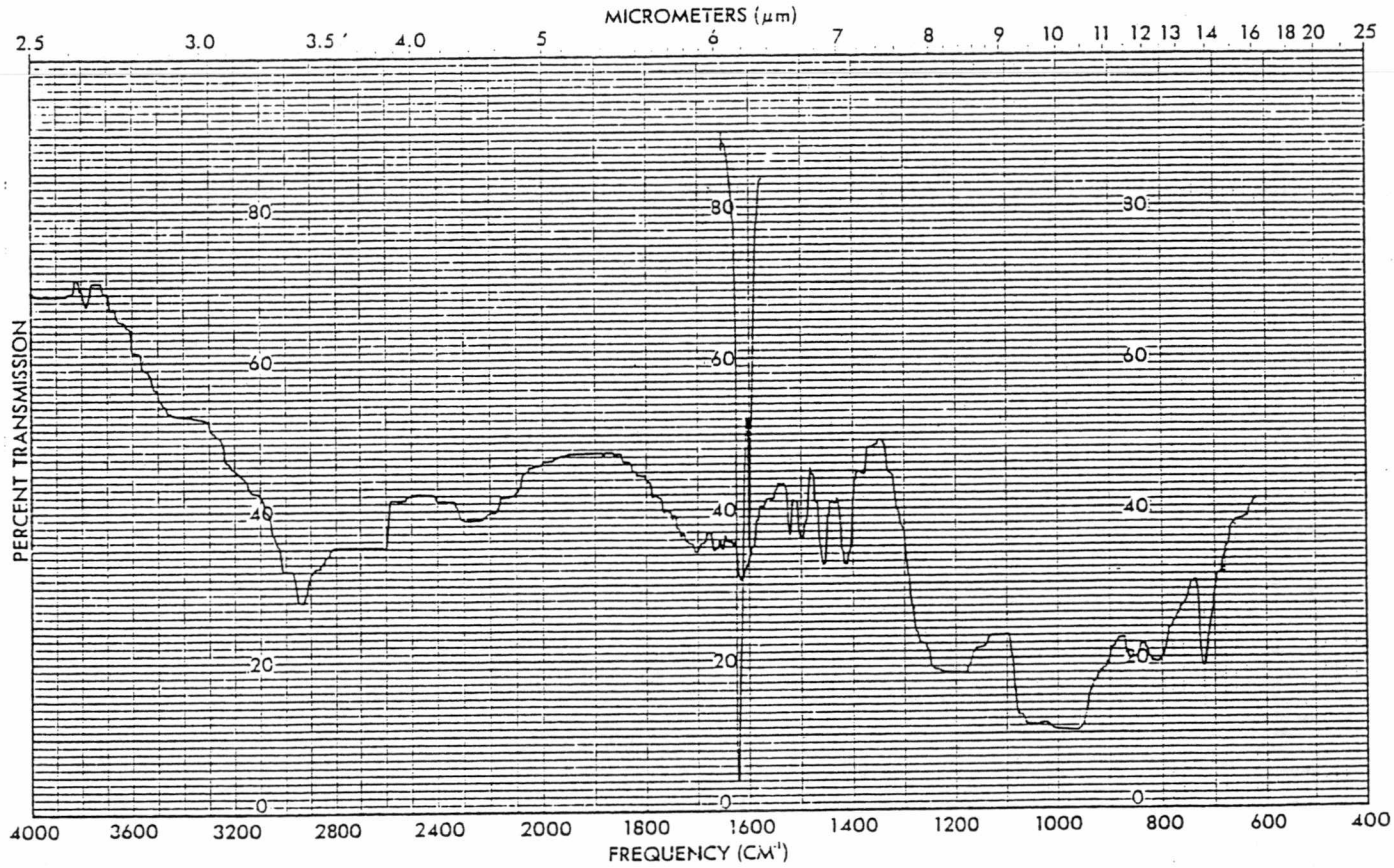

Figure 31. IR spectrum of -100+200 mesh monoester resin.

did not increase until after the entire quench solution had been added and stirred for approximately 30 min. The second quench solution was subsequently added and heated to reflux in order to produce the monoester resin. The resin formed by this reaction (DQ-04-233) was characterized as follows: tot(P) = 3.01 mequiv/g, tot(OH) = 2.63 mequiv/g, % monoester = 80.7, % diester = 16.0 and % diacid = 3.3. Whole beads were not produced by this reaction, however, and the beads were of mixed colors. Assuming 100% substitution of all benzyl chloride groups with phosphorus ligands and the experimental values for the distribution of functional groups, the theoretical phosphorus capacity is calculated to be 3.98 mequiv/g. The experimental result is considerably lower than the theoretical capacity and may be the result of incomplete phosphorylation due to limited PCl_3 accessibility into the tightly cross-linked polymer matrix.

Attempts to prepare both 10 and 15% cross-linked monoester resins also resulted in the production of fractured beads which were non-uniform in color. As with the 5% cross-linked resins, these results indicate that diffusion of the quench solution was limited in the 10 and 15% cross-linked resins. That the solvolysis reaction occurred very slowly or not at all during the addition of the first quench solution was indicated by the fact that no pyridinium hydrochloride was formed and no increase in reaction temperature was observed. The more highly cross-linked resins fractured to a greater extent than the 2% cross-linked ones. Because bead brittleness increases with increasing cross-link level, the 10 and 15% cross-linked resin were more sensitive to the thermal stresses encountered in the highly exothermic ethanolysis

reaction. Although the 15% cross-linked resin was too badly fractured to analyze, the 10% cross-liked resin was found to have a tot(OH) = 2.69 mequiv/g, tot(P) = 2.34 mequiv/g, and an acid capacity at the breakpoint of the titration curve = 2.54 mequiv/g. Because the breakpoint acid capacity was greater than the total phosphorus capacity, the distribution of functional groups could not be calculated for this resin. The theoretical maximum phosphorus capacity of 3.59 mequiv/g, however, can be approximated for this resin by assuming the average functional group distribution of 82% monoester, 14% diester, and 4% diacid from Table 19 (page 103). As with the 5% cross-linked resin, this value was lower than the observed acid capacity, likely due to limited reagent accessibility in the phosphorylation reaction.

The synthesis of a phosphonate monoester resin was carried out using $FeCl_3$ as the Friedel-Crafts functionalization catalyst instead of $AlCl_3$ and without the use of pyridine in the quench solution. The 2% cross-linked gel poly(VBC) copolymer was functionalized with PCl_3 and 0.77 mole $FeCl_3$ per mole of VBC groups at 76 °C for 4 h. The resulting $-CH_2PCl_4$ groups were quenched with ethanol at 0-5 °C. After stirring for 1 h, the first quench solution was removed and a second portion of ethanol was added. The resin was refluxed in ethanol for 17 h and was then conditioned and characterized to have tot(OH) = 3.15 mequiv/g, tot(P) = 2.58 mequiv/g, % monoester = 45.3, % diester = 16.3, and % diacid = 38.4. The fact that a mixed ester resin was formed in this reaction rather than a monoester is best explained by the absence of pyridine in the quench solution. Apparently, pyridine complexes the HCl liberated in the esterification reaction and allows for its attack

on the ethoxy group of the diester groups leading to the formation of the monoester moiety.

An attempt was made to increase the number of monoester groups on the mixed ester resin by heating it in water. A mixed ester resin was heated in water for 30 min at 90 °C and then for 18 h at 60 °C. A titration curve was carried out to detect any scrambling of the ester groups that may have occurred at the elevated temperatures. The titration curve gave an acid capacity at the breakpoint of 2.52 mequiv/g, consistent with the original value for the mixed ester of 3.02 mequiv/g. This result demonstrates that no changes in the functional group distribution occurred upon heating of the resin in water.

Synthesis of Phosphonate Diester Resins

A mild ethanolysis reaction was required to obtain a resin with a high percentage of diester groups. The use of partially functionalized resins ensured a non-exothermic solvolysis reaction. Diester resins were prepared as illustrated in Figure 32 by partial phosphorylation at 40 °C followed by ethanolysis at 0-5 °C in a solution of 0.7 mole ethanol (per 10 g of polymer) and 50 wt% toluene.

Table 20 reports the results of diester synthesis using $AlCl_3$ levels of 0.77 and 1.2 mole per mole of VBC groups. Degrees of esterification greater than 85% were achieved when $AlCl_3$ levels of 0.77 mole were used. Slightly lower levels of esterification were obtained when 1.2 mole $AlCl_3$ was employed and for the large scale (100 g) esterification (DQ-03-273C). In contrast to the mixed ester and

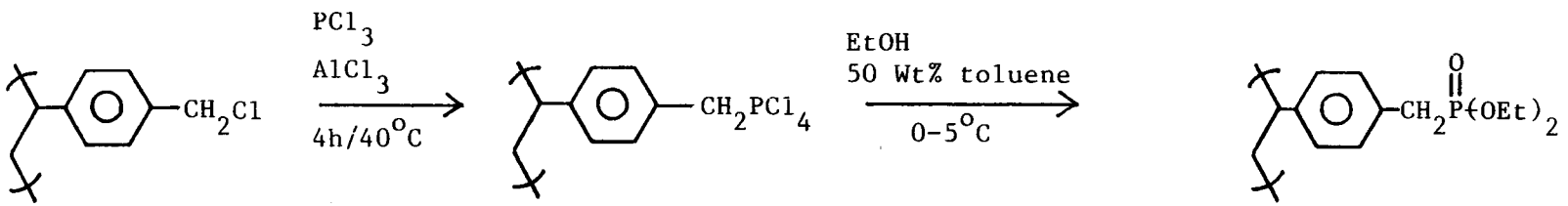

Figure 32. Synthesis of diethyl ester resin.

Table 20

Characterization of Diethyl Ester
Resins Synthesized with $AlCl_3$ at 40 °C[a]

Resin Code	capacity (mequiv/g)			% ester.
	tot(OH)	tot(P)	tot(Cl)	
DQ-03-026B[b]	0.19/0.13[c]	1.88	0.64	94.95
DQ-03-145A	0.81	2.86	f	85.84
DQ-03-145B[d]	1.11	3.54	f	84.32
DQ-03-151	0.41	1.80	f	88.61
DQ-03-173	0.32	1.64	f	90.24
DQ-03-273C[e]	0.68	2.05	f	83.41

[a] Synthesized from 2% cross-linked poly(VBC) beads (20g) at 40 °C with 0.77 mole $AlCl_3$ unless noted otherwise. Quenched in 0.70 mole ethanol(pyridine)/10g polymer and 50 wt% toluene.

[b] 0.59 g/g.

[c] tot(OH) determined using 0.1 M KOH in a solution of 20% water/80% dioxane for increased accessibility into hydrophobic resin.

[d] 1.2 mole $AlCl_3$ used.

[e] 100 g batch.

[f] Not determined.

monoester resins, the diester beads produced from the mild ethanolysis reaction were not fractured and were uniform in color (white).

Because of the hydrophobic nature of the diester resins (% solids > 65%), accessibility of an aqueous NaOH solution into the resin pores may be limited and thus lead to artificially low tot(OH) values. Therefore, the acid capacity was determined using both aqueous 0.1M NaOH and 0.1M KOH in an aqueous solution of 80% dioxane. Use of dioxane solvent should result in greater hydroxide ion accessibility into the polymer matrix. Both aqueous and dioxane acid capacities are given in Table 20 for diester resin DQ-03-026B. The excellent agreement of the two results suggests that aqueous accessibility into the diester resin was not limited.

A loss of chlorine capacity for the diester resin DQ-03-026B is indicated by the results in Table 20. The % yield for the functionalized resin can be quantified through a g/g calculation. The g/g value measures the grams of functional groups and unreacted benzyl chloride per gram of VBC groups available for functionalization. A sample g/g calculation is given below for DQ-03-026B. The diester capacity is given by the difference of the phosphorus capacity and the acid capacity; the acid capacity of the resin is attributed to monoester groups only.

$$\text{g diester/g resin} = (\text{MW diester})(\text{diester capacity})/1000$$

$$= (254.3 \text{ g mol}^{-1})(1.72 \text{ mequiv g}^{-1})/1000 \text{ mequiv mol}^{-1}$$

$$= 0.44 \text{ g/g}$$

$$\text{g monoester/g resin} = (226.2\ \text{g mol}^{-1})(0.16\ \text{mequiv g}^{-1})/1000\ \text{mequiv mol}^{-1}$$
$$= 0.036\ \text{g/g}$$

$$\text{g VBC/g resin} = (152.6\ \text{g mol}^{-1})(0.64\ \text{mequiv g}^{-1})/1000\ \text{mequiv mol}^{-1}$$
$$= 0.098\ \text{g/g}$$

$$\text{total g functional groups/g resin} = 0.57$$

One gram of 2% cross-linked polymer actually contains only 0.964 g VBC groups available for functionalization (DVB contains 44.6% ethylvinylbenzene). Therefore, the g/g value is calculated to be:

$$\text{g/g} = 0.57/0.964$$
$$= 0.59$$

This result indicates that a significant amount of VBC groups on the diester resin remains unaccounted for. The low g/g value is most likely the result of $AlCl_3$-catalyzed cross-linking between neighboring VBC groups which can occur during the toluene wash of the phosphorylated intermediate. A small portion of the partially functionalized polymer used to make diester resin DQ-03-026B was removed before the toluene wash and quenched in water to produce a phosphonic resin. This resin was analyzed to have a g/g value of 1.08, tot(P) = 1.88 mequiv/g, tot(OH) = 4.30 mequiv/g and tot(Cl) = 1.88 mequiv/g. These results demonstrate that the loss of chlorine does not occur during the

functionalization reaction, but rather during either the toluene wash or ethanol quench.

Although higher levels of esterification are achieved when mild functionalization conditions were employed, the diester resins obtained by this route are of low capacity. High capacity resins are desired for use in metal ion recovery in order to minimize column length needed and maximize kinetic performance. For these reasons, a synthetic method to produce a high capacity diester resin was sought.

In order to obtain a high capacity diester resin using mild quench conditions, the synthesis was carried out using Friedel-Crafts catalysts which are less active than $AlCl_3$. Results are presented in Table 21 for diester resins synthesized using 0.77 mole $FeCl_3$, $SnCl_4$, and $ZnCl_2$ Friedel-Crafts catalysts. No phosphorylation was achieved using $ZnCl_2$, the weakest Friedel-Crafts catalyst. Although a higher level of functionalization was obtained using $SnCl_4$, no esterification was achieved. The results using $FeCl_3$ show that high levels of both functionalization and esterification were attained without any loss of chlorine.

The effect of $FeCl_3$ catalyst level on the extent of functionalization and esterification was investigated. The phosphorylated intermediates were prepared by refluxing 2% cross-linked poly(VBC) beads in PCl_3 for 4 h with levels of $FeCl_3$ ranging from 0.11 to 2.0 mole per mole of VBC groups. Esterification was achieved by quenching the resin in solution of ethanol and toluene. Diethyl ester resins were synthesized from different sizes of polymer beads in order to determine if the functionalization occurred completely to the inner

Table 21

Characterization of Diethyl Ester Resins
Synthesized with $FeCl_3$, $SnCl_4$ and $ZnCl_2$
Friedel-Crafts Catalysts[a]

Resin Code	Catalyst	capacity (mequiv/g)			g/g	% ester.
		tot(OH)	tot(P)	tot(Cl)		
DQ-03-031A	$FeCl_3$	0.35/0.34[b]	1.78	2.99	0.93	90.3
DQ-30-031B	$SnCl_4$	3.80[c]	1.59	2.31	0.69	0
DQ-03-031C	$ZnCl_2$	0	0.19	5.84	0.92	0

[a] 2% cross-linked gel copolymer used, catalyst level = 0.77 mole/mole VBC groups; Functionalization temperature = 76 °C.

[b] tot(OH) determined using 0.1 M KOH in a solution of 20% water/ 80% dioxane for increased accessibility into hydrophobic resin.

[c] Average of three results; standard deviation = 1.32 mequiv/g.

resin core using $FeCl_3$ catalyst. As indicated by the results in Table 22, the smaller beads (-60 and -60+100 mesh cuts) were functionalized to a higher level than the larger beads (-20+40 mesh cut) for all catalyst levels studied. The theoretical phosphorus capacity assuming 100% substitution to diester groups is calculated to be 3.79 mequiv/g for a 2% cross-linked resin. The phosphorus capacities in Table 22 indicate that a catalyst level of 2.0 mole and a bead mesh size of -60 or -60+100 is required to obtain a fully functionalized diester resin. The relationship of the phosphorus and chlorine capacities to $FeCl_3$ catalyst level for diester resin synthesized from -60 and -60+100 mesh beads is illustrated in Figure 33.

In order to determine if the degree of functionalization can be increased for -20+40 beads using longer reaction times, diester resin DQ-03-167 was refluxed in PCl_3 for 70 h using 2.0 mole $FeCl_3$ (see Table 22). The longer reflux period, however, did not increase the level of phosphorylation over that achieved for a 4-h reflux period. In fact, the degree of esterification decreased to 76.4% when the 70-h reflux period was employed.

The g/g results reported in Table 22 suggest that less chlorine loss occurs using $FeCl_3$ as the catalyst than with $AlCl_3$. Apparently, $FeCl_3$ did not catalyze the cross-linking reaction between neighboring VBC groups. In general, higher g/g values were obtained as the level of $FeCl_3$ catalyst increased. In fact, relatively high (>0.88) g/g values were attained using 2.0 moles $FeCl_3$.

The % esterification results given in Table 22 range from 74 to 98%. The level of esterification achieved greatly depended on the

Table 22

$FeCl_3$ Catalyst Level Study in the Synthesis of Diethyl Ester Resins[a]

Resin Code	$FeCl_3$ (mole)	Mesh Cut	capacity (mequiv/g) tot(OH)	tot(P)	tot(Cl)	g/g	% ester.[f]
DQ-05-112D	0.11	-60+100	0.16/0.42[b]	0.69	3.30	0.70	88.4
DQ-05-112C	0.33	-60+100	0.29/0.70[b]	1.43	2.83	0.82	89.9
DQ-05-112B	0.55	-60+100	0.15/0.48[b]	1.89	1.08	0.67	96.0
DQ-03-031A	0.77	-20+40	0.35/0.34[b]	1.78	2.99	0.93	90.3
DQ-03-042	0.77	-20+40	0.37	2.13	2.46	0.94	91.3
DQ-03-286A	0.77	-60	1.22	2.43	1.05	0.77	74.9
DQ-04-003A	0.77	-60	0.28	2.43	1.44	0.86	94.2
DQ-04-003B	0.77	-60	0.17	2.50	1.09	0.83	96.6
DQ-04-156A	0.77	-60	0.33/0.46[b]	2.07	1.51	0.78	92.0
DQ-04-156B	0.77	-60	0.36/0.43[b]	2.31	1.28	0.80	92.2
DQ-04-156C	0.77	-60	0.27/0.41[b]	2.44	1.24	0.83	94.5
DQ-04-278C	0.77	-60+100	0.36	2.49	1.33	0.86	92.8
DQ-05-112A	0.77	-60+100	0.46/0.62[b]	2.19	1.56	0.81	89.5
DQ-03-162A	1.2	-20+40	0.28	1.74	2.61	0.86	92.0
DQ-03-286B	1.2	-60	0.32	3.12	0.62	0.91	94.9
DQ-03-162B	2.0	-20+40	0.44	2.55	1.75	0.94	91.4
DQ-03-167[c]	2.0	-20+40	1.13	2.39	0.94	0.75	76.4
DQ-03-286C	2.0	-60	0.30	3.45	0.44	0.97	95.7
DQ-04-072C	2.0	-60	0.25	3.47	g	g	96.4
DQ-04-244B	2.0	-60	0.44	3.38	g	g	93.5
DQ-04-272B[d]	2.0	-60+100	0.88	3.19	g	g	86.2
DQ-04-278B	2.0	-60+100	0.35	3.40	g	g	94.9
DQ-05-242A	2.0	-60+100	0.35	3.26	g	g	94.6
DQ-06-129A	2.0	-60+100	0.41	3.39	0.0	0.88	94.0
DQ-06-129A	2.0	-60+100	0.10[e]	3.49[e]	0.0	0.92[e]	98.6[e]
DQ-06-129B	2.0	-60+100	0.40	3.37	0.0	0.88	94.1

[a] All reactions carried out at reflux (76 °C) for 4 h using 2% cross-linked gel poly(VBC) beads unless noted otherwise; All reactions quenched in 0.70 mole ethanol(pyridine)/10g polymer and 50 wt% toluene.

[b] Tot(OH) determined using 0.1M KOH in 20% water/80% dioxane.

[c] Functionalization time of 70 h.

[d] Quench solution added over a long period (approximately 17 h).

[e] Capacity measured after resin soxhleted in water and reconditioned.

[f] Calculated using aqueous tot(OH) results.

[g] Not determined.

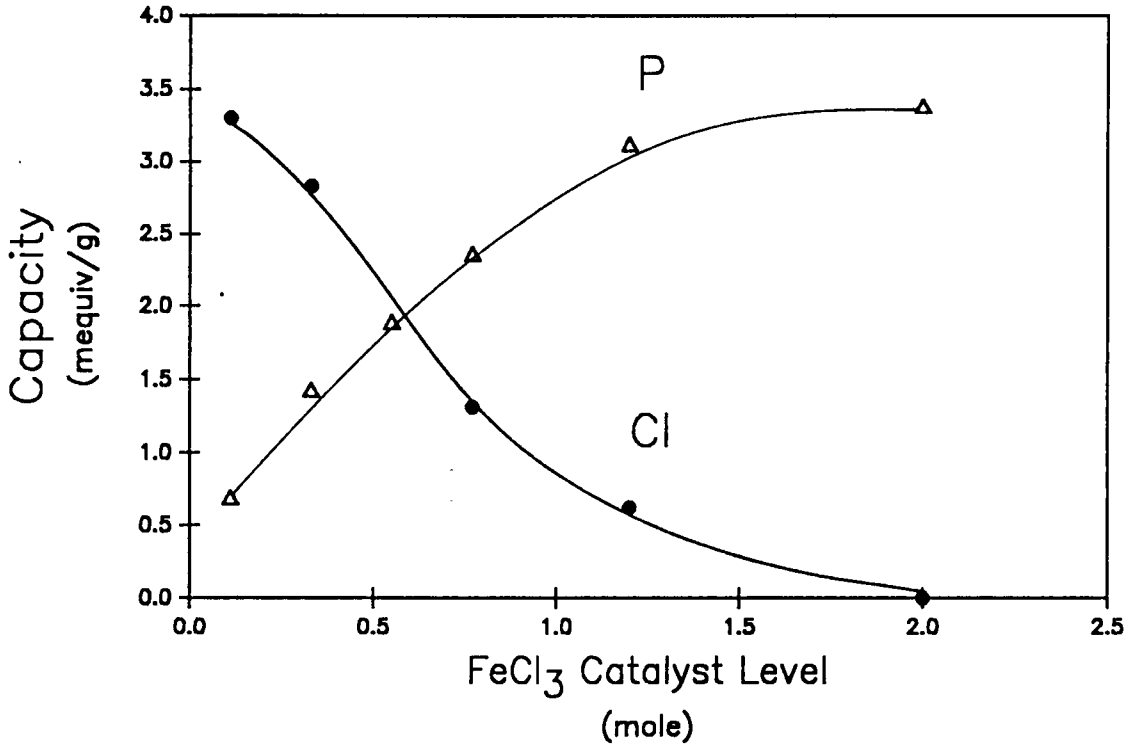

Figure 33. Phosphorus and chlorine capacities of diethyl ester resins as a function of $FeCl_3$ catalyst level.

amount of exposure of the reaction mixture to moisture. Higher degrees of esterification were obtained when a nitrogen sweep was used during the quench. An attempt was made to increase the degree of esterification by carrying out a very slow addition of the quench solution (see resin DQ-04-272B, Table 22). Extending the usual 4-h addition period to 17 h, however, resulted in a lower % esterification, most likely because of a longer exposure time of the reactive polymer to moisture from the atmosphere.

The effect of polymer cross-linking and macroporosity on the degree of functionalization and esterification of diethyl esters prepared with $FeCl_3$ was investigated. Ester resins were synthesized from 2% crosslinked gel and 5% cross-linked MR polymer beads (-60 mesh) using 1.2 mole $FeCl_3$. The results presented below demonstrate that the levels of functionalization and esterification, and g/g values were identical for the two resins. Thus, reagent accessibilty was not limited in either the phosphorylation or ethanolysis reactions using the more highly cross-linked resin.

Effect of Cross-linking and Macroporosity on Diester Synthesis

Resin Code	Capacity (mequiv/g)			%ester	g/g
	tot(OH)	tot(P)	tot(Cl)		
DQ-03-189A	0.46	3.24	0.80	92.9	0.97
DQ-03-189B	0.61	3.17	1.17	90.4	1.00

Diester resins were prepared containing methyl, *n*-propyl and *n*-butyl groups by solvolysis of the phosphorylated intermediate in a 50 wt% solution of the corresponding alcohol in toluene. In addition, the

synthesis of cyclic diester resins was attempted by quenching in 1,2-ethanediol and 1,3 propanediol. Table 23 presents the results of these syntheses. In order to attain a high degree of esterification, the alcohol required distillation from a drying agent just prior to use. This fact is illustrated by the low % esterification results for the dipropyl esters DQ-04-244C and DQ-04-272C, for which the alcohol was not purified before use. By comparison, a very high level of esterification was obtained for dipropyl ester DQ-05-268B, which was prepared using freshly dried and distilled 1-propanol. As with the diethyl ester synthesis, the use of a long addition period decreased the degree of esterification (see resins DQ-04-272A and DQ-04-272C). A general trend of increasing degree of esterification with increasing alkyl group size is indicated by the results in Table 23.

The acidity of the ester resins was determined in both aqueous NaOH and in a solution of KOH prepared in 80% dioxane/20% water. As seen in Table 23, generally good agreement was obtained between the two sets of results. The slight differences in tot(OH) values for the dipropyl and dimethyl esters may be due to experimental error, given the excellent agreement in the two values for the very hydrophobic dibutyl ester. These results strongly suggest high accessibility of aqueous reagents into these hydrophobic diester resins.

As shown in Table 23, very low levels of esterification were achieved for the cyclic diester resins. These resins were synthesized by solvolysis of 10 g of phosphorylated polymer in 0.35 mole of the diol

Table 23

Synthesis of Diester Resins of
Varying Alkyl Groups[a]

Resin Code	Alcohol Used in Quench	capacity (mequiv/g) tot(OH)	tot(P)	% ester.
DQ-04-244A	methanol	0.68	3.63	90.6
DQ-04-272A	methanol	0.84	3.66	88.5
DQ-04-278A	methanol	0.50	3.82	93.5
DQ-05-268A	methanol	0.59/1.07[b]/0.65[c]	3.70	92.0/85.5[b]/91.2[c]
DQ-04-244C	1-propanol	1.00	3.17	84.2
DQ-04-272C	1-propanol	1.21	3.15	80.8
DQ-05-003A	1-propanol	0.18	3.12	97.1
DQ-05-268B	1-propanol	0.19/0.60[b]	3.09	96.9/90.3[b]
DQ-05-286C	1-butanol	0.15/0.46[b]/0[c]	2.85	97.4/91.9[b]/100[c]
DQ-06-116A	1,2-ethanediol[d]	3.46	3.33	48.1
DQ-06-116B	1,3-propanediol[d]	1.89	3.22	70.7

[a] Unless noted otherwise, all resins functionalized for 4 h at 76 °C using -60 mesh cut, 2% cross-linked gel poly(VBC) beads.
[b] tot(OH) determined using 0.1M KOH in 20% water/ 80% dioxane.
[c] Determined after soxhleting and reconditioning resin.
[d] Quenched in 0.35 mole alcohol/10g polymer in 100 mL dioxane.

in 100 mL of dioxane. The following are the possible ester reaction products for the resin quenched in 1,2-ethanediol:

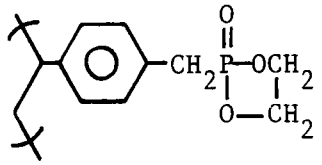

I

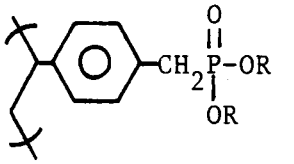

R = -H, $-CH_2CH_2OH$

II

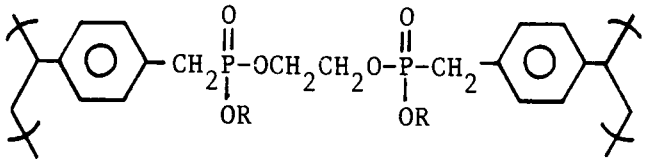

R = -H, $-CH_2CH_2OH$

III

In order to fully characterize these resins, a method such as selective oxidation of the unreacted alcohol groups with chromic acid, must be developed to distinguish the amount of cyclic diester from structure II. This technique would not, however, differentiate structure I from III. To maximize the formation of the cyclic structure I, a very dilute quench solution of the purified diol should be added to the phosphorylated intermediate over a long addition period.

Synthesis of Amine/Ester Resins

Amine/ester resins were prepared by amination of the unreacted benzyl chloride groups of partially functionalized diester resins using primary or secondary amines as shown in Figure 34. This bifunctional

resin contains two groups which are both capable of metal ion complexation. The amine group can extract metals through ion association whereas the phosphoryl oxygen of the phosphonate ester can complex metal ions through coordination. In solvent extraction systems, weak synergistic effects (6-10 fold increases in distribution coefficient values) have been observed for the extraction of metal ions by mixtures of tertiary or quaternary amines and neutral organophosphorus reagents.[92] For example, synergistic enhancement has been observed in the extraction of cerium(III) from 3M HNO_3 by mixtures of TBP and trilauryl ammonium nitrate.[93] The synergistic effect was attributed to the formation of mixed anionic complexes of metal nitrate-TBP-alkylammonium nitrate. The amine/ester resins were synthesized in order to determine if similar synergistic enhancements are possible for metal ion extraction with bifunctional resins.

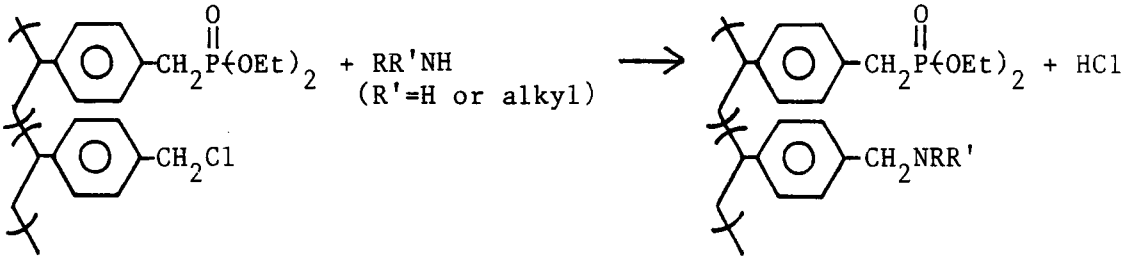

Figure 34. Synthesis of amine/diethyl ester resin.

The first variable studied in the synthesis of amine/ester resins was the effect of amination temperature on amine capacity. Table 24 reports the results of the amination of diester resin DQ-02-195B at 0,

Table 24

Study of Amination Temperature in the Synthesis of Dimethylamine/Ester Resins[a,b]

Resin Code	Temp (°C)	Capacity (mequiv/g)[c]				
		tot(OH)	Δtot(OH)[d]	tot(P)	TAEC	tot(Cl)
DQ-02-198A	0	0.64	-0.01	2.49	0.19	0.43
DQ-02-198B	25	0.65	0	2.16	0.18	0.69
DQ-02-198C	40	0.65	0	1.83	0.20	0.58
DQ-02-198D	60	1.17	0.52	1.78	0.16	0.45

[a] Amination carried out on ester resin DQ-02-195B; tot(OH) = 0.65 mequiv/g, tot(P) = 2.41 mequiv/g, % ester = 86.5, tot(Cl) = 0.67 mequiv/g, g/g = 0.77.

[b] Amination conditions : 40 wt% aqueous solution of dimethyl amine used; reaction time = 4 h.

[c] Determined on the resin in the protonated chloride form.

[d] $\Delta tot(OH) = tot(OH)_{after\ amination} - tot(OH)_{before\ amination}$.

25, 40 and 60 °C with a 40 wt% aqueous solution of dimethylamine. A small amount of NaOH was added in all aminations to neutralize the HCl formed in the reaction. The capacities presented in Table 24 were determined on the chloride form of the amine/ester resin. The acid capacity is a measure of both the amine groups and the acidic groups of the starting diester. The difference in the acid capacity of the amine/ester and the pure diester thus quantifies the amine capacity of the resin. Another measure of the amine content is the total anion exchange capacity (TAEC). To determine the TAEC, the amine group was first converted to the chloride form by elution with 4 wt% HCl. The chloride counterion was then exchanged for nitrate by elution with 4 wt% $NaNO_3$. The eluant was collected and titrated for chloride. The amount of chloride exchanged per gram of dry resin is termed the TAEC. The chlorine capacity was measured by elemental analysis of the resin in either the chloride or free amine form. The chlorine capacity of the free amine resin measures the unreacted benzyl chloride groups; both the amount of amine groups and unreacted benzyl chloride is given by the chlorine capacity of the chloride form of the resin.

As indicated in Table 24, very little amination was achieved for all the temperatures studied. Because of the low chlorine capacity of the starting diester resin (0.67 mequiv/g), the maximum amine capacity of the amine/ester resins is calculated to be 0.52 mequiv/g. Although all TAEC values were lower than the theoretical capacity, the results point out that the diester groups were stable to the amination conditions used in this experiment. This is evidenced by the fact that the Δtot(OH) values did not exceed the TAEC. All subsequent aminations

with dimethylamine were carried out at 52 °C, the reflux temperature of a 40 wt% aqueous solution of the amine.

The results of all dimethylamine/ester syntheses are given in Table 25. The bifunctional resins were prepared by refluxing a partially functionalized diester resin in 40 wt% dimethylamine for 4 h, unless noted otherwise. The capacities for both the amine/ester and starting diester are reported in Table 25. In general, good agreement was obtained for the two measures of amine capacity, Δtot(OH) and TAEC. For the 4-h reaction, slightly lower amine capacities were obtained than the theoretical values calculated from the chlorine content of the starting diester. When a 7-h reflux period was employed (as for DQ-04-161), the theoretical and experimental amine capacities were in closer agreement. Comparison of the amination results for the 2% cross-linked diester (DQ-03-202A) to those for a 5% cross-linked MR (DQ-03-202B) shows no differences in resin properties based upon cross-link level or macroporosity.

A cross-linking reaction can occur between neighboring rings to lead to the formation of a quaternary amine, as shown in Figure 35. The amount of quaternary amine groups was determined as the salt-splitting anion exchange capacity (SSAC). In this procedure, the chloride form of the resin was eluted with 4 wt% NaOH. This placed the tertiary amine groups in the free amine form and exchanged the chloride counterion of the quaternary amine for a hydroxide counterion. Elution with 4 wt% $NaNO_3$ exchanged the hydroxide ion for nitrate. The amount of hydroxide ion exchanged per gram of dry resin was determined by titration of the eluant with standard acid. This quantity is termed the SSAC. A SSAC

Table 25

Synthesis of Dimethylamine/Ester Resins[a]

Resin Code	capacity (mequiv/g)[b,c]					
	tot(OH)	tot(P)	tot(Cl)	Δtot(OH)	TAEC	theory
DQ-03-037A	2.71(0.35)	(1.78)	2.14(2.99)	1.82	2.00	2.31
DQ-03-045	1.88(0.37)	2.10(2.13)	1.92(2.46)	1.51	1.67	1.90
DQ-04-020	0.93(0.17)	(2.50)	0.73(1.09)	0.76	0.38	0.84
DQ-04-161[d]	1.63(0.36)	2.19(2.31)	1.15(1.28)	1.27	1.01	0.99
DQ-03-202A	(0.46)	(3.24)	(0.80)		0.10	0.62
DQ-03-202B[e]	(0.61)	(3.17)	(1.17)		0.36	0.90

[a] All resins synthesized by refluxing a 2% cross-linked gel diester resin in 40 wt% dimethylamine for 4 h unless otherwise noted.

[b] Capacities determined on the amine/ester resin in the chloride form.

[c] Values in parentheses are for the starting diester resin.

[d] 7-h reflux period.

[e] 5% cross-linked MR.

determination on dimethylamine/ester resin DQ-03-045 gave a quaternary amine capacity of zero. This result can be explained by the limited amount of benzyl chloride sites available for cross-linking on the partially functionalized diester resin. Due to the presence of diester groups, it is unlikely that an amine group can come in close enough proximity to a benzyl chloride group for quaternization to occur. As will be seen later, this was not the case for the high capacity monofunctional dimethylamine resin.

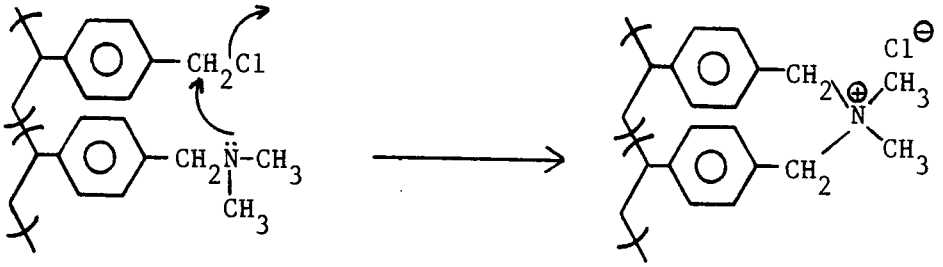

Figure 35. Formation quaternary amine sites by cross-linking.

In addition to dimethylamine/esters, amine/ester resins were synthesized containing ethylamine, diethylamine and di-*n*-propylamine groups. The synthesis conditions and characterization results for these resins are summarized in Table 26. Both the ethylamine/ester and diethylamine/ester were prepared under mild conditions to nearly maximum amine capacity without hydrolysis of the ester groups. The amination conditions used for the dipropylamine/ester resin DQ-04-218A, however, led to hydrolysis of some of the ester groups. This is evidenced by the increased Δtot(OH) value over that of the TAEC capacity. The results of

Table 26

Synthesis of Ethylamine/Ester, Diethylamine/Ester and Dipropylamine/Ester Resins

Resin Code	Amine	Amination Conditions	Capacity (mequiv/g)[a,b]					
			tot(OH)	tot(P)	tot(Cl)	Δtot(OH)	TAEC	theory
DQ-04-020B	ethyl	39°C/13h	0.56(0.17)	(2.50)	0.55(1.09)	0.39	0.35	0.84
DQ-04-162A	ethyl	39°C/8h	1.60(0.27)	2.40(2.44)	0.93(1.24)	1.33/1.23[c]	0.69	0.95
DQ-04-163A	diethyl	55°C/6h	1.44(0.33)	1.85(2.07)	1.36(1.51)	1.11/1.10[c]	1.18	1.02
DQ-04-218A	dipropyl	91°C/8h	2.73(0.28)	(2.43)	0.91(1.44)	2.45	0.64	0.87
DQ-04-289[d]	dipropyl	55°C/24h	0.83(0.36)	2.53(2.49)	0.83(1.33)	0.47	0.82	0.80

[a] Capacities determined on the amine ester resin in the chloride form.
[b] Values in parentheses are for the starting diester resin.
[c] Δtot(OH) determined in 0.1 M KOH/80% dioxane/20% water to increase OH^- accessibility.
[d] 50% aqueous solution if di-n-propyl amine used with ethanol as cosolvent.

a control experiment carried out by refluxing the diester resin in water and a slight amount of NaOH showed no increase in acid capacity of the resin. Despite these findings, amination under milder conditions did not lead to ester hydrolysis. Complete amination of the diester resin was accomplished by reaction with a 50 wt% aqueous solution of di-*n*-propyl amine (with ethanol as co-solvent) at 55 °C for 24 h. Examination of the Δtot(OH) and TAEC values from Table 26 demonstrates that the ester groups were stable to these conditions.

Synthesis of Amine Resins

Monofunctional amine resins were prepared so that their metal ion complexing abilities could be compared to the bifunctional amine/ester and amine/acid resins. The resins were synthesized by amination of 2% cross-linked gel poly(VBC) beads with either primary or secondary amines as indicated in Figure 36.

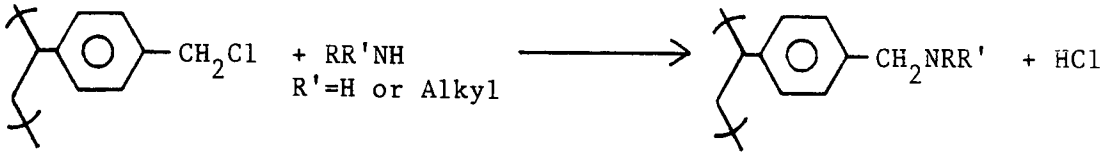

Figure 36. Synthesis of amine resin.

Resins containing dimethyl, ethyl, diethyl, di-*n*-propyl and di-*n*-butyl amine groups were prepared. Table 27 summarizes the reaction conditions and the characterization results for these resins. The capacities reported were determined on the chloride form of the resins. For resins prepared from secondary amines, the formation of both

Table 27

Synthesis of Amine Resins[a]

Resin Code	Amine	Conditions	capacity (mequiv/g)[b] tot(OH)[c]	tot(Cl)	TAEC	SSAC	3° amine	theory[d]	% reaction
DQ-03-089B	dimethyl	4h/52°C	3.01	4.22	3.53				
DQ-04-161B	dimethyl	7h/52°C	3.87/4.07	4.19	4.41	0.52	3.89	4.05	96.0
DQ-04-162B	ethyl	8h/39°C	3.86/3.69	4.40	3.82	0		3.08(3°)/4.87(2°)	124(3°)/78.4(2°)
DQ-04-163B	diethyl	6h/55°C	0.59/1.93	4.22	4.13	0	4.13	4.27	96.7
DQ-04-218B	di-n-propyl	8h/93°C	0.32	3.44	3.72	e	3.72	3.80	97.9
DQ-05-192	di-n-butyl	4h/90°C		3.44/3.35[f]	3.35	0	3.35	3.42	98.0

[a] From 2% cross-linked gel poly(VBC) beads.
[b] Determined on resins in the chloride form.
[c] Aqueous/dioxane acid capacity.
[d] Theoretical capacity for the 3° amine (unless noted otherwise); calculated assuming the experimental value for SSAC.
[e] Assume SSAC = 0.
[f] Chlorine capacity after elution with 4% NaOH (see text).

tertiary and quaternary amine groups was possible. The tertiary amine capacity of these resins is given by the difference of the TAEC and SSAC values. The theoretical tertiary amine capacities in Table 27 are calculated assuming the quaternary amine capacities are given by the experimental values of the SSAC.

The results for amination with dimethylamine show that a higher TAEC was obtained for the 7-h than the 4-h reaction. The theoretical tertiary amine capacity cannot be calculated for the 4-h amination because the SSAC was not determined for this resin. The results for the 7-h reaction demonstrate that practically complete substitution to tertiary amine groups was achieved (96% reaction). The close agreement between the aqueous and dioxane acid capacities indicates that the resin was completely accessible to aqueous reagents.

The ethylamine resin was found to have a SSAC value of zero. For amination with a primary amine such as ethylamine, the likelihood of quaternization is very small because it involves a cross-linking reaction between three neighboring rings. In this case, the TAEC measures both the secondary amine and cross-linked tertiary amine capacities. The theoretical capacity for substitution to only secondary amine groups is calculated to be 4.87 mequiv/g; exclusive tertiary amine substitution leads to a theoretical capacity of 3.08 mequiv/g. The observed TAEC lies between these two values, indicating a mix of secondary and tertiary substitution.

No quaternary amine groups were observed in the amination with diethylamine, di-*n*-propylamine or di-*n*-butylamine. These results suggest that for alkyl groups larger than methyl, quaternization is

prohibited due to steric hindrance. The % reaction values for these resins show that the amination reactions all occurred nearly to completion. The hydrophobic nature of these resins is evidenced by the low tot(OH) results. Although the acid capacity for the diethylamine resin was greater in dioxane than water, it was still significantly lower than the TAEC value.

The results of chlorine elemental analysis on the different forms of the di-*n*-butyl resin suggest that it cannot be converted to the free amine form by elution with NaOH. The chloride form of the resin was eluted with 4 wt% NaOH over a 1-h period in an attempt to transform the resin to its free amine form. Chlorine elemental analysis of the eluted resin gave a capacity of 3.35 mequiv/g, in close agreement with the value for the resin in the chloride form (3.44 mequiv/g). These results may be explained by limited aqueous NaOH accessibility into the hydrophobic resin matrix. However, elutions using 50% ethanol as the solvent instead of water still resulted in a resin with a chlorine capacity of 3.22 mequiv/g. When the chloride form of the resin was eluted with 4 wt% $NaNO_3$, the chlorine capacity was found to be 0.17 mequiv/g, indicating that the chloride counterion was exchanged for nitrate. A possible explanation for these findings is that the large butyl groups prevent close approach of the hydroxide ion to the proton on nitrogen, thus prohibiting conversion of the resin to the free amine form. The associated chloride ion, however, is not shielded to such a large extent by the butyl groups and therefore is not sterically hindered to counterion exchange.

Synthesis of Phosphonic Acid Resins

Phosphonic acid resins were prepared as indicated in Figure 37. Cross-linked poly(VBC) beads were phosphorylated with PCl_3 in the presence of a Friedel-Crafts catalyst of $AlCl_3$. The intermediate tetrachlorophosphonium groups were then hydrolyzed to yield the phosphonic acid resin. The effects of catalyst level, hydrolysis method, and percent DVB cross-linking were examined in the synthesis of phosphonic acid resins.

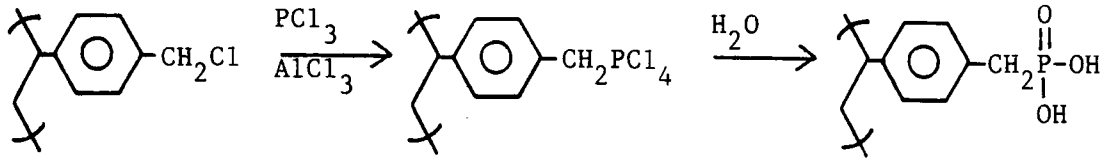

Figure 37. Synthesis of phosphonic acid resin.

Partially substituted phosphonic resins were prepared by functionalization at 40 °C using 0.77 mole $AlCl_3$ catalyst. Bifunctional polymers can be synthesized from these resins by further reaction of the remaining benzyl chloride groups. For example, bifunctional amine phosphonic resins were prepared by amination of partially functionalized phosphonic resins, as will be discussed in the next section. Presented below are the results of partial functionalization of 2% cross-linked gel and 5% cross-linked MR beads at 40 °C with 0.77 mole $AlCl_3$.

Synthesis of Partially Functionalized Phosphonic Acid Resins

Resin Code	type	Capacity (mequiv/g) tot(OH)	tot(P)	tot(Cl)	% rxn	g/g	tot(OH)/ tot(P)
DQ-03-083B	2% gel	4.42	2.79	2.82	57.4	1.02	1.58
DQ-04-211	2% gel	4.42	2.60	2.64	53.5	0.95	1.70
DQ-02-214	5% MR	5.27	2.41	3.05	52.5	1.04	2.19

These results demonstrate that mild synthesis conditions of 40 °C/0.77 mole $AlCl_3$ led to approximately 50% functionalization for both 2% gel and 5% MR beads. The high g/g levels signify that all of the VBC groups were accounted for by the measured phosphorus and chlorine capacities. Although the acid capacity of the phosphonic resin should equal twice its phosphorus capacity, the ratios of tot(OH) to tot(P) for the gel resins were less than 2. The low acid capacities are likely due to inaccessibility of the aqueous hydroxide ion into the partially functionalized resin matrix. For the incompletely functionalized gel resins, the phosphorus capacity is a better measure of functionality because it is carried out on solubilized resins and is therefore not subject to accessibility problems. For the MR resin, the increased accessibility due to the macroporous network resulted in a tot(OH) to tot(P) ratio of 2.19. A titration curve was carried out on the MR resin in order to verify the presence of diacid groups. The second proton of the phosphonic acid, however, was not detected due to its weak acidity. The acid capacity at the breakpoint was found to be 2.78 mequiv/g, in good agreement with the phosphorus capacity.

The synthesis of fully functionalized phosphonic resins was carried out at 76 °C using 1.2 mole $AlCl_3$. Table 28 presents the results of the syntheses. Hydrolysis of the $-CH_2PCl_4$ intermediate was accomplished by three different methods. The first method, rapid hydrolysis in ice water, led to bead fracturing, especially when large beads were used. In the second method, milder hydrolysis conditions were employed by slow addition of aqueous dioxane in an attempt to maintain bead integrity. Prior to their hydrolysis, the beads were washed in dioxane to remove $AlCl_3$ from the resin pores and thus produce a less exothermic reaction within the resin matrix. The third hydrolysis method was carried out using the same conditions as for esterification by the dropwise addition of a solution of water and pyridine to the $-CH_2PCl_4$ intermediate.

Both -20+40 and -60+100 mesh cuts of polymer beads were used in the preparation of phosphonic acid resins. In general, slightly lower % reaction values were obtained for the larger beads. For example, examination of Table 28 shows that the average % reaction for -20+40 beads was 81%, whereas for -60+100 beads it was 90%. These findings imply that PCl_3 and/or $AlCl_3$ accessibility was restricted from the inner core of the larger -20+40 beads.

As indicated in Table 28, a lower acid capacity than that predicted by twice the phosphorus content was observed for all the -20+40 phosphonic resins. The possibility was examined that the presence of phosphinic acid groups on the resin resulted in an acid content lower than twice the phosphorus capacity. Ag^+ oxidation of phosphonic resin DQ-03-002A at both 25 and 50 °C indicated that no

Table 28

Synthesis of Fully Functionalized
Phosphonic Acid Resins[a]

Resin Code	Quench	Mesh Size	Capacity (mequiv/g)[b] tot(OH)$_{aq}$	tot(OH)$_{diox}$	tot(P)	tot(Cl)	tot(OH)$_{aq}$ / tot(P)	tot(OH)$_{diox}$ / tot(P)	% reaction
DQ-03-232	ice/H_2O	-20+40	7.73		4.18		1.86		86.0
DQ-03-083A	ice/H_2O	-20+40	7.61		4.06	0.84	1.87		83.5
DQ-06-168B	ice/H_2O	-60+100	8.47(8.97)		4.60(4.51)		1.84(1.99)		93.7
DQ-06-268A	ice/H_2O	-60+100	9.11(9.26)		4.58		1.99		94.2
DQ-05-162A	70% dioxane	-20+40	6.44(7.14)[c]	6.66(7.36)[c]	3.70(3.59)[c]	0.77	1.74(1.99)	1.00(2.05)	75.0
DQ-05-162B	70% dioxane	-60+100	6.94(7.42)[c]	7.17(7.82)[c]	3.93(4.09)[c]	0.44	1.77(1.81)	1.02(1.91)	82.5
DQ-05-222B	70% dioxane	-60+100	(9.03)	(9.40)	(4.40)		(2.05)	(2.14)	90.5
DQ-03-002A	H_2O/pyr.	-20+40	6.16		3.07	0.78	1.59		79.6

[a] Synthesized with 1.2 mole $AlCl_3$ at 76°C using 2% cross-linked gel beads.

[b] Values in parentheses were determined after resin was soxhleted in water and reconditioned.

[c] Resin soxhleted in dioxane instead of water.

oxidizable P-H bonds were present on the polymer. Limited hydroxide ion accessibility is a possible explanation for the low acid capacities in the -20+40 beads. Inconsistent with this explanation, however, are the acid capacities determined in dioxane for DQ-05-162A. Whereas a significant increase in acid capacity would be expected when determined in a swelling solvent, only a very slight increase in acid capacity was observed. In addition, the dioxane acid capacity was still considerably lower than twice the phosphorus capacity.

Phosphorus and acid capacities were determined on phosphonic resins after soxhleting (in water or dioxane) followed by reconditioning. These capacities are presented in parentheses in Table 28. Soxhleting of the resins produced a white solid which was most likely an aluminum salt that remained in the resin pores after conditioning. Examination of the results in Table 28 shows that although the phosphorus content was unchanged, the acid capacity increased after soxhleting. The ratios of tot(OH) to tot(P) were closer to the expected value of 2 when the acid capacity was determined after soxhleting.

A study of the influence of cross-link level on phosphonic resin capacity was carried out at DVB levels of 10 and 15%. The following table reports the results for the syntheses carried out at 76 °C using 0.77 mole $AlCl_3$.

Capacities of 10 and 15% Cross-Linked Phosphonics

Resin Code	X'link Level	rxn time	capacity (mequiv/g) tot(OH)	tot(P)	tot(Cl)	g/g	% rxn
DQ-04-190A	10%	4h	3.04	1.86	3.10	1.03	44.9
DQ-04-190B	15%	4h	0.35	0.73			19.9
DQ-04-205	15%	17h	0.67	0.82			22.3

As indicated by the low % reaction values, accessibility of PCl_3 and $AlCl_3$ was greatly reduced at the higher cross-link levels. The acid capacities for both cross-link levels were significantly lower than predicted by the phosphorus capacity. The hydrophobic nature of these resins was evidenced by their high % solids: 67% for the 10% cross-linked resin and 85% for the 15% cross-linked resins. No increase in functionalization was observed for the 15% resin when the reaction time was lengthened to 17 h.

Phosphonic acid resins were also synthesized at DVB levels of 0.6 and 1.5%. They are compared in the table below to the 2% cross-linked resins described previously. All resins were synthesized using $AlCl_3$ levels of 1.2 mole at 76 °C. The capacities presented in parentheses were determined after soxhleting and reconditioning of the resin. Comparable % reaction values were obtained for all resins regardless of cross-link level.

Capacities of 0.6, 1.5 and 2% Cross-Linked Phosphonic Acid Resins

Resin Code	X'link Level	Mesh size	Capacity (mequiv/g) tot(OH)	tot(P)	tot(OH) tot(P)	% rxn
DQ-06-268B	0.6%	-60+100	9.21(9.38)	4.54	2.03(2.07)	90.9
DQ-06-250	1.5%	-40+60	8.73(8.82)	4.50	1.94(1.96)	91.6
DQ-06-168B	2.0%	-60+100	8.47(8.97)	4.60(4.51)	1.84(1.99)	93.7
DQ-06-268A	2.0%	-60+100	9.11(9.26)	4.58	1.99(2.02)	94.2

Synthesis of Amine Phosphonic Resins

Bifunctional amine phosphonic resins were prepared as shown in Figure 38 according to previously described procedures.[94] A partially functionalized phosphonic resin (tot(OH) = 4.42 mequiv/g; tot(P) = 2.79 mequiv/g; tot(Cl) = 2.82 mequiv/g) was converted to the sodium salt form and was then refluxed (52 °C) for 4 h in a 40% aqueous solution of dimethylamine. A slight amount of 50% NaOH was added to neutralize the HCl formed by the reaction. The chloride form of the resulting amine phosphonic resin was characterized to have the following: tot(OH) = 6.21 mequiv/g,; tot(P) = 2.15 mequiv/g; tot(Cl) = 2.10 mequiv/g; TAEC = 1.45 mequiv/g. The theoretical amine capacity of the amine phosphonic resin is calculated to be 2.18 mequiv/g based on the chlorine content of the starting phosphonic resin. The results indicate that the amination reaction occurred to only 67% completion, a lower value than previously found.[94]

Recent results with bifunctional trimethylamine phosphonic resins have suggested that the amine sites and the phosphonic acid sites may not be located on the same bead.[95] The partially functionalized

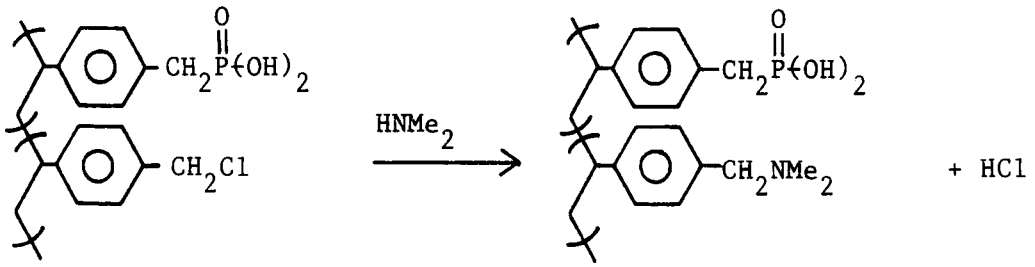

Figure 38. Synthesis of amine phosphonic resin.

phosphonic resin may in fact contain some beads which are completely functionalized and some which are entirely unreacted. Amination of this partial phosphonic resin would not result in the formation of a bifunctional resin, but would instead produce a resin containing both monofunctional amine and phosphonic beads. In addition, other studies have shown that phosphorylation conditions of 0.77 mole $AlCl_3$/40 °C lead to only surface functionalization of the beads. Thus, amination occurs only in the resin core, resulting in isolation of the amine and the phosphonic acid sites. Current investigations are focusing upon the development of synthetic methods to ensure homogeneous partial functionalization of phosphonic resins.

Synthesis of Thiol and Thiol Phosphonic Resins

An ion-exchange/coordination polymer incorporating sulfur ligands was developed with the aim of achieving metal ion selectivities distinct from other DMBP's. For example, the soft thiol ligand would be expected to exhibit different selectivities from the hard amine group.

Monofunctional sulfur-containing resins have been found to complex or precipitate most of the heavy metal transition metal ions.[50]

Frechet and coworkers have attached thiol groups to polymer supports by reaction of lithiated polystyrene with elemental sulfur followed by reduction of the di- and polysulfides with lithium aluminum hydride:[96]

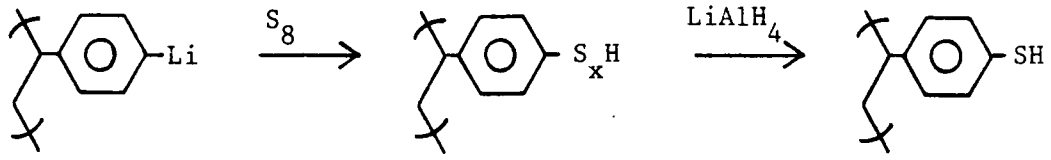

However, the reduction of the sulfide groups was suspected to be incomplete, thus producing additional cross-links in the polymer.[97] As shown in Figure 39, an alternate method of thiolation involves reaction of poly(VBC) with thiourea.[97,98] Hydrolysis of the resulting isothiouronium chloride yields the thiol resin. The latter approach was undertaken in the present work for the synthesis of thiol and thiol phosphonic resins.

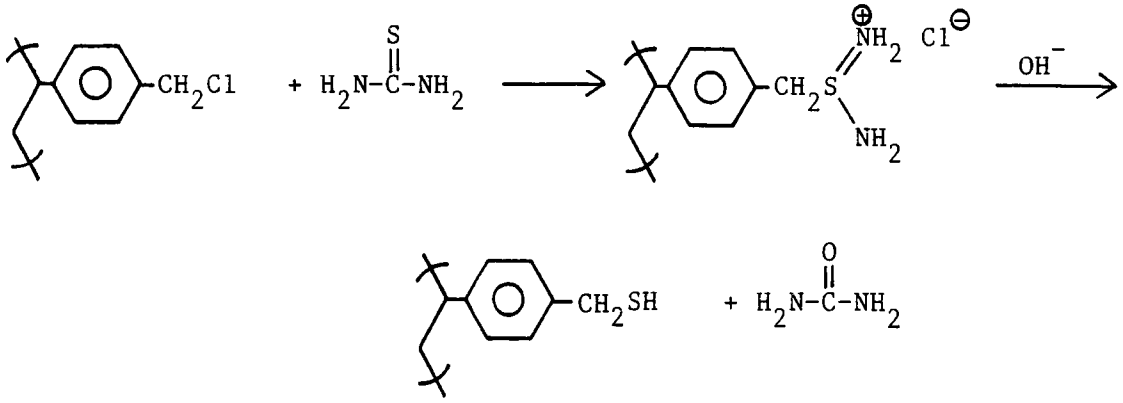

Figure 39. Synthesis of thiol resin.

The first step of thiolation was accomplished by reaction of the $-CH_2Cl$ groups of poly(VBC) beads or partially functionalized phosphonic resins with thiourea in a 1:2 mole ratio. The poly(VBC) beads were pre-swelled in ethylene dichloride (EDC) to increase reagent accessibility into the polymer matrix. The reaction with thiourea was carried out in ethanol for 24 h at 79 °C. Hydrolysis of the resulting isothiouronium groups was achieved by refluxing the resins in 10 wt% NaOH for 24 h. A small amount of urea by-product was observed in the reaction. No care was taken to exclude oxygen from the hydrolysis reaction. According to Frechet[97], disulfide groups are produced unless the hydrolysis is carried out in an inert atmosphere. Thus, -S-S- groups may have been formed in the hydrolysis rather than -SH groups.

The stability of the isothiouronium group to acidic and basic conditions was investigated by TAEC analysis. In this procedure, the amount of isothiouronium groups on the monofunctional resin was determined by titration of the chloride counterions exchanged upon elution of the resin with $NaNO_3$. The TAEC was determined on the resin after each of the following sets of elutions: (1) H_2O, 4 wt% HCl, H_2O, 4 wt% $NaNO_3$; (2) H_2O, 4 wt% HCl, H_2O, 4 wt% $NaNO_3$; (3) H_2O, 0.01 M NaOH, H_2O, 4 wt% HCl, H_2O, 4 wt% $NaNO_3$. The following capacities were found: TAEC 1 = 4.20 mequiv/g; TAEC 2 = 4.12 mequiv/g; TAEC 3 = 3.71 mequiv/g. Comparison to the theoretical capacity of 4.21 mequiv/g shows that complete substitution to isothiouronium groups was accomplished. The first two TAEC results demonstrate that the isothiouronium group was stable to acidic conditions because no decrease in capacity was observed after the second elution with HCl. The fact that the TAEC decreased

after the resin was eluted with 0.01 M NaOH indicates the instability of the isothiouronium group to basic conditions. The stability of the resin in basic media was further studied by stirring it in 0.1M NaOH at 25 °C for three days. After elution of the resin with H_2O, 4 wt% HCl and H_2O, the TAEC was determined to be 0.13 mequiv/g. These results demonstrate that hydrolysis of the isothiouronium groups should readily occur under conditions of refluxing 10% NaOH, but do not indicate whether the hydrolysis products are -SH or -S-S- groups.

The resins produced by isothiouronium hydrolysis in refluxing 10% NaOH were analyzed for their chlorine and acid capacities. These results are summarized in Table 29 for two sets of thiolation reactions. The loss of chlorine from the starting VBC polymers and phosphonic resins indicates substitution of the benzyl chloride groups. The absence of chlorine, however, does not prove that thiol groups are present on the polymer. Qualitative proof of sulfur on the resin was given by elemental analysis. After the resins were digested by sodium fusion, the fusion solution was acidified and lead acetate was added. The formation of a black precipitate of lead sulfide confirmed the presence of sulfur. No increase in acid capacity over that of the initial phosphonic resin was observed for the thiol phosphonic resins. If the thiol group is in fact the reaction product, it is apparently too weakly acidic (pK_a of thiobenzyl alcohol = 9.43[99]) to be measured by the excess NaOH technique.

An attempt was made to determine the amount of thiol groups on the monofunctional resin by their oxidation to sulfonic acids, which can then be quantified by titration. Oxidations were carried out by

Table 29

Synthesis of Thiol and Thiol Phosphonic Resins

Resin Code	type	Capacity (mequiv/g) tot(OH)	tot(Cl)
DQ-03-169A[a]	thiol phosphonic	4.79	0.13
DQ-04-238B[b]	thiol phosphonic	5.03	0.31
DQ-03-169C[c]	thiol	0.01	0.14
DQ-04-238A	thiol	0.05	1.56

[a] Starting phosphonic: tot(OH) = 4.40 mequiv/g; tot(Cl) = 3.15 mequiv/g.

[b] Starting phosphonic: tot(OH) = 4.42 mquiv/g; tot(Cl) = 2.64 mequiv/g.

[c] Chlorine capacity of starting VBC polymer = 6.32 mquiv/g.

refluxing the resin in 1.15% H_2O_2 in 1M NaOH for 4h and 16 h, and by reacting the resin with 4 M HNO_3 for 17 h at room temperature. As indicated by acidity measurements on the resins, none of the oxidation reactions led to the formation of sulfonic acid groups. Harsher oxidation conditions than those employed may be necessary for complete oxidation to sulfonic acid groups.

Ag^+ extraction studies were carried out on the monofunctional thiol resins. Resin DQ-04-238A (Table 29) was contacted for 5 h with $AgNO_3$ at an R_i of 1.0 (thiol capacity assumed to be 4.76 mequiv/g, the difference in the starting and final chlorine capacities). The fact that very low amount of Ag^+ was absorbed by the resin (0.9%) may be attributed to the resin's hydrophobic nature. Indeed, a major drawback of all thiol resins for metal ion extraction is their low accessibility due to the hydrophobic polymer matrix.[52] This conclusion is supported by the observation that the % Ag^+ absorbed increased to 10.8% when determined on a crushed thiol resin.

Although sulfur substitution of the benzyl chloride groups with a sulfur ligand is suggested by the characterization results on the thiol and thiol phosphonic resins, it was not determined whether the groups were present as thiols or disulfides. Conclusive proof of the reaction products may be obtained by IR and sulfur elemental analyses.

Attempted Synthesis of a Phosphinate Monoester Resin

The synthesis of a phosphinate monoester from a phosphinic acid was undertaken. This resin represents a new type of dual mechanism bifunctional polymer. In contrast to the Class I DMBP, the phosphinate

monoester resin would have a coordinative interaction as the access mechanism rather than an ion-exchange reaction; the recognition mechanism would be provided by the P-H bond through selective metal ion reduction. Unfortunately, several attempts to prepare this resin were unsuccessful. The synthetic conditions and reaction results are summarized in Table 30.

The first synthesis involved reaction of the phosphinic resin with triethylphosphite:

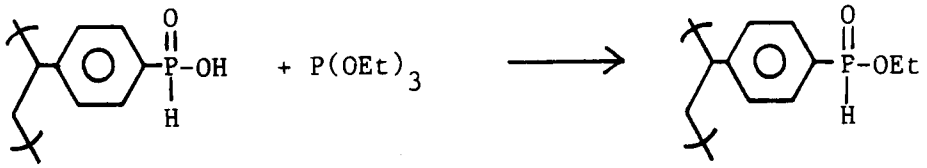

The phosphinic resin was first azeotroped in heptane to dehydrate it and was then reacted with $P(OEt)_3$ in dioxane solvent. The reaction was maintained at 60 °C for 19.5 h. The second reaction was carried out at 100 °C for 19.5 h in neat $P(OEt)_3$. The reaction time for the third esterification attempt was increased to 114 h using a reaction temperature of 86 °C. As indicated by the acid capacities reported in Table 30, none of these reactions with $P(OEt)_3$ led to esterification of the phosphinic resin.

Another attempt at esterification involved treatment of the phosphinic resin with ethanol in the presence of the dehydrating agent dicyclohexylcarbodiimide (DCC):

Table 30

Attempted Synthesis of Phosphinate Ester Resins

Resin	Reactant	Rxn temp.	Rxn time	tot(OH) mequiv/g	
				initial	final
DQ-04-276	$P(OEt)_3$[a]	60	19.5	4.98	4.85
DQ-04-280	$P(OEt)_3$[b]	100	19.5	4.98	4.93
DQ-04-283	$P(OEt)_3$[a]	86	114	4.98	4.88
DQ-05-099	DCC/EtOH	79	24	4.96	4.70

[a] In dioxane solvent.
[b] Neat.

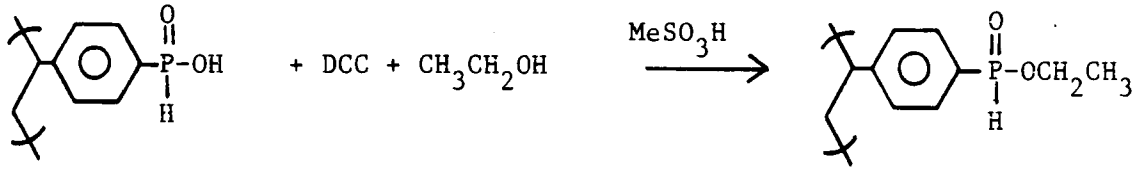

This reaction was carried out on azeotroped resin in ethanol solvent in the presence of a small amount of methanesulfonic acid catalyst. The reaction was refluxed at 79 °C for 24 h. After reaction, the beads were soxhleted in ethanol to remove any dicyclohexylurea formed in the reaction. After full conditioning, the resin's acid capacity was determined to be 4.70 mequiv/g, in close agreement with the capacity of the original phosphinic acid resin (Table 30). This result shows that no esterification of the phosphinic resin was achieved. The most probable cause for failure of the reactions is limited reagent accessibility into the resin matrix. Future work on this synthesis should include a model reaction of a small molecule phosphinic acid with both DCC and $P(OEt)_3$ to determine if in fact limited reagent accessibility prevents resin esterification.

CHAPTER III

COMPLEXATION OF LANTHANIDES AND ACTINIDES WITH CLASS I AND CLASS II DUAL MECHANISM BIFUNCTIONAL POLYMERS

Introduction

The selective recovery of lanthanide and actinide ions from aqueous solutions is important for both environmental and economic considerations. Solvent extraction of these ions from aqueous solutions has been extensively investigated.[100] This chapter details the ability of some Class I and Class II DMBP's to complex trace quantities of some lanthanide and actinide ions. The extraction of Eu^{3+}, Th^{4+}, UO_2^{2+}, Pu^{4+} and Am^{3+} has been studied using the phosphinic acid resin in various nitric acid solutions, both at varying and constant ionic strength. Oftentimes, the aqueous waste stream contains only a trace quantity of the desired metal in a background of innocuous ions such as sodium. Therefore, the resin's ability to complex the targeted metal ion in the presence of excess sodium ions was investigated. The mechanisms and results of metal ion extraction by the phosphinic acid resin were compared to that of the strongly acidic sulfonic resin.

Radiotracer Analysis

A radiotracer technique was used to carry out the trace-level metal ion studies. In these experiments, enough resin to yield one milliequivalent of active sites was contacted with 5-mL of a background solution which varied in nitric acid concentration. When constant ionic

strength was desired, enough $NaNO_3$ was added to the solution to give a 4M nitrate background. To the background solution and resin, a trace level of the radioactive lanthanide or actinide metal ion was added. The concentration of metal was estimated to be no greater than 10^{-10}M. After the metal-containing solution was equilibrated with the resin, a 1-mL aliquot was removed and counted using either an alpha or gamma scintillation counter depending on the type of radiation emitted by the radioisotope. To determine the amount of metal absorbed by the resin from the solution, the sample counts per minute (cpm_f) were compared to those of a blank (cpm_i). The percentage of metal ions absorbed by the resin was thus given by:

$$\% \text{ abs} = [(cpm_i - cpm_f)/cpm_i] [100\%]$$

The amount of metal extracted by the resin can also be expressed by a distribution coefficient, D. This quantity is defined as the ratio of metal absorbed by the resin per gram of resin to the amount of metal remaining in solution per milliliter of solution. For these experiments, D was calculated as follows:

$$D = 5[cpm_i - cpm_f]/[(cpm_f)(\text{g of resin})]$$

Log D vs. pH Plots

The trace-level metal ion extraction data was analyzed by plotting the log of the distribution coefficient versus the equilibrium solution pH. The slope of the linear plot provides information as to the

mechanism of metal ion extraction. Working from the equilibrium constant expression for the ion-exchange reaction, the relationship of log D to pH can be determined. The ion-exchange reaction is given by:

$$M^{n+} + nA^- + n\overline{R\text{-}H} \rightleftharpoons \overline{R_n\text{-}M} + nH^+ + nA^-$$

where
M^{+n} = metal ion in aqueous phase
A^- = counterion of M^{+n}
$\overline{R\text{-}H}$ = resin in protonated form
$\overline{R_n\text{-}M}$ = resin in metal-exchanged form

The equilibrium constant for this reaction is thus:

$$K_{eq} = \frac{[\overline{R_n\text{-}M}]\ [H^+]^n}{[M^{n+}]\ [\overline{R\text{-}H}]^n} = \frac{D\ [H^+]^n}{[\overline{R\text{-}H}]^n}$$

Taking the logarithm of each side and rearranging leads to:

$$\log K_{eq} = \log D + n\ (\log[H^+] - \log[\overline{R\text{-}H}])$$

At trace levels of metal ions, the term $[\overline{R\text{-}H}]$ remains constant so that:

$$\log D = -n \log [H^+] + \log K_{eq} + \text{constant}$$

Given that $pH = -\log[H^+]$, then:

$$\log D = n\ pH + \log K_{eq} + \text{constant}$$

Thus, for extraction by ion exchange, the slope of the log D vs. pH plot is equal to the number of protons exchanged by the resin for each metal ion transferred onto the resin phase. As will be seen later, values of n which are less than the valence of the metal ion may indicate that an extraction mechanism other than ion exchange is operating, such as coordination of the neutral metal salt.

Determination of Solution pH

For background solutions without added $NaNO_3$, no change in pH from that of the initial solution is expected after equilibration with the resin because only a trace amount of protons are released into solution upon metal exchange with the resin. When $NaNO_3$ is added to the solution, however, exchange of the resin protons for sodium ions can significantly lower the pH from that of the original solution. Furthermore, the solution pH cannot be measured with a pH meter because of interference from the excess sodium ions. Thus, titrimetry was used to determine the equilibrium solution pH. Enough resin to contain one milliequivalent of active sites was contacted for 17 h with 5 mL of each of the following solutions which were also 10^{-4}N in ferric, manganese or mercuric nitrate: 4M HNO_3; 2M HNO_3; 1M HNO_3; 0.2M HNO_3; 2M HNO_3/2M $NaNO_3$; 1M HNO_3/3M HNO_3; and 0.2M HNO_3/3.8M $NaNO_3$. Following the equilibration period, a portion of the solution was removed and titrated with 0.1 M NaOH. The results for the phosphinic, sulfonic, and monoester resins are presented in Table 31. As anticipated, no decrease in pH was observed for any of the resins in the absence of $NaNO_3$. Furthermore, the solution pH did not decrease from that of the initial solution for

Table 31

Determination of Solution pH After Equilibration with Sulfonic, Phosphinic, and Monoester Resins[a]

Resin	Solution Concentration, N			-log[H^+] (titrated)	
	$M^{n+}(NO_3)_n$	HNO_3	$NaNO_3$	initial	after equilibration
	1×10^{-4} $Mn(NO_3)_2$	4.0	0	-0.60[b]	-0.58
phosphinic	1×10^{-4} $Mn(NO_3)_2$	2.0	0	-0.30[b]	-0.28
	1×10^{-4} $Mn(NO_3)_2$	1.0	0	0.00[b]	0.02
	1×10^{-4} $Mn(NO_3)_2$	0.2	0	0.70[b]	0.68
	1×10^{-4} $Hg(NO_3)_2$	4.0	0	-0.60	-0.58
phosphinic	1×10^{-4} $Hg(NO_3)_2$	2.0	2.0	-0.29	-0.27
	1×10^{-4} $Hg(NO_3)_2$	1.0	3.0	0.00	0.02
	1×10^{-4} $Hg(NO_3)_2$	0.2	3.8	0.70	0.69
	1×10^{-4} $Fe(NO_3)_2$	4.0	0	-0.59	-0.59
sulfonic	1×10^{-4} $Fe(NO_3)_2$	2.0	0	-0.29	-0.29
	1×10^{-4} $Fe(NO_3)_2$	1.0	0	0.00	0.02
	1×10^{-4} $Fe(NO_3)_2$	0.2	0	0.69	0.69
	1×10^{-4} $Hg(NO_3)_2$	4.0	0	-0.60	-0.59
sulfonic	1×10^{-4} $Hg(NO_3)_2$	2.0	2.0	-0.29	-0.30
	1×10^{-4} $Hg(NO_3)_2$	1.0	3.0	0.00	-0.05
	1×10^{-4} $Hg(NO_3)_2$	0.2	3.8	0.20	0.45
	1×10^{-4} $Hg(NO_3)_2$	4.0	0	-0.60	-0.57
monoester	1×10^{-4} $Hg(NO_3)_2$	2.0	2.0	-0.29	-0.26
	1×10^{-4} $Hg(NO_3)_2$	1.0	3.0	0.00	0.03
	1×10^{-4} $Hg(NO_3)_2$	0.2	3.8	0.70	0.74

[a] 17-h equilibration period used.

[b] Calculated values for -log[H^+] given; initial solutions were not titrated.

the moderately acidic phosphinic and monoester resins in the presence of $NaNO_3$. In contrast, the strongly acidic sulfonic resin exchanged protons for sodium ions in both the 1M HNO_3/3M $NaNO_3$ and 0.2M HNO_3/3.8M $NaNO_3$ solutions, as evidenced by the decreases in pH from that of the initial solutions. The equilibrium solution pH of -0.05 corresponds to exchange of 61% of the available protons on the sulfonic resin with sodium ions in the 1M HNO_3/3M $NaNO_3$ solution; in the 0.2M HNO_3/3.8M $NaNO_3$ solution, the pH value of 0.45 indicates that 77% of the resin protons exchanged for sodium ions. The results of this study were used as a guideline to determine the equilibrium solution pH values in all the trace-level lanthanide and actinide studies. In the solutions without $NaNO_3$, the equilibrium solution pH was determined to be the same as the initial solution pH. Additionally, for the moderately acidic resins in the presence of $NaNO_3$, the final solution pH was assumed to be the same as that of the initial solution. However, the equilibrium solution pH for the sulfonic resin was calculated from the fact that 61% of the available protons exchanged for sodium in the 1M HNO_3/3M $NaNO_3$ solution and 77% exchanged for sodium in the 0.20M HNO_3/3.8M $NaNO_3$ solution.

Complexation of Europium and Americium by Phosphinic and Sulfonic Resins

The time required to reach equilibrium in trace-level lanthanide and actinide extraction by phosphinic and sulfonic resins was established. Presented in Table 32 are the results of Eu extraction at equilibration periods of 2, 17, 41, and 65 h for the two resins. Background solutions of 4M HNO_3, 0.2M HNO_3 and 0.2M HNO_3/3.8M $NaNO_3$ were employed for the phosphinic resin. Extractions using the sulfonic resin

Table 32

Equilibration Time Study on Europium Extraction
by Phosphinic And Sulfonic Resins

Resin	Bkg. Solution	time (h)	log (D)	% Abs
phosphinic	4M HNO_3	2	0.70	16.75
		17	1.32	45.94
		41	1.45	54.12
		65	1.52	56.71
phosphinic	0.2M HNO_3	2	2.81	98.86
		17	3.39	99.06
		41	3.24	98.77
		65	3.81	99.64
phosphinic	0.2M HNO_3/3.8M $NaNO_3$	17	3.09	97.86
		65	3.29	98.79
sulfonic	4M HNO_3	2	0.72	17.11
		17	0.84	20.70
		41	0.75	18.15
		65	0.98	27.79
sulfonic	0.05M HNO_3	2	3.22	98.46
		17	3.09	97.99
		41	3.34	98.87
		65	3.61	99.40

were carried out in 4M HNO_3 and 0.05M HNO_3. The results for the sulfonic resin show that equilibrium was reached in as little as 2 h for both concentrations of nitric acid. An equilibration period of between 2 and 17 h, however, was required for the phosphinic resin. The results at varying HNO_3 concentrations for both resins indicate that the time to reach equilibrium was independent of solution acidity within the time frame studied. Moreover, further equilibration time was not required by the phosphinic resin upon the addition of excess sodium ions. In light of these findings, a standard 17-h contact time was established to ensure that equilibrium was attained in all lanthanide and actinide extraction studies.

The complexing ability of the phosphinic and sulfonic resins for Eu and Am are illustrated in Figures 40 and 41. The log D's were determined over a pH range of -0.78 to +0.70 (6M to 0.2M HNO_3) at both varying and constant ionic strength. At pH values greater than approximately 0.70, the distribution coefficient decreased for the extraction of both metals. For example, in Am extraction, the log D values decreased from 3.76 and 4.80 at pH 0.70 (0.2M HNO_3) for the phosphinic and sulfonic resins, respectively, to 3.33 and 3.24 at pH 1.30 (0.05M HNO_3). Similar results were obtained for Eu extraction. These results are confirmed by solvent extraction studies in which the complexation of Am and Eu from HNO_3 by TOPO was found to be a maximum at approximately 0.25M HNO_3.[100] The decline in distribution coefficient in

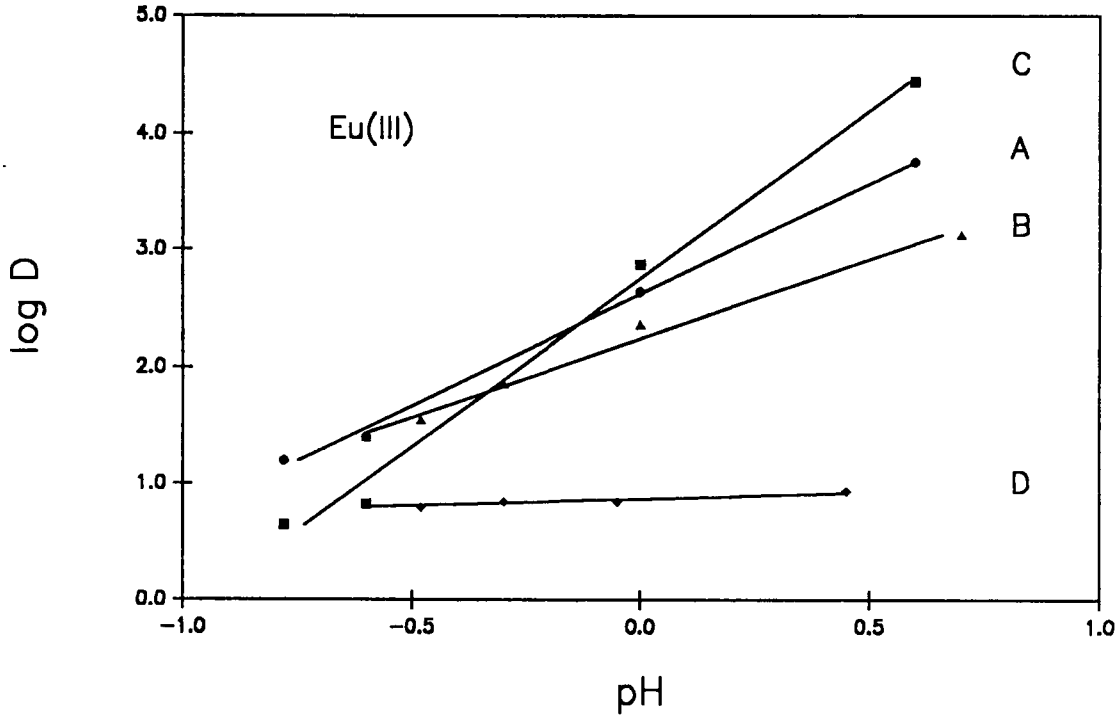

Line A: phosphinic resin, varying [HNO_3], slope = 1.9.
Line B: phosphinic resin, constant [NO_3^-], slope = 1.3.
Line C: sulfonic resin, varying [HNO_3], slope = 2.9.
Line D: sulfonic resin, constant [NO_3^-].

Figure 40. Europium extraction by phosphinic and sulfonic resins.

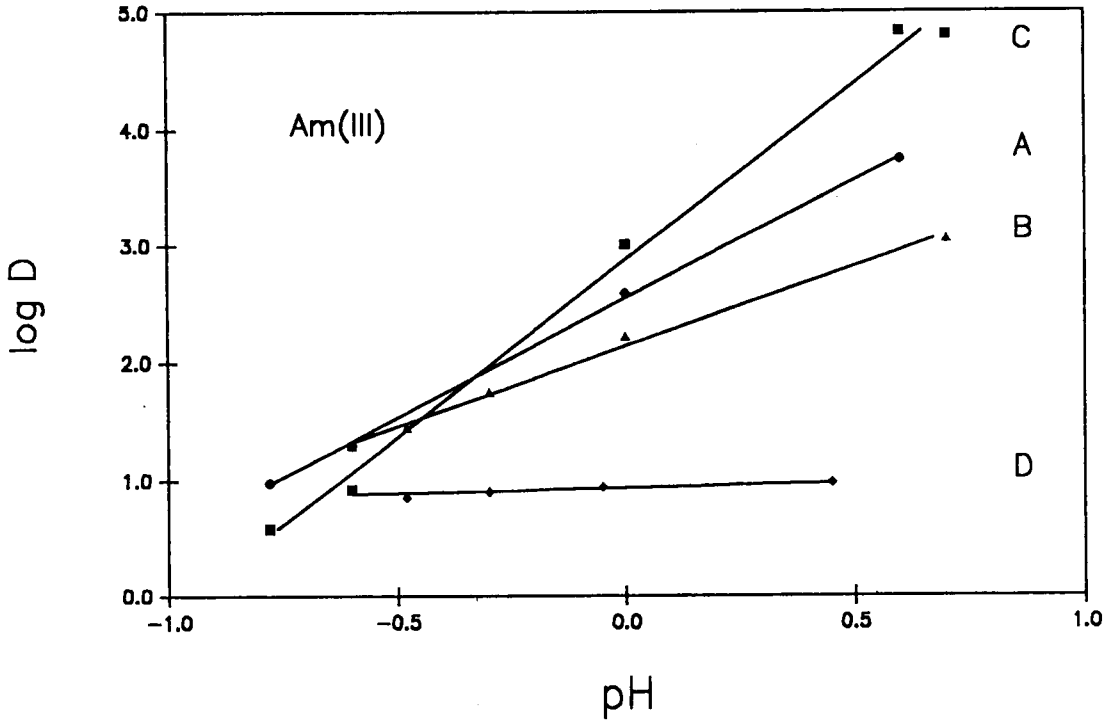

Line A: phosphinic resin, varying [HNO_3], slope = 2.0.
Line B: phosphinic resin, constant [NO_3^-], slope = 1.4.
Line C: sulfonic resin, varying [HNO_3], slope = 3.0.
Line D: sulfonic resin, constant [NO_3^-].

Figure 41. Americium extraction by phosphinic and sulfonic resins.

the higher pH region is most likely the result of metal ion hydrolysis as represented below:

$$M(H_2O)^{n+} \rightleftharpoons M(OH)^{(n-1)+} + H^+$$

Formation of metal hydroxide complexes can then give rise to polynuclear hydroxy complexes as the pH is further increased:

$$2M(OH) \rightleftharpoons MOM + H_2O$$

Once these metal hydroxide species have precipitated, they have little tendency for extraction, thus resulting in a decrease in the distribution coefficient.

In the log D vs. pH plots, lines A and C represent metal ion extraction from solutions of varying nitric acid concentration for the phosphinic and sulfonic resins, respectively; lines B and D denote extraction from solutions of constant 4M nitrate background through the addition of $NaNO_3$. Whereas the results for both metals are similar, the extraction behavior of the two resins is notably different. Complexation of both metals by the sulfonic resin from solutions of varying acidity (line C) occurs by an ion-exchange process as indicated by the slopes of 2.9 for Eu and 3.0 for Am. The ion-exchange reaction for the sulfonic resin is illustrated below:

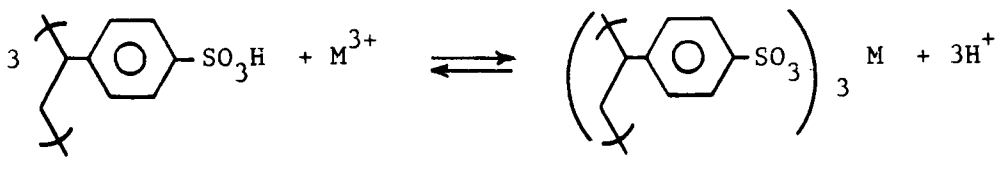

This behavior is contrasted by the phosphinic resin which gives a slope of 1.9 for Eu and 2.0 for Am. These results suggest that the phosphinic resin, due to its ability to coordinate the neutral trinitrate salt via the phosphoryl oxygen, extracts Eu and Am by a mix of coordination and ion-exchange as depicted below:

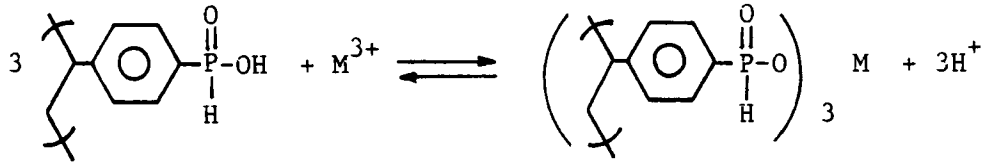

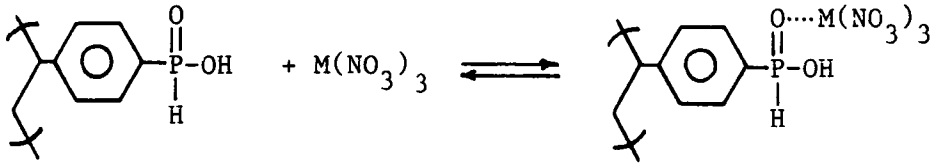

The extraction of metal salts by coordination to the phosphoryl oxygen of the phosphinic acid resin most likely occurs in the same manner as for neutral phosphorus liquid extractants such as TBP and TOPO. A slope of 3 for the log D vs. pH plot would be expected for the ion-exchange process alone; if coordination was the sole extraction mechanism, a slope of zero would be anticipated. The slopes of 1.9 and 2.0 imply that the two extraction processes occur in a given ratio to yield the observed slopes. An alternate explanation for the slopes of 2 is extraction of the mononitrate salts $EuNO_3^{2+}$ and $AmNO_3^{2+}$ by the phosphinic resin. The sulfonic results, however, clearly indicate extraction of the trivalent cation under the same conditions. The importance of the coordinative component of the phosphinic resin was also indicated by its

superior performance in the lowest pH regions. Whereas the ion-exchange reaction was suppressed in the highly acidic solutions, the coordination mechanism is not affected. This is evidenced by the higher log D values for the phosphinic over the sulfonic in the low pH regions. The sulfonic resin only outperformed the phosphinic at pH values greater than about -0.4 for Am extraction and -0.2 for Eu extraction.

A striking contrast in behavior between the phosphinic and sulfonic resins was observed at constant nitrate concentration (lines B and D) in the extraction of Am and Eu. Whereas the log D declined only slightly for the phosphinic resin upon the addition of excess sodium ions, a large decrease in log D was observed for the sulfonic resin. The phosphinic resin thus exhibited much greater selectivity for Am and Eu over sodium than the sulfonic resin. The strongly acidic sulfonic resin was unable to distinguish between the targeted metal ion and a sodium ion and thus became saturated with sodium ions which were present in large excess. The differences in reaction free energies for ion exchange of Na, Am and Eu with the sulfonic resin are not sufficient for selectivity to be observed. As with the experiment at varying nitric acid, the slope values observed for the phosphinic resin at constant ionic strength (1.3 for Eu and 1.4 for Am) were significantly lower than the value expected for extraction by ion exchange alone. These results indicate that the previous observations in varying nitric acid were not merely due to the changing ionic strength of the solution and that extraction also occurred by both ion exchange and coordination in the presence of excess sodium ions.

Complexation of Uranium by Phosphinic and Sulfonic Resins

The results of uranyl nitrate extraction by phosphinic and sulfonic resins are presented in Figure 42. As with Am and Eu, widely disparate results were obtained for the two resins. For the phosphinic resin, the slopes of the log D vs. pH plots were found to be 0.01 in HNO_3 alone (line A) and 0.06 at constant ionic strength (line B). The insensitivity of the distribution coefficient on the solution pH indicates that the phosphinic resin extracts uranium solely by coordination. The resin complexed slightly more uranium in the presence of added $NaNO_3$ than in HNO_3 alone. This result may be due to the fact that the addition of $NaNO_3$ favors the formation of the neutral uranyl nitrate salt, hence increasing the amount of uranium that can be extracted by coordination. The plot of log D vs. pH for the sulfonic resin in solutions without added $NaNO_3$ gave a slope of 1.0 in the lower pH region; only at pH values greater than -0.30 did the slope increase to the expected value of 2. These findings suggest that even the weakly basic sulfonyl oxygen was capable of some coordination of uranyl nitrate in the most highly acidic solutions. As the nitric acid concentration decreased, however, ion exchange occurred exclusively to give the predicted slope of 2. The insensitivity of the coordination mechanism to added $NaNO_3$ in the pH range of -0.6 to -0.3 is indicated by the very small decrease in log D upon the addition of $NaNO_3$ (cf. lines C and D). This result can be contrasted to those for Eu and Am (Figures 40 and 41) in which much larger decreases in log D were observed for the sulfonic resin in the presence of excess sodium ions. The phosphinic resin, through its superior coordinative ability, again showed higher log D

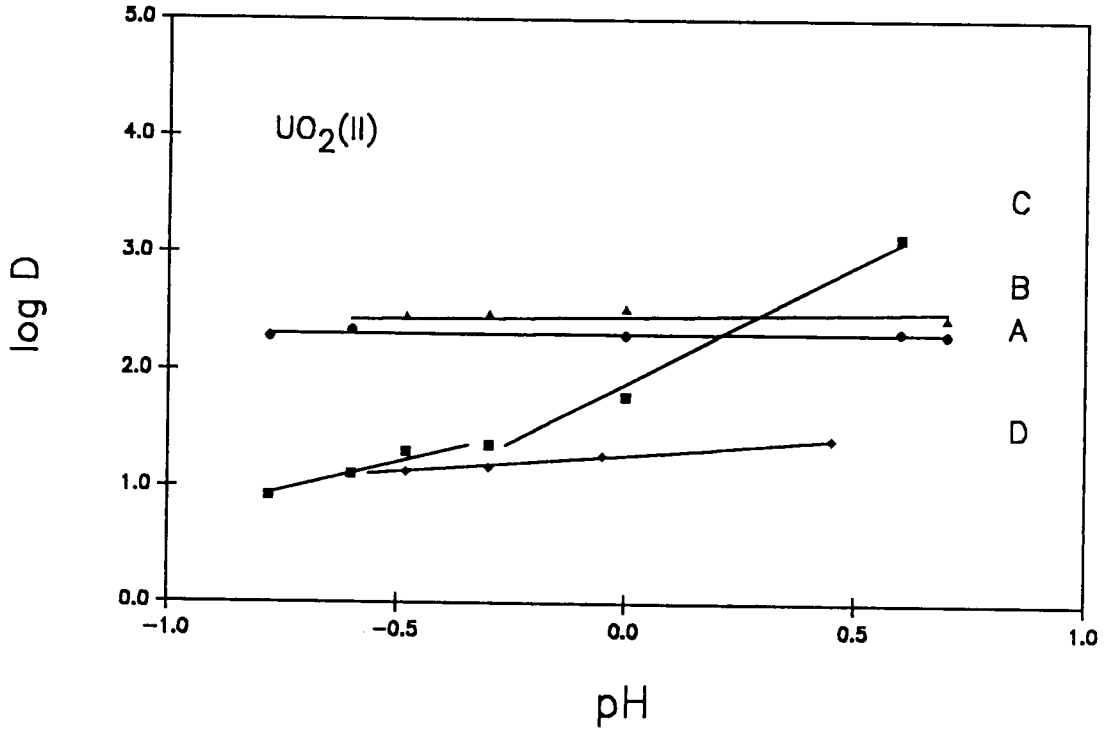

Line A: phosphinic resin, varying [HNO_3], slope = 0.01.
Line B: phosphinic resin, constant [NO_3^-], slope = 0.06.
Line C: sulfonic resin, varying [HNO_3], slope = 0.96 → 2.02.
Line D: sulfonic resin, constant [NO_3^-].

Figure 42. Uranium extraction by phosphinic and sulfonic resins.

values in the most acidic solutions. For example, the log D was 2.28 for the phosphinic resin in 6M HNO_3, whereas for the sulfonic resin it was 0.92. Only at HNO_3 concentrations greater than about 0.5M did the sulfonic resin outperform the phosphinic.

Complexation of Thorium by Phosphinic and Sulfonic Resins

Thorium extraction results for the phosphinic and sulfonic resins are shown in Figure 43. As with Eu and Am, the distribution coefficients decreased for both resins at pH values greater than approximately 0.7, presumably due to metal ion hydrolysis. A slope of 2.5 rather than the expected value of 4 was found for the extraction of Th by the sulfonic resin from solutions of varying HNO_3 concentration. Peppard and Mason have reported the extraction of Th in the form of both mono- and dinitrate salts by mono-acidic organophosphorus extractants from nitric acid media.[101] The results for the sulfonic resin suggest that extraction of both salts occurred in a proportion to give the slope of 2.5. The phosphinic resin operated primarily by a coordinative mechanism as indicated by the slopes of 0.40 and 0.49 for solutions of varying and constant ionic strength, respectively. The phosphinic's coordinative mechanism was also evidenced by its insensitivity to the addition of sodium ions and its better performance over the sulfonic resin in highly acidic solutions. As with the other metal ions studied, thorium absorption by the sulfonic resin was greatly diminished in the presence of excess sodium ions.

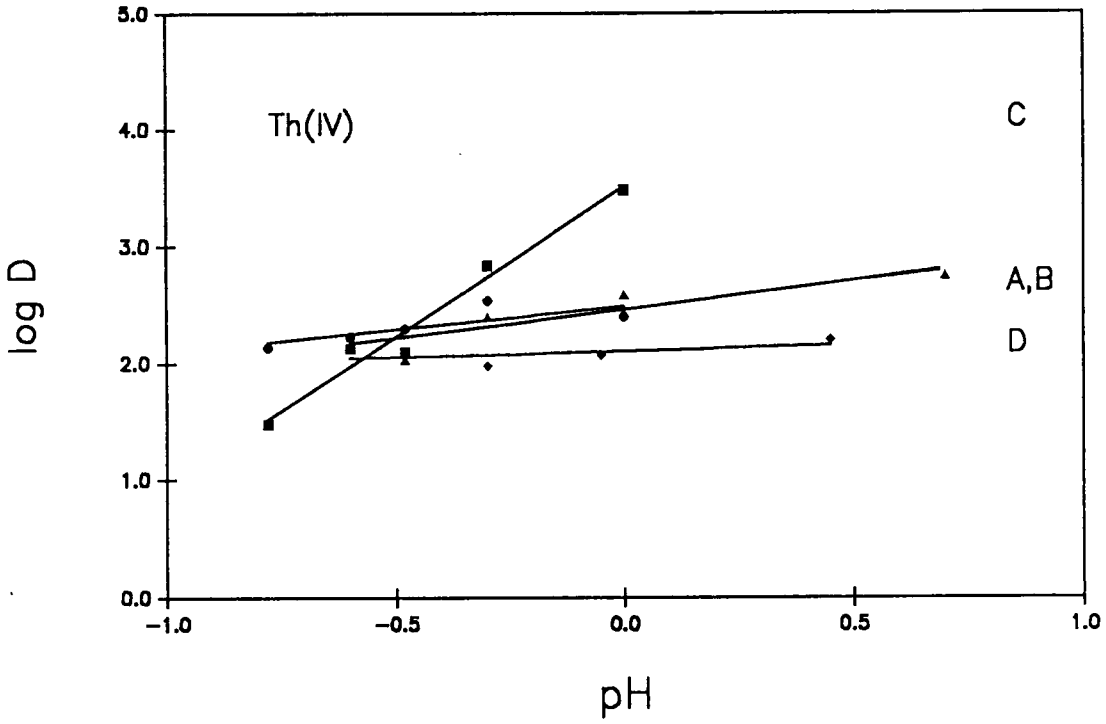

Line A: phosphinic resin, varying [HNO_3], slope = 0.40.
Line B: phosphinic resin, constant [NO_3^-], slope = 0.49.
Line C: sulfonic resin, varying [HNO_3], slope = 2.6.
Line D: sulfonic resin, constant [NO_3^-].

Figure 43. Thorium extraction by phosphinic and sulfonic resins.

Complexation of Plutonium by Phosphinic and Sulfonic Resins

Analysis of plutonium extraction data is complicated by its complex solution chemistry. For example, Pu^{4+} can hydrolyze to form $PuOH^{3+}$ and polynuclear ions, although at low concentrations formation of polynuclear species is unlikely. Furthermore, disproportionation of quadrivalent plutonium to the following oxidation states is known to occur at low acidity:[102]

$$3Pu^{4+} + 2H_2O \rightleftarrows PuO_2^{2+} + 2Pu^{3+} + 4H^+$$

$$2Pu^{4+} + 2H_2O \rightleftarrows PuO_2^{+} + Pu^{3+} + 4H^+$$

$$PuO_2^{+} + Pu^{4+} \rightleftarrows PuO_2^{2+} + Pu^{3+}$$

Thus all four oxidation states of plutonium can be simultaneously present in solution. Probably as a result of these complicating factors, interpretation of the log D vs. pH plots for Pu extraction was not instructive. Some general conclusions regarding Pu complexation by the phosphinic and sulfonic resins, however, were drawn from the data in Table 33. In contrast to the sulfonic resin, the extraction of Pu by the phosphinic resin was unaffected by the addition of excess sodium ions. For instance, in the 1M HNO_3 solution, the amount of Pu absorbed by the phosphinic decreased by only 7% when 3M $NaNO_3$ is added, whereas a 70% decline in % absorbed was observed for the sulfonic resin in the same solutions. The data also point to a slight advantage for the phosphinic resin in highly acidic solutions: 50% of the Pu was absorbed by the phosphinic resin in 6M HNO_3 compared to 39% for the sulfonic.

Table 33

Plutonium Extraction by Phosphinic and Sulfonic Resins

Resin	No Na^+			with Na^+		
	$[HNO_3]$	log D	% Abs	$[HNO_3]/[NaNO_3]$	log D	% Abs
phosphinic	6.0	1.41	49.9			
	4.0	1.57	59.1			
	3.0	1.52	56.1	3.0/1.0	2.04	81.2
	2.0	1.76	69.7	2.0/2.0	1.52	56.4
	1.0	2.28	88.0	1.0/3.0	2.04	81.2
	0.25	2.38	90.4			
	0.20	2.06	80.4	0.20/3.8	2.50	92.7
	0.05	1.65	64.3			
sulfonic	6.0	1.27	39.0			
	4.0	1.22	55.1			
	1.0	2.87	96.6	1.0/3.0	0.99	27.4
	0.25	2.80	96.0			
	0.20	3.34	98.8	0.20/3.8	0.76	18.0
	0.05	2.65	94.6			

The Am^{3+}, Eu^{3+}, UO_2^{2+}, Th^{4+} and Pu^{2+} results clearly demonstrate the superiority of the phosphinic resin over the sulfonic in complexing trace levels of these ions from background solutions containing both excess sodium ions and high concentrations of nitric acid. The strong coordinative ability of the phosphoryl oxygen accounts for its advantage in highly acidic solutions. Its enhanced ion-exchange selectivity and coordinative ability also result in its superiority in $NaNO_3$ solutions.

Complexation of Uranium by the Mixed Ester Resin

The results of uranyl nitrate extraction for mixed ester, phosphinic and sulfonic resins at both varying and constant ionic strength are presented in Figure 44. The mixed ester resin contained the following distribution of functional groups: 72% diester, 4.4% monoester and 23.6% diacid. Slightly higher levels of uranium were extracted by the mixed ester than by the phosphinic. In contrast to the phosphinic results which were completely independent of pH, a small effect of solution acidity on log D values was observed for the mixed ester resin (slopes of 0.31 and 0.10 at varying and constant ionic strength, respectively). The higher slopes for the mixed ester suggest that a slight amount of ion-exchange of UO_2^{2+} occurred in addition to coordination of neutral metal salt, $UO_2(NO_3)_2$. As previously indicated, the sulfonic resin combines ion-exchange and coordination mechanisms at pH values less than zero, whereas in the pH range of zero to 0.7, complexation occurs solely by ion-exchange (slope = 1.9). The strong coordinative ability of the phosphoryl oxygen was again indicated in the

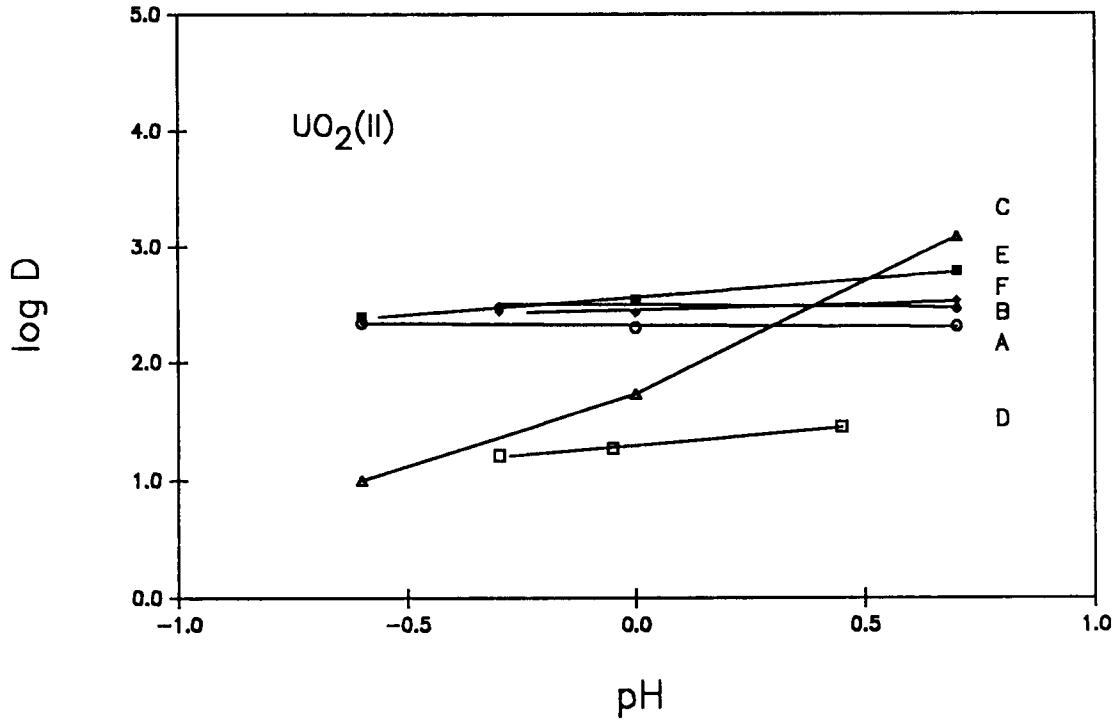

Line A: phosphinic resin, varying [HNO_3], slope = -0.02.
Line B: phosphinic resin, constant [NO_3^-], slope = -0.03.
Line C: sulfonic resin, varying [HNO_3], slope = 1.2 → 1.9.
Line D: sulfonic resin, constant [NO_3^-].
Line E: mixed ester resin, varying [HNO_3], slope = 0.3.
Line F: mixed ester resin, constant [NO_3^-], slope = 0.1.

Figure 44. Uranium extraction by mixed ester, phosphinic and sulfonic resins.

region of lowest pH where both the mixed ester and phosphinic resin surpassed the sulfonic.

The phosphorus-based resins exhibit a decided advantage over the sulfonic when extracting uranium from solutions containing excess sodium ions. For instance, upon the addition of 3M $NaNO_3$ to a 1M HNO_3 solution, the log D values increased from 2.30 to 2.53 for the phosphinic resin and decreased modestly from 2.54 to 2.43 for the mixed ester; by contrast, the log D declined from 1.73 to 1.27 for the sulfonic resin under the same conditions. The results with the phosphinic and mixed ester resins clearly demonstrate the advantage of phosphorus-based resins for extraction of uranium from both highly acidic and sodium-containing solutions.

Effect of Ligand Acidity and Coordinative Ability on Americium Extraction

Trace-level Am extraction was investigated using the phosphinic, phosphonic, sulfonic, and monoester resins. The log D/pH correlations were determined at constant ionic strength (4M nitrate ion) through the addition of $NaNO_3$ to HNO_3 solutions ranging from 2M to 0.2M.

As shown in Figure 45, widely different results were obtained for Am extraction by the three different phosphonic resins. Resins DQ-03-002A and B^2-01-043B were both fully functionalized and possessed comparable acid and phosphorus capacities. Phosphonic resin B^2-01-082A was only partially functionalized to a phosphorus capacity of 2.15 mequiv/g. Comparison of the two resins of similar capacity shows that DQ-03-002A extracted much higher levels of Am than B^2-01-043B. The

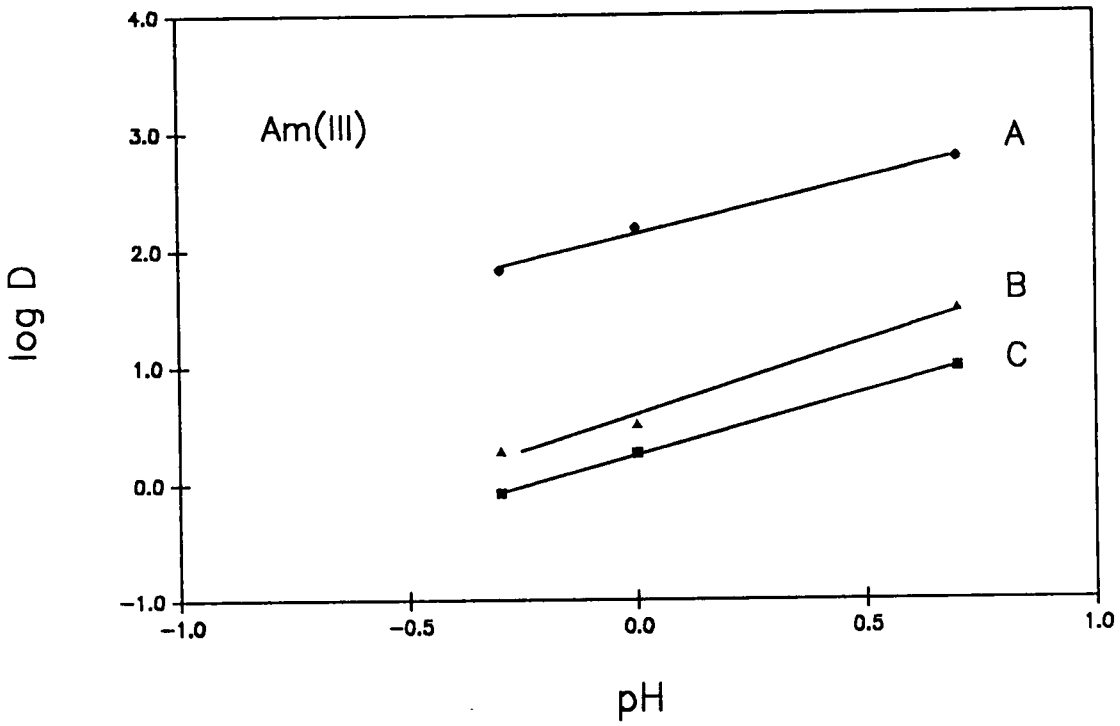

Line A: DQ-03-002A, slope = 0.93.
Line B: B^2-01-043B, slope = 1.2.
Line C: B^2-01-082B, slope = 1.1.

Figure 45. Americium extraction by phosphonic resins in the presence of excess sodium ions.

disparate extraction results may be related to the different conditioning methods used for the two resins. Phosphonic B^2-01-043B was conditioned by continuous 1 h elutions of water, 4 wt% NaOH, water, 4 wt% HCl, and water. In contrast, DQ-03-002A was conditioned using a batch process in which the resin was stirred for a 15-30 min period with 300-mL portions of water, 4 wt% NaOH, water, 4 wt% HCl and water. The batch conditioning process may have been inadequate for the removal of aluminum salts remaining in the resin pores from the functionalization reaction. Although no differences in Hg^{2+} extraction were observed for the two resins at an R_i of 1.0 (59% absorbed by B^2-01-043B and 62% absorbed for DQ-03-002A), the presence of impurities within the resin matrix appears to greatly affect trace-level metal extraction.

Figure 45 also indicates that the partially functionalized phosphonic resin B^2-01-082A extracted lower levels of Am than the fully functionalized B^2-01-043B. As discussed in Chapter II, the incompletely substituted 2% gel phosphonic resins were subject to inaccessibility of hydroxide ion into the polymer matrix. This was evidenced by tot(OH) values which were lower than twice the phosphorus capacity (e.g., tot(OH)/tot(P) = 1.60 for B^2-01-082A). The reduced accessibility of aqueous reagents into the partially functionalized polymer network may account for the lower Am extraction results. Because phosphonic resin B^2-01-043B was completely functionalized and conditioned to remove catalyst impurities, it was used in all further Am extraction studies.

Figure 46 presents the log D/pH relationships for four resins of varying ligand acidity and coordinative ability: phosphinic, phosphonic, monoester and sulfonic. As previously noted, the strongly acidic

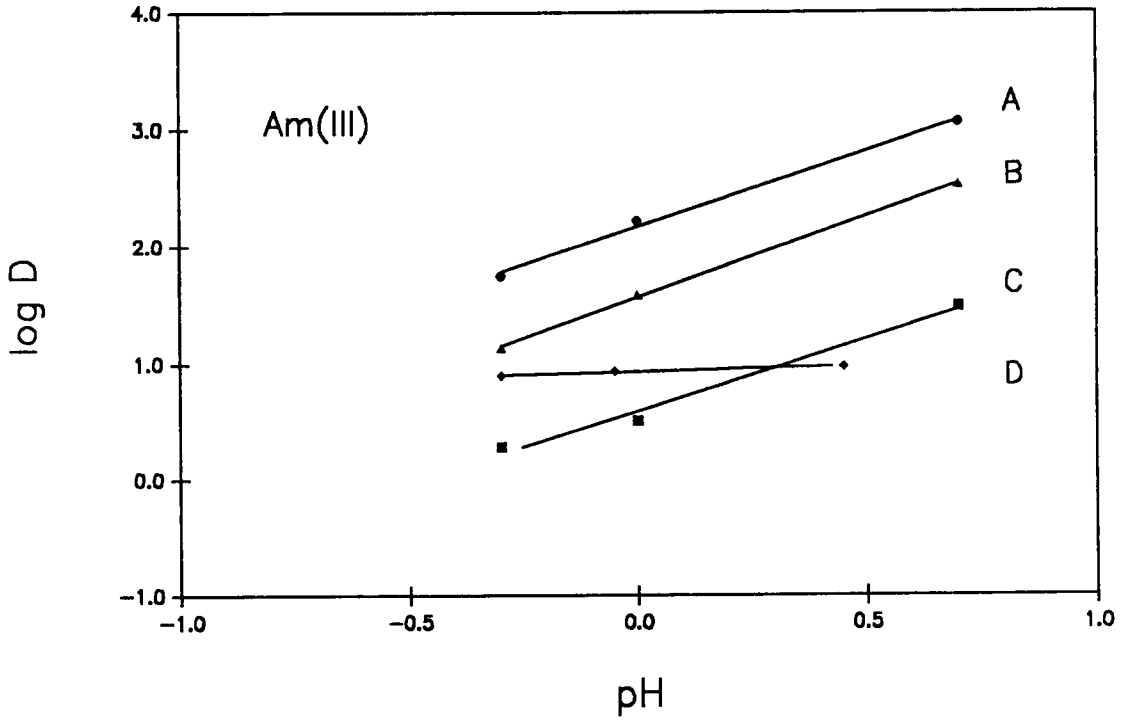

Line A: phosphinic, slope = 1.3.
Line B: monoester, slope = 1.4.
Line C: phosphonic, slope = 1.2.
Line D: sulfonic.

Figure 46. Effect of resin ligand acidity and coordinative ability on americium extraction in the presence excess sodium ions.

sulfonic resin exhibited no selectivity for Am over the excess sodium ions in solution. This non-selective behavior was contrasted, however, by the three phosphorus resins which showed a higher affinity for Am than sodium. The phosphorus-based resins had comparable slopes (1.29, 1.38 and 1.24, for the phosphinic, monoester and phosphonic, respectively), suggesting that they complex Am by a combination of ion-exchange and coordination mechanisms. Therefore, both resin ligand acidity and coordinative ability must be considered in explaining the extraction order in Figure 46. The extraction results paralleled the relative acid strength of the resins, which was estimated from model compounds to be in the order phosphinic> monoester> phosphonic (pK_a of 3.49 for phenylphosphinic acid[81], 3.83 for cyclohexylphenyl phosphonate monoester[103] and 3.96 for phenylphosphonic acid[103]).

The ability of the resins to extract Am also appears to be correlated to the degree of softness of the phosphoryl oxygen. Electron withdrawal by the two oxygens on the monoester and phosphonic resins decreases the polarizability and degree of softness of the phosphoryl oxygen relative to that of the phosphinic resin. In the monoester resin the electron withdrawal of oxygen is diminished by the electron donation of the ethyl group, thus rendering it slightly more polarizable (softer) than the phosphonic. The extraction order follows that of increasing polarizability and softness of the phosphoryl oxygen: phosphinic > monoester > phosphonic. These results are in contrast with those predicted by HSAB principles. The hard Am^{3+} cation is expected to preferentially bind with hard bases. Thus, the extraction order would be expected to decrease with increasing phosphoryl oxygen softness. The

observed results can be explained by the fact that Am is not present in the nitric acid/sodium nitrate background solutions as the bare cation but rather as the dinitrate, $Am(NO_3)_2^+$, or the neutral trinitrate salt, $Am(NO_3)_3$. The decreased charge on Am renders it softer than the bare cation and thus increases its tendency to coordinate soft bases. The Am results illustrate that differences in selectivity can be achieved through variation in P=O softness due to the electronic nature of the substituents attached to phosphorus.

Americium Extraction by Resins of Mixed Functionality

The log D/pH plots for Am extraction by mixed ester, monoester, diester, and phosphonic resins are given in Figure 47. Eight mixed ester resins of varying functional group distributions were studied as shown in Table 34. Extractions were carried out in the pH range of -0.3 to 0.7 at constant ionic stregth. With the exception of the diester, all resins were found to have slopes ranging between 1.1 and 1.3, suggesting extraction by both ion-exchange and coordination. The log D's for all of the mixed ester resins were between those of the monoester and phosphonic. As seen in Table 34 and Figure 47, the level of Am extraction generally decreased with increasing percentage of diacid groups on the mixed ester resin. Apparently, Am extraction was dominated by the monoester ligand in the absence of any diacid groups (resins II-VI). However, as the amount of phosphonic acid on the mixed ester increased (resins VII-X), the results were governed by the diacid groups, as evidenced by the further decreases in log D. The very low levels of Am complexed by the pure diester resin (XI) indicate that the

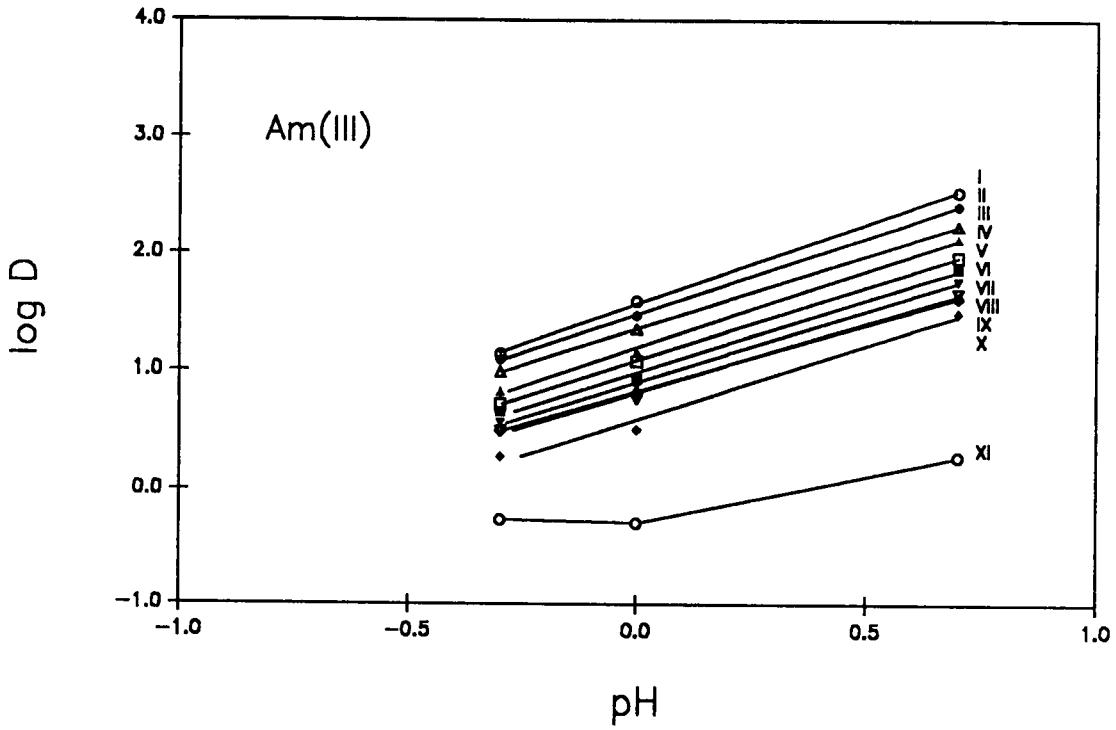

Resin I: monoester.
Resins II-IX: mixed esters (see Table 34).
Resin X: phosphonic.
Resin XI: diester.

Figure 47. Americium extraction by mixed ester, monoester, phosphonic and diethyl ester resins in the presence of excess sodium ions.

Table 34

Functional Group Percentage of Resins Studied in Americium Extraction[a]

Code	Resin	Type	%		
			diester	monoester	diacid
I	DQ-02-259D	monoester	17	83	0
II	DQ-02-284D	mixed ester	68	32	0
III	DQ-02-259A	mixed ester	77	16	7
IV	DQ-03-002D	mixed ester	82	18	0
V	DQ-02-284C	mixed ester	30	51	19
VI	DQ-03-002B	mixed ester	12	30	58
VII	DQ-03-002C	mixed ester	15	45	40
VIII	DQ-02-259C	mixed ester	7	37	56
IX	DQ-02-259B	mixed ester	16	39	45
X	B^2-01-043B	phosphonic	0	0	100
XI	DQ-03-026B	diester	95	5	0

[a] See Figure 47 for log D vs. pH plots of these resins.

diester moiety itself played no role in the extraction by mixed ester resins.

Presented in Figure 48 are the log D/pH correlations for Am extraction by amine, amine phosphonic, diester and phosphonic resins. Extractions with the mono- and bifunctional amine resins were performed on the protonated form of the resin with nitrate as the counterion. As in the previous studies, solutions of 2M to 0.2M HNO_3 were employed at a constant 4M nitrate background. The purely coordinating monofunctional amine and diester resins extracted very low levels of Am. It is possible that the poor performance of the diester resin is the result of reduced accessibility of the americium nitrate salt into the hydrophobic resin matrix. However, identical acid capacities were obtained on the diester resin in water and in dioxane, suggesting that aqueous reagent accessibility was not limited. The bifunctional amine ester resin, which outperformed both of its monofunctional counterparts, most likely extracted Am by the monoester and phosphonic acid groups present on the starting diester resin, which was only 91% esterified. Indeed, similar extraction mechanisms for the three resins are suggested by their comparable slopes (1.09, 1.24 and 1.38 for the amine ester, phosphonic and monoester resins, respectively).

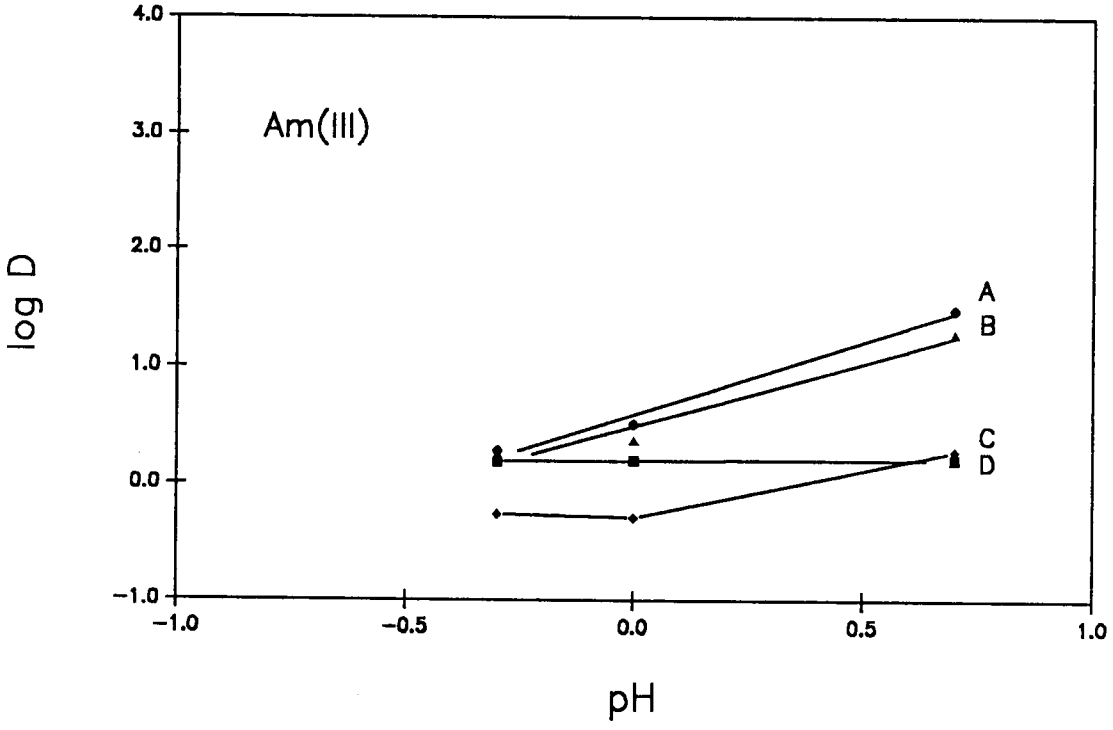

Line A: phosphonic, slope = 1.2.
Line B: amine ester, slope = 1.1.
Line C: amine, slope = 0.02.
Line D: diester.

Figure 48. Americium extraction by amine ester, amine, diethyl ester and phosphonic resins in the presence of excess sodium ions.

CHAPTER IV

COMPLEXATION OF TRANSITION METAL IONS WITH CLASS I AND CLASS II DUAL MECHANISM BIFUNCTIONAL POLYMERS

Introduction

An understanding of the polymer ligand/metal ion interactions is required for the development of resins with targeted metal ion selectivities. The aim of the research presented in this chapter is to formulate a general theory for the observed ligand-to-metal interactions of DMBP's using the principles of hard-soft acid-base theory. To this end, the complexing ability of Class I and Class II DMBP's was investigated under a variety of experimental conditions for a series of transition metal ions of varying hard-soft character.

Copper(II) Complexation by Class I and Class II DMBP's

The ability of some Class I and Class II DMBP's to extract divalent copper was investigated. The initial extraction studies employed a copper-selective electrode to measure the Cu concentration before and after resin contact. The experiment was performed using an initial $Cu(NO_3)_2$ concentration of 1×10^{-4}N ($R_i = 1 \times 10^{-3}$). Difficulties in the analysis, such as scattered mV readings for repeat samples, were encountered probably as the result of the low concentrations of Cu employed. The limit of detection for the copper electrode was found to be approximately 5×10^{-6} N, corresponding to 95%

of the initial Cu concentration. Thus, when high levels of Cu were removed from solution by the resin, the final concentration approached the limit of detection for the electrode. Furthermore, interferences from other ionic impurities in solution became more critical as the Cu concentration reached the limit of detection.[104] As a result of the limitations of the copper-selective electrode, further Cu determinations were carried out by titrimetry.

The effect of added Na ions on Cu extraction by ion-exchange/redox and ion-exchange/coordination polymers was examined. Presented in Table 35 are the results of Cu complexation at an R_i of 0.10 by amine, amine phosphonic, phosphonic, mixed ester, monoester, diester, phosphinic and sulfonic resins from solutions containing no added $NaNO_3$, 5 X 10^{-3}M $NaNO_3$ and 4M $NaNO_3$. Extractions with the dimethylamine resin were performed on both the protonated (nitrate counterion) and free amine forms of the resin. Strikingly different extraction behavior was found for the two resin forms. Extraction by the protonated resin can be considered to occur by solvation of the neutral copper nitrate molecule by the amine salt:[105]

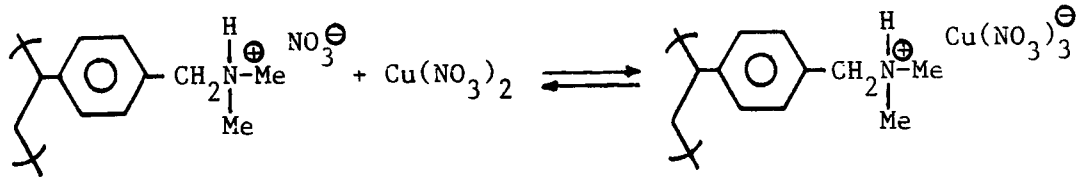

Whereas the amine salt extracted only very low levels of Cu from the background solutions containing no $NaNO_3$ and 5 X 10^{-3}M $NaNO_3$, it absorbed 48% of the Cu in the presence of 4M $NaNO_3$. Precedence for this behavior

Table 35

Effect of $NaNO_3$ on Cu(II) Extraction
by Class I and Class II DMBP's[a]

Resin Code	Type	% Absorbed		
		no $NaNO_3$	5 X 10^{-3}M $NaNO_3$	4M $NaNO_3$
B^2-01-055A	amine·HNO_3	1.2	0.4	48.4
B^2-01-055A	amine[b]	31.5	85.7	13.8
B^2-01-084	amine phosphonic[c]	92.6	92.4	20.8
B^2-01-082B	phosphonic[d]	93.5	89.5	
DQ-03-002A	phosphonic[e]	100	97.5	
B^2-01-043B	phosphonic[f]	100	98.2	14.6
DQ-02-259A	mixed ester[g]	68.8	69.9	27.2
DQ-02-259B	mixed ester[h]	100	96.2	20.9
DQ-02-259C	mixed ester[i]	100	96.3	20.8
DQ-02-259D	monoester[j]	100	95.6	35.8
DQ-02-284C	mixed ester[k]	83.0	90.0	19.9
DQ-03-002B	mixed ester[l]	100	95.9	
DQ-03-002C	mixed ester[m]	100	92.1	9.8
DQ-03-026B	diester	7.3	7.5	2.1
DQ-02-109	phosphinic	100	100	46.8
DW-01-060C	sulfonic	100	100	1.3

[a] R_i = 0.10
[b] Free-amine form
[c] Protonated form of amine used (nitrate counterion). tot(P) = 2.03 mequiv/g, TAEC = 2.20 mequiv/g
[d] Partially functionalized; tot(P) = 2.15 mequiv/g
[e] Fully functionalized; tot(P) = 3.87 mequiv/g
[f] Fully functionalized; tot(P) = 3.59 mequiv/g
[g] 77% diester, 16% monoester, 7% diacid
[h] 16% diester, 39% monoester, 45% diacid
[i] 7% diester, 37% monoester, 56% diacid
[j] 17% diester, 83% monoester
[k] 30% diester, 51% monoester, 19% diacid
[l] 12% diester, 30% monoester, 58% diacid
[m] 15% diester, 45% monoester, 40% diacid

exists in solvent extraction studies using high molecular weight amines. Horwitz and coworkers have reported that the use of high concentrations of nitrate salts as salting-out agents in the extraction of trivalent *trans*plutonium ions by tertiary and quaternary amines was required to achieve high extraction coefficients.[106] In contrast to the amine salt, the free amine form of the resin extracted the lowest amount of Cu from 4M $NaNO_3$. The mechanism of complexation by this resin likely involves the coordination of Cu through the lone electron pair on nitrogen. It is unclear why a maximum in % absorbed is obtained for the 5 X 10^{-3}M $NaNO_3$ background solution.

Comparison of the results for the amine phosphonic to those of the monofunctional amine salt and partially functionalized phosphonic resins suggests that the bifunctional resin complexes Cu through the phosphonic group alone. As with americium extraction (Figure 45, page 174), slightly lower loadings were observed for the partially functionalized phosphonic B^2-01-082A than for the fully functionalized resins DQ-03-002A and B^2-01-043B. This result can be ascribed to the accessibility limitations of the partially substituted resin. In contrast to americium extraction in which DQ-03-002A greatly outperformed B^2-01-043B, identical copper extraction results were obtained for the two phosphonic resins. Apparently the catalyst impurities remaining in the resin pores of DQ-03-002A have no effect on the extraction of macro levels of Cu ions.

Both the monoester and phosphonic resins extracted nearly 100% of the Cu ions from solutions containing no $NaNO_3$ and 5 X 10^{-3}M $NaNO_3$; conversely, the diester resin absorbed only a small percentage of Cu

from all of the solutions examined. The mixed ester results can be correlated to the amount of acidic groups present on the resin: less Cu was extracted by mixed ester resins which contain appreciable amounts of diester groups (≥30%) than by mixed esters containing a higher percentage of mono- and diacid ligands. These findings indicate the greater importance of the ion-exchange mechanism over coordination in the extraction of Cu by the ion-exchange/coordination resins.

The results in Table 35 point to a marked contrast in extraction behavior by the phosphinic and sulfonic resins. Although reduction of cupric ions to metallic copper by the phosphinic resin is possible at very long contact periods (oxidation of 80% of the P-H bonds requires 240 h[107]), it is unlikely that a significant amount of reduction occurred during the 17-h equilibration period used in this experiment. Both the phosphinic and sulfonic resins absorbed 100% of the Cu from the solution without added $NaNO_3$ and also from the solution which contained a 5-fold mole excess of Na ions over Cu ions. This result is a reflection of the ion-exchanger's preference for the divalent over monovalent cation when the monovalent ion is not present in an overwhelming excess. The more highly selective nature of the phosphinic resin over the sulfonic was evidenced by the results in 4M $NaNO_3$. When Na ions were present in an 8000-fold excess over Cu ions, the amount of Cu extracted by the sulfonic decreased dramatically to 1.3%; in contrast, the phosphinic resin still absorbed 46.8% of the Cu from solution. The sulfonic resin became saturated with excess Na ions and therefore absorbed few Cu ions.

The influence of nitric acid on the extraction of Cu by phosphonic, amine phosphonic, monoester, mixed ester and sulfonic resins was examined. The extractions were performed at an R_i of 0.10 in solutions of 2M and 0.20M HNO_3. To eliminate the influence of varying solution ionic strength, a constant 4M nitrate background was achieved by the addition of $NaNO_3$. The results in Table 36 show that Cu extraction by the phosphorus resins was severely depressed by the addition of nitric acid. For example, the phosphinic resins absorbed less than 7% of the Cu from solutions of 2M and 0.2M HNO_3 compared to 46.8% from the solution without added HNO_3. The strong dependence of the extraction results on the solution acidity suggests that the phosphorus resins extract Cu primarily by an ion-exchange reaction rather than by coordination which is insensitive to changes in solution pH.

Silver Complexation by Class I and Class II DMBP's

Presented in Table 37 are the results of Ag extraction (R_i = 0.10) from background solutions of water, 0.19M $NaNO_3$, 0.19M $NaNO_3$/0.10M HNO_3, 3.8M $NaNO_3$/0.20M HNO_3 and 2.0M $NaNO_3$/2.0M HNO_3 by some Class I and Class II DMBP's. Both the phosphinic and sulfonic resins removed nearly 100% of the Ag from a water background solution. Whereas the sulfonic can extract Ag only through ion-exchange, the phosphinic resin is also capable of reduction of Ag ions to metallic silver through the primary acid ligand. The phosphinic resin has been shown to operate exclusively by the redox process until all of the primary acid ligands (2.92 mequiv/g in this case) have been oxidized after which ion-exchange

Table 36

Effect of HNO_3 on Cu(II) Extraction
by Class I and Class II DMBP's[a]

Resin Code	Type	% Absorbed		
		4M $NaNO_3$	2M HNO_3/ 2M $NaNO_3$	0.2M HNO_3/ 3.8M $NaNO_3$
DQ-02-109	phosphinic	46.8	6.6	0
B^2-01-043B	phosphonic	14.6	0	0
B^2-01-084	amine phosphonic	20.8	3.1	0
DQ-02-259D	monoester	35.8	0.8	0
DQ-02-259A	mixed ester	27.2	7.5	0
DW-01-068C	sulfonic	1.3	3.0	0

[a] $R_i = 0.10$

Table 37

Influence of $NaNO_3$ and HNO_3 on Ag(I) Extraction by Class I and Class II DMBP's[a]

Resin Code	Type	% Abs.				
		H_2O	0.19M $NaNO_3$	0.19M $NaNO_3$ 0.01M HNO_3	3.8M $NaNO_3$ 0.2M HNO_3	2M $NaNO_3$ 2M HNO_3
DQ-02-109	phosphinic	95.9	59.1	28.0	10.4	5.8
B^2-01-043B	phosphonic	81.2	55.6	37.4	21.5	7.9
DQ-02-259D	monoester	82.4	49.5	37.5	26.2	11.0
DQ-02-259A	mixed ester[b]	59.0		16.5	12.7	13.0
DW-01-068C	sulfonic	97.3	31.0	33.0	7.6	2.0

[a] $R_i = 0.10$

[b] 77% diester, 16% monoester, 7% diacid

occurs.[75] The redox process is thus dominant over ion-exchange as a result of the resin's strong tendency to reduce Ag ions ($E°_{ox}$ = +0.50 V for $H_3PO_2 \rightarrow H_3PO_3$; $E°_{red}$ = +0.80 V for $Ag^+ \rightarrow Ag°$).[84] In this case, at an R_i of 0.10 based on total phosphorus sites, only reduction of Ag ions should occur because there exists a 6:1 surplus of P-H sites available over Ag ions. The results for the ion-exchange/coordination polymers show that the phosphonic and monoester resins removed approximately equal amounts of Ag from water, while the mixed ester resin (77% diester, 16% monoester and 7% diacid) complexed slightly lower levels of Ag. These findings indicate that the diester groups did not contribute to the extraction of Ag by the mixed ester resin. Thus, it appears that only the ion-exchange mechanism was operative in these resins under these experimental conditions.

A significant decrease in Ag extraction was observed for all the resins upon the addition of a 190:1 excess of Na to Ag ions. The large drop in % absorbed by the sulfonic resin illustrates the resin's lack of selectivity for Ag over Na ions. Smaller decreases in % absorbed were observed for the less acidic phosphonic and monoester resins, an indication of their superior Ag/Na selectivity over that of the sulfonic resin.

The percentage of Ag extracted by the phosphinic resin declined from 95.9% when performed in pure water to 59.1% in 0.19M $NaNO_3$. Previous studies on Ag extraction at an R_i of 1.0 established that the decrease in Ag absorption from sodium-containing solutions came almost completely at the expense of the redox process.[107] That is, a constant percentage of Ag was found to be extracted by ion-exchange with the

resin in both the presence and absence of added sodium ions, whereas the amount of Ag removed from solution by the redox process decreased when sodium ions were added. Although changes in reaction EMF resulting from the varying solution ionic strength should also be considered in explaining the results, it appears that sodium ions hinder the redox process by occupying the ion-exchange sites.

The results of Ag extraction by ion-exchange/redox and ion-exchange/coordination resins from a background solution of 0.19M $NaNO_3$/0.01M HNO_3 are also given in Table 37. The addition of HNO_3 to the $NaNO_3$ solution caused further decreases in Ag extraction for all resins except the sulfonic resin, which gave the same results in both solutions. The decline in % absorbed for the phosphonic, monoester and mixed ester resin resulted from a shifting of the ion-exchange equilibrium toward the reactants upon the addition of acid to the solution. The sulfonic resin, due to its greater acid strength, was less affected by the addition of acid. The phosphinic resin also showed a decrease in Ag absorption in the presence of 0.01M HNO_3. A decrease in the EMF for the redox reaction upon the addition of acid is predicted by the Nernst equation thus decreasing the amount of Ag reduced by the resin. Additionally, based on the results of the other phosphorus resins, a decrease in the % extracted by ion-exchange would also be expected for the phosphinic resin. The conclusions concerning Ag extraction by the phosphinic resin from solutions of $NaNO_3$ and HNO_3 at an R_i of 0.10 were verified by similar studies at an R_i of 0.25. For example, Ag absorption decreased from 88% when determined in pure water

to 12% in 3.8M $NaNO_3$ and further declined to 8% when carried out in 3.8M $NaNO_3$/0.20M HNO_3.

Ag extraction with Class I and Class II resins was also examined from solutions of constant ionic strength at an R_i of 0.10. As indicated in Table 37, the percentage of Ag extracted by all of the resins decreased even further in background solutions of 3.8M $NaNO_3$/0.20M HNO_3 and 2M $NaNO_3$/2M HNO_3. The decrease in Ag absorption can be attributed to the additional loss of selectivity and suppression of the ion-exchange reaction (and also the redox reaction for the phosphinic resin) in the presence of the higher levels of $NaNO_3$ and HNO_3. In contrast to the 0.10M HNO_3 results discussed previously, the sulfonic resin also showed a decline in Ag extraction at these elevated levels of added acid: a decrease in % absorbed for 7.6% to 2.0% was observed when the HNO_3 concentration increased from 0.2M to 2M.

Extraction of Ag at an R_i of 0.10 from solutions of 0.19M $NaNO_3$ and 0.19M $NaNO_3$/0.10M HNO_3 by mixed ester resins was compared to that by phosphonic, monoester and diester resins. The data in Table 38 show a slight drop in the % absorbed for all resins when 0.01M HNO_3 was added to the background solution resulting from the shift of the ion-exchange equilibrium toward the reactants thus decreasing the amount of Ag transferred onto the resin. For both background solutions, nearly equal amounts of Ag were absorbed by the monoester, phosphonic and mixed ester resins containing less than approximately 30% diester groups. As seen in Table 38, considerably lower levels of Ag were extracted by mixed ester resins DQ-02-245A and DQ-02-259A, which contained 72% and 77% diester groups, respectively, than for mixed ester DQ-02-259C which had

Table 38

Extraction of Ag(I) by Phosphonic, Monoester, Diester and Mixed Ester Resins from $NaNO_3$ and HNO_3 Solutions[a]

Resin Code	Type	% Absorbed	
		0.19M $NaNO_3$	0.19M $NaNO_3$/0.01M HNO_3
DQ-02-259D	monoester	49.5	37.5
B^2-01-043B	phosphonic	55.6	37.4
DQ-02-259C	mixed ester[b]	64.1	55.1
DQ-03-002B	mixed ester[c]	50.8	38.1
DQ-03-002C	mixed ester[d]	46.2	31.1
DQ-02-259B	mixed ester[e]	45.1	26.1
DQ-02-284C	mixed ester[f]	40.9	27.7
DQ-02-245A	mixed ester[g]	35.1	25.5
DQ-02-259A	mixed ester[h]		16.5
DQ-03-026B	diester	13.6	15.0

[a] $R_i = 0.10$
[b] 7% diester, 37% monoester, 56% diacid
[c] 12% diester, 30% monoester, 58% diacid
[d] 15% diester, 45% monoester, 40% diacid
[e] 16% diester, 39% monoester, 45% diacid
[f] 30% diester, 51% monoester, 19% diacid
[g] 72% diester, 4% monoester, 24% diacid
[h] 77% diester, 16% monoester, 7% diacid

only 7% diester groups. These results, along with those for the pure diester resin, indicate that under these experimental conditions the diester ligands play only a very limited role in the complexation of Ag.

Ag extraction was also examined for phosphonic, amine phosphonic, amine, dimethylamine/ester and diester resins. Presented in Table 39 are the results of extraction at an R_i of 0.10 from background solutions of 0.19M $NaNO_3$ and 0.19M $NaNO_3$/0.01M HNO_3. For all extractions, the amine groups were present in the protonated form with the nitrate group as the counterion. If both groups present on the bifunctional resin function independently, the amount of metal which they absorb can be predicted from the extraction results of their monofunctional analogues. If the experimental outcome exceeds that calculated from the monofunctional results, then the two groups may be operating synergistically. The predicted % absorbed values can be calculated in the following manner for Ag extraction from 0.19M $NaNO_3$ by the amine phosphonic resin. The contribution of the amine groups to the amount of Ag absorbed by the bifunctional resin is determined to be 26.7% based upon the amount of Ag absorbed by the pure amine resin (55.6%) and the fraction of the amine groups on the bifunctional resin (0.48). Likewise, the contribution by the phosphonic ligands is computed to be 6.1%. Thus, a value of 32.8% absorbed is predicted for the independent operation of the two functional groups, a result slightly lower than the experimental value of 41.8%. Similarly, for Ag extraction by the amine phosphonic from 0.19M $NaNO_3$/0.01M HNO_3 solution, a value of 23.3% absorbed was predicted compared to 25.2% determined experimentally. It must be noted that the calculation of % absorbed values for the

Table 39

Extraction of Ag(I) by Phosphonic, Amine Phosphonic, Amine Ester and Diester Resins from $NaNO_3$ and HNO_3 Solutions[a]

Resin Code	Type	% Absorbed	
		0.19M $NaNO_3$	0.19M $NaNO_3$/0.01M HNO_3
B^2-01-043B	phosphinic	55.6	37.4
B^2-01-084	amine phosphonic[b]	41.0	25.1
B^2-01-055A	amine[c]	11.7	10.3
DQ-03-045	amine/ester[d]	98.3	98.7
DQ-03-0266B	diester	13.6	15.0

[a] R_i = 0.10

[b] Protonated amine form used (NO_3^- counterion); tot(P) = 2.03 mequiv/g; TAEC = 2.20 mequiv/g.

[c] Protonated amine form used (NO_3^- counterion); TAEC = 4.45 mequiv/g.

[d] Protonated amine form used (NO_3^- counterion); tot(P) = 2.10 mequiv/g; TAEC = 1.67 mequiv/g; tot(OH) of starting diester = 0.37 mequiv/g.

bifunctional resins from the monofunctional resin results is only an approximation because the R_i values with respect to the individual functional groups on the bifunctional resin are higher than for the sum of the two groups. For example, the R_i with respect to the amine groups alone is 0.19 and with respect to the phosphonic groups is 0.21, whereas for the sum of the two groups it is 0.10. If an increased R_i leads to an increased % absorbed for each individual group, the predicted results would be higher than those obtained experimentally. Thus, the slightly higher levels of Ag extraction by the bifunctional amine phosphonic resin over those predicted by independent operation of the two groups is most likely the result of changes in the R_i rather than synergism. In contrast to the amine phosphonic resin, the results for the amine/ester resin indicate that the amine and ester groups may operate synergistically in the extraction of Ag. Experimentally, the bifunctional resin was found to complex 98.3% and 98.7% of the Ag from background solutions of 0.19M $NaNO_3$ and 0.19M $NaNO_3$/0.01M HNO_3, respectively, whereas values of 12.8% and 12.9% are predicted if the two groups act independently. The fact that the experimental results were approximately 86% higher for the bifunctional resin than estimated for independent operation of the two groups suggests that they function synergistically in the extraction of Ag. Before definite conclusions on synergism can be made, however, several additional studies must be performed. The influence of the R_i level on Ag extraction by the monofunctional amine and diester resins must be determined in order to accurately establish the % absorbed value for the independent operation of the two functional groups of the bifunctional resin. Furthermore,

the effect of the small amount (0.37 mequiv/g measured before amination) of acidic phosphorus groups (mono- and diacid) on Ag complexation by the amine/ester resin must be determined before synergistic extraction of Ag by the amine and ester groups can be proven.

Mercury (II) Complexation by Class I and Class II DMBP's

The influence of added HNO_3 was examined in the extraction of Hg by ion-exchange/redox and ion-exchange/coordination resins. The findings are presented in Table 40 for complexation from background solutions of 0.19M $NaNO_3$ and 0.19M $NaNO_3$/0.01M HNO_3 by phosphinic, sulfonic, phosphonic and monoester resins. In Table 41 the % absorbed values are given for Hg extraction at an R_i of 0.15 by phosphinic, sulfonic, amine phosphonic, amine and monoester resins from the following background solutions of constant ionic strength: 0.19M $NaNO_3$/0.01M HNO_3, 0.15M $NaNO_3$/0.05M HNO_3, 0.10M $NaNO_3$/0.10M HNO_3. The Hg results can be contrasted to those for Ag extraction by Class I and Class II resins. Comparison of Table 37 (page 190) and Table 40 for the results at R_i of 0.10 shows that higher levels of Hg were extracted by both the phosphorus and sulfonic resins than Ag. Neglecting the small differences in R_i, the protonated amine resin was found to extract comparable levels of Hg and Ag. Whereas Ag absorption decreased for the ion-exchange/redox and ion-exchange/coordination polymers upon the addition of 0.01 M HNO_3 (see Table 37, page 190), nearly identical results were obtained for Hg extraction from 0.19M $NaNO_3$ and 0.19M $NaNO_3$/0.01M HNO_3 background solutions. The results at constant ionic

Table 40

Hg Extraction at R_i = 0.1 from Background
Solutions of 0.19M $NaNO_3$ and 0.19M $NaNO_3$/0.01M HNO_3

Resin Code	Type	% Absorbed	
		0.19M $NaNO_3$	0.19M $NaNO_3$/0.01M HNO_3
DQ-02-109	phosphinic	98.4	97.8
DW-01-068C	sulfonic	77.7	71.7
MB-01-085C	phophonic	92.0	89.6
DQ-02-259D	monoester	97.6	97.0

Table 41

Hg Extraction at R_i = 0.15 from Background Solutions of Constant Ionic Strength

Resin Code	Type	% Absorbed		
		0.19M $NaNO_3$ 0.01M HNO_3	0.15M $NaNO_3$ 0.05M HNO_3	0.10M $NaNO_3$ 0.10M HNO_3
DQ-02-109	phosphinic	96.2	98.2	99.1
B^2-01-192	sulfonic		78.7	79.7
B^2-01-055A	amine	13.1	19.1	14.7
B^2-01-084	amine phosphonic	82.5		89.1
DQ-02-259D	monoester	88.1	97.1	93.4

strength (Table 41) also demonstrate that Hg extraction is independent of acid strength over the range of 0.01M to 0.10M HNO_3 for all of the resins studied. The independence of the Hg extraction results on the acid concentration for the phosphorus resins contrasts their behavior with Ag, suggesting that they complex Hg by a coordination mechanism rather than by ion-exchange. Previous studies with the phosphinic resin have shown that Hg extraction occurs exclusively by the redox process until all of the primary acid ligands have been oxidized after which extraction occurs by ion-exchange and/or coordination.[107] The present experiments were performed at a 6:1 or 4:1 excess of primary acid ligands to Hg ions (R_i's of 0.10 and 0.15; primary acid capacity = 2.97 mequiv/g) so that extraction should occur solely by reduction of the mercuric ions. As noted in the previous section, however, a decline in the amount of Hg extracted by the redox process is expected upon the addition of acid as predicted by the Nernst equation. In Hg extraction by the phosphinic resin, the amount of metal absorbed from solution remains constant (within experimental error) at approximately 98% over the range of HNO_3 concentration from 0.01M to 0.10M. These results suggest that if indeed the redox process is inhibited by the addition of acid, then the pH-independent coordination mechanism takes over to give almost quantitative removal of Hg from solution. Although not determined in this experiment, the effect of added acid on the redox process could be established by titrating the resin after contact with Hg to quantify the number of primary phosphinic ligands which have been oxidized to phosphonic acid groups. As with Ag extraction, the strongly

acidic sulfonic resin shows no dependence on background solution acidity in the range of 0.01M to 0.10M HNO_3.

Attempted Methods of Trace-Level Transition Metal Ion Analysis

The investigation of trace-level transition metal complexation by Class I and Class II DMBP's required a method for determining the concentrations of metal ions from very dilute solutions which also contained high levels of $NaNO_3$ and HNO_3. A technique having a limit of detection as low as 1 X 10^{-7}N was desired so that final concentrations could be determined when 99% of the metal was removed by the resin from a 1 X 10^{-5}N metal ion solution. In addition to the radiotracer technique described in Chapter III, colorimetric and atomic absorption techniques were attempted for trace-level transition ion analysis. Unfortunately, serious limitations of both methods precluded their use in the trace-level study.

One advantage of the colorimetric method is its insensitivity to added $NaNO_3$. Colorimetric analysis was undertaken in the determination of Fe^{3+}, employing both potassium thiocyanate and 1,10-phenanthroline as chromogens. The use of 1,10-phenanthroline necessitated the reduction of Fe^{3+} to Fe^{2+} by hydroquinone and adjustment of the solution pH to the required operating range of 2-9 by the addition of sodium citrate.[108] The absorbance of the resulting orange-red phenanthroline complex was measured at 508 nm; the solution concentration was determined from the linear Beer's Law plot. The lowest $Fe(NO_3)_3$ concentration which could be measured by this technique was approximately 1 X 10^{-4}N, a value too high for the trace-level study. Although the results using potassium

thiocyanate were more promising, the detection limit of 5 X 10^{-6}N $Fe(NO_3)_3$ was still considerably higher than the desired concentration of 1 X 10^{-7}N. Thus, % absorbed values no greater than 95% could be determined using this technique when the initial $Fe(NO_3)_3$ concentration was 1 X 10^{-4}N.

Generally lower limits of detection can be obtained using atomic absorption spectroscopy than with colorimetry. For some of the transition metal ions of interest to this study (namely, Fe, Hg, Mn and Ag) the detection limits were still too high for metal studies to be carried out at initial concentrations of 1 X 10^{-4}N and 1 X 10^{-5}N.[109] The initial atomic absorption studies were performed using $Hg(NO_3)_2$ in background solutions of 4M HNO_3, 2M HNO_3/2M $NaNO_3$, 1M HNO_3/3M $NaNO_3$ and 0.2M HNO_3/3.8M $NaNO_3$. The absorption sensitivity (the concentration of metal required to produce a 1% absorption signal) for Hg has been reported to be 2 X 10^{-5}N[109]; experimentally, a 1 X 10^{-5}N $Hg(NO_3)_2$ solution gave an absorbance reading of 0.006. Thus, the maximum measurable % absorbed value from a solution which was initially 1 X 10^{-4}N in $Hg(NO_3)_2$ is approximately 90%. In addition to concentration restrictions, the atomic absorption technique is limited to solutions which contain only very low levels of $NaNO_3$. Deposits of $NaNO_3$ were found to clog the burner and aspirator when salt concentrations greater than 3M were used. Furthermore, even when lower levels of $NaNO_3$ were used in the background solutions, variations in the nebulizer efficiency occur as a result of changes in the salt concentration, thus necessitating the use of background solutions containing the same levels of $NaNO_3$ for both standards and samples.[110]

In light of the difficulties encountered with colorimetric and atomic absorption techniques, the radiotracer method was chosen for the trace-level transition ion study. This technique provides several advantages over the methods previously discussed. First, extremely low levels of metal ions can be determined by the radiotracer technique. As will be seen later, metal ion concentrations as low as 1 X 10^{-7}N have been measured by this method when the resin absorbed 99% of the metal ions from a solution which was initially 1 X 10^{-5}N. Second, a wide range of transition metal ions have long-lived gamma-emitting isotopes which can be measured by scintillation techniques. Third, the radiotracer analysis is insensitive to the background solution composition. Fourth, although not examined in the present work, competitive extractions from solutions containing two or more radioactive ions can be carried out without interference if the energies of the two radioactive ions are sufficiently distinct. The experimental considerations of the radiotracer technique are addressed in the next section.

Application of the Radiotracer Technique to the Transition Metal Ion Study

The radiotracer analysis was performed in the same manner as described in Chapter III for the lanthanides and actinides except that non-tracer levels of non-radioactive metal ions were used in addition to the radioactive tracer. For example, the background solutions in this study contained a given concentration of the target metal (as the nitrate salt) along with varying levels of HNO_3 and $NaNO_3$. Enough resin

to provide one milliequivalent of active sites was shaken for 17 h with 5 mL of the background solution and a radiotracer level of the metal ion of interest. The concentration of radioactive metal after dilution to 5 mL was estimated to be no greater than approximately 4 X 10^{-10}N. After equilibration, a portion of the radioactive solution was removed and counted with a gamma-scintillation counter. The amount of metal absorbed by the resin was determined by comparison of the sample counts to those of a blank solution. The results were analyzed in terms of % absorbed and log D as described in Chapter III. The decrease in solution pH as a result of exchange of resin protons with the added Na ions was determined by titration of the background solution after equilibration with the resin.

A number of factors, such as the purity of the background solutions and resins and the attrition of the polymer beads during the equilibration process, were found to influence the results of trace-level extractions. Solution purity was important because even small amounts of impurities were found to affect trace-level determinations. Therefore, the water used in solution preparation was deionized by passage through a mixed-bed ion-exchange column; further purification to remove any remaining inorganic or organic impurities was carried out by double distillation from $KMnO_4$. Additionally, the $NaNO_3$ used in solutions containing $AgNO_3$ was recrystallized from 95% methanol to remove chloride impurities and thus prevent the precipitation of AgCl. To prepare the background solutions for radiotracer analysis, stock solutions of metal nitrate and $HNO_3/NaNO_3$ were combined in the appropriate proportions to yield the final desired concentrations of

metal, nitric acid and sodium nitrate. For example, to prepare a background solution containing 1 X 10^{-4}N $Hg(NO_3)_2$, 2M $NaNO_3$ and 2M HNO_3, a 10-mL portion of 1 X 10^{-3}N $Hg(NO_3)_2$ was diluted to 100 mL with a solution of 2.22M HNO_3/2.22M $NaNO_3$. Precautions were taken to avoid hydrolysis in the metal solution before mixing with the acidic $HNO_3/NaNO_3$ stock solution. To prevent hydrolysis, the pH of all stock metal nitrate solutions was adjusted to 1.5 by the addition of small amounts of concentrated HNO_3.

Trace-level extraction results can also be influenced by impurities in the resin pores, such as catalyst remaining from the phosphorylation reaction which may be only partially removed by the conditioning process. Indeed, the extraction of americium by the incompletely conditioned phosphonic resin DQ-03-002A (see Figure 45, p. 174) indicated that the presence of aluminum salts in the resin pores can affect the results of trace-level extractions. As discussed in Chapter I, complete purification of the resin pores was accomplished by soxhleting the resin in water. Because the pores collapsed upon soxhleting (as evidenced by the increase in % solids from 50% to 70% after soxhleting) the resins also required reconditioning in order to re-swell the polymer matrix. Presented in Table 42 are the results of trace-level extraction of Fe, Hg and Ag by three different samples of phosphinic resin: unsoxhleted, soxhleted (not reconditioned), and soxhleted (reconditioned). Due to the decreased metal ion accessibility into the collapsed polymer matrix, a decline in the distribution coefficient was observed for all three metals after the resin was soxhleted. The log D values increased after reconditioning of the

Table 42

Effect of Soxhleting and Reconditioning of the Phosphinic Resin on the Trace-Level Extraction of Fe, Hg, and Ag[a]

Metal	Background[b] Solution	log D		
		unsoxhleted	soxhleted	soxhleted/reconditioned
Fe	4/0	2.75	0.85	3.13
	2/2	3.08	0.85	3.42
	1/3	3.25	0.92	3.48
	0.2/3.8	3.20	1.14	3.50
Hg	4/0	1.70	0.88	1.74
	2/2	2.47	1.06	2.49
	1/3	2.51	1.26	2.17
	0.2/3.8	2.70	2.00	2.67
Ag	4/0	1.54	0.99	1.06
	2/2	1.42	0.97	1.31
	1/3	1.43	1.09	1.29
	0.2/3.8	1.47	1.35	1.44

[a] Initial metal nitrate concentration = 1 X 10^{-4}N

[b] $[HNO_3]$,M/$[NaNO_3]$,M

resin, resulting from enhanced accessibility through re-swelling of the polymer network. The effect of resin purification can be seen by comparing the unsoxhleted results to those after soxhleting and reconditioning: although little difference was observed after soxhleting for Hg and Ag, a slight increase in log D was noted for Fe extraction by the purified resin. Consequently, it appears that the effects of resin soxhleting are more pronounced when very high levels of metal are removed from solution. This is likely because small variations in the final solution activity can result in large log D differences when the final solution counts are very low. For example, consider two samples (0.25 g of resin in each) which have final solution activities of 20,000 and 200 cpm, respectively. Assuming an activity of 40,000 cpm for the blank, the log D value is calculated to be 1.30 for the former sample and 3.60 for the latter. If due to an experimental error, the solution activity was decreased by 50 cpm in both samples, no change in log D would be observed for the former sample, but the log D for the latter would increase to 3.73. To ensure that the extraction results were not influenced by impurities within the polymer matrix, all resins (except the amine and sulfonic which were not functionalized using a Freidel-Crafts catalyst) were soxhleted and reconditioned through two complete cycles before use in trace-level transition metal ion studies.

Trace-level extraction results were also found to be affected by bead attrition. Fracturing of resins can occur during the synthesis as a result of the exothermic solvolysis reaction and during the conditioning process due to the swelling and de-swelling of the polymer matrix. The presence of fines in the resin sample can in turn cause

difficulty in pipetting an aliquot for counting which is free of bead fragments. Resin fines in the 1-mL aliquot were found to increase the solution's activity, leading to error in the distribution coefficient, especially when high levels of metal were absorbed by the resin. For example, in the extraction of 1 X 10^{-4}N $Hg(NO_3)_2$ from a background solution of 0.20M HNO_3/3.8M $NaNO_3$ by the phosphonic resin, two separate 1-mL aliquots containing differing amounts of fines yielded cpm values of 7414 and 5119, corresponding to log D values of 1.82 and 2.02, respectively. Thus, a difference of 0.20 log D units occurred as the result of counting bead fragments in addition to the solution. As discussed previously, the effect of small changes in solution activity became even more pronounced when the final solution activity was very low. In an effort to avoid contamination by bead fragments, the samples were passed through a filter paper before counting. Table 43 gives the results of Hg extraction by phosphinic and phosphonic resins before and after filtration. The samples obtained before filtering were carefully pipetted to obtain as few fines as possible. After filtering, the activity decreased for all samples, resulting in a significant increase in log D. As indicated by the 2.6% decrease in counts for the blank, however, some of the radioactive metal was lost in filtering. Thus, to prevent scatter in the log D values as a result of counting bead fragments and to avoid the loss of activity upon filtration of the radioactive solutions, the resins were sieved before extraction to remove the fines. The results of Hg extraction by a phosphinic resin which was sieved prior to use (Table 43) show good agreement with those obtained before filtration.

Table 43

Effect of Bead Fragments on Extraction of Hg by Phosphinic and Phosphonic Resins[a]

Resin	Background Solution[b]	cpm/log D		
		unfiltered	filtered	sieved
phosphinic	4/0	4600/2.17	1027/2.87	3285/2.32
	2/2	1695/2.65	247/3.50	1691/2.63
	1/3	727/3.04	89/3.95	825/2.95
	0.2/3.8	378/3.32	47/4.22	315/3.38
phosphonic	4/0	14324/1.38	13359/1.42	
	2/2	3970/2.14	769/2.89	
	1/3	4398/2.10	895/2.83	
	0.2/3.8	5119/2.02	874/2.84	
Blank	4/0	31513	30694	

[a] $[Hg(NO_3)_2]_i = 1 \times 10^{-4}N$; $R_i = 5 \times 10^{-4}$

[b] $[HNO_3]$,M/$[NaNO_3]$,M

Unreliable extraction data were obtained in a study of metal ion extraction as a function of cross-link level. Extractions of Fe, Hg and Ag were performed using 2, 10, 15 and 30% cross-linked gel phosphinic resins; 2, 5, 10 and 15% cross-linked gel phosphonic resins; and 2 and 5% cross-linked gel monoester resins. The large amount of scatter in the results was attributed to the presence of fines in the resin samples, as indicated by the reproducible Hg and Fe extraction data obtained when the solutions were centrifuged to remove the fines.

Bead attrition can also occur during the 17-h equilibration period. This is indicated by the presence of a polymer residue after centrifuging background solutions which had been vigorously shaken with the resin. Extractions were carried out using either a Burrell wrist-action shaker for strong agitation or an Eberbach reciprocating shaker for gentle mixing. Some representative results are given in Table 44 which illustrate the effects of shaking method and solution centrifugation on trace-level ($R_i = 5 \times 10^{-4}$) transition metal extraction. For extractions carried out on the wrist-action shaker, an increase in log D was observed after centrifuging when high levels of metal ion were absorbed from solution (e.g. extraction of Fe by the phosphinic and phosphonic resins). In contrast, for moderate and low levels of metal extraction, such as extraction of Ag by the phosphinic resin, no significant change in log D was observed after centrifuging. Even though only moderate amounts of Hg were extracted by the phosphinic resin, the log D increased considerably after centrifuging, possibly due to the removal of reduced metal from solution. For all phosphorus resins, a white residue was obtained after centrifugation of the

Table 44

Effect of Centrifugation and Method of Shaking on Transition Metal Ion Extraction by Phosphinic, Sulfonic and Phosphonic Resins at an R_i of 5 X 10^{-4} [a]

Resin	Metal	Bkg. Sol.[b]	log D			
			wrist-action shaker[c]		Eberbach shaker[d]	
			uncent	cent	uncent	cent
phosphinic	Fe	4/0	3.15	3.62	3.67	3.74
		2/2	3.62	4.03	4.04	3.94
		1/3	3.53	4.15	3.92	4.24
		0.2/3.8	3.44	4.38	4.00	4.64
phosphinic	Hg	4/0	1.33	3.39	3.80	3.93
		2/2	1.78	3.59	3.76	4.18
		1/3	2.27	3.70	4.02	4.58
		0.2/3.8	2.09	3.60	3.78	4.12
phosphinic	Ag	4/0	0.85	1.03	0.95	
		2/2	0.93	1.04	1.07	
		1/3	1.03	1.06	1.15	
		0.2/3.8	1.26	1.31	1.29	
phosphinic	Mn	4/0	0.35	0.25		
		2/2	0.46	0.44		
		1/3	0.67	0.67	0.71	
		0.2/3.8	1.38	1.40		
phosphinic	Co	4/0	0.00	0.08		
		2/2	-0.04	-0.10		
		1/3	0.11	0.23	-0.01	
		0.2/3.8	0.40	0.43		
phosphinic	Zn	4/0	-0.16	-0.38		
		2/2	0.28	0.22		
		1/3	0.20	0.20	0.00	
		0.2/3.8	0.60	0.60		
sulfonic	Fe	4/0	0.90	0.84	0.94	0.94
		2/2	0.82	0.78	0.84	0.86
		1/3	0.76	0.76	0.88	0.86
		0.2/3.8	0.97	0.98	0.98	0.96
sulfonic	Hg	4/0	0.69	0.74	0.61	0.54
		2/2	0.75	0.73	0.67	0.67
		1/3	0.77	0.78	0.73	0.70
		0.2/3.8	0.93	0.92	0.89	0.88

Table 44 (continued)

Resin	Metal	Bkg. Sol.[b]	log D			
			wrist-action shaker[c]		Eberbach shaker[d]	
			uncent	cent	uncent	cent
sulfonic	Ag	4/0	0.77	0.84	0.79	0.88
		2/2	0.75	0.80	0.84	0.86
		1/3	0.84	0.83	0.66	0.57
		0.2/3.8	0.96	0.96	0.78	0.66
phosphonic	Fe	4/0	2.99	3.22	3.34	3.32
		2/2	3.16	3.44	3.59	3.63
		1/3	3.28	3.66	3.87	3.81
		0.2/3.8	2.86	3.59	3.88	4.23
phosphonic	Hg	4/0	0.70	0.74		
		2/2	1.40	1.44		
		1/3	1.39	1.54		
		0.2/3.8	1.48	1.60		
phosphonic	Ag[e]	4/0	1.41	2.08		
		2/2	1.26	1.65		
		1/3	1.25	1.61		
		0.2/3.8	1.23	1.56		

[a] initial metal nitrate concentration = 1×10^{-4} N.
[b] Background solution [HNO_3],M/[$NaNO_3$],M.
[c] vigorous shaking.
[d] gentle shaking.
[e] $NaNO_3$ used to prepare the Ag solutions was not recrystallized, therefore some precipitation of AgCl may have occurred.

background solution; the amine and sulfonic resins did not produce a solid after centrifuging. ESCA analysis was performed on the solid obtained upon centrifuging a background solution of 1 X 10^{-4}N $AgNO_3$/4M HNO_3 after it had shaken for 17 h on the wrist-action shaker with a phosphonic resin. The results in Table 45 show that the residue was primarily composed of C, O, P and Cl with amounts of Na, Si, I and F which were probably present as impurities from the sample holder. Apparently the concentration of Ag in the resin was too low to be measured by this technique. Although close agreement between the observed and predicted percentages of oxygen and chlorine was not obtained, the ESCA results nonetheless suggest that the residue was polymer which had fractured during the shaking process. The identification of the residue as polymer by ESCA is consistent with the extraction results: before centrifuging an erroneously high solution activity was measured due to the presence of polymer fragments containing radioactive metal. A significant error in log D thus occurred when the polymer extracted large amounts of metal. At lower levels of absorption, however, the resin fragments had much less effect on the extraction.

In an attempt to prevent bead attrition, subsequent extractions were performed using the more gentle side-to-side agitation of the Eberbach shaker. The log D values for extraction of several metals by the phosphinic and sulfonic resins using the Eberbach shaker obtained before and after centrifuging are included in Table 44. No polymer residue was observed after centrifugation for any of the samples which were equilibrated by the Eberbach shaker. Close agreement was obtained

Table 45

ESCA Results on Residues Obtained After Centrifugation

Element	Concentration (%)	
	Found	Predicted
C	62	65
O	23	9
P	6	6
Cl	2	13
Na	2	0
Si	3	0
I	0.7	0
F	2	0

for the centrifuged wrist-action and the uncentrifuged Eberbach results. This finding indicates that equilibrium was reached within 17 h using the less vigorous shaking method. As shown in Table 44, increases in log D were again observed after centrifugation when high levels of metal were extracted, such as absorption of Hg and Fe by the phosphinic resin. These changes in log D, however, cannot be attributed to bead attrition because no polymer residue was obtained after centrifuging. The observed increases in log D corresponded to the loss in solution radioactivity of only 40 to 50 cpm, approximately 0.2% of the original solution activity. The activity of the blank solutions also decreased upon centrifuging. On the average, 0.6% of the original activity was lost from Hg solutions and 0.2% from Fe solutions, thus suggesting that the decrease in counts upon centrifuging is due to an experimental error, such as the loss of lint fibers which had absorbed small amounts of radioactive metal.

As shown in Table 46, the conclusions drawn for phosphinic, sulfonic and phosphonic resins at an R_i of 5×10^{-4} are consistent with those determined at an R_i of 5×10^{-3}. The use of the wrist-action shaker again caused bead attrition as indicated by the presence of polymer residue after centrifuging. When large amounts of metal were extracted, as for Fe absorption by the phosphinic and phosphonic resins, an increase in log D was noted after centrifuging. As with the previous extractions, no polymeric residue was obtained after equilibration using the Eberbach shaker although an increase in the log D was found after centrifugation when high levels of metal were absorbed. The effects of centrifuging were also examined at an R_i of 5×10^{-2} for Hg, Fe and Ag

Table 46

Effect of Centrifugation and Method of Shaking on Transition Metal Ion Extraction by Phosphinic, Sulfonic and Phosphonic Resins at an R_i of 5 X 10^{-3} [a]

Resin	Metal	Bkg. Sol.[b]	log D			
			wrist-action shaker[c]		Eberbach shaker[d]	
			uncent	cent	uncent	cent
phosphinic	Fe	4/0	3.39	3.53	3.42	3.50
		2/2	3.56	3.77	3.68	3.74
		1/3	3.54	4.02	3.94	4.03
		0.2/3.8	3.75	4.17	4.14	4.19
phosphinic	Hg	4/0	2.75	3.66	4.09	4.29
		2/2	3.21	4.09	3.86	4.33
		1/3	3.20	4.19	3.74	4.43
		0.2/3.8	3.18	4.47	3.87	4.77
phosphinic	Ag	4/0	0.41	0.50	0.51	0.47
		2/2	0.76	0.77	0.41	0.47
		1/3	0.89	0.88	0.43	0.52
		0.2/3.8	1.04	1.08	0.63	0.67
phosphinic	Mn	4/0	0.39	0.39		
		2/2	0.63	0.59		
		1/3	0.77	0.74		
		0.2/3.8	1.43	1.43		
phosphinic	Co	4/0	0.08	0.08		
		2/2	0.20	0.11		
		1/3	0.18	0.18		
		0.2/3.8	0.51	0.50		
phosphinic	Zn	4/0	0.25	-0.08		
		2/2	0.16	0.05		
		1/3	0.18	0.02		
		0.2/3.8	0.51	0.50		
sulfonic	Fe	4/0	0.85	0.89	0.93	0.94
		2/2	0.73	0.77	0.84	0.83
		1/3	0.82	0.81	0.85	0.85
		0.2/3.8	0.87	0.85	0.97	0.96
sulfonic	Hg	4/0	0.57	0.57	0.61	0.60
		2/2	0.76	0.76	0.81	0.83
		1/3	0.85	0.88	0.96	0.96
		0.2/3.8			1.25	1.25

Table 46 (continued)

Resin	Metal	Bkg. Sol.[b]	log D			
			wrist-action shaker[c]		Eberbach shaker[d]	
			uncent	cent	uncent	cent
sulfonic	Ag	4/0	0.74	0.68	0.76	0.73
		2/2	0.81	0.78	0.80	0.79
		1/3	0.85		0.81	0.84
		0.2/3.8	0.96	1.00	0.93	0.93
phosphonic	Fe	4/0	2.72	2.75		
		2/2	2.82	3.00		
		1/3	3.05	3.28		
		0.2/3.8	3.09	3.79		
phosphonic	Hg	4/0	2.01	2.10		
		2/2	1.10	1.10		
		1/3	1.38	1.32		
		0.2/3.8	1.69	1.69		
phosphonic	Ag	4/0	0.91	0.90		
		2/2	0.85	0.86		
		1/3	0.88	0.90		
		0.2/3.8	1.10	1.11		

[a] initial metal nitrate concentration = 1 X 10^{-3} N.
[b] Background solution [HNO_3],M/[$NaNO_3$],M.
[c] vigorous shaking.
[d] gentle shaking.

extraction by phosphinic and phosphonic resins using the wrist-action shaker. The results in Table 47 indicate that, although polymer was centrifuged out of solution, no significant change in log D was observed for most samples. This is most likely because at the higher R_i a smaller percentage of the metal absorbed onto the polymer is radioactive, thus giving less error when polymer-absorbed metal is counted in addition to the solution.

The results using the wrist-action shaker show that attrition of the polymer beads occurred with vigorous shaking. Errors in the distribution coefficients at R_i levels of 5×10^{-3} and 5×10^{-4} resulted from counting polymer-absorbed metal in addition to the radioactive metal remaining in solution, especially when high levels of metal were absorbed. To obviate the problems caused by bead attrition and centrifugation, extractions were carried out on the Eberbach shaker, and the solutions generally were not centrifuged prior to counting. The centrifuged results obtained using the wrist-action shaker are reported only when very low levels of metal were extracted (e.g. extraction of Mn, Co and Zn by all resins except the phosphinic) and for extractions using the amine resin, which did not fracture during shaking.

Counting errors can also influence the results of metal ion analyses. Background errors, statistical errors and coincidence errors are the three major sources of inaccuracy in the counting procedure.[111] Errors from background radiation, which was generally low and constant, were eliminated by measuring the background activity and subtracting it from the observed sample and blank counts. Statistical measurement errors occur because radiation is emitted from sources at random

Table 47

Effect of Centrifugation on Transition Metal Ion Extraction by Phosphinic and Phosphonic Resins at an $R_i = 5 \times 10^{-2}$ [a]

Resin	Metal	Bkg. Soln.[b]	log D[c] uncent.	log D[c] cent.
phosphinic	Fe	4/0	2.75	2.78
		2/2	3.00	3.04
		1/3	3.23	3.25
		0.2/3.8	3.58	3.62
phosphinic	Hg	4/0	1.85	1.87
		2/2	2.23	2.27
		1/3	2.86	2.91
		0.2/3.8	3.11	3.99
phosphinic	Ag	4/0	0.30	0.29
		2/2	0.11	0.18
		1/3	0.06	0.17
		0.2/3.8	0.62	0.62
phosphonic	Fe	4/0	2.48	2.50
		2/2	2.61	2.61
		1/3	2.79	2.87
		0.2/3.8	2.93	3.09
phosphonic	Hg	4/0	1.16	1.18
		2/2	1.23	1.25
		1/3	1.53	1.54
		0.2/3.8	2.27	2.27
phosphonic	Ag	4/0	0.76	0.81
		2/2	0.77	0.78
		1/3	0.73	0.78
		0.2/3.8	0.90	0.95

[a] Initial metal nitrate concentration = 1×10^{-2}N.
[b] $[HNO_3]$,M/$[NaNO_3]$,M
[c] Extractions carried out using wrist-action shaker.

intervals. The probable error caused by the random nature of radioactive decay is taken to be the square root of the measured activity. Thus, a smaller statistical error is associated with a sample having a count rate of 10,000 ± 100 cpm (1% error) than with one having a count rate of 100 ± 10 cpm (10% error). Coincidence errors occur when more than one pulse strikes the detector within its response time. The "dead-time" is the period after each recorded count during which the counter is unresponsive and cannot record a subsequent count. Normally, errors due to dead-time are significant only at high count rates. The multichannel analyzer utilized in this study corrected for dead-time by counting for an additional period of time depending on the activity of the sample. As will be seen later, errors from dead-time can still occur at very high count rates even with this correction.

A study was undertaken to determine the level of radioactivity required to balance the effects of statistical and coincidence counting errors. Presented in Table 48 are the results of extraction of 1×10^{-4}N $Mn(NO_3)_2$ and $Fe(NO_3)_3$ by the phosphinic resin using different initial activities for the radioactive spike. For Mn extractions, initial count rates of 1616, 22,848 and 29,551 cpm were used. Close agreement was obtained for the two highest spike levels. These results differed from those of the lowest spike level, probably due to the loss of sensitivity for the lower count rate. In the case of Fe, the blank solution counting 183,185 cpm required dilution to decrease the amount of dead-time. Before dilution the sample counted 159,000 cpm with a dead-time of 15%; after a 5:1 dilution, the dead-time was reduced to 3% and a count rate of 36,637 was obtained, corresponding to 183,185 cpm

Table 48

Effect of Initial Solution Radioactivity on Mn and Fe Extraction Results Using the Phosphinic Resin[a]

Metal[b]	Bkg. Soln.[c]	Solution Activity, cpm		log D
		Initial	Final	
Mn	4/0	1616	1554	-0.22
	2/2	1616	1393	0.54
	1/3	1616	1386	0.57
	0.2/3.8	1616	845	1.35
Mn	4/0	22944	21224	0.25
	2/2	22944	20629	0.43
	1/3	22944	19231	0.69
	0.2/3.8	22944	11307	1.42
Mn	4/0	29551	27222	0.25
	2/2	29551	26669	0.44
	1/3	29551	24931	0.67
	0.2/3.8	29551	14640	1.40
Fe	4/0	183186	976	3.67
	2/2	183186	632	3.84
	1/3	183186	446	3.99
	0.2/3.8	183186	261	4.24
Fe	4/0	18945	83	3.75
	2/2	18945	84	3.75
	1/3	18945	48	3.99
	0.2/3.8	18945	54	3.94

[a] Wrist-action shaker used; Centrifuged results reported.
[b] As the nitrate salt; initial concentration = 1 X 10^{-4}N.
[c] $[HNO_3]$,M/$[NaNO_3]$,M.

after correction for dilution. Thus approximately 24,000 counts were not detected in the undiluted sample due to dead-time losses. Consistent Fe extraction results were obtained for samples having initial count rates of 183,185 and 18,945 cpm, even when the final solution counts were very low, as for extraction from the 0.2M HNO_3/3.8M $NaNO_3$ background solution. In order to increase the counting accuracy for samples having a very low count rate, a longer sampling time can be used, although this was generally not found to lead to significant differences in the count rate. For instance, a background count sampled for 10 min gave a count of 28.8 cpm while two 1-min counting periods gave an average result of 31.5 cpm. In most extractions an initial solution activity of 30,000 - 40,000 cpm was used in order to obviate problems with both statistical and dead-time counting errors.

The effects of resin hydration and stock metal solution pH were examined in the complexation of Ag (at an R_i of 5 X 10^{-3}) by phosphonic and diethyl ester resins. For both the phosphonic and diester, the same results were obtained for the dried and hydrated resin forms. For example, a log D value of 0.85 was observed from the 1M HNO_3/3M $NaNO_3$ solution for both the hydrated and dried phosphonic resins. Similarly, the dried and hydrated diethyl ester resins gave log D values of 1.45 and 1.41, respectively from a background of 1M HNO_3/3M $NaNO_3$. However, later experiments with more hydrophobic diester resins suggested that drying of the resin may in fact lead to scattered results. Thus to ensure adequate hydration, all resins were fully conditioned through two cycles and were stored in water rather than in their suction-dried form until just prior to use in the radiotracer experiments. Although the pH

of the stock $AgNO_3$ solution was found to have no effect on the extraction results (for the phosphonic resin from a background of 1M HNO_3/3M $NaNO_3$ a log D of 0.85 was obtained from $AgNO_3$ initially at pH 1.5 compared to 0.86 from $AgNO_3$ solution with unadjusted pH) hydrolysis is more likely to be significant for metals such as Hg and Fe which have lower hydrolysis constants than Ag (pk_{hyd} = 6.9 for Ag^+, 3.70 for Hg^{2+} and 2.19 for Fe^{3+}).[112]

Complexation of Trace Levels of Ag and Hg by Amine and Amine/Ester Resins

Previous results with the dimethylamine/ester resin suggested that the ester and amine groups operated synergistically in the extraction of macro levels of silver. The possibility of synergism between the amine and ester moieties was further examined in the trace-level complexation of Ag and Hg with the following resins which contained both diethyl ester and amine groups (in their protonated form with nitrate as counterion): dimethylamine/ester, ethylamine/ester and diethylamine/ester. The extractions from background solutions of 4M HNO_3, 2M HNO_3/2M $NaNO_3$, 1M HNO_3/3M $NaNO_3$ and 0.20M HNO_3/3.8M $NaNO_3$ were performed at an R_i of 5 X 10^{-4} using the nitrate salt of the target metal cation. The Ag and Hg extraction results (% absorbed and log D values) are presented in Tables 49 and 50 for the bifunctional amine/esters and the monofunctional amine and diethyl ester analogues. Also given in the tables are the predicted % absorbed values for the bifunctional resins based upon the independent operation of the two functional groups. As discussed earlier, the predicted values are

Table 49

Trace-Level Ag Extraction by Amine and Amine Ester Resins[a]

Resin	Bkg. Soln.[b]	log D	% Absorbed	
			observed	predicted
dimethylamine ester	4/0	2.09	88.41	66.46
	2/2	2.24	91.42	73.15
	1/3	1.99	85.53	71.56
	0.2/3.8	1.85	81.77	71.30
dimethylamine	4/0	0.96	30.53	
	2/2	1.16	39.56	
	1/3	1.21	42.38	
	0.2/3.8	1.27	46.13	
ethylamine ester	4/0	2.20	90.87	72.23
	2/2	2.18	90.36	89.23
	1/3	2.16	90.16	81.14
	0.2/3.8	2.06	87.80	79.72
ethylamine	4/0	1.19	32.74	
	2/2	1.85	57.53	
	1/3	1.87	66.42	
	0.2/3.8	1.88	67.61	
diethylamine ester	4/0	2.32	93.17	71.05
	2/2	2.38	93.99	76.53
	1/3	2.33	93.27	78.27
	0.2/3.8	2.11	89.28	77.17
diethylamine	4/0	1.35	51.79	
	2/2	1.44	57.10	
	1/3	1.63	67.28	
	0.2/3.8	1.65	67.84	
diethylester	4/0	1.94	83.37	
	2/2	2.15	88.96	
	1/3	2.00	85.29	
	0.2/3.8	1.93	83.14	

[a] $[AgNO_3]_i = 1 \times 10^{-4}$

[b] $[HNO_3]$,M/$[NaNO_3]$,M

Table 50

Trace-Level Hg Extraction by Amine and Amine Ester Resins[a]

Resin	Bkg. Soln.[b]	log D	% Absorbed	
			observed	predicted
dimethylamine ester	4/0	0.71	23.09	26.18
	2/2	1.13	46.72	31.73
	1/3	1.31	56.12	42.20
	0.2/3.8	1.63	72.92	60.11
dimethylamine	4/0	1.11	36.45	
	2/2	1.26	44.43	
	1/3	1.38	51.99	
	0.2/3.8	1.56	63.82	
ethylamine ester	4/0	0.67	23.19	24.61
	2/2	0.96	36.99	30.86
	1/3	1.15	49.29	41.91
	0.2/3.8	1.48	67.07	60.45
ethylamine	4/0	1.04	36.17	
	2/2	1.25	48.94	
	1/3	1.41	57.24	
	0.2/3.8	1.65	74.80	
diethylamine ester	4/0	0.79	29.08	26.20
	2/2	1.10	46.07	33.68
	1/3	1.29	56.66	42.30
	0.2/3.8	1.65	74.80	58.39
diethylamine	4/0	1.02	33.79	
	2/2	1.18	42.44	
	1/3	1.30	49.66	
	0.2/3.8	1.46	58.44	
diethylester	4/0	0.68	21.35	
	2/2	0.79	25.76	
	1/3	1.30	49.66	
	0.2/3.8	1.39	58.36	

[a] $[HgNO_3]_i = 1 \times 10^{-4}$
[b] $[HNO_3]$,M/$[NaNO_3]$,M

calculated from the monofunctional results and the fraction of amine and diester groups on the bifunctional resin. These calculations do not take into account the differences in R_i for the monofunctional resin and for the bifunctional resin with respect to each functional group, and they assume no participation in the extraction from the small amount of phosphonic acid groups on the resin. The extractions were carried out prior to determining the necessity for purification of the water, resins and sodium nitrate. Therefore, although this set of results are useful to compare to one another, they should not be equated to later results obtained using purified reagents. The most significant error likely occurs in the extraction of Ag as a result of its precipitation with chloride from the impure $NaNO_3$.

Comparison of the performance of the three amine/ester resins in the complexation of Ag shows that the ethylamine/ester and the diethylamine/ester behave similarly and slightly outperform the dimethylamine/ester. Likewise, comparable results were obtained for the monofunctional ethyl- and diethylamine resins, and both were found to extract higher levels of Ag than the dimethylamine resin. The extraction results (dimethylamine > ethylamine $\approx$ diethylamine) roughly parallel the pK_b's of the amine groups (3.28 for dimethylamine, 3.25 for ethylamine and 3.02 for diethylamine[113]). Although the pk_b's of the dimethylamine and ethylamine resins are similar, the superior performance of the ethylamine resin may be the result of its decreased steric hindrance to ion-pair complexation. The observed % absorbed values for the bifunctional dimethylamine/ester and diethyl/amine resins were significantly greater (12-22%) than those predicted for independent

operation of the two groups, suggesting synergistic extraction by the amine and diester moieties. The extent of the synergistic enhancement appeared to decrease with increasing pH and $NaNO_3$ content. Only modest increases, which were likely due to R_i differences rather than synergistic enhancement, were observed for the ethylamine/ester resin. The Ag extraction results suggest that synergism occurs only with the tertiary amine/ester resins.

In general, lower levels of Hg were extracted by the bifunctional amine/ester, monofunctional amine and diethyl ester resins than for Ag, although erroneously high Ag results may have occurred as a result of AgCl precipitation. Whereas nearly the same Hg results were obtained by the three amine resins, the ethylamine/ester resin was found to absorb slightly lower levels of Hg than the dimethylamine/ester and diethylamine/ester resins. As was observed in Ag extraction, no synergistic interaction was indicated between the amine and ester groups of the ethylamine ester resin. By contrast, the two tertiary amine/ester resins demonstrated a significant increase (12-17%) in the observed over the predicted % absorbed values, suggesting synergistic extraction by the amine and ester groups. Although these results imply synergistic extraction of both Ag and Hg by the bifunctional dimethylamine/ester and diethylamine/ester resins, further study should be conducted to determine the effect of changes in R_i and the role of the phosphonic acid groups in the extractions.

Determination of the Selectivity Series

A metal ion selectivity series was established in order to fully define the ability of Class I and Class II DMBP's to complex the following transition metal ions: Fe^{3+}, Mn^{2+}, Co^{2+}, Zn^{2+}, Hg^{2+} and Ag^{+}. The extractions were performed at R_i levels of 5×10^{-3} and 5×10^{-4} from background solutions of 4M HNO_3, 2M HNO_3/2M $NaNO_3$, 1M HNO_3/3M $NaNO_3$ and 0.2M HNO_3/3.8M $NaNO_3$. The complexing ability of ion-exchange/coordination polymers having P=O coordinating ligands of varying degrees of softness was investigated as a function of the hard/soft character of the metal ion. The transition metals examined ranged from hard (Fe^{3+}, Mn^{2+}) to borderline (Co^{2+}, Zn^{2+}) to soft (Hg^{2+}, Ag^{+}) as described by Pearson's hard-soft acid-base (HSAB) theory.[114]

As described in Chapters I and II, the phosphorylated precursors to the phosphinic and phosphonic resins can be hydrolyzed by two different procedures: by rapid addition of the unwashed intermediate into an ice bath (Method I) and by dropwise addition of aqueous dioxane to the dioxane-washed intermediate (Method II). The latter approach was carried out in an attempt to produce a resin containing a lower level of catalyst impurities. Transition ion extractions were performed on phosphinic and phosphonic resins synthesized by both techniques at R_i levels of 5×10^{-4} and 5×10^{-3}. As seen from Table 51, similar Fe, Hg, Mn and Ag extraction results were obtained for the phosphinic resins synthesized by the two different methods. In contrast, the two phosphonic resins complexed different amounts of Hg and Ag at an R_i of 5×10^{-4}, as indicated by the results in Table 52. At the higher loading level, however, the two resins performed similarly in the

Table 51

Extraction by Phosphinic Resins Quenched by Different Methods[a]

Metal[b]	Background Solution[c]	log D (% Absorbed) Method I	Method II
Fe	4/0	3.62(99.40)	3.57(99.40)
	2/2	4.03(99.77)	3.90(99.71)
	1/3	4.15(99.82)	4.02(99.78)
	0.2/3.8	4.38(99.96)	4.27(99.88)
Hg	4/0	3.39(99.00)	3.31(99.01)
	2/2	3.59(99.36)	3.30(98.88)
	1/3	3.70(99.50)	3.52(99.34)
	0.2/3.8	3.60(99.39)	3.97(99.76)
Ag	4/0	1.03(29.82)	1.12(36.02)
	2/2	1.04(31.75)	1.42(53.80)
	1/3	1.06(32.04)	1.19(40.26)
	0.2/3.8	1.31(44.86)	1.31(44.86)
Mn	4/0	0.25(6.65)	0.26(7.35)
	2/2	0.43(9.85)	0.58(14.02)
	1/3	0.69(16.41)	0.69(17.92)
	0.2/3.8	0.42(50.95)	1.38(51.98)

[a] Method I: rapid hydrolysis of phosphorylated intermediate in an ice bath; Method II: dropwise addition of aqueous dioxane into dioxane-washed intermediate.

[b] Initial metal nitrate concentration = 1×10^{-4}N; $R_i = 5 \times 10^{-4}$

[c] $[HNO_3]$,M/$[NaNO_3]$,M

Table 52

Extraction by Phosphonic Resins Quenched by Different Methods[a]

Metal	Ri	Background Solution[b]	log D (% Absorbed) Method I	log D (% Absorbed) Method II
Fe	5×10^{-4}	4/0	3.22(98.76)	3.34(98.99)
		2/2	3.55(99.43)	3.59(99.44)
		1/3	3.92(99.75)	3.87(99.71)
		0.2/3.8	4.42(99.92)	3.88(99.71)
Hg	5×10^{-4}	4/0	1.06(33.45)	0.44(10.81)
		2/2	1.30(46.54)	0.49(12.36)
		1/3	2.30(89.65)	1.19(41.53)
		0.2/3.8	2.68(95.50)	1.32(49.64)
Ag	5×10^{-4}	4/0	1.14(39.52)	1.77(72.53)
		2/2	1.08(36.48)	1.68(68.84)
		1/3	1.02(33.16)	1.51(59.49)
		0.2/3.8	1.24(45.57)	1.52(60.01)
Fe	5×10^{-3}	4/0	3.16(98.76)	3.22(98.69)
		2/2	3.48(99.43)	3.50(99.32)
		1/3	3.87(99.75)	3.78(99.63)
		0.2/3.8	4.91(99.92)	3.79(99.64)
Hg	5×10^{-3}	4/0	0.95(28.66)	0.89(26.74)
		2/2	1.44(55.43)	1.18(40.63)
		1/3	1.60(64.25)	1.63(66.92)
		0.2/3.8	2.22(88.09)	2.20(87.73)
Ag	5×10^{-3}	4/0	0.77(22.59)	0.89(26.03)
		2/2	0.76(21.22)	0.81(22.95)
		1/3	0.74(20.14)	0.87(25.29)
		0.2/3.8	1.13(39.74)	1.07(34.97)

[a] Method I: rapid hydrolysis of phosphorylated intermediate in an ice bath; Method II: dropwise addition of aqueous dioxane into dioxane-washed intermediate.

[b] $[HNO_3]$,M/$[NaNO_3]$,M

extraction of all four metals. Additionally, no differences were observed in the macroscopic characterization results of the two resins: the acid and phosphorus capacities were found to be 9.26 and 4.58 mequiv/g, respectively, for the phosphonic resin prepared by Method I, compared to values of 9.03 and 4.40 mequiv/g obtained for the resin quenched by Method II. These results suggest that the dissimilarities between the two phosphonic resins are only detectable at trace-level determinations. Because the effect of the dioxane wash and quench on the resulting resin structure and properties was not fully defined, phosphinic and phosphonic resins synthesized by Method I were employed for the selectivity series determinations.

The effect of the degree of functionalization of the phosphonic resin on the extraction of transition metal ions was investigated. Presented in Table 53 are the results of Hg, Fe and Ag extraction at an R_i of 5 X 10^{-4} from the 1M HNO_3/3M $NaNO_3$ background solution using five phosphonic resins having degrees of functionalization ranging from 30 to 99%. The Fe extraction data demonstrate that metal ion accessibility was reduced for the phosphonic resin which was only 30% substituted. Comparable log D values were obtained for the resins which were 65 to 99% functionalized, an indication that no accessibility limitations exist with these resins in the extraction of Fe. The Hg and Ag extraction results, however, were less clear-cut. The Hg data in Table 53 show no clear relationship between the degree of substitution and log D. Although the log D's were scattered for the resins which were 30 to 84% functionalized, the data nonetheless indicate that accessibility was reduced for the partially functionalized resins compared to the fully

Table 53

Extraction of Fe, Hg and Ag by Phosphonic Resins of Varying Degrees of Functionalization

% Functionalization	log D (1M HNO_3/3M $NaNO_3$)		
	Fe	Hg	Ag
30	2.82	2.07	3.00
65	3.59	1.91	3.18
76	3.66	1.49	2.98
84	3.59	2.93	3.00
99	3.74	3.61	1.72

substituted one. In the case of Ag complexation, accessibility does not appear to be limited in the range of 30 to 84% substitution, although an unexpected decrease in log D was observed for the fully functionalized resin. From this data it is unclear why the partially functionalized resins outperform the fully substituted one in Ag complexation. Further clarification of the effect of the degree of functionalization on the extraction of Ag and Hg most likely requires examination of the complete log D/pH plot. To enhance metal ion accessibility, the selectivity series experiments were carried out using a fully substituted (94%) phosphonic resin.

The influence of bead size on the extraction of Hg by the phosphonic resin was also studied. A series of phosphonic resins were synthesized under conditions of 0.77 mole $AlCl_3$ at 40 °C using polymer beads of the following mesh cuts: -20+30, -30+40, -60+80 and -80+100. As the data in Table 54 indicate, a decrease in chlorine capacity was observed with decreasing mesh size without a concomitant increase in phosphorus capacity. In addition, the ratio of the acid to phosphorus capacity increased from 1.5 for the largest beads to the expected value of 2.0 for both the -60+80 and -80+100 mesh cuts. In light of these differences in the characterization results, the resins were studied in the trace-level ($R_i = 5 \times 10^{-4}$) extraction of Hg. Examination of the data in Table 54 shows no difference in extraction behavior for the four resins despite their dissimilar characterization data. A fully functionalized phosphonic resin having a mesh size of -60+100 was utilized in the selectivity series determination owing to the good

Table 54

Hg Extraction by Phosphonic Resins of Varying Mesh Size [a]

Mesh Size	Capacity (mequiv/g)			tot(OH)/tot(P)	log D ([HNO_3],M/[$NaNO_3$],M)			
	tot(OH)	tot(P)	tot(Cl)		4/0	2/2	1/3	0.2/3.8
-20 + 30	3.41	2.25	3.66	1.52	0.92	1.27	2.11	2.61
-30 + 40	3.94	2.30	3.50	1.71	0.93	1.29	2.04	2.73
-60 + 80	4.91	2.49	3.00	1.97	1.06	1.60	2.30	2.86
-80 + 100	5.20	2.57	2.85	2.02	0.66	1.23	2.30	2.73

[a] $[Hg(NO_3)_2]_i = 1 \times 10^{-4}N$; $R_i = 5 \times 10^{-4}$

agreement between its phosphorus and acid capacities: tot(P) = 4.58 mequiv/g and tot(OH) = 9.26 mequiv/g.

Figures 49-55 present the log D/pH correlations for the extraction of Fe, Hg, Ag, Mn, Co and Zn at an R_i of 5 X 10^{-4} from background solutions of 4M HNO_3, 2M HNO_3/2M $NaNO_3$, 1M HNO_3/3M $NaNO_3$ and 0.2M HNO_3/3.8M $NaNO_3$ by five DMBP's (phosphinic, phosphonic, amine phosphonic, monoester and diethyl ester) and the monofunctional amine and sulfonic resins. Comparison of the log D/pH plots shows that much wider separation of the six transition metal ions was achieved with the phosphorus acid resins than with the strongly acidic sulfonic resin. For example, the Fe/Hg separation factor (SF, the ratio of distribution coefficients for the two metals from the 1M HNO_3/3M $NaNO_3$ background solution) was 42 for the phosphonic resin compared to 1.4 for the sulfonic. The non-specific nature of the sulfonic resin is attributed to the narrow range of reaction free energy values for its ion exchange with the transition metal ions. Indeed, Boyd and coworkers have found a variation in reaction free energies of only 1-2 kcal/mole for the ion exchange of a wide range of metal ions with the sulfonic acid resin.[48] Moreover, due to its ion exchange with the sodium ions present in excess, the sulfonic resin absorbs only moderate levels of the target transition metal ions. For example, 22.6% of Fe was absorbed from the 1M HNO_3/3M $NaNO_3$ background solution by the sulfonic resin in comparison to 99.7% absorbed by the phosphinic resin.

The log D/pH plots were also determined at an R_i of 5 X 10^{-3} for the six transition metal ions and seven resins described above (Figures 56-62). As with the extractions at an R_i of 5 X 10^{-4}, greater ion

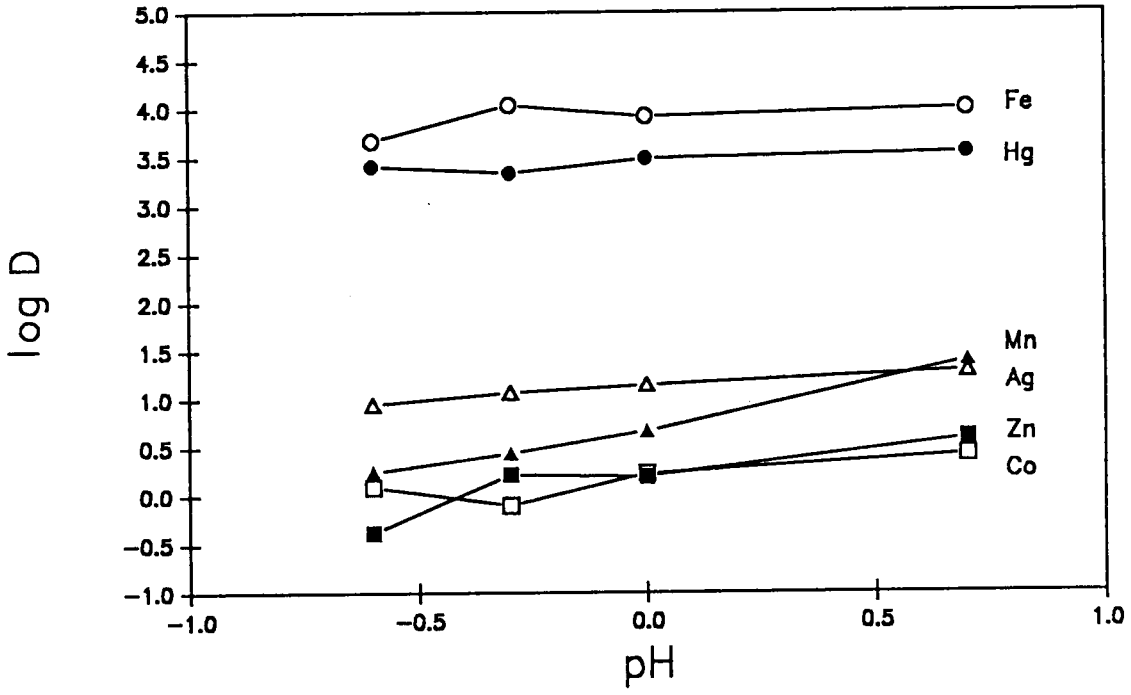

Figure 49. Plots of log D versus pH for Fe, Hg, Ag, Mn, Co and Zn extraction by the phosphinic resin determined at an R_i of 5 X 10^{-4} in the presence of excess sodium ions.

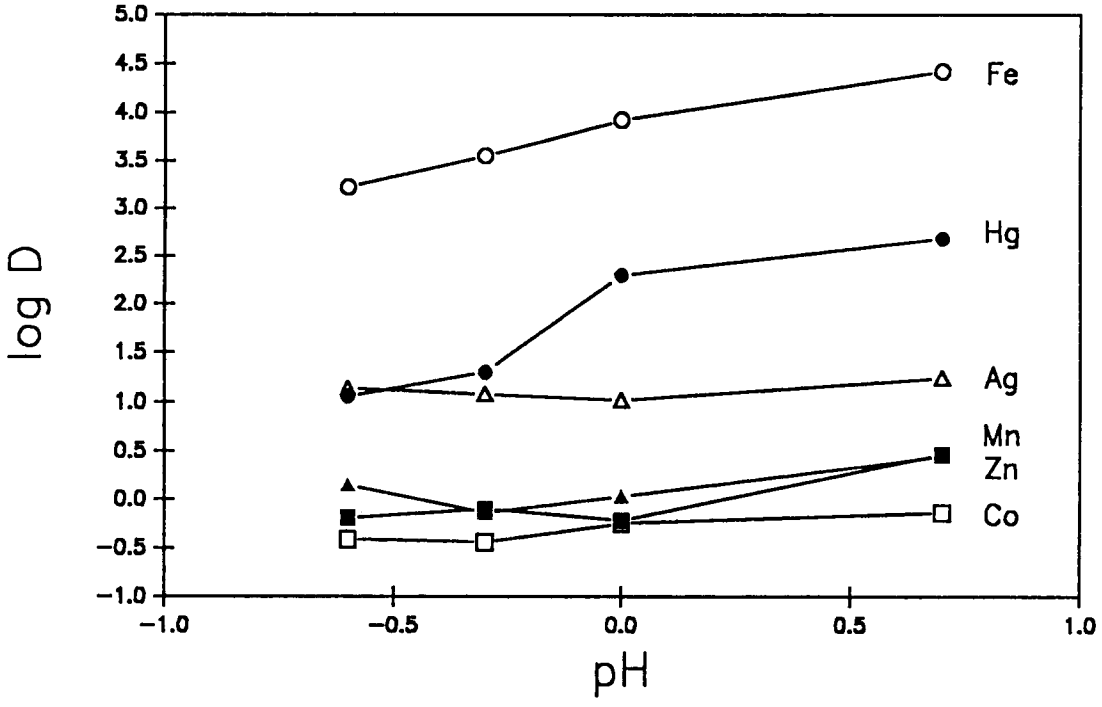

Figure 50. Plots of log D versus pH for Fe, Hg, Ag, Mn, Co and Zn extraction by the phosphonic resin determined at an R_i of 5 X 10^{-4} in the presence of excess sodium ions.

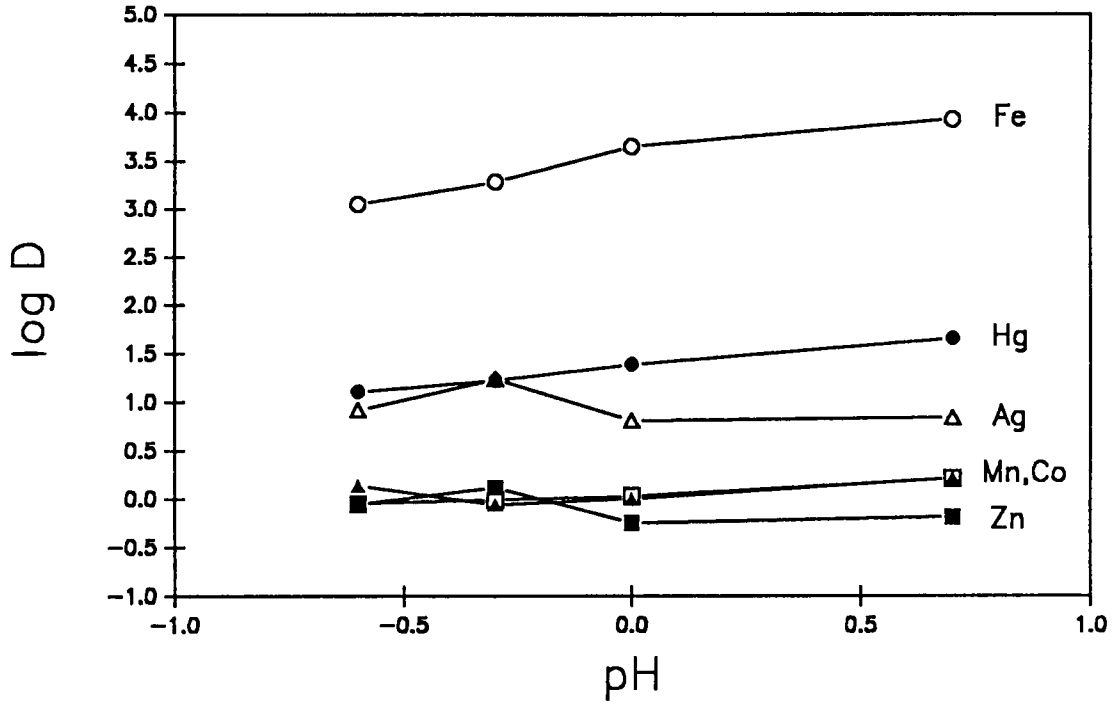

Figure 51. Plots of log D versus pH for Fe, Hg, Ag, Mn, Co and Zn extraction by the amine phosphonic resin determined at an R_i of 5 X 10^{-4} in the presence of excess sodium ions.

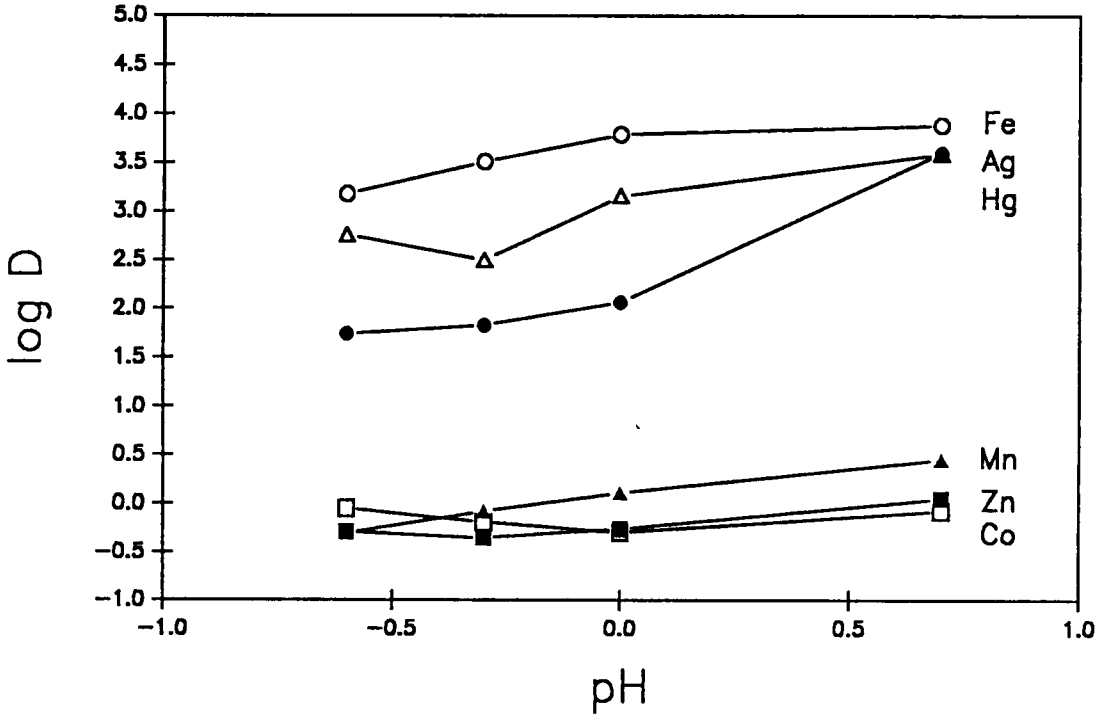

Figure 52. Plots of log D versus pH for Fe, Hg, Ag, Mn, Co and Zn extraction by the monoester resin determined at an R_i of 5×10^{-4} in the presence of excess sodium ions.

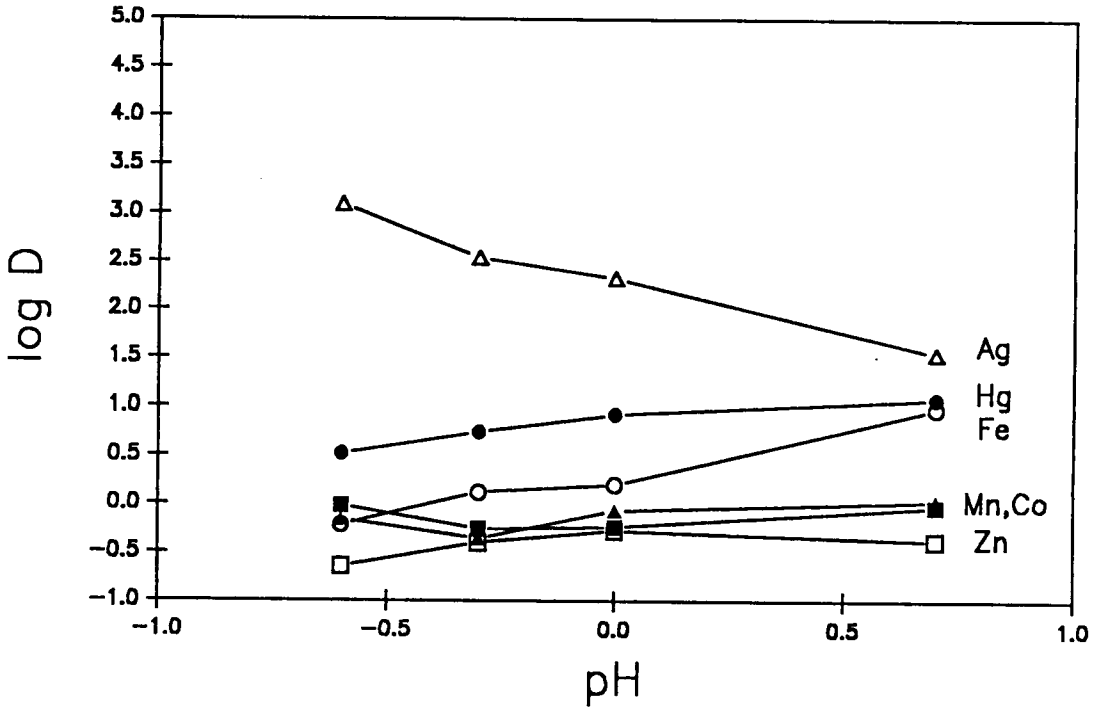

Figure 53. Plots of log D versus pH for Fe, Hg, Ag, Mn, Co and Zn extraction by the diethyl ester resin determined at an R_i of 5×10^{-4} in the presence of excess sodium ions.

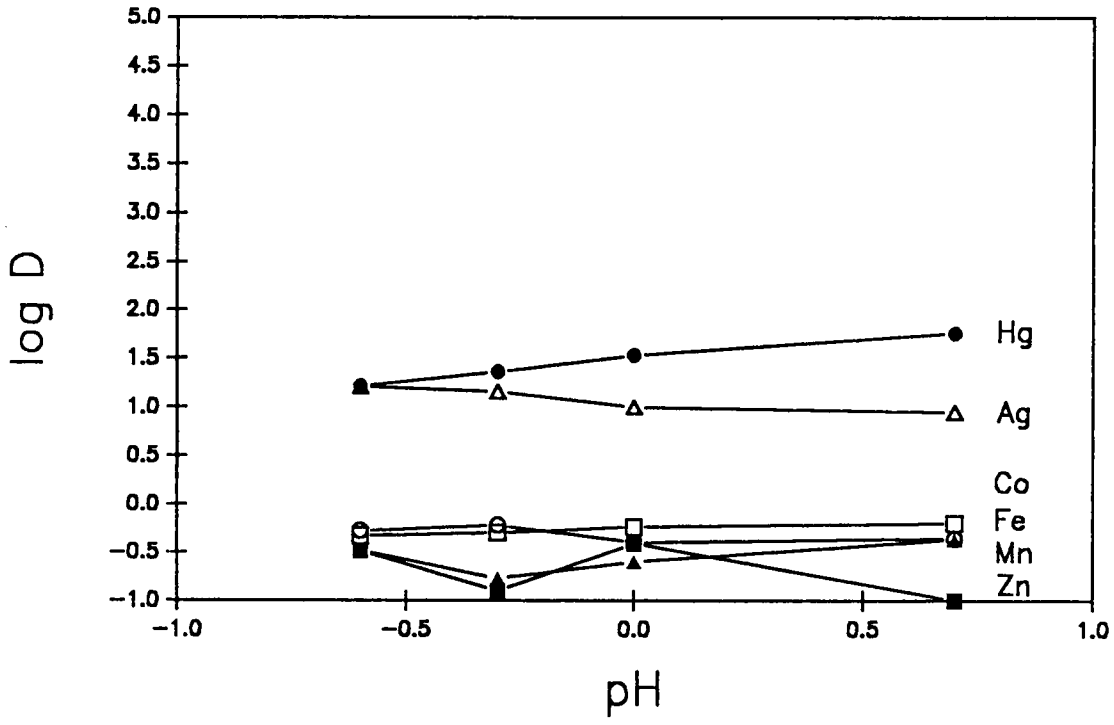

Figure 54. Plots of log D versus pH for Fe, Hg, Ag, Mn, Co and Zn extraction by the amine resin determined at an R_i of 5×10^{-4} in the presence of excess sodium ions.

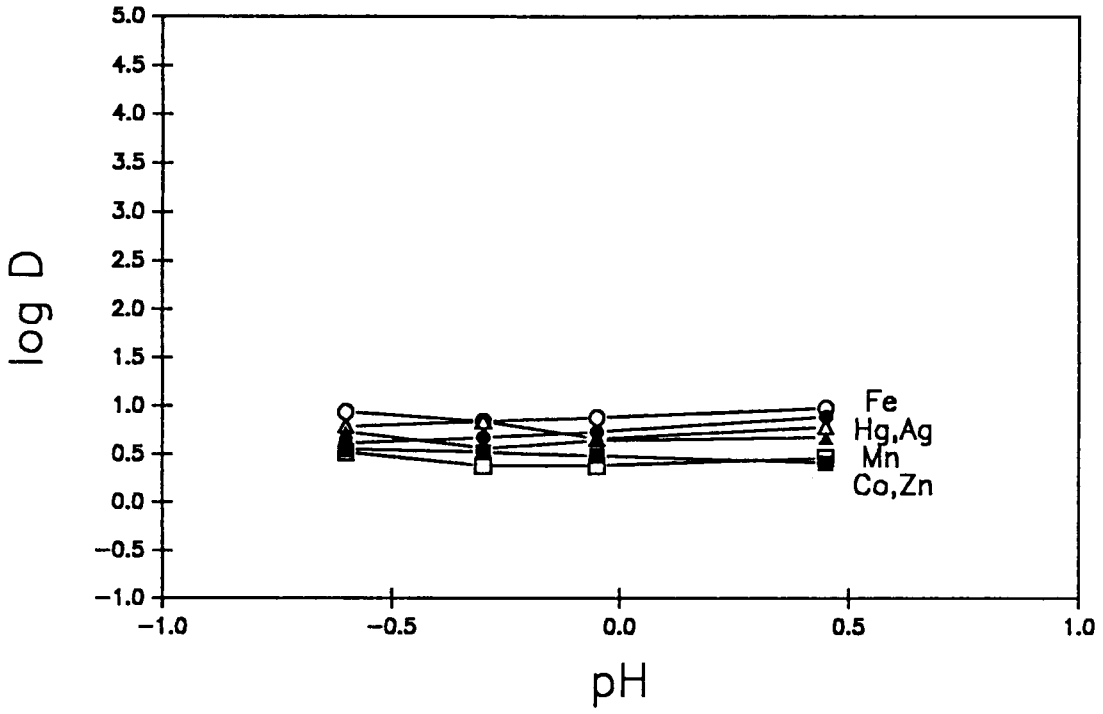

Figure 55. Plots of log D versus pH for Fe, Hg, Ag, Mn, Co and Zn extraction by the sulfonic resin determined at an R_i of 5×10^{-4} in the presence of excess sodium ions.

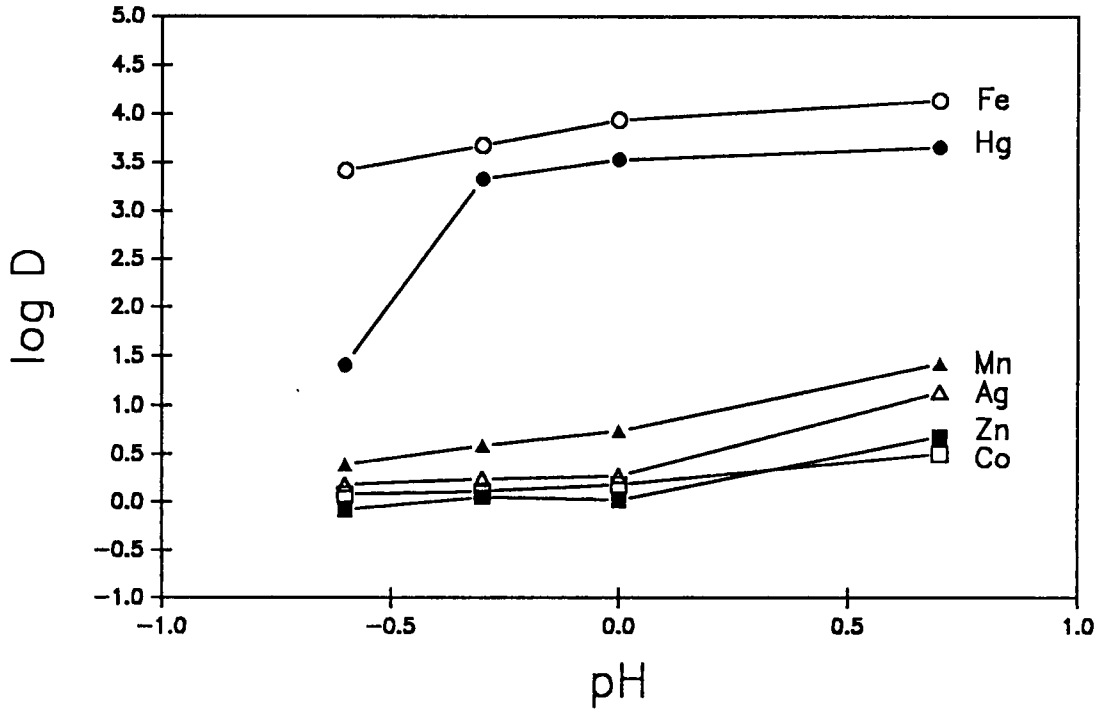

Figure 56. Plots of log D versus pH for Fe, Hg, Ag, Mn, Co and Zn extraction by the phosphinic resin determined at an R_i of 5 X 10^{-3} in the presence of excess sodium ions.

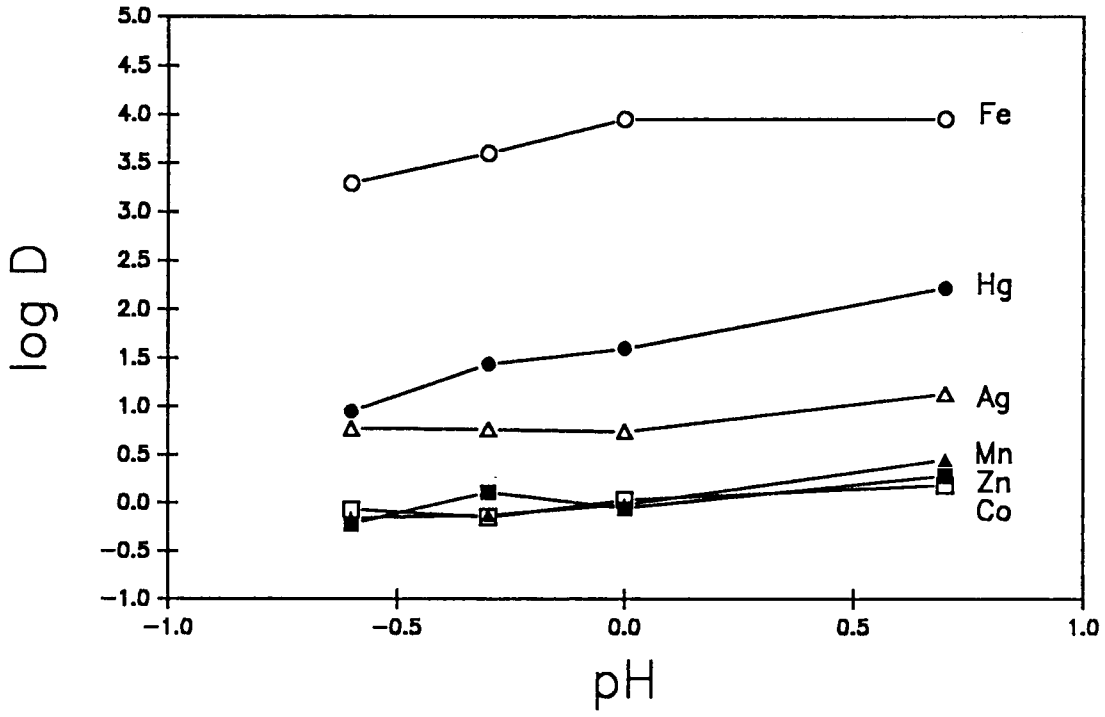

Figure 57. Plots of log D versus pH for Fe, Hg, Ag, Mn, Co and Zn extraction by the phosphonic resin determined at an R_i of 5×10^{-3} in the presence of excess sodium ions.

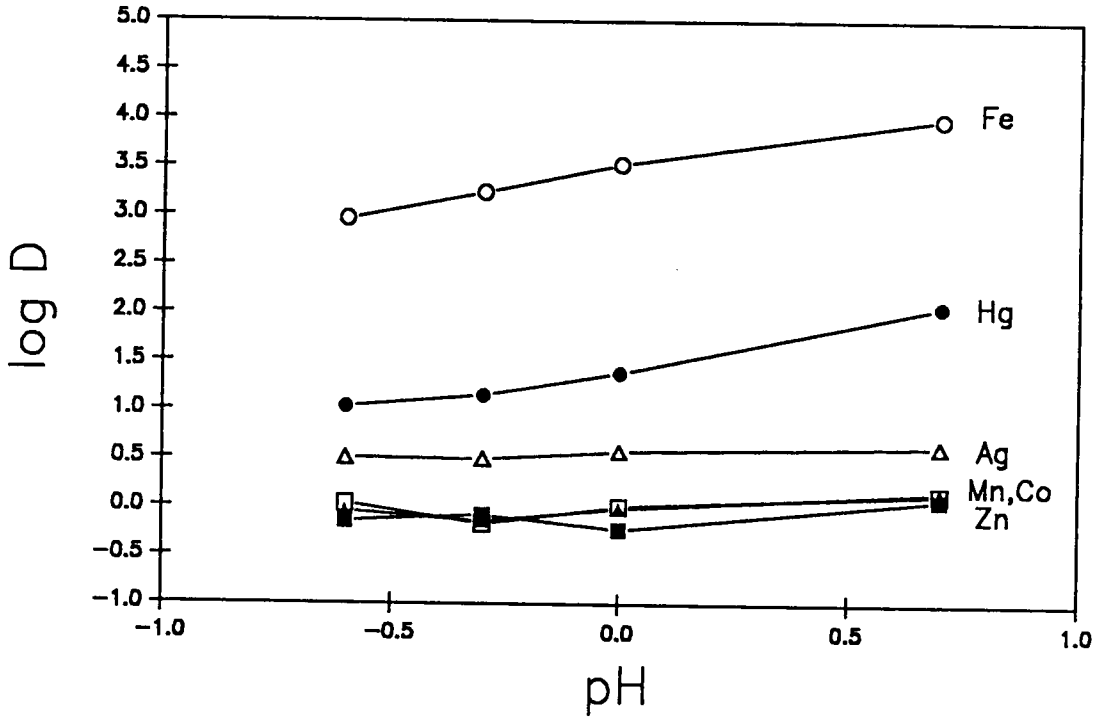

Figure 58. Plots of log D versus pH for Fe, Hg, Ag, Mn, Co and Zn extraction by the amine phosphonic resin determined at an R_i of 5 X 10^{-3} in the presence of excess sodium ions.

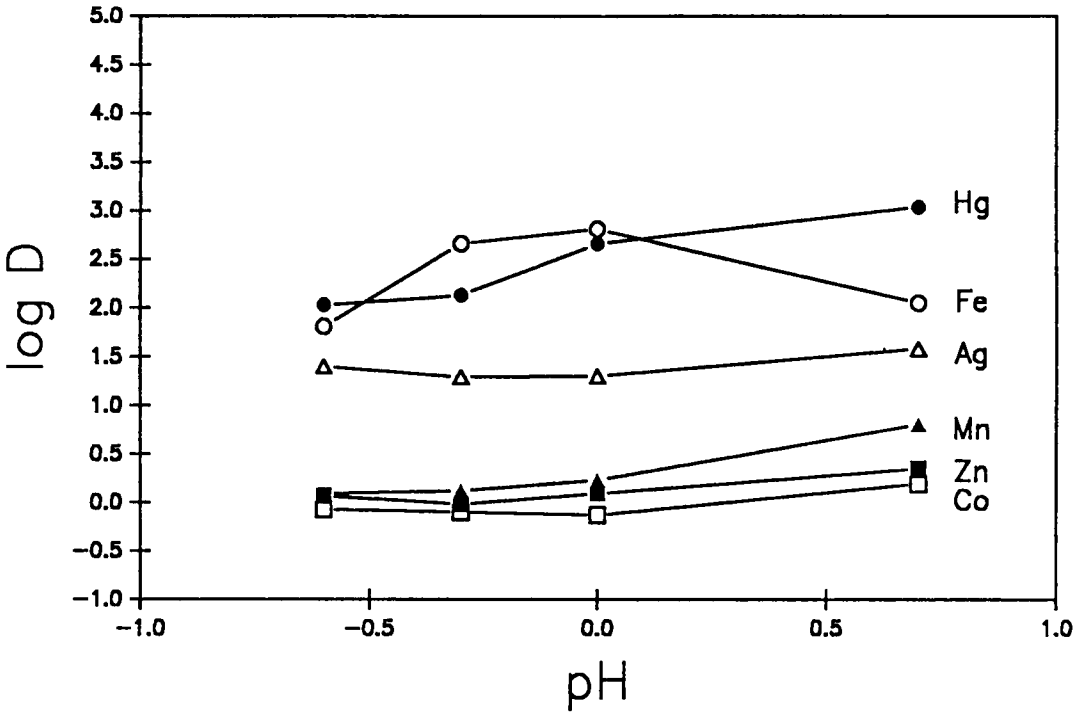

Figure 59. Plots of log D versus pH for Fe, Hg, Ag, Mn, Co and Zn extraction by the monoester resin determined at an R_i of 5 X 10^{-3} in the presence of excess sodium ions.

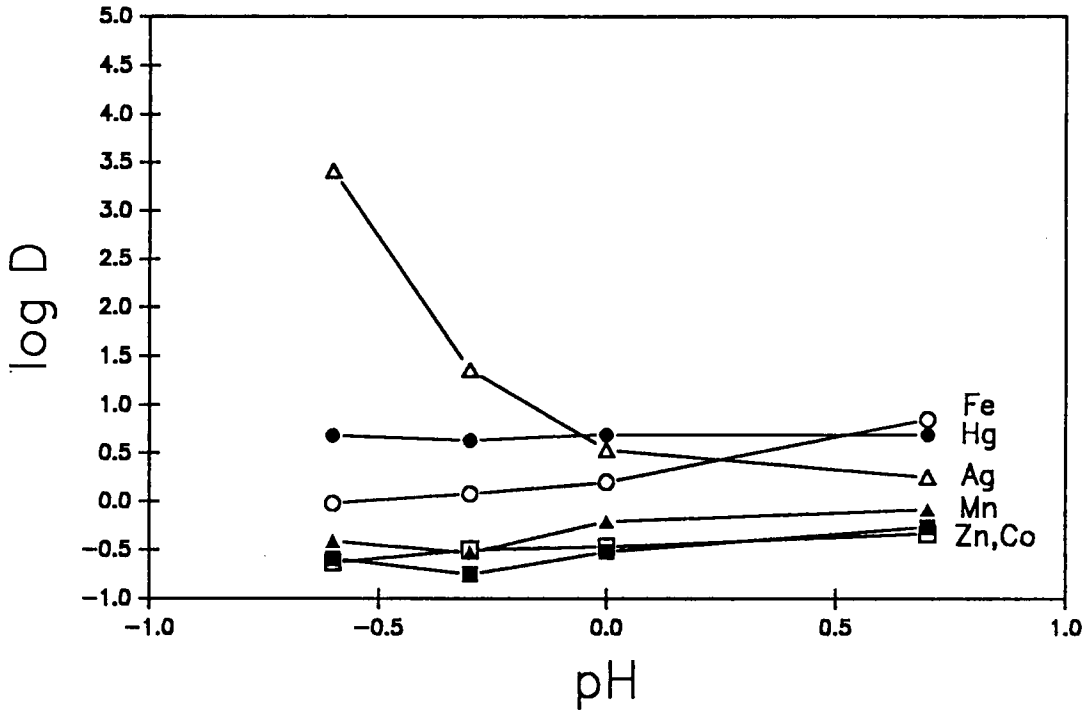

Figure 60. Plots of log D versus pH for Fe, Hg, Ag, Mn, Co and Zn extraction by the diethyl ester resin determined at an R_i of 5×10^{-3} in the presence of excess sodium ions.

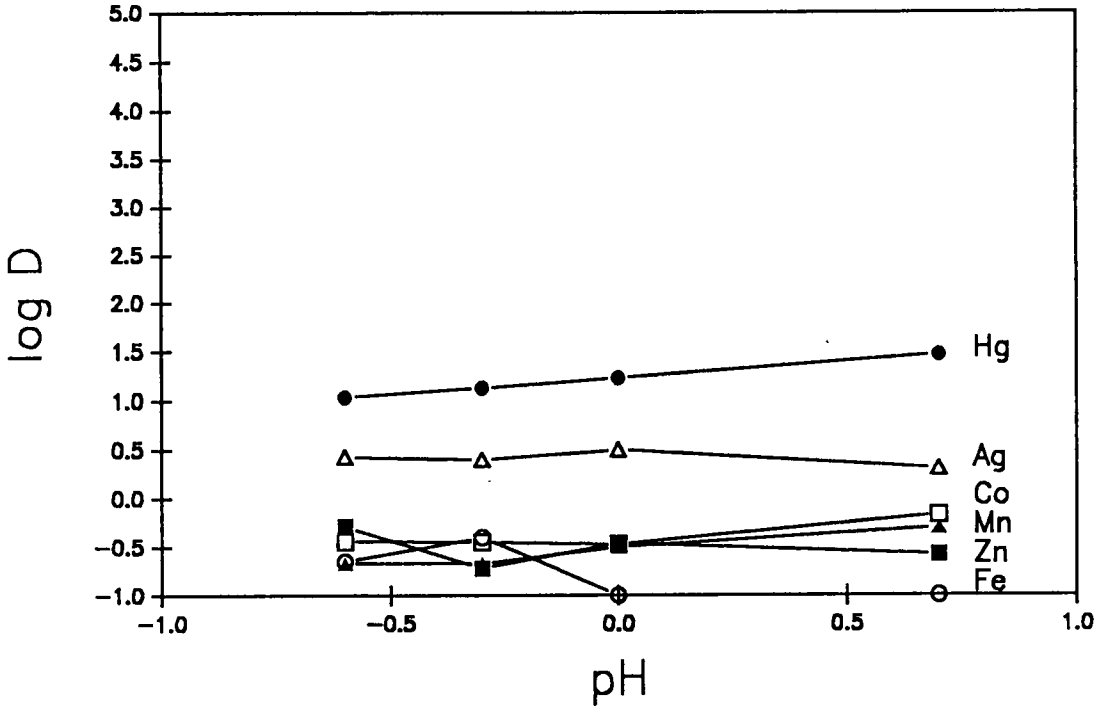

Figure 61. Plots of log D versus pH for Fe, Hg, Ag, Mn, Co and Zn extraction by the amine resin determined at an R_i of 5×10^{-3} in the presence of excess sodium ions.

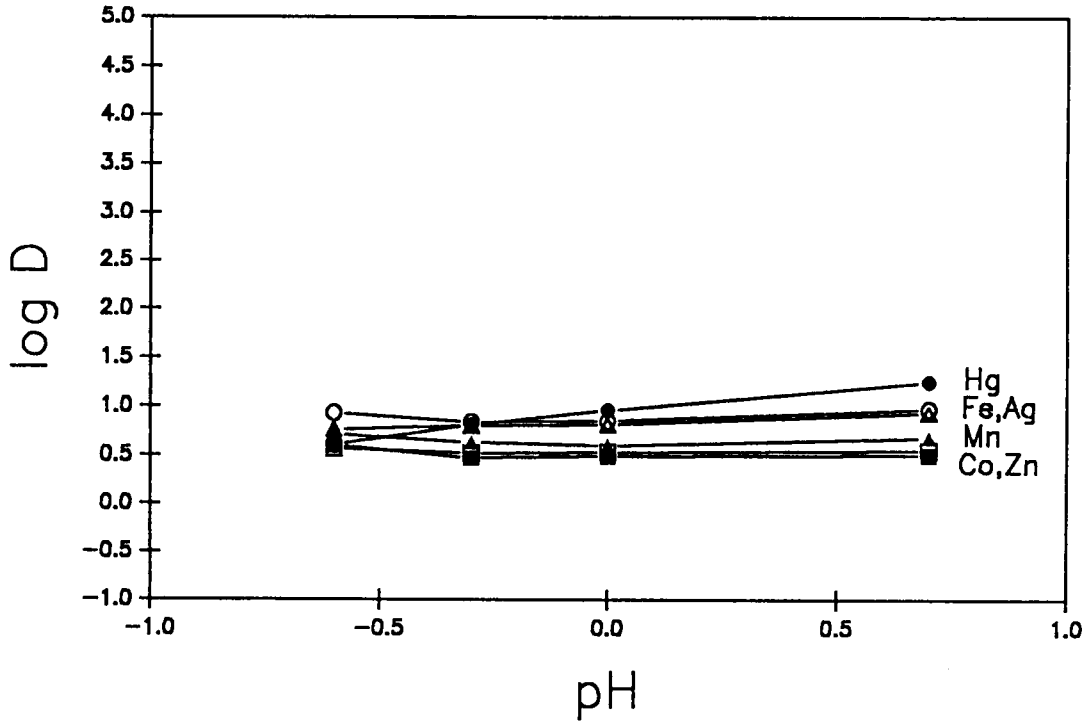

Figure 62. Plots of log D versus pH for Fe, Hg, Ag, Mn, Co and Zn extraction by the sulfonic resin determined at an R_i of 5 X 10^{-3} in the presence of excess sodium ions.

separation was obtained with the DMBP's than with the sulfonic. Changes in metal ion absorption were observed for some of the resins with increasing R_i. For example, dramatically lower levels of Ag were sorbed by the diethyl ester at an R_i of 5×10^{-3} than at 5×10^{-4}. As a result, the Ag/Fe selectivity factor decreased for the resin from 135 to 1.7. Extraction of Hg by the monoester resin increased by 0.6 log D units at the higher R_i, resulting in decreased Fe/Hg separation compared to the lower loading level.

Figure 63 gives the log D/pH plots for the extraction of Fe, Hg, Ag, Mn, Co and Zn by the sulfonic resin from background solutions of 4M HNO_3, 2M HNO_3, 1M HNO_3 and 0.2M HNO_3 at an R_i of 5×10^{-4}. As discussed in Chapter III, in the absence of excess $NaNO_3$, the slope of the log D/pH plot should equal the valence of the metal ion if extraction occurs solely by ion exchange. The slope values reported in Figure 63 verify that the sulfonic resin operates by ion exchange in the extraction of the six transition metal ions, although for Hg and Fe, the slopes were slightly different than predicted. In the case of Fe extraction, a slope of 2.5 was observed rather than the expected value of 3 for the ferric ion. One explanation for this result is that the log D value of 4.06 obtained for the highest pH solution was erroneously low due to the difficulty in measuring the low count rate of the solution after extraction. A log D of 4.65 is required to give the expected slope of 3 (with a correlation of 1.00) using the data for the three remaining background solutions. Given the background count rate of 30,000 cpm, the final solution activity needed to give a log D of 4.65 is calculated to be 17 cpm, a value even lower than the background count of 34 cpm.

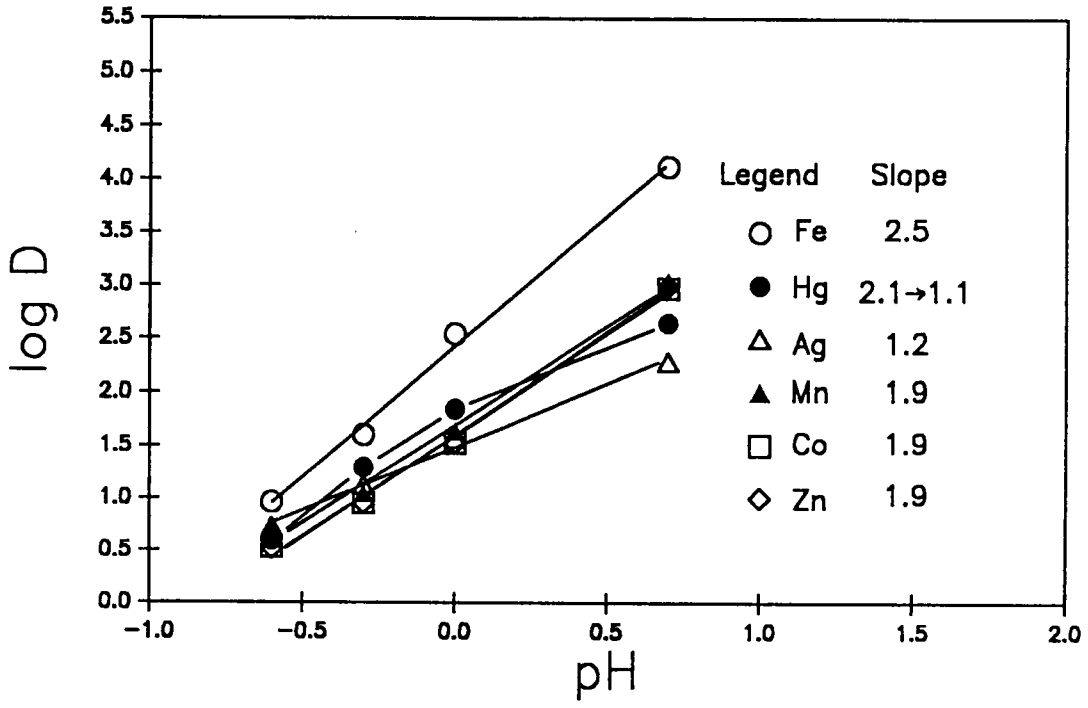

Figure 63. Plots of log D versus pH for Fe, Hg, Ag, Mn, Co and Zn extraction by the sulfonic resin determined at an R_i of 5×10^{-4} in the absence of added sodium ions.

To examine the possibility that the log D value was limited by the very low final count rate, the extraction was also performed using an initial solution activity of 128,000 cpm. This count rate requires a final solution activity of 71 cpm to give a log D value of 4.65. The log D value of 4.12 (corresponding to a final solution activity of 250 cpm) obtained using this higher count rate, however, was in excellent agreement with the previous result of 4.06, indicating that the lower than expected slope was not due to counting errors. An alternate explanation for the slope of 2.5 is that the sulfonic resin extracted both the ferric ion and its mononitrate salt, $FeNO_3^{2+}$, in equal proportions to yield the observed slope. Precedence for this behavior was noted in Chapter III in the extraction of thorium as both mono- and dinitrate salts by the sulfonic resin to give a slope of 2.5 rather than 4.

In the case of Hg extraction by the sulfonic resin, the expected slope of 2 was observed only in the pH region from -0.6 to 0.0. At the higher pH range from 0.0 to 0.7, the slope decreased to 1.1. To examine the possibility that ionic accessibility was limited for the 10% cross-linked gel sulfonic thus leading to the reduced slope, extractions were also carried out using a 3% cross-linked MR resin. Figure 64 presents the results of this study for the extraction of both Fe and Hg by the 3% cross-linked MR sulfonic resin. Slopes of 2.2 and 0.22 were observed for the extraction of Fe and Hg, respectively. These results were likely in error, however, due to leaching of linear sulfonated polymer from the resin pores into the background solutions as evidenced by the orange color of the solutions after shaking with the resins.

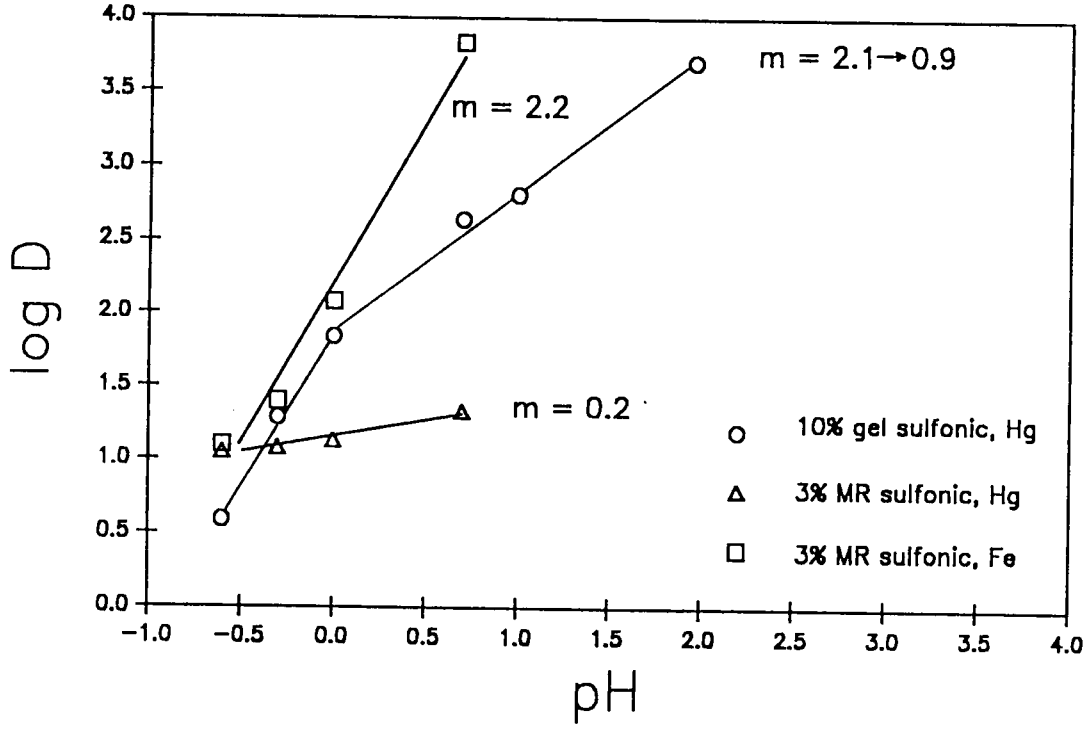

Figure 64. Plots of log D versus pH for Fe and Hg extraction by a 3% cross-linked MR sulfonic and for Hg extraction by a 10% cross-lined gel sulfonic determined at an R_i of 5×10^{-4} in the absence of sodium ions.

Erroneously low extraction data would result from counting the metal sorbed by the linear polymer in addition to the uncomplexed metal remaining in solution. Figure 64 also presents the results of Hg extraction by the 10% cross-linked sulfonic resin over a wider pH range than previously studied. The reduction in slope from 2.1 to approximately 1 was also found to hold over the extended pH range of 0.0 to 2.0. At the present time it is unclear as to why the slope of the log D/pH plot changed with increasing pH for Hg extraction by the sulfonic resin.

The selectivity series results are summarized in Figure 65 for extractions performed at an R_i of 5 X 10^{-4}. In these plots, the log D values are presented for the extraction of the six transition metal ions by all seven resins from a single representative background solution (1M HNO_3/3M $NaNO_3$). At these highly acidic conditions, coordination is expected to be the dominant extraction mechanism for the intermediate strength phosphorus acid resins. Focusing first on the selectivity series determined at an R_i of 5 X 10^{-4}, the following observations can be made. As noted previously, the DMBP's exhibit higher selectivity for extraction of the transition metal ions over sodium ions than the sulfonic resin. The sulfonic resin was found to load to log D levels less than 1 due to ion exchange with the excess Na ions present in solution. Additionally, the sulfonic resin was unable to distinguish between the six transition metal ions it absorbed as shown by its log D values which ranged from 0.4 for Co to 0.9 for Fe. Of the six transition metals studied, the DMBP's showed the highest affinity for Fe, Hg and Ag with the exception of the diethyl ester resin which

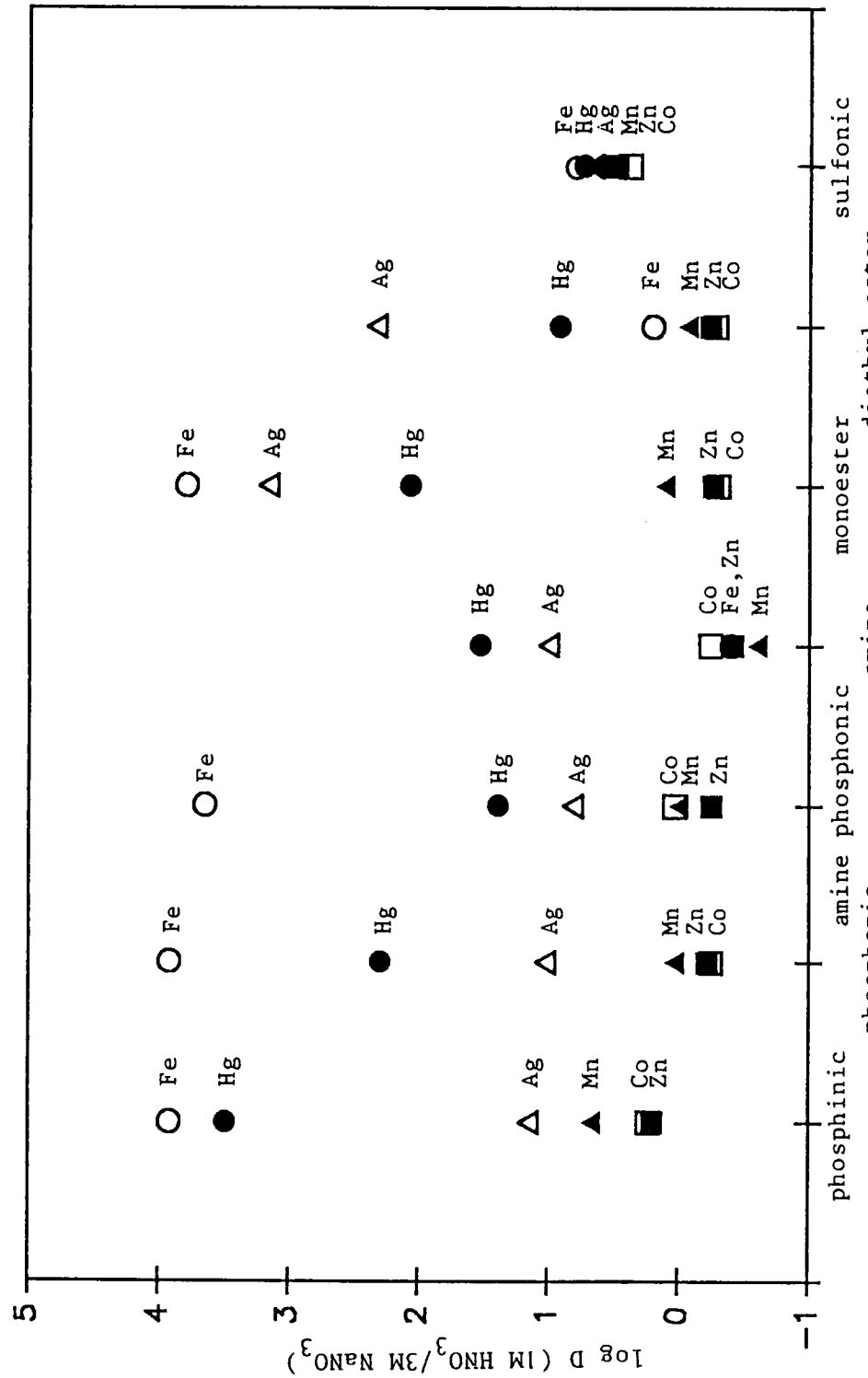

Figure 65. Selectivity series determined at an R_i of 5 X 10^{-4}.

extracted only low levels of Fe. The phosphinic, phosphonic and amine phosphonic sorbed these three metals in the order Fe> Hg> Ag, whereas the trend reversed to Ag> Hg> Fe for the diethyl ester and to Fe> Ag> Hg for the monoester. These reversals in the affinity trend make possible the selective recovery of certain metals using the DMBP's. For example, Ag can be selectively recovered from Fe-containing solutions using the diethyl ester resin. In contrast, selective removal of Fe from Ag is possible using the phosphinic, phosphonic and amine phosphonic resins. Of all the DMBP's, the phosphinic resin displayed the highest affinity for Hg, probably due to its ability to reduce mercuric ions to mercury metal as has been observed at higher R_i's. At $Hg(NO_3)_2$ concentrations as low as 1 X 10^{-4}N, however, the reduced metal cannot be observed in solution nor can the increase in acid capacity due to oxidation of the P-H bond be measured in order to prove that metal ion reduction has occurred. Nevertheless, the higher affinity of the phosphinic resin for Hg compared to the structurally similar phosphonic resin by over one log D unit strongly suggests the participation of the phosphinic's redox component. At the pH conditions employed in this study, sorption of Hg by the phosphinic resin most likely occurs as a mix of coordination and reduction processes, whereby access of the metal into the polymer network is given by the coordinative component and metal ion recognition leading to the enhanced affinity of the resin for Hg is provided through metal ion reduction.

In contrast to the Hg results, the phosphinic and phosphonic resins were found to have similar affinities for Ag, suggesting that Ag ions were not reduced by the phosphinic resin under these conditions.

Although the phosphinic resin has been shown to reduce Ag^{+} to Ag° at higher loading levels[75], stoichiometric considerations apparently preclude reduction or significantly slow its rate at very dilute $AgNO_3$ concentrations. The probability that two silver ions will come into close enough proximity to one P-H bond for the transfer of two electrons is greatly lessened at dilute solution conditions. The dependence of the phosphinic's reduction component on the metal ion concentration is examined in a subsequent section.

Comparison of the Fe, Hg and Ag extraction results for the amine phosphonic resin to those of its monofunctional amine and phosphonic counterparts suggests that the two groups operate independently in the bifunctional resin. The amine phosphonic appears to complex Ag and Hg through the amine group alone and to extract Fe solely by the phosphonic acid moiety. As was previously observed for Ag complexation at an R_i of 0.10, no synergistic enhancement was indicated for the extraction of trace levels of Ag, Hg or Fe. In fact, slightly lower levels of Hg, Ag and Fe were absorbed by the amine phosphonic resin than by the amine and phosphonic resins.

The polymer ligand-to-metal interactions indicated by the selectivity series results can be best described using the principles of HSAB theory. Examination of the affinity series results for the R_i of 5×10^{-4} shows that the hard Mn and borderline Co and Zn cations are extracted to low levels ($\log D < 1$) by all of the phosphorus-based resins. The low affinity of DMBP's for these ions can be explained by the fact that the relatively soft phosphoryl oxygen has little tendency to coordinate hard or borderline metal ions. Furthermore, in the highly

acidic solutions used in this study, little ion exchange is expected to occur with the medium-strength phosphorus acids, thus resulting in low degrees of extraction of these metals. In contrast, much higher levels of the soft Hg and Ag ions were complexed by the phosphorus resins. This interaction can be described as an enthalpy-driven coordination of the soft phosphoryl oxygen with the soft metal ions. The high affinity of the phosphorus resins for the hard ferric ion (with the exception of the diethyl ester resin) cannot be ascribed to an enthalpy-driven coordination process, however, given the Mn results which indicate that hard ions are extracted primarily through ion exchange. It is thus postulated that Fe interacts with the phosphoryl oxygen through an entropy-driven coordination process whereby the driving force for complexation is the entropically favored release of the waters of hydration of the ferric nitrate salt upon coordination with the phosphoryl oxygen. Literature precedent exists for entropically driven metal ion complexation by polymers. The sorption of lanthanide ions by poly(methacrylic acid) and its copolymers has been attributed to the very large positive entropy change obtained upon complex formation caused by the dehydration of the polymer ligand and the trivalent lanthanide ion.[115] In a 4M nitrate background used in this study, however, the ferric nitrate salt may not be fully hydrated, thus making its need for solvolysis the driving force behind the coordinative interaction. To examine this possibility, extractions of Fe and Hg were performed with the phosphinic resin from solutions of nitric acid alone and containing total nitrate levels of 4M and 1M through the addition of the appropriate amounts of $NaNO_3$. The results are presented as plots of

% absorbed and log D vs. pH in Figures 66 and 67 for Fe and Hg extraction, respectively. Although small variations in log D were observed for the three sets of solutions, almost identical % absorbed values were obtained regardless of the nitrate concentration, clearly indicating that both metals are fully hydrated in a background of 4M nitrate. As will be discussed later, the concept of enthalpy- and entropy-driven coordination has been further examined in extractions performed over a wide pH range both in the presence and absence of $NaNO_3$.

Figure 68 presents the selectivity series determined at an R_i of 5×10^{-3}. Although the results for the sulfonic resin were found to be independent of loading level, changes in the affinity trends with increasing R_i were observed for some of the DMPB's. For example, Ag extraction decreased by 0.9 log D units such that the selectivity trend reversed from Ag > Mn at an R_i of 5×10^{-4} to Mn > Ag at an R_i of 5×10^{-3}. For the monoester resin, the metal ion affinity changed from Fe > Ag > Hg at the lower loading level to Fe ~ Hg > Ag at the higher loading level. Furthermore, much greater separation of the three metals was achieved at the lower R_i. For example, the Fe/Hg SF for the monoester decreased from 53 at an R_i of 5×10^{-4} to 1.4 and 5×10^{-3}. In addition, the diethyl ester resin gave higher Hg/Ag separation at the lower R_i. Whereas Fe extraction by the diethyl ester remained constant and Hg absorption decreased only slightly, a precipitous decline in the log D for Ag of over 1.8 units resulted in a decrease in the SF from 26 at an R_i of 5×10^{-4} to 0.7 at an R_i of 5×10^{-3}. The influence of loading level on the observed metal ion selectivity was examined from an

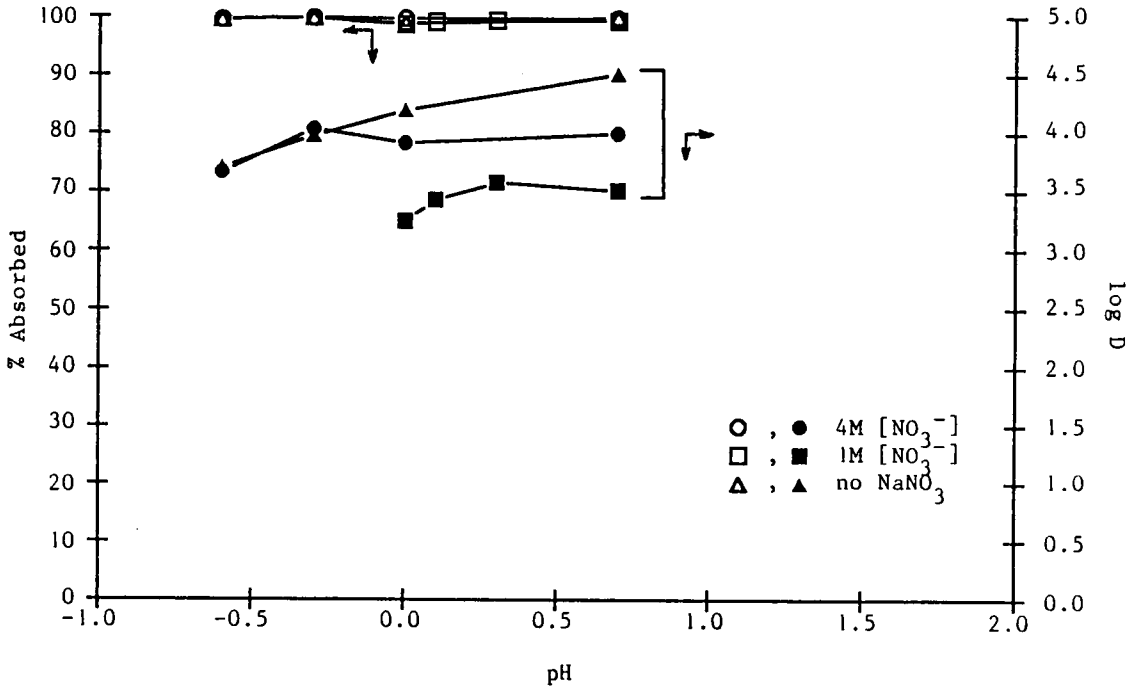

Figure 66. Plots of % absorbed and log D versus pH for Fe extraction by the phosphinic resin at an R_i of 5 X 10^{-4} from background solutions of varying nitrate concentration.

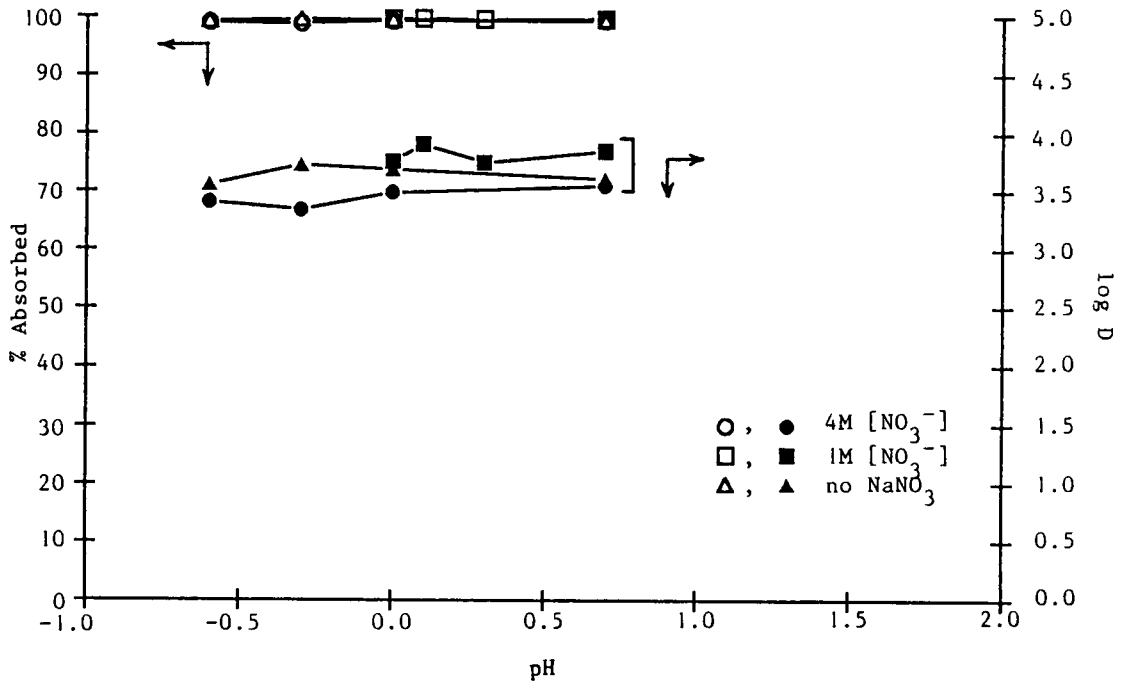

Figure 67. Plots of % absorbed and log D versus pH for Hg extraction by the phosphinic resin at an R_i of 5 X 10^{-4} from background solutions of varying nitrate concentration.

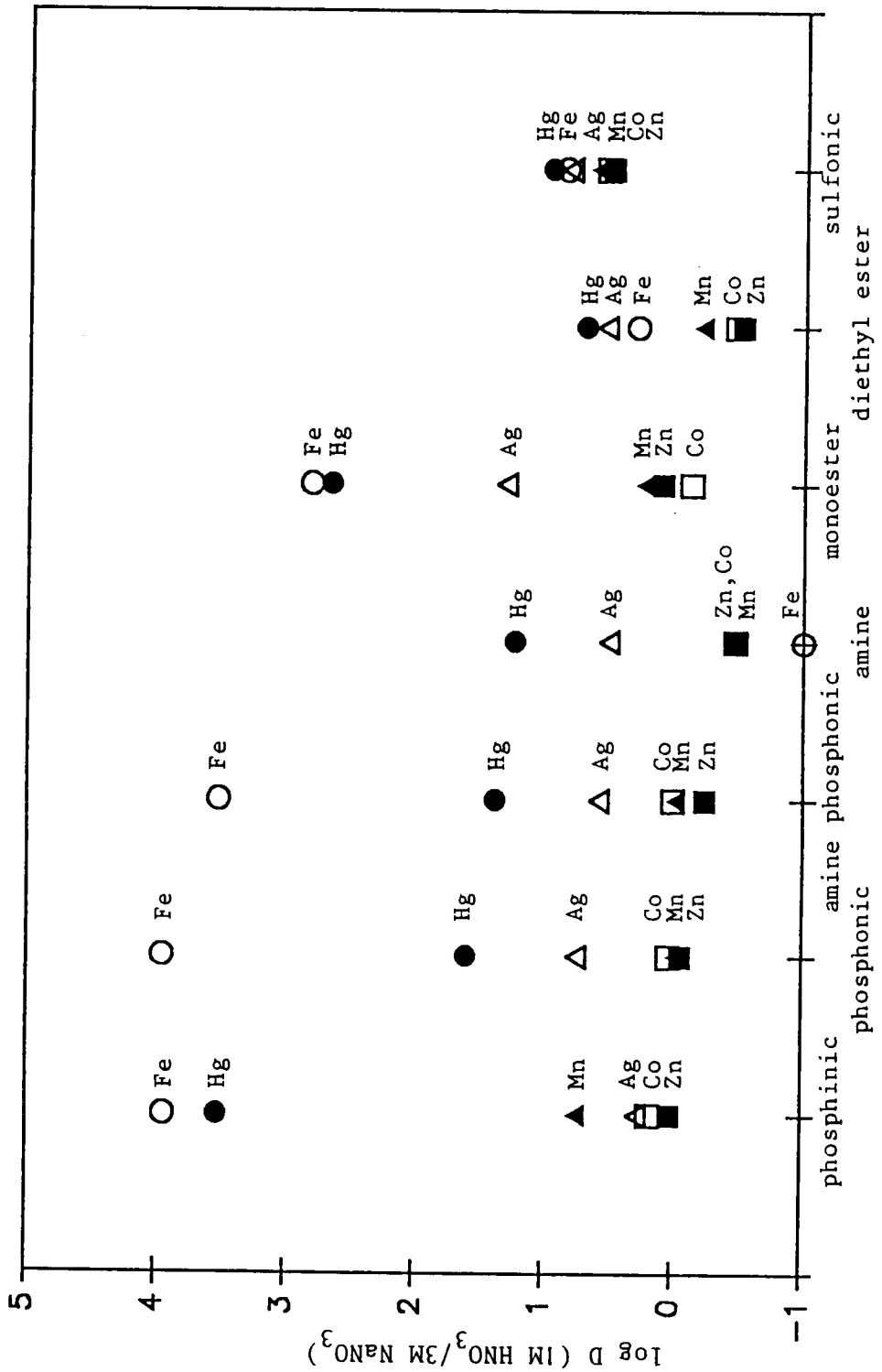

Figure 68. Selectivity series determined at an R_i of 5 X 10^{-3}.

R_i of 5 X 10^{-5} to 1.0 for the phosphinic and phosphonic resins as will discussed subsequently.

The selectivity series results indicate that enhanced ionic recognition by DMBP's can be determined through either **reaction control** or **steric control** of the extraction process. An example of reaction control is the reduction of mercuric ions to the zerovalent metal at an R_i of 5 X 10^{-4} by the phosphinic resin thus leading to a much higher selectivity for Hg over Ag (SF = 219) than is attained using the phosphonic (SF = 19) or amine phosphonic (SF = 4) resins. Enhanced ionic recognition through steric control of extraction is illustrated by the diethyl ester resin which has a higher preference for Ag over Hg (SF = 25) than the monoester resin (SF = 12). The enhanced Ag selectivity achieved with the diethyl ester resin is likely because of steric hindrance of the phosphoryl oxygen coordination site by the two ethyl groups. This results in the resin's preference to coordinate the less bulky $AgNO_3$ over $Hg(NO_3)_2$. In the next section, steric control of ionic recognition is examined for diester resins of varying alkyl group size.

Effect of Diester Alkyl Group Size on Fe, Hg, and Ag Complexation

The influence of diester alkyl group size on transition metal ion extraction was examined using dimethyl, diethyl, di-*n*-propyl and di-*n*-butyl ester resins. The extractions were performed at R_i's of 5 X 10^{-4} and 5 X 10^{-3} from background solutions of 4M HNO_3, 2M HNO_3/2M $NaNO_3$, 1M HNO_3/3M $NaNO_3$ and 0.2M HNO_3/3.8M $NaNO_3$. Figures 69-71 give the log D/pH correlations performed at an R_i of 5 X 10^{-4} for the extraction of Fe and Hg by dimethyl, diethyl, di-*n*-propyl and di-*n*-butyl ester resins and for

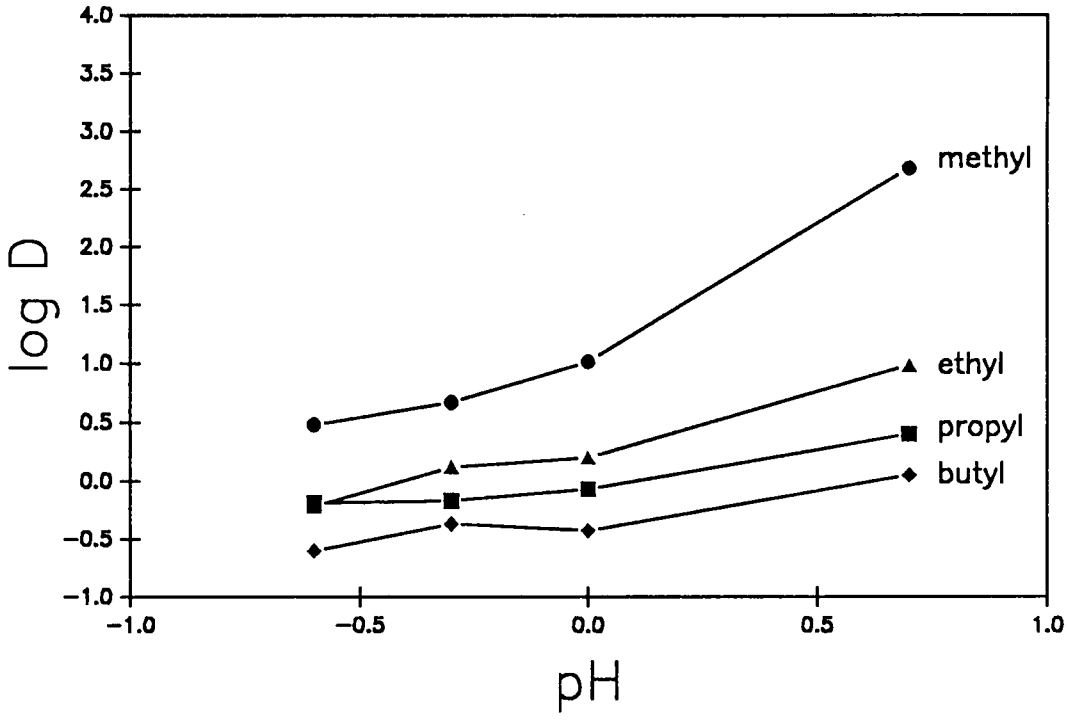

Figure 69. Log D versus pH correlations for Fe extraction by diester resins at an R_i of 5 X 10^{-4} in the presence of sodium ions.

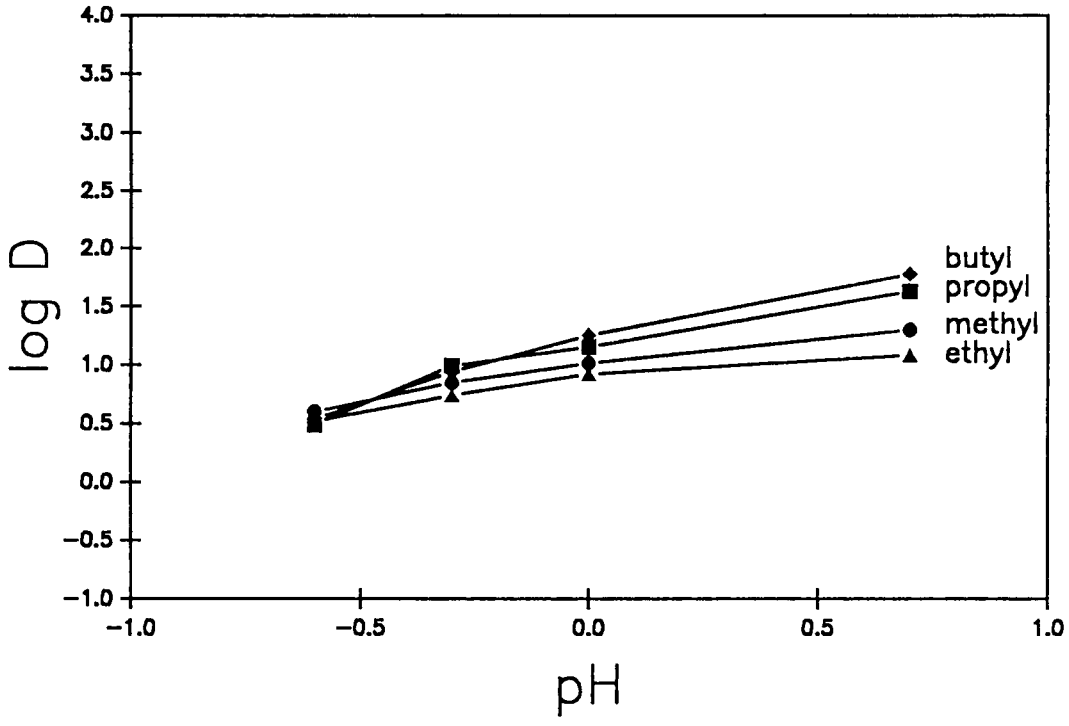

Figure 70. Log D versus pH correlations for Hg extraction by diester resins at an R_i of 5 X 10^{-4} in the presence of sodium ions.

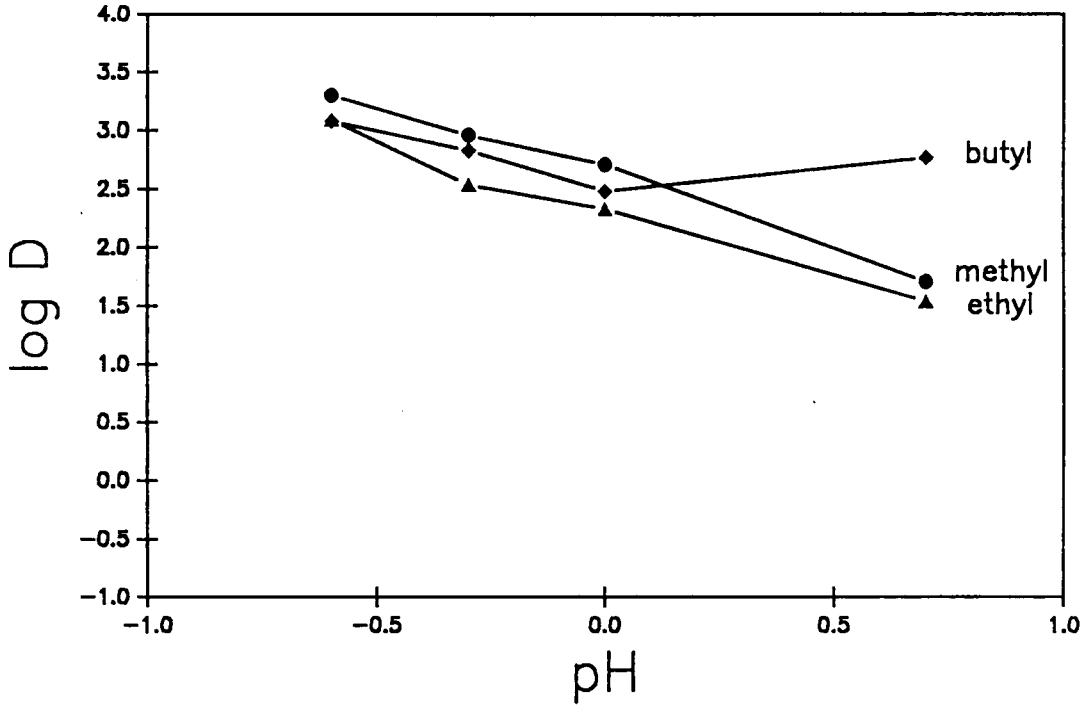

Figure 71. Log D versus pH correlations for Ag extraction by diester resins at an R_i of 5 X 10^{-4} in the presence of sodium ions.

extraction of Ag by dimethyl, diethyl and di-*n*-butyl resins. The results for Fe, Hg and Ag extraction by dimethyl, diethyl and di-*n*-butyl esters at an R_i of 5×10^{-3} are presented in Figures 72-74. A strong dependence of alkyl group size on the results was observed in the extraction of Fe by the diesters. The order of Fe absorption (dimethyl > diethyl > di-*n*-propyl > di-*n*-butyl) parallels that of increasing substituent size. Complexation of Hg and Ag by the diesters, however, was found to be independent of the size of the alkyl moiety. Only slight variation in Hg sorption was observed for the four resins at both R_i's, following the extraction order di-*n*-butyl > di-*n*-propyl > dimethyl > diethyl. Likewise, the extraction results were not correlated to the alkyl substituent size for Ag complexation. For example, at an R_i of 5×10^{-4}, nearly identical results were obtained for the diester resins, with the exception of the di-*n*-butyl resin which extracted higher levels of Ag from the 0.2M HNO_3/3.8M $NaNO_3$ background solution than the other resins. Considerably larger differences in Ag complexation were found for the three resins at loadings of 5×10^{-3} than at 5×10^{-4}, especially in the highest acid region. At an R_i of 5×10^{-3}, the metal ion separation was found to be greatest in the 4M HNO_3 solution with diethyl >> di-*n*-butyl >> dimethyl. With increasing pH, however, the separation width decreased substantially and the selectivity trend changed to di-*n*-butyl > dimethyl > diethyl in the 0.2M HNO_3/3.8M $NaNO_3$ background solution.

The differences in Fe affinity for the diester resins are most likely related to steric crowding of the P=O coordinating site since the order of increasing metal absorption follows that of decreasing alkyl

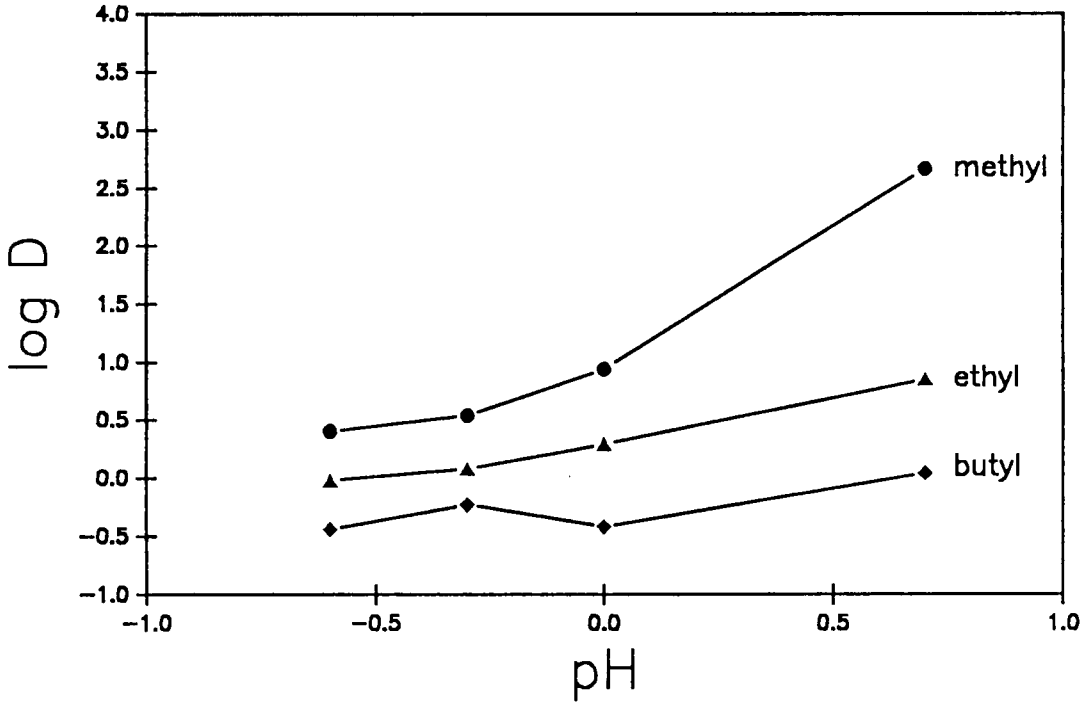

Figure 72. Log D versus pH correlations for Fe extraction by diester resins at an R_i of 5 X 10^{-3} in the presence of sodium ions.

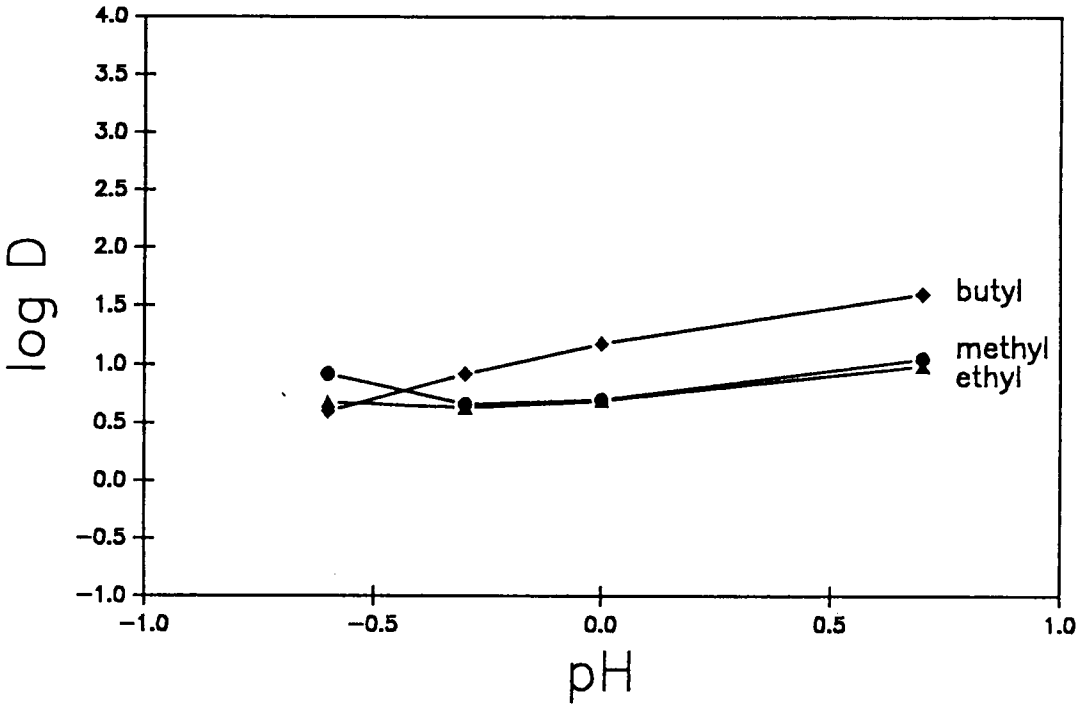

Figure 73. Log D versus pH correlations for Hg extraction by diester resins at an R_i of 5 X 10^{-3} in the presence of sodium ions.

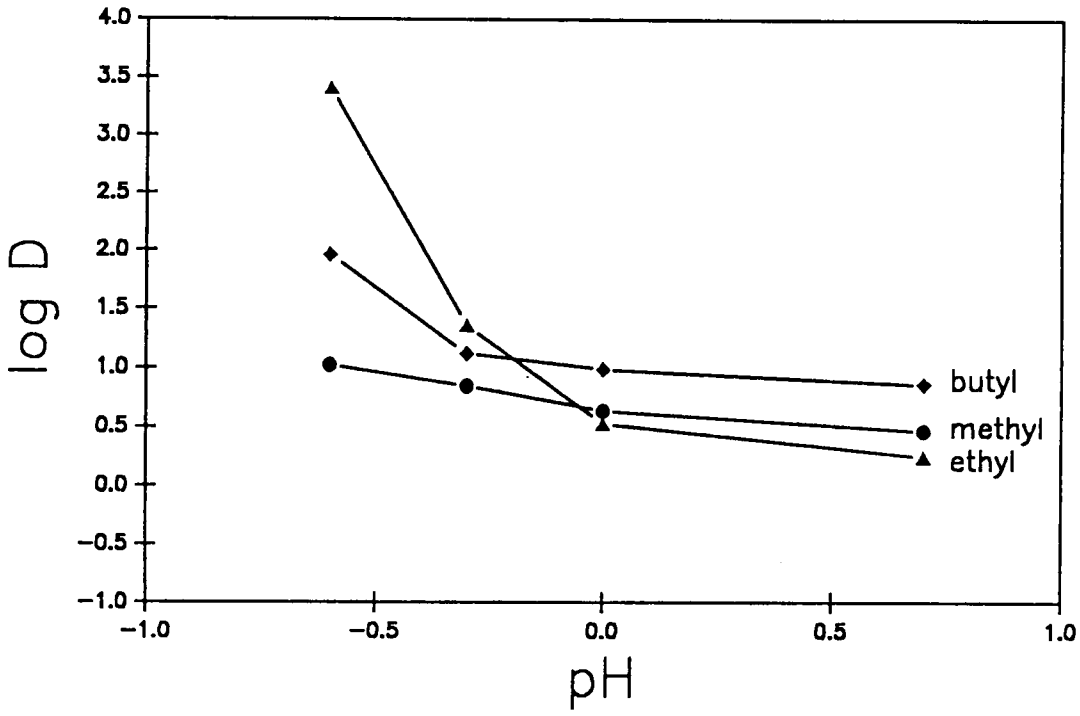

Figure 74. Log D versus pH correlations for Ag extraction by diester resins at an R_i of 5 X 10^{-3} in the presence of sodium ions.

group size. The dissimilar behavior of Hg and Ag is probably due to the smaller size of $Hg(NO_3)_2$ and $AgNO_3$ in relation to $Fe(NO_3)_3$ with its nine waters of hydration. The Fe extraction results, however, can also be correlated to the amount of phosphonic acid groups present as impurities on the diester resin. In general, the amount of acidic impurities (as phosphonic and/or monoester groups) decreased with increasing size of the diester alkyl group. For example, an acid capacity of 0.65 mequiv/g was obtained for the dimethyl ester resin (91.2% esterification) compared to 0.15 mequiv/g for the di-*n*-butyl ester resin (97.4% esterification). In Figure 75 the log D value for Fe extraction at R_i's of 5×10^{-4} and 5×10^{-3} from the 1M HNO_3/3M $NaNO_3$ background solution is plotted against the milliequivalents of acid sites present in one milliequivalent of phosphorus sites for all of the diester resins studied. With the exception of one datum point obtained for the di-*n*-propyl ester at an R_i of 5×10^{-4}, excellent agreement was found between the log D value and the amount of acid groups present in the diester sample (correlation coefficient = 0.9975). Although it appears that Fe extraction by the diester resins is an example of enhanced ionic recognition achieved through steric control, the possibility that the extractions are governed by the level of acidic groups present cannot be ruled out. Therefore, the extractions should also be carried out using diester resins containing equal amounts of acidic impurities to determine the source of the observed Fe selectivity.

The Hg, Fe, and Ag extraction results for the dimethyl, diethyl and di-*n*-butyl ester resins are summarized in the selectivity series plots presented in Figures 76 and 77 for R_i's of 5×10^{-4} and 5×10^{-3},

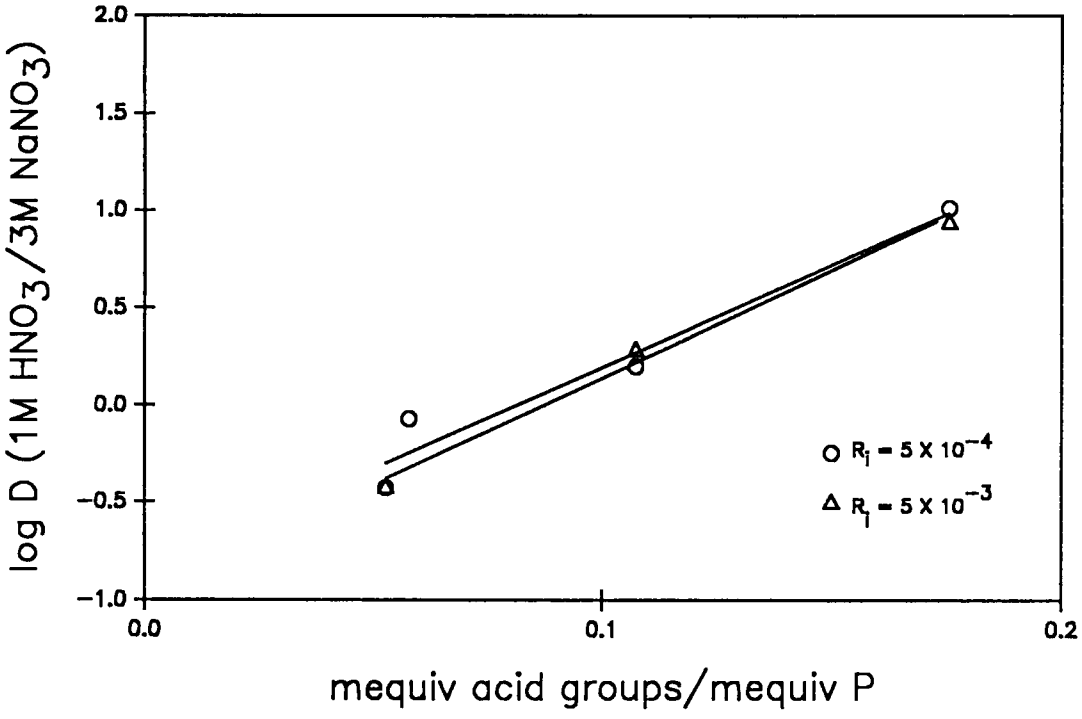

Figure 75. Variation in log D as a function of the mequiv of acid groups/mequiv P for the diester resins in the extraction of Fe at an R_i of 5 X 10^{-4} from 1M HNO_3/3M $NaNO_3$.

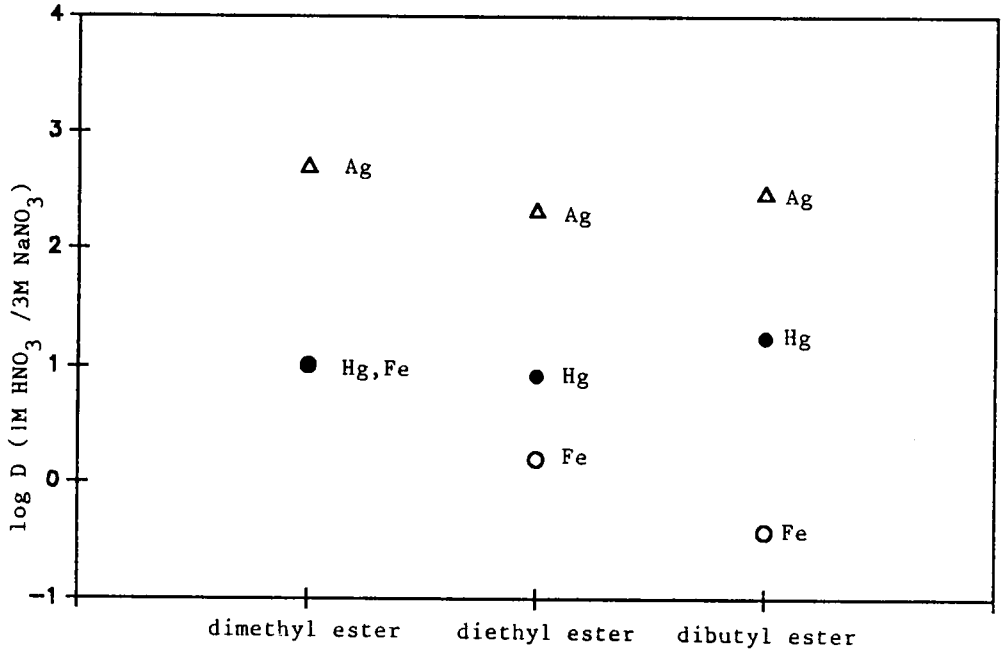

Figure 76. Selectivity series for diester resins determined at an R_i of 5 X 10^{-4}.

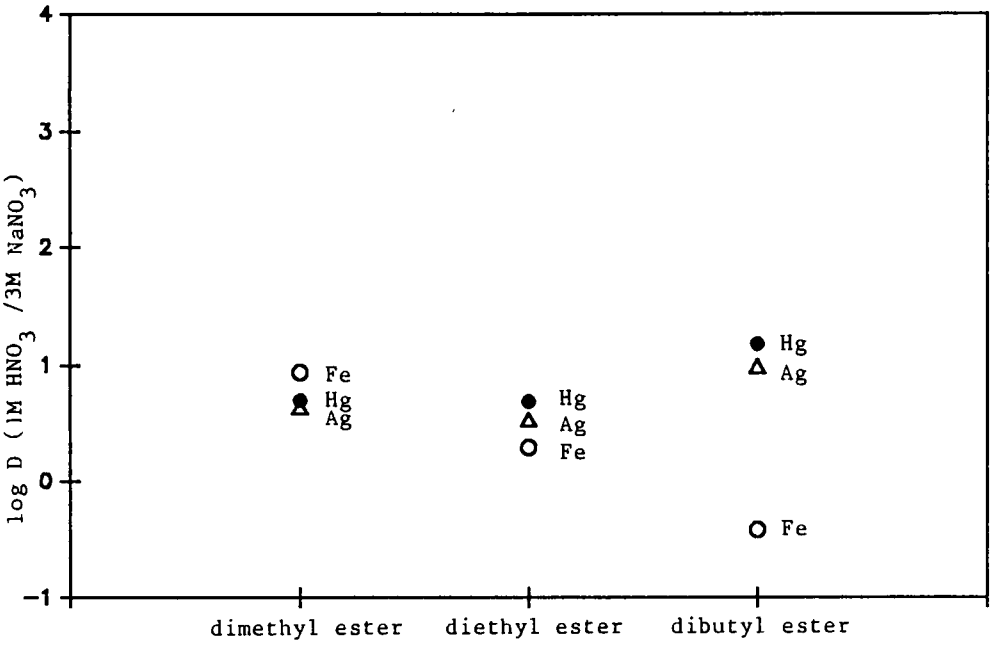

Figure 77. Selectivity series for diester resins determined at an R_i of 5 X 10^{-3}.

respectively. Both sets of results show increasing metal ion separation with increasing size of the alkyl group, mainly due to decreased Fe absorption. Much poorer separation of Fe, Hg and Ag was achieved, however, at the higher R_i as a result of the precipitous decline in Ag absorption with increased loading level. For example, Ag/Hg separation factors of 50, 26 and 18 were obtained for the dimethyl, diethyl and di-*n*-butyl resins, respectively, at an R_i of 5×10^{-4} compared to 0.87, 0.69 and 0.65 at an R_i of 5×10^{-3}.

Neutral liquid organophosphorus reagents such as TBP can complex nitric acid from aqueous solutions through coordination to the phosphoryl oxygen.[4] This same behavior was observed with the phosphorus-based resins. The nitric acid complexing ability of some DMBP's and liquid extractants was quantified in the following manner. The resin or liquid extractant solution was contacted with a 1M aqueous solution of HNO_3 in a 1 to 2.5 ratio of phosphorus sites to HNO_3. After a contact period of 15-17 h, a portion of the nitric acid solution was titrated to determine the amount of acid absorbed by the extractant. As shown by the results in Table 55, much higher levels of nitric acid were extracted by the phosphorus-based resins than by the sulfonic, an indication of the superior coordinative ability of the phosphoryl oxygen over the sulfonyl oxygen. Comparison of the results for the phosphorus resins, demonstrates that higher nitric acid capacities were obtained for the esterified resins than for the phosphinic and phosphonic resins. Similar extraction behavior was observed for the three diester resins regardless of the alkyl substituent. This observation has been previously noted for HNO_3 extraction by liquid trialkyl phosphates with

Table 55

Extraction of HNO_3 by DMBP's and Liquid Extractants[a]

Extractant	mequiv HNO_3 extracted/mequiv P
phosphinic	0.18
phosphonic	0.16
monoester	0.33
dimethyl ester	0.33
diethyl ester	0.33
di-n-propyl ester	0.30
sulfonic	0.02[e]
tri-octyl-phosphine oxide	0.78[b]
tri-n-butyl phosphate	0.12[b]/0.14[c]
Cyanex-272[d]	0.07[b]

[a] Measured as HNO_3 uptake from a 1M aqueous solution at a loading ratio of 10 mequiv HNO_3/4 mequiv phosphorus sites.
[b] In toluene.
[c] In dodecane.
[d] Di(2,2,4-trimethyl pentyl) phosphinic acid.
[e] Mequiv HNO_3 extracted/mequiv S

alkyl groups ranging from *n*-butyl to *n*-octyl.[116] The liquid extractant results demonstrate that the neutral phosphorus reagents complex greater amounts of HNO_3 than the acidic extractant, di-(2,4,4-trimethylpentyl) phosphinic acid (Cyanex 272). Comparison of the results for the two neutral extractants indicates that the phosphine oxide is a stronger coordinator of nitric acid that the phosphate ester. This is attributed to the electron donation of the three alkyl groups of the phosphine oxide, thus increasing its phosphoryl oxygen basicity relative to the phosphate ester which has three electron-withdrawing alkoxy groups attached to phosphorus.

The high affinity of the diester resins for HNO_3 apparently plays an important role in their extraction of Ag. As shown in Figures 53 (page 241), 60 (page 248), 71 (page 266) and 74 (page 271), the absorption of Ag by the diester resins increased with increasing solution acidity, giving a negative slope to the log D/pH plot. That this behavior is not an artifact of decreasing $NaNO_3$ concentration is indicated by the results in Figure 78 for the extraction of Ag by the diethyl ester resin in both the presence and absence of added $NaNO_3$. The observed dependence of the results on the nitric acid concentration is best explained by the extraction of a protonated $AgNO_3$ complex by the diester resins. It is interesting to note that this behavior occurs only for Ag extraction by the diesters and not for Hg or Fe.

Metal Ion Complexation over an Extended pH Range

The complexing ability of the phosphinic and sulfonic resins for Fe, Hg and Mn at an R_i of 5×10^{-4} was examined over an extended range

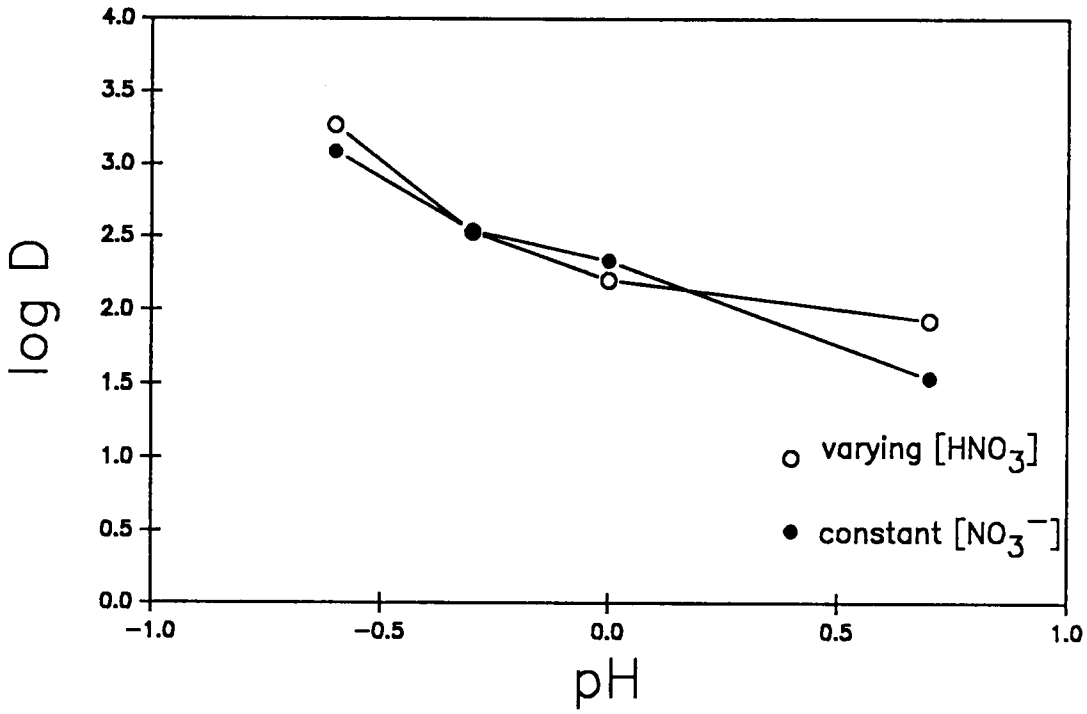

Figure 78. Extraction of Ag by the diethyl ester resin in the presence and absence of $NaNO_3$ at an R_i of 5 X 10^{-4}.

of solution acidities (4M to 1 X 10^{-4}M) both in the presence and absence of $NaNO_3$. Depending on the solution pH, the access mechanism of the Class I and Class II DMBP's can be provided by either ion exchange or coordination. The ion-exchange mechanism is expected to be inoperative for the intermediate strength phosphinic acid ($pK_a \sim 4$) in the solutions of highest acidity. In the acid region of approximately 0.10 to 10^{-4}N HNO_3, access is most likely provided by a mix of ion exchange and coordination. Only at pH values greater than the resin's pK_a would ion exchange become the predominant access pathway. Metal ion extraction was thus studied from a wide range of nitric concentrations in order to determine the effect of solution pH on the phosphinic resin's access mechanism. The recognition mechanism of the phosphinic is given either by coordination or reduction of the target metal ion and is governed by the hard/soft character and reduction potential of the metal ion. Thus, Fe(III), Mn(II) and Hg(II) were chosen for study in order to provide a wide range of hard/soft character and reduction potentials for the target metal ion.

The complexation of Fe, Hg and Mn was also studied using the liquid phosphorus-based extractants dicyclohexyl phosphinic acid (DCHPA) and DEHP under conditions identical to those described above so that the extraction mechanisms of the small-molecule and polymer-supported extractants could be compared. The two liquid extractants were chosen for study in order to examine the influence of the electronic properties of the phosphoryl oxygen on the complexing ability of the extractant. Thus, the nature of the substituents attached to phosphorus were varied

from the electron-withdrawing alkoxy groups of DEHP to the electron-releasing alkyl groups of DCHPA.

The solutions used in the study comprised the target metal nitrate present at 1 X 10^{-4}N in a background of varying concentrations of nitric acid (4M, 2M, 1M, 0.2M, 0.1M, 10^{-2}M, 10^{-3}M and 10^{-4}M). In addition, to maintain constant ionic strength, the following background solutions containing sodium nitrate were also used: 2M HNO_3/2M $NaNO_3$, 1M HNO_3/3M $NaNO_3$, 0.2M HNO_3/3.8M $NaNO_3$, 0.1M HNO_3/3.9M $NaNO_3$, 10^{-2}M HNO_3/3.99M $NaNO_3$, 10^{-3}M HNO_3/3.999M $NaNO_3$ and 10^{-4}M HNO_3/3.9999M $NaNO_3$. In preparing the solutions, a 1 to 10 dilution of 1 X 10^{-3}N stock metal solution was performed using a stock background solution of HNO_3(/$NaNO_3$) of appropriate concentration to yield the desired concentration after dilution. For example, to prepare a solution of 1 X 10^{-4}N metal nitrate in 2M HNO_3/2M $NaNO_3$, 10 mL of 1 X 10^{-3}N stock metal nitrate was diluted to 100 mL with 2.22M HNO_3/2.22 M $NaNO_3$ stock background solution. The pH of all stock metal nitrate solutions was adjusted to 1.5-1.7 with HNO_3 to prevent metal ion hydrolysis. Thus, in calculating the pH of the metal solution after dilution with stock background solution, the contribution of the protons from the stock metal nitrate solution must be included, particularly for the higher pH solutions. For example, the pH of the background solution containing 1 X 10^{-4}M HNO_3 would not be 4 as expected, but rather 2.49 if the pH of the stock metal nitrate solution was 1.5 ($[H^+] = [10(10^{-1.5}) + 90(1.111 \text{ X } 10^{-4})]/100 = 3.33 \text{ X } 10^{-3}$; pH = 2.49). Thus, the metal ion extraction results were not complicated by hydrolysis of the metal ions as would be the case for both Fe^{3+} and Hg^{2+} in pH 3-4 solutions.

The equilibrium pH of each series of solutions was determined both by titrimetry and pH electrode measurements for the two resins. The initial solution pH values were calculated as described above using the measured pH of the stock metal solution and the calculated acid concentration of the stock background solution. In Tables 56 and 57 the initial pH values are compared with the equilibrium pH values measured after 17-h contact of the resins (present at 1 milliequivalent) with 5 mL of background solution. In the case of the sodium-containing solutions, pH measurements with a standard calomel electrode were unreliable due to the high concentration of sodium ions and therefore were not included in the table. As shown in Table 56, close agreement between the initial and final pH values for both resins indicates that the extractant makes no contribution to the solution acidity in the absence of $NaNO_3$. The amount of H^+ released into solution due to exchange with the target metal ion present at trace levels is negligible. Comparison of the initial and final pH values for solutions containing $NaNO_3$ in Table 57 shows that exchange of resin acid sites with Na^+ occurs with both resins but to different amounts. Because of the errors associated with the titration of very dilute acid solutions and with the pH measurement of sodium-containing solutions using a standard pH electrode, the equilibrium pH values used in the % absorbed versus pH plots were calculated based on the results of Tables 56 and 57. The following assumptions were used in the calculations:

(1) In the absence of $NaNO_3$, neither the phosphinic nor sulfonic resins contributes protons to the solution.

Table 56

Comparison of Calculated and Experimental pH Values for Phosphinic and Sulfonic Resins in the Absence of $NaNO_3$

Resin	Bkg Soln $[HNO_3]$,M	Cal'd pH_i	Measured pH_f[a]	
			titrimetry	pH meter
sulfonic[b]	4	-0.60	-0.59	-0.59
	2	-0.30	-0.29	-0.25
	1	0.00	0.02	0.09
	0.2	0.70	0.69	0.78
	10^{-1}	0.99	1.00	1.07
	10^{-2}	1.91	d	1.90
	10^{-3}	2.47	d	2.36
	10^{-4}	2.60	d	2.48
phosphinic[c]	4	-0.60	-0.58	
	2	-0.30	-0.28	
	1	0.00	0.02	
	0.2	0.70	0.68	
	10^{-1}	0.99	0.99	
	10^{-2}	1.90	1.80	1.87
	10^{-3}	2.46	d	2.55
	10^{-4}	2.59	d	2.63

[a] Measured after shaking 5 mL of solution with resin (present at 1 mequiv) for 17 h.

[b] 1 X 10^{-3} stock $Fe(NO_3)_3$ solution used; initial pH 1.622.

[c] 1 X 10^{-3} stock $Mn(NO_3)_2$ solution used; initial pH 1.605.

[d] $[H^+]$ concentration too low for accurate titration.

Table 57

Comparison of Calculated and Experimental pH Values for Phosphinic and Sulfonic Resins in the Presence of $NaNO_3$

Resin	Bkg. Soln[a,b]	Calc'd pH_i	Measured pH_f[c] (titrimetery)	% acid sites exchanged
	4/0	-0.60	-0.59	0.0
	2/2.0	-0.30	-0.30	0.0
	1/3.0	0.00	-0.05	61.0
sulfonic	0.2/3.8	0.69	0.45	75.3
	10^{-1}/3.9	0.99	0.56	86.5
	10^{-2}/3.99	1.91	0.73	87.0
	10^{-3}/3.999	2.47	0.72	93.6
	10^{-4}/3.9999	2.60	0.74	89.7
	4/0	-0.60	-0.58	0.0
	2/2.0	-0.30	-0.27	0.0
	1/3.0	0.00	0.02	0.0
phosphinic	0.2/3.8	0.70	0.69	2.3
	10^{-1}/3.9	0.99	0.96	3.6
	10^{-2}/3.99	1.91	1.42	12.8
	10^{-3}/3.999	2.47	1.48	14.9
	10^{-4}/3.9999	2.60	1.48	15.3

[a] $[HNO_3]$,M/$[NaNO_3]$,M

[b] 1 X 10^{-3}N $Fe(NO_3)_3$ stock solution used; initial pH 1.622.

[c] Measured after shaking 5 mL of solution with resin (present at 1 mequiv.) for 17 h.

(2) The sulfonic resin exchanges 61% of its protons for sodium in the 1M HNO_3/3M $NaNO_3$ background solution, 75% in the 0.2M HNO_3/3.8M $NaNO_3$ solution and 100% in the sodium nitrate solutions with concentrations of HNO_3 greater than or equal to 0.10M.

(3) The phosphinic resin does not exchange for sodium ions until the 10^{-2}M HNO_3/3.99M $NaNO_3$ solution at which point it exchanges for 15% of the resin acid sites in that and the 10^{-3}M HNO_3/3.999M $NaNO_3$ and 10^{-4}M HNO_3/3.9999M $NaNO_3$ solutions.

Any errors in the pH values determined using these assumptions are considered to be small compared to those associated with the titrimetric and electrode measurements and do not affect the overall conclusions of the metal ion study.

The % absorbed/pH plots for the sulfonic resin are presented in Figure 79 for extraction of Fe, Hg and Mn from nitric acid solutions. The resin sorbed the three metals in the order Fe > Hg > Mn until a pH of approximately 0.7, after which the extraction of all three metals was nearly quantitative. This behavior is contrasted with that in the presence of $NaNO_3$, as shown in Figure 80. The dramatic decrease in absorption of the target metal ions upon the addition of $NaNO_3$ illustrates the nonselective nature of the sulfonic resin. Because of the competing ion-exchange reaction with the preponderance of sodium ions in solution, the sulfonic resin absorbs only very low levels (10-30%) of the transition metal ions. The sulfonic's extraction behavior in the presence of excess $NaNO_3$ confirms the results of the equilibrium pH study which demonstrate that resin protons exchanged with the sodium ions in solution.

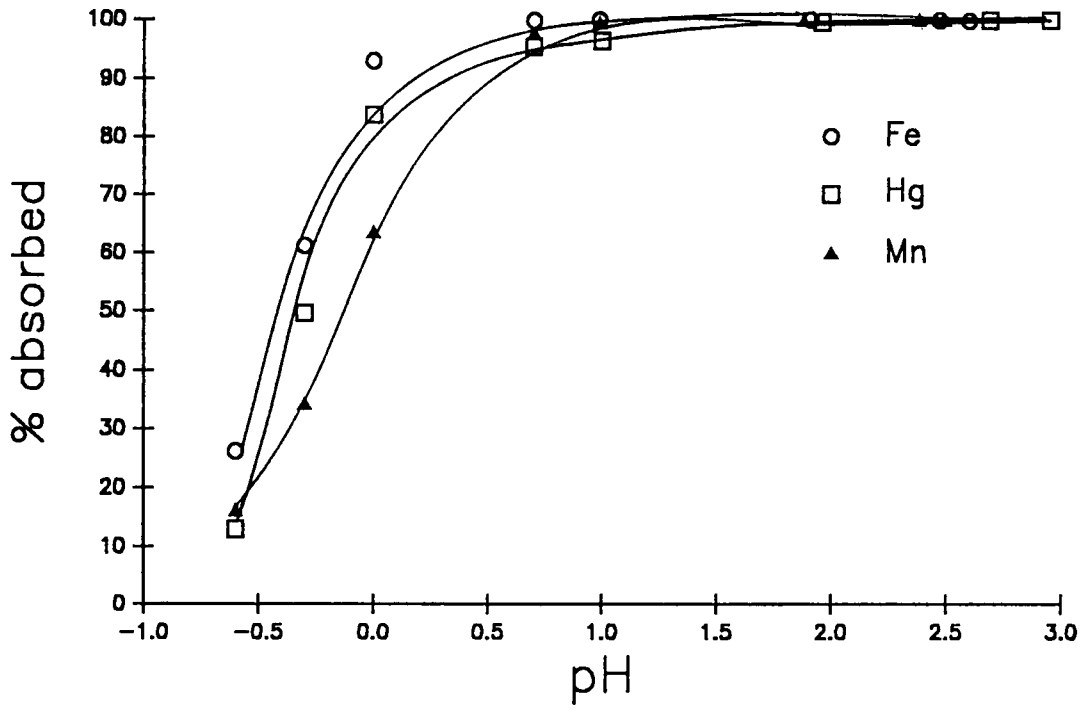

Figure 79. Plots of % absorbed versus pH for Fe, Hg and Mn extraction by the sulfonic resin from nitric acid solutions at an R_i of 5 X 10^{-4}.

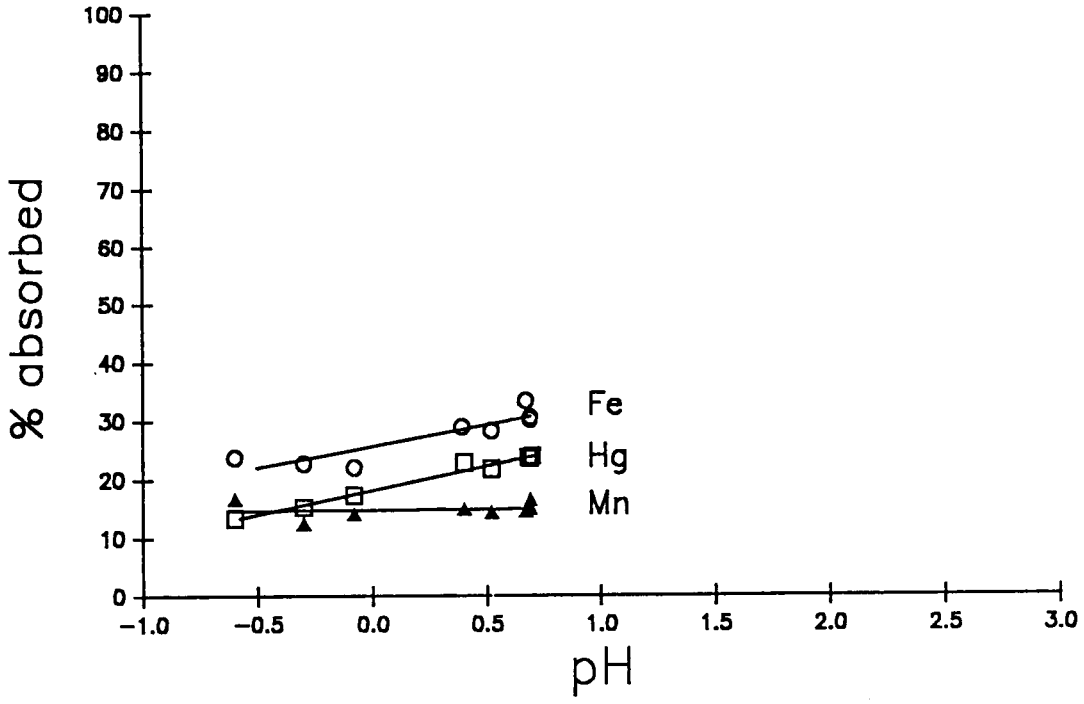

Figure 80. Plots of % absorbed versus pH for Fe, Hg and Mn extraction by the sulfonic resin at an R_i of 5 X 10^{-4} in the presence of sodium ions.

The phosphinic resin's results are markedly different from those of the sulfonic as shown by Figures 81 and 82. The sorption of Fe and Hg was quantitative over the entire pH range studied, both in the presence and absence of added $NaNO_3$. Whereas the extraction of Hg and Fe was completely unaffected by the addition of Na^+, a slight decrease in Mn extraction was observed in the solutions containing sodium nitrate. The more selective nature of the phosphinic resin for the transition metal ions over sodium is evident upon comparison of its results to those of the sulfonic. For example, Mn extraction from the 0.10M HNO_3 solution decreased by only 21% for the phosphinic resin when 3.9M $NaNO_3$ was added compared to a decrease of 85% for the sulfonic.

Further comparison of the results for the phosphinic and sulfonic resins points to some conclusions regarding their mechanisms of metal ion extraction. The tremendous decrease in sorption by the sulfonic resin upon the addition of sodium ions is consistent with an ion-exchange extraction mechanism. The fact that the phosphinic complexes Hg and Fe to the same degree both with and without added $NaNO_3$ indicates that the extraction occurs by a coordination mechanism. Further evidence for coordination is provided by the high levels of Hg and Fe sorption from the lowest pH solutions where ion exchange is not likely for the medium-strength phosphinic acid. From this data it cannot be established whether the recognition mechanism for Hg is provided by reduction. Based upon the selectivity series data presented earlier and the results from higher loading levels, however, reduction of Hg^{2+} is likely to occur, although the extent of reduction cannot be measured at the trace metal levels.

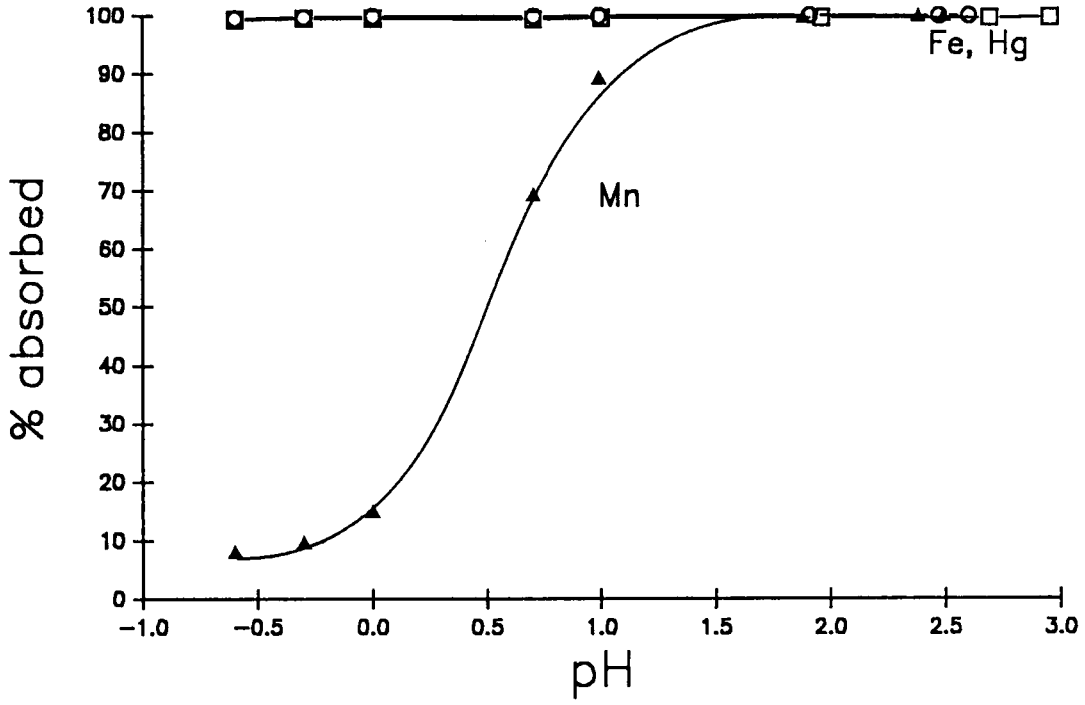

Figure 81. Plots of % absorbed versus pH for Fe, Hg and Mn extraction by the phosphinic resin from nitric acid solutions at an R_i of 5×10^{-4}.

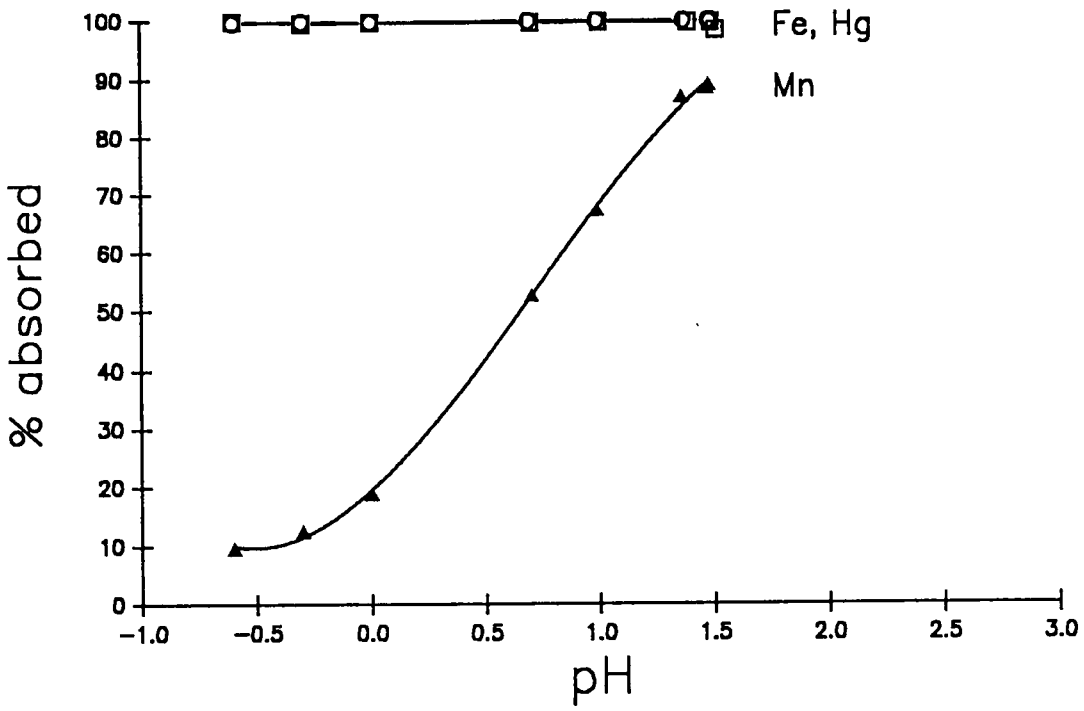

Figure 82. Plots of % absorbed versus pH for Fe, Hg and Mn extraction by the phosphinic resin at an R_i of 5 X 10^{-4} in the presence of sodium ions.

The sensitivity of the Mn results to added $NaNO_3$ at pH values greater than approximately 0.5 for the phosphinic resin points to an ion-exchange extraction mechanism. In addition, only very low levels of Mn were absorbed in the lowest pH region (0.6 to 0), further indication that the phosphinic resin has little tendency to coordinate Mn. Only at pH values greater than zero does the % absorbed rise significantly due to the onset of the ion-exchange reaction.

The Hg and Fe results of the wide pH study are consistent with the enthalpy/entropy-driven coordination hypotheses proposed earlier. Coordination of Hg occurs by an enthalpy-driven coordination process between a soft metal ion and a soft phosphoryl oxygen. In light of the contrasting extraction behavior of the two hard ions studied, the coordination of Fe by the P=O cannot be ascribed to an enthalpy-driven process. Rather, it is postulated to be an entropy-driven process in which the release of the waters of hydration around the ferric nitrate salt is the driving force for the complexation. The lack of coordination of Mn by the phosphinic resin can be justified in terms of HSAB theory. The soft P=O has little propensity to complex a hard metal ion, and thus extraction can only occur by ion exchange.

The results of Fe and Hg extraction are given as plots of % absorbed versus pH in Figures 83 and 84 for DEHP and Figures 85 and 86 for DCHPA. As with the resins, the extractions were performed over the extended pH range in both the presence and absence of $NaNO_3$. Presented in Table 58 are the pH values of the sodium-containing background solutions measured by titration after equilibration with the extractants. In contrast to the phosphinic resin, the results for DEHP

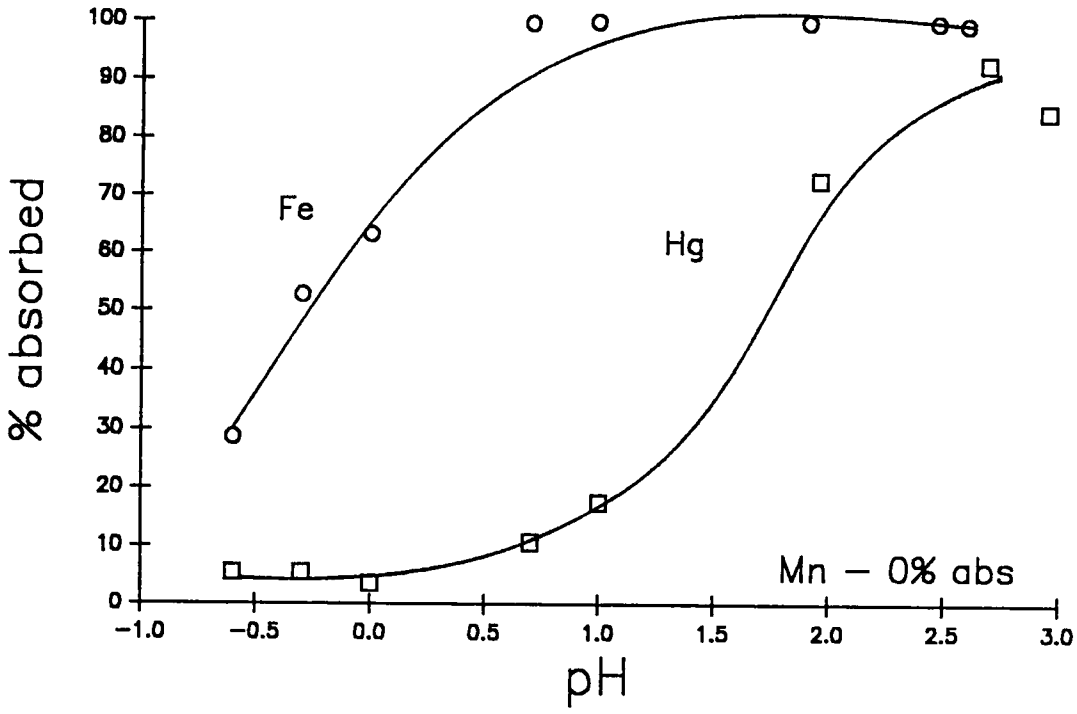

Figure 83. Plots of % absorbed versus pH for Fe and Hg extraction by DEHP from nitric acid solutions at an R_i of 5 X 10^{-4}.

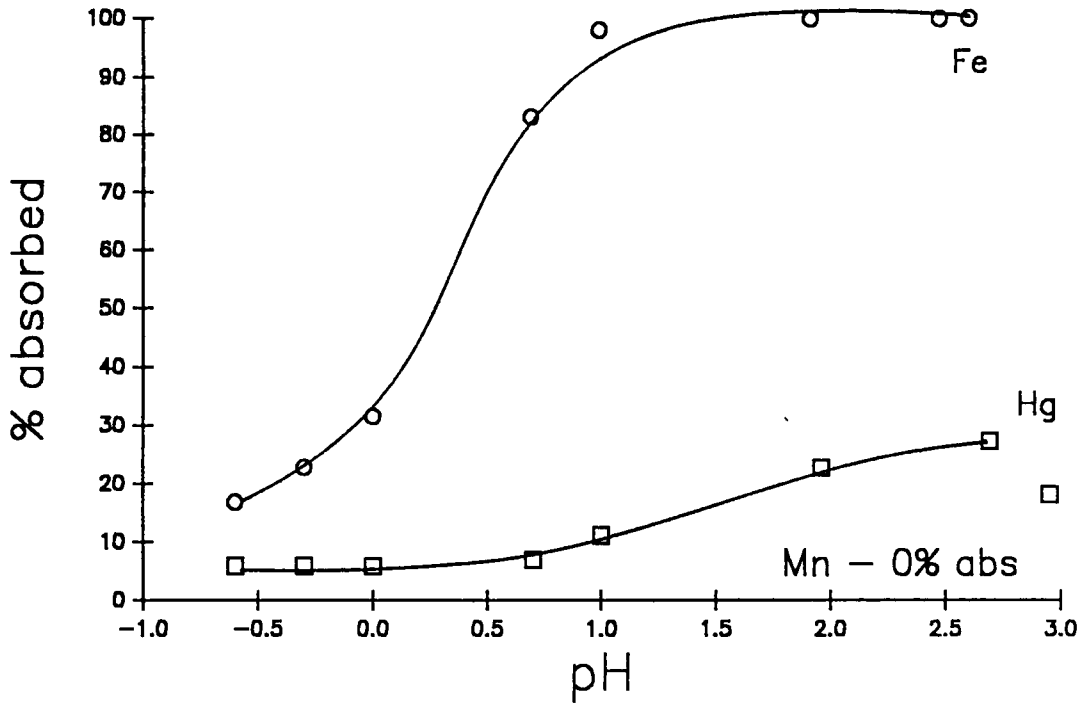

Figure 84. Plots of % absorbed versus pH for Fe and Hg extraction by DEHP at an R_i of 5 X 10^{-4} in the presence of excess sodium ions.

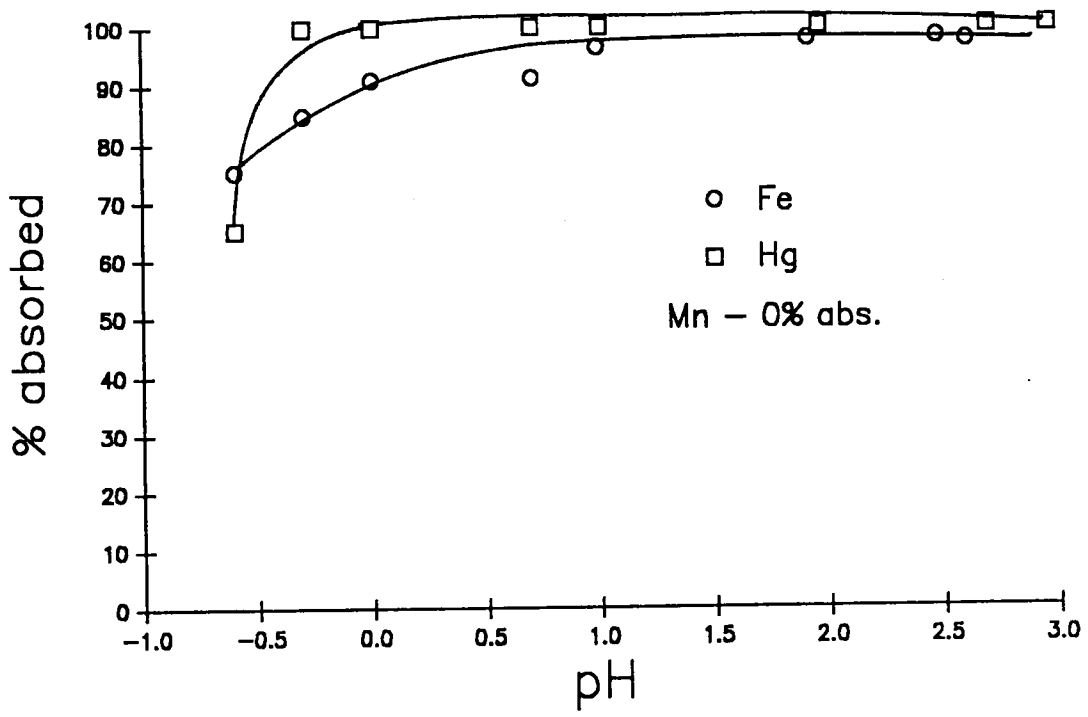

Figure 85. Plots of % absorbed versus pH for Fe and Hg extraction by DCHPA from nitric acid solutions at an R_i of 5 X 10^{-4}.

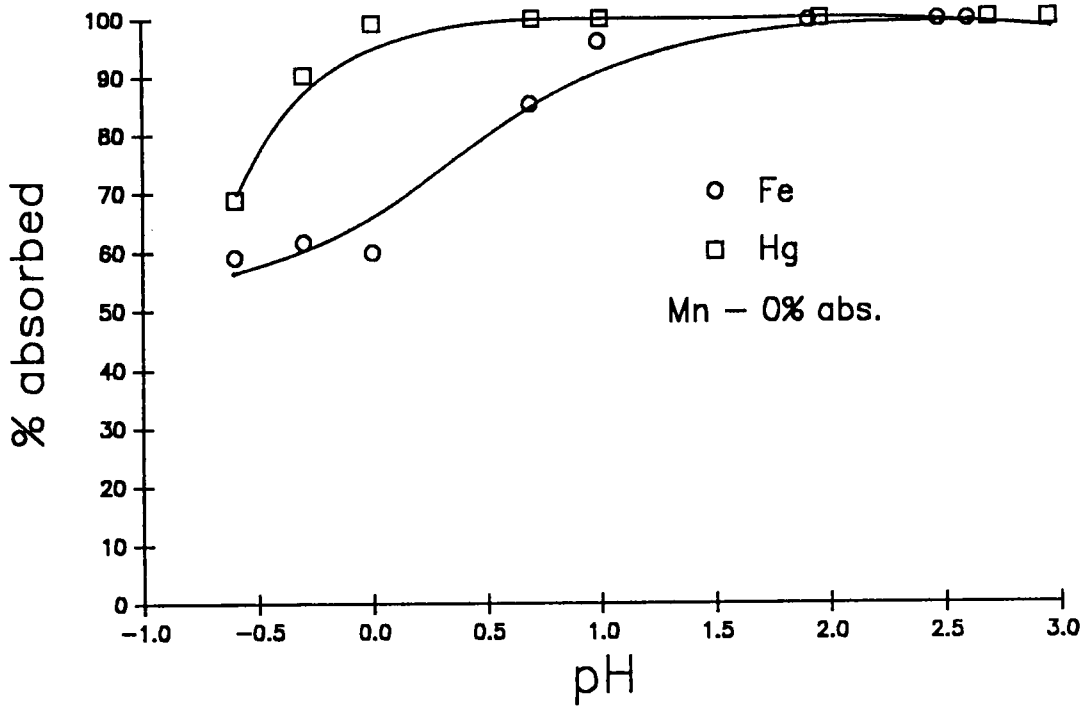

Figure 86. Plots of % absorbed versus pH for Fe and Hg extraction by DCHPA at an R_i of 5 X 10^{-4} in the presence of excess sodium ions.

Table 58

Comparison of Calculated and Experimental pH Values for DEHP and DCHPA in the Presence of $NaNO_3$

Resin	Bkg. Soln[a,b]	Calc'd pH_i	Measured pH_f[c] (titrimetery)	% acid sites exchanged
	4/0	-0.60	-0.59	0.0
	2/2.0	-0.30	-0.30	0.0
	1/3.0	0.00	0.00	0.0
DEHP	0.2/3.8	0.69	0.69	0.0
	10^{-1}/3.9	0.99	0.98	1.2
	10^{-2}/3.99	1.91	1.81	1.6
	10^{-3}/3.999	2.47	2.21	1.4
	10^{-4}/3.9999	2.60	2.21	1.8
	4/0	-0.60	-0.59	0.0
	2/2.0	-0.30	-0.29	0.0
	1/3.0	0.00	0.01	0.0
DCHPA	0.2/3.8	0.69	0.71	0.0
	10^{-1}/3.9	0.99	1.00	0.0
	10^{-2}/3.99	1.91	1.77	2.3
	10^{-3}/3.999	2.47	2.12	2.1
	10^{-4}/3.9999	2.60	2.18	2.0

[a] $[HNO_3]$,M/$[NaNO_3]$,M

[b] 1 X 10^{-3}N $Fe(NO_3)_3$ stock solution used; initial pH 1.622.

[c] Measured after contacting 5 mL of a 0.2M solution of extractant in toluene with 5 mL of a background solution for 17 h.

and DEHP indicate no exchange of the acid sites for Na^+ over the entire pH range.

A decrease in Fe absorption by DEHP was observed with the addition of sodium ions over the pH range of -0.6 to 2.0. This behavior, however, cannot reflect that extraction occurs by ion exchange in the highly acidic solutions given the intermediate strength of the phosphoric acid derivative. It is much more likely that the metals were extracted by coordination in the low pH region. The reason for the decreased absorption in $NaNO_3$ is not clear at this time, but may be an artifact of the change in solution ionic strength with added $NaNO_3$.

The Hg results with DEHP are more straightforward than those for Fe. Very low levels of Hg were sorbed over the pH range from -0.6 to 0.7 both with and without added sodium ions. At pH values greater than 0.70, a dramatic increase in sorption occurred for the solutions without Na^+ in comparison to only a very slight increase for the solutions containing sodium. These findings indicate that ion exchange is suppressed in the high acid region and that the very low levels of Hg extracted from these solutions occurs by coordination. As the pH increased above 0.7, however, the % absorbed increased dramatically due to ion exchange. The effect of the competing ion-exchange reaction is indicated in the results with sodium ions which were much lower than those without added sodium. For example, 73% of Hg was absorbed from the 0.01M HNO_3 background solution, compared to 23% from the 0.01M HNO_3/3.9M $NaNO_3$ solution.

A decline in Fe extraction was also observed with DCHPA in the highly acidic regions (pH -0.6 to 1.0) upon addition of sodium. As with

DEHP, this behavior cannot be attributed to ion exchange in this pH region, but is more likely due to variation in the aqueous phase ionic strength with the addition of $NaNO_3$. Contrasting results to those for DEHP, however, were observed for Hg extraction. The same levels of Hg absorption were obtained in the solutions with and without added sodium ions, an indication of the coordinative interaction between Hg and the phosphoryl oxygen over the entire pH range.

In comparing the results of DEHP and DCHPA, it is evident that DCHPA is an overall stronger extractant for both Hg and Fe than DEHP, especially in the high acid regions. For example, DCHPA absorbed 75% of Fe and 65% of Hg from the 4M HNO_3 background solution compared to 29% of Fe and 5% of Hg by DEHP. This can be related to the variation in P=O basicity for the two extractants which results from the difference in the electronic properties of the attached substitutents. The electron-withdrawing alkoxy groups of DEHP remove electron density from the phosphoryl oxygen, rendering it a poorer coordinator than DCHPA, which has electron-releasing alkyl groups attached to phosphorus. Because the phosphoryl oxygen can also complex nitric acid, competition exists between H^+ and the target metal ion for the coordination sites. Thus, the lower degree of Hg absorption by DEHP in the highly acidic solutions suggests that it is a harder base than DCHPA, preferring to complex the hard H^+ over the soft Hg^{2+}.

The results discussed above were determined for extractant concentrations of 0.2M. The influence of extractant concentration on the degree of metal absorption was investigated in order to verify that the observed differences between the two extractants were indeed related

to variations in P=O basicity and not merely artifacts of the solution concentration. The results of Fe extraction (present at 1 X 10^{-4}N) from background solutions of varying HNO_3 concentration are given in Figure 87 for DCHPA and Figure 88 for DEHP. The following extractant concentrations were studied: 0.05M, 0.10M, 0.15M and 0.2M. The volume of the organic phase was held constant at 5 mL so that the R_i varied from 2 X 10^{-3} to 5 X 10^{-4}. No differences in extraction mechanism were evident with changing concentration for either extractant. The variation in extractant concentration resulted in a general decrease in absorption with increasing R_i for DCHPA: Fe extraction was found to decrease in the order 0.20M > 0.15M > 0.10M > 0.05M. The concentration dependence for DEHP were not as clear-cut as those for DCHPA, however, following the order 0.15M > 0.10M > 0.20M > 0.05M. Comparison of the results for all concentrations of DCHPA and DEHP nonetheless shows DCHPA to be a better extractant and hence stronger coordinator of Fe than DEHP.

In addition to Hg and Fe, the complexation of Mn was studied using DEHP and DCHPA. As indicated in the % absorbed/pH plots, no Mn was absorbed by the extractants from either set of background solutions. These findings stand in contrast to the phosphinic resin results shown in Figures 81 and 82 (pages 289 and 290, respectively). The dissimilar behavior of the small molecule and polymer-supported extractants is most likely related to differences in the organic phase environments of the two extractants. The hydrophilic resin matrix provides greater accessibility to the hydrated Mn ion than the hydrophobic toluene solution of the small molecule extractant.

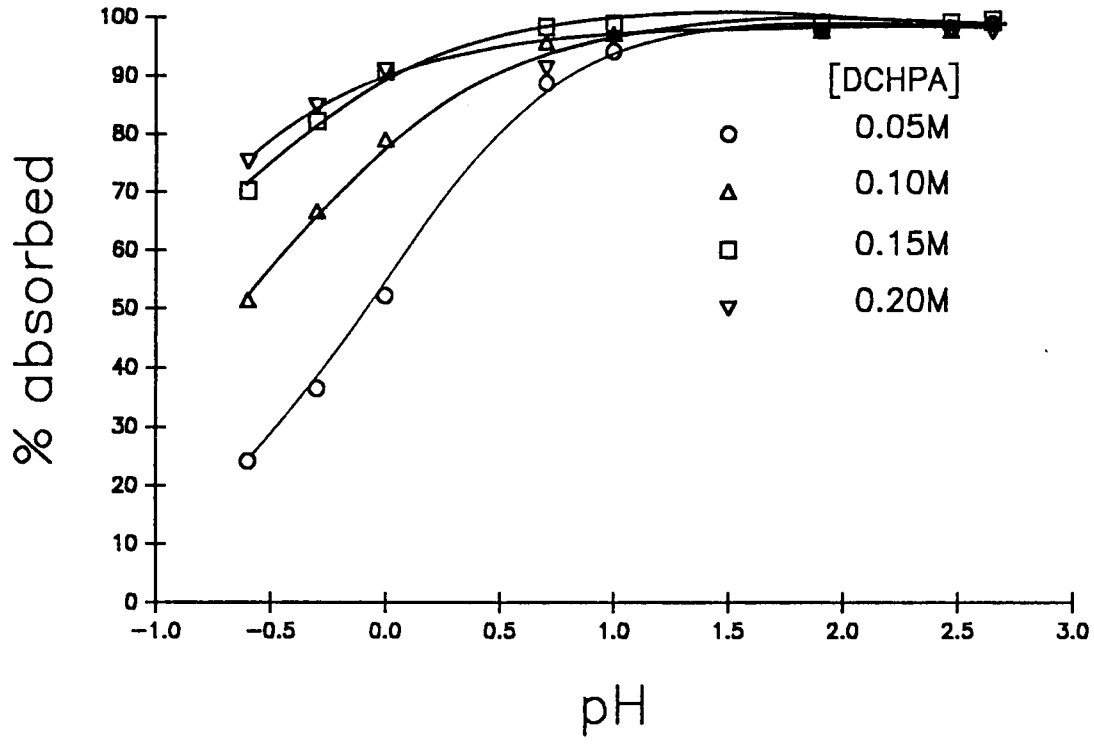

Figure 87. Effect of DCHPA concentration on Fe extraction from nitric acid solutions at an R_i of 5 X 10^{-4}.

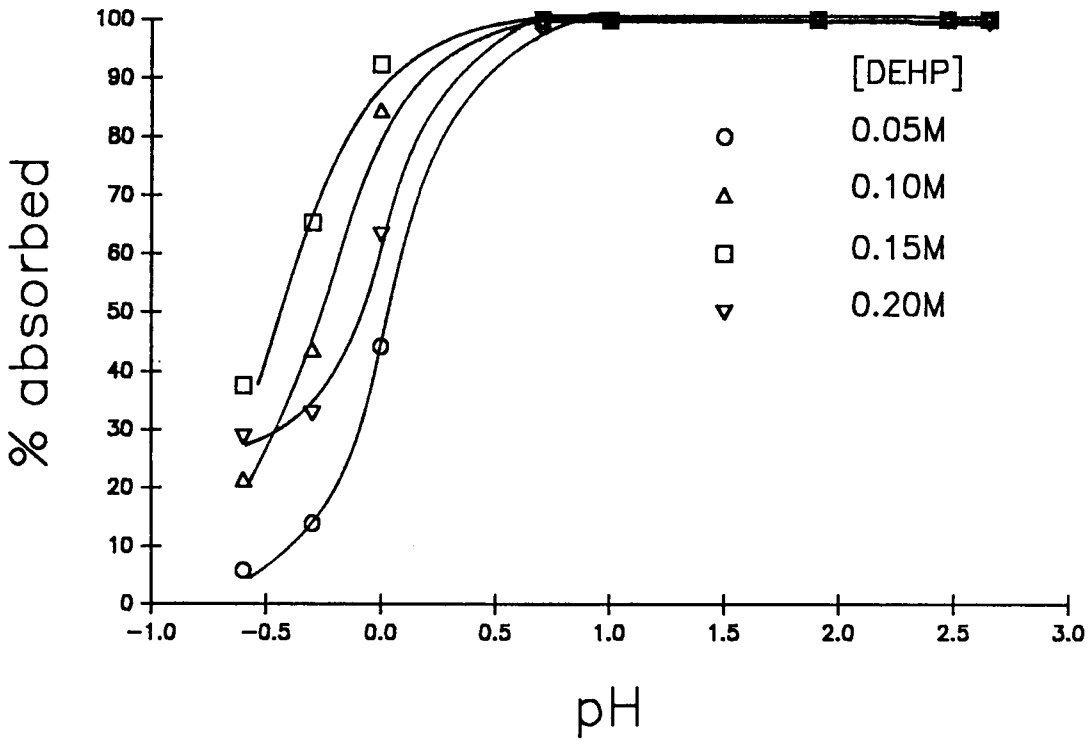

Figure 88. Effect of DEHP concentration on Fe extraction from nitric acid solutions at an R_i of 5 X 10^{-4}.

Metal Ion Complexation by Neutral and Acidic Organophosphorus Extractants

The complexation of trace levels of Fe, Hg, Mn and Ag was investigated for five phosphorus-based extractants: DCHPA; 2,4,4-trimethylpentyl phosphinic acid (Cyanex 272); DEHP; TOPO; and TBP. Metal studies using a liquid sulfonic acid extractant, di-dodecylnaphthyl sulfonic acid (HDDNS), were unsuccessful as a result of the extractant's solubility into the aqueous phase. The extractions were performed at an R_i of 5 X 10^{-4} over a pH range of -0.60 to 0.70, where coordination is expected to be the predominant extraction mechanism. The nitric acid solutions also contained enough $NaNO_3$ to provide a constant 4M nitrate background. The extraction results were analyzed in terms of the differing electronic properties of the phosphoryl oxygen coordinating ligand, as influenced by the electron-withdrawing alkoxy or electron-donating alkyl groups bonded to phosphorus.

A problem occasionally encountered in liquid-liquid extraction systems is the formation of a third phase. This phenomenon, indicated by a low material balance for the system, was observed in the extraction of 1 X 10^{-4}N $Hg(NO_3)_2$ by Cyanex 272. The extraction results in Table 59 show that over 30% of the Hg initially present in the 0.20M HNO_3/3.8M $NaNO_3$ background solution was lost to a third phase. Several variables in the extraction process were examined in an attempt to obviate third phase formation. These included using a more gentle method for equilibration of the two phases, centrifuging the sample to try to disperse the third phase, lowering the background $NaNO_3$ concentration

Table 59

Extraction of Hg by Cyanex 272[a]

Bkg. Soln.[b]	log D	% Abs.	material balance[c] (% of total)
4/0	-0.77	17.32	-3.23
2/2	-0.56	23.78	-2.73
1/3	0.60	81.55	-7.55
0.2/3.8	2.11	99.46	-30.29

[a] R_i = 5 X 10^{-4}; Organic phase = 5 mL of 0.2M Cyanex 272 in toluene; Aqueous phase = 5 mL of 1 X 10^{-4}N $Hg(NO_3)_2$ in $HNO_3/NaNO_3$ solutions.

[b] $[HNO_3]$,M/$[NaNO_3]$,M

[c] Comparison of the initial radioactivity with the total measured radioactivity in aqueous and organic phases after equilibration.

and increasing the extractant concentration. Significant material balance losses, however, were encountered in all the above experiments. With the exception of Ag extraction by TOPO and TBP, all other liquid-liquid extraction systems studied gave acceptable material balances. At the present time, the cause of third phase formation in these systems and in Hg extraction by Cyanex has not been determined.

The % absorbed versus pH plots for Hg extraction by DCHPA, TOPO, TBP and DEHP at an R_i of 5 X 10^{-4} are presented in Figure 89. Due to the material balance problems discussed above, the results for Cyanex were not included. The phosphinic extractant DCHPA greatly outperformed the phosphoric acid derivative, DEHP. Whereas quantitative extraction of Hg was achieved with DCHPA at pH values greater than zero, less than 10% was absorbed by DEHP over the entire range of solution acidities. Of the two neutral extractants, TOPO extracted much higher levels of Hg than TBP, especially in the higher pH regions.

Figure 90 presents the results of 1 X 10^{-4}N Fe extraction by all five phosphorus reagents. As observed with Hg, the phosphinic acids were also found to be better extractants for Fe than DEHP. Comparison of the two phosphinic acids shows Cyanex 272 to be the more powerful extractant for Fe. In contrast to TBP, which did not absorb Fe from any of the background solutions studied, TOPO extracted significant levels of the metal, particularly from solutions with pH values greater than 0.5. Both the phosphinic and phosphoric acid complexed higher amounts of Fe than both neutral extractants, an observation also made for the polymer-supported analogues.

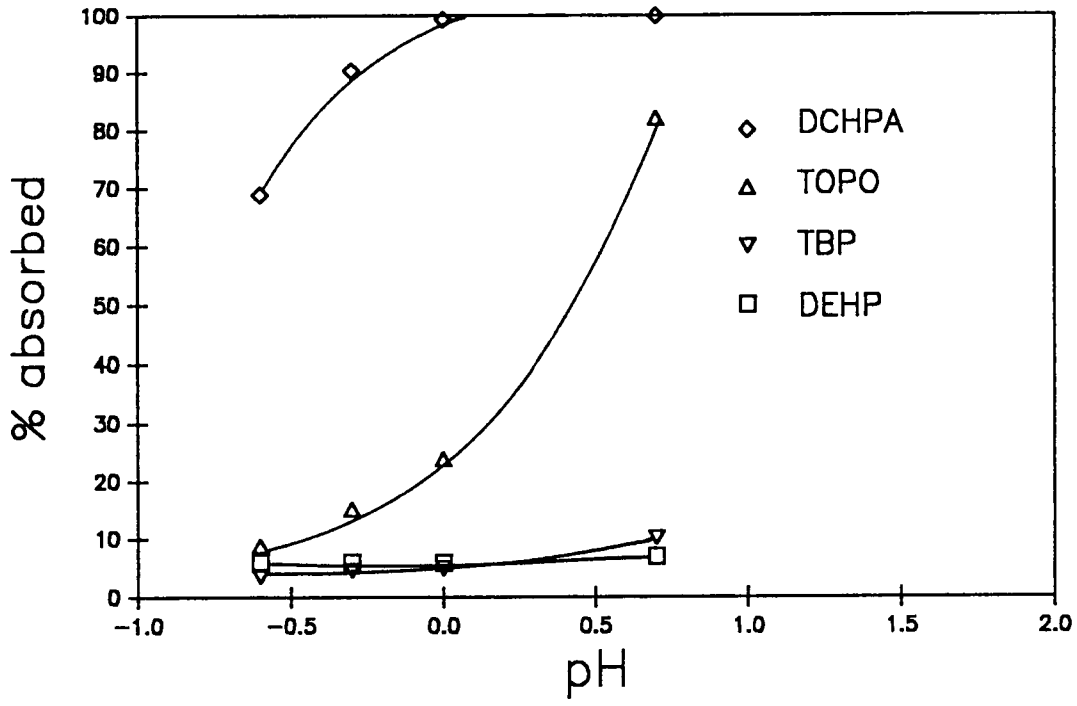

Figure 89. Extraction of Hg by DCHPA, TOPO, TBP and DEHP determined at an R_i of 5 X 10^{-4} from solutions of 4M nitrate background.

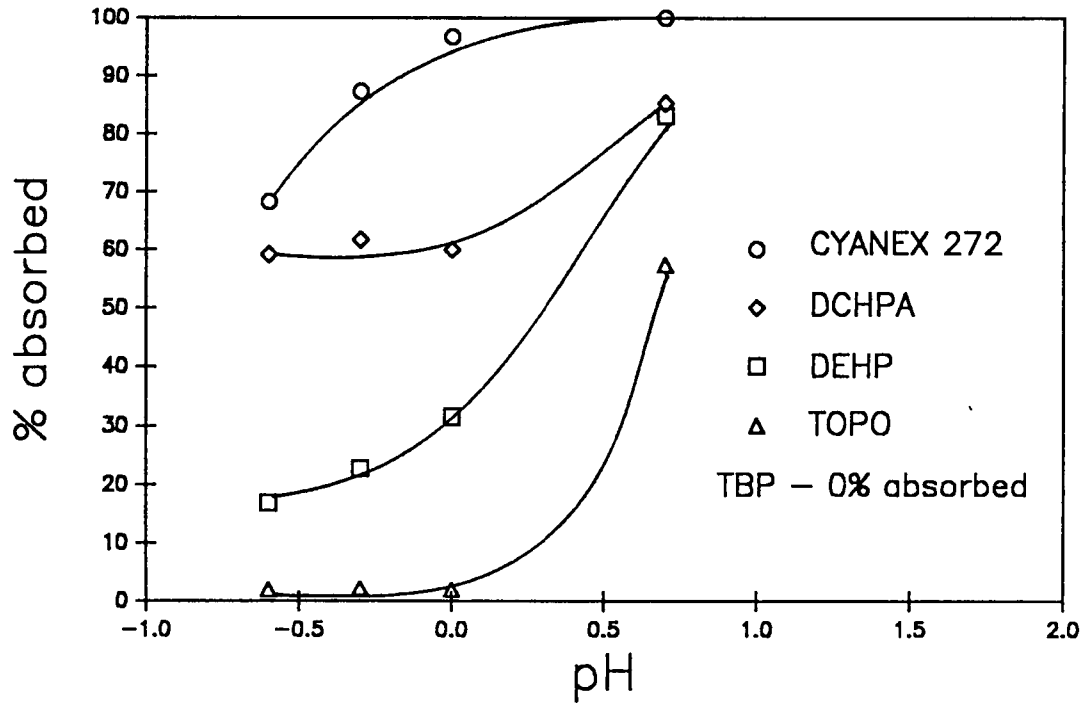

Figure 90. Extraction of Fe by Cyanex 272, DCHPA, DEHP, TOPO and TBP determined at an R_i of 5 X 10^{-4} from solutions of 4M nitrate background.

The extraction of Hg by Cyanex 272, DEHP and TOPO (Figure 91) and the extraction of Fe by Cyanex 272 and DEHP (Figure 92) was also studied at an R_i of 5 X 10^{-3}. Examination of both sets of results shows the phosphinic acid to outperform the phosphoric acid, as was also seen at an R_i of 5 X 10^{-4}. In some cases, the degree of metal ion extraction was found to depend on the loading level. For example, comparison of the results for R_i levels of 5 X 10^{-3} and 5 X 10^{-4} shows that significantly lower levels of Hg sorption were obtained for TOPO at the higher R_i. In contrast, Fe extraction by DEHP increased only slightly at the higher loading level. The dependence of the degree of metal extraction on the R_i will be examined in greater detail in the following section.

The results at both R_i's demonstrate the phosphinic acids to be stronger complexing agents for Fe and Hg than the phosphoric acid derivative. Likewise, the phosphine oxide was superior to the phosphate in the extraction of both metals. These findings are consistent with the greater coordinative ability of the P=O which is bonded to electron donating alkyl groups. The phosphinic resins outperformed TOPO particularly in the solutions of lowest pH for extraction of both Fe and Hg. The poor performance of TOPO in the high acid concentrations suggests that H^+ can favorably compete with the target metal for the coordination site.

The results of Ag extraction by Cyanex 272, TOPO and TBP and of Mn extraction by Cyanex 272 are shown in Table 60. Loss of Ag to a third phase was significant for both TOPO and TBP as evidenced by the very low material balances for these systems. The percentage of Ag absorbed from

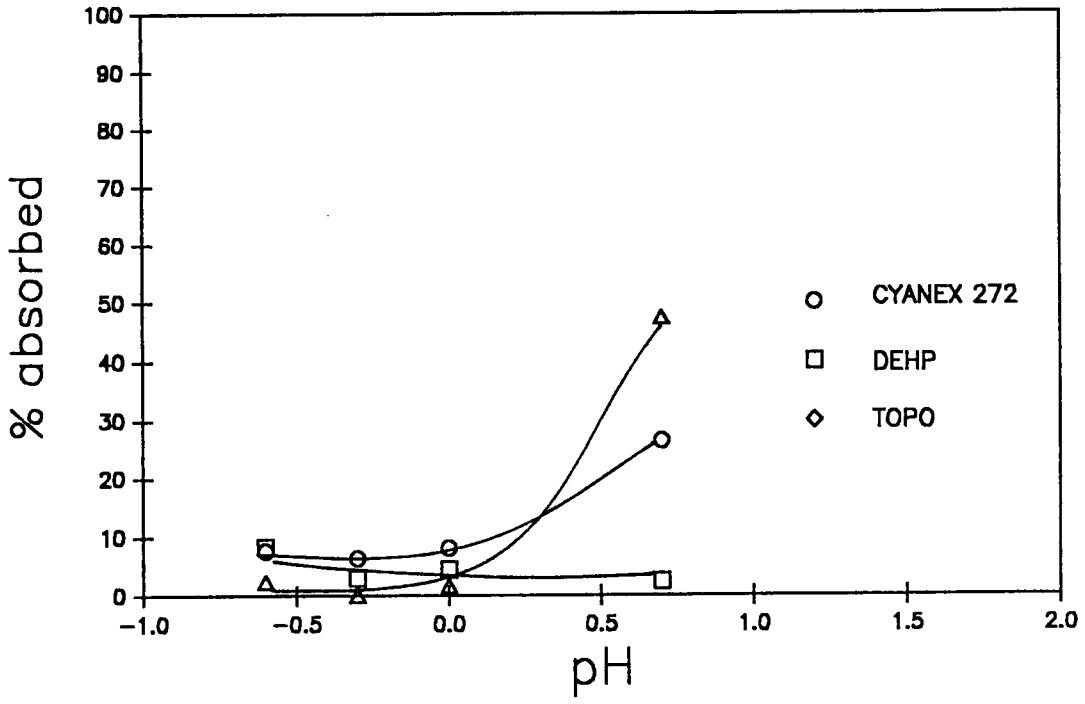

Figure 91. Extraction of Hg by Cyanex 272, DEHP and TOPO determined at an R_i of 5 X 10^{-3} from solutions of 4M nitrate background.

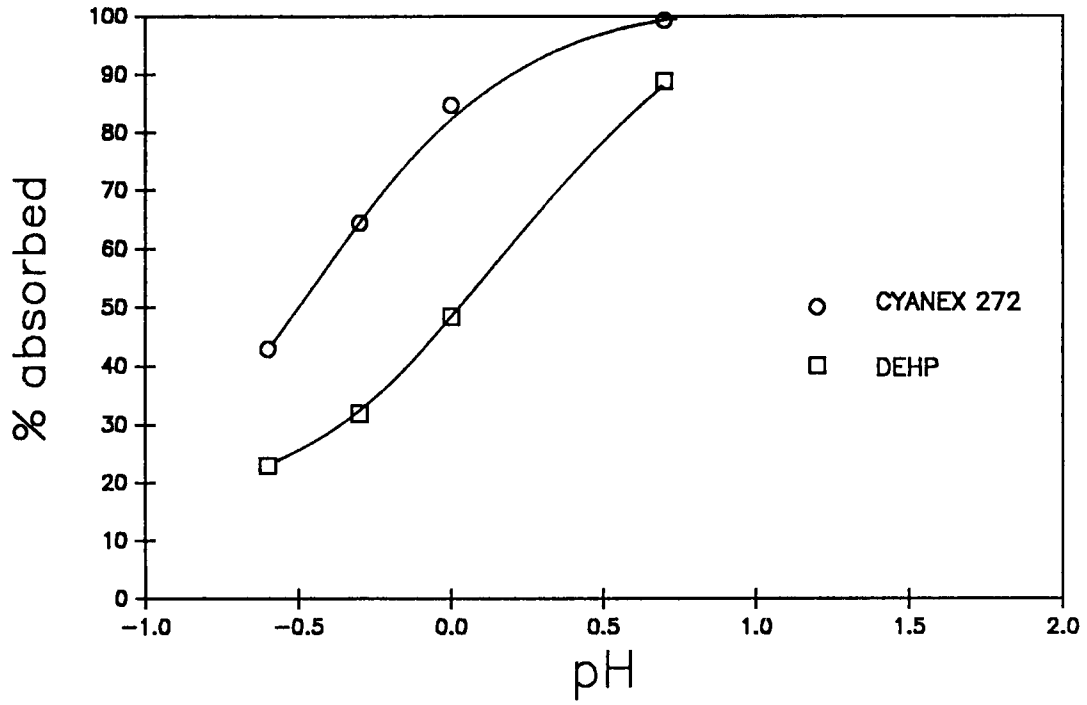

Figure 92. Extraction of Fe by Cyanex 272 and DEHP determined at an R_i of 5 X 10^{-3} from solutions of 4M nitrate background.

Table 60

Extraction of Ag and Mn by Organophosphorus Extractants[a]

Extractant	Metal[b]	Bkg. Soln.[c]	% Absorbed	Material Balance (% of total)
Cyanex 272	Ag	4/0	0.05	0.01
		2/2	1.33	-1.30
		1/3	0.25	0.20
		0.2/3.8	1.29	-1.18
TOPO	Ag	4/0	9.19	-9.15
		2/2	6.37	-6.37
		1/3	11.24	-11.24
		0.2/3.8	8.66	-8.54
TBP	Ag	4/0	7.92	-8.04
		2/2	2.81	-2.86
		1/3	0.00	1.33
		0.2/3.8	12.79	-13.64
Cyanex 272	Mn	4/0	0.00	1.42
		2/2	0.00	0.37
		1/3	0.00	1.15
		0.2/3.8	0.00	0.16

[a] Extractions performed using 5 mL aqueous phase and 5 mL of 0.2M extractant (in toluene) as organic phase.

[b] Initial concentration = 1 X 10^{-4}N, as the nitrate.

[c] $[HNO_3]$,M/$[NaNO_3]$,M

the aqueous phase directly corresponded to the material balance loss, suggesting that the Ag was not extracted into the organic phase but rather into a third phase. In spite of the complications of third phase formation, these results demonstrate the low affinity of both the acidic and neutral organophosphorus reagents to complex Ag. As formerly observed with DEHP and DCHPA, no Mn was extracted by Cyanex 272.

Effect of Loading Level on Metal Ion Complexation by Phosphinic and Phosphonic Resins

The extraction of Fe, Hg, Mn and Ag was examined over a range of R_i values from 1.0 to 5 X 10^{-5} from the following background solutions: 4M HNO_3, 2M HNO_3/2M $NaNO_3$, 1M HNO_3/3M $NaNO_3$, 0.2M HNO_3/3.8M $NaNO_3$, and 0.01M HNO_3. These solution conditions were employed in order to determine the influence of metal ion concentration and solution acidity on the access and recognition mechanisms displayed by the phosphinic and phosphonic resins.

A decrease in metal sorption can occur at high R_i's as a result of unfavorable electrostatic interactions within the resin. As indicated in Figure 93, a loading effect was apparent for the 2% cross-linked gel phosphinic resin in the extraction of Fe from all background solutions at R_i values of 1 and 0.5. The results in Table 61 also indicate a loading effect in Fe complexation from both 4M and 0.01M HNO_3 (11.99% absorbed at an R_i of 1.0 compared to 99.52% at 5 X 10^{-4} in 4M HNO_3; 8.90% absorbed at an R_i of 1.0 versus 99.77% at 5 X 10^{-4} in 0.01M HNO_3). These findings demonstrate that the loading effect for Fe extraction by the phosphinic resin is independent of the resin's access mechanism

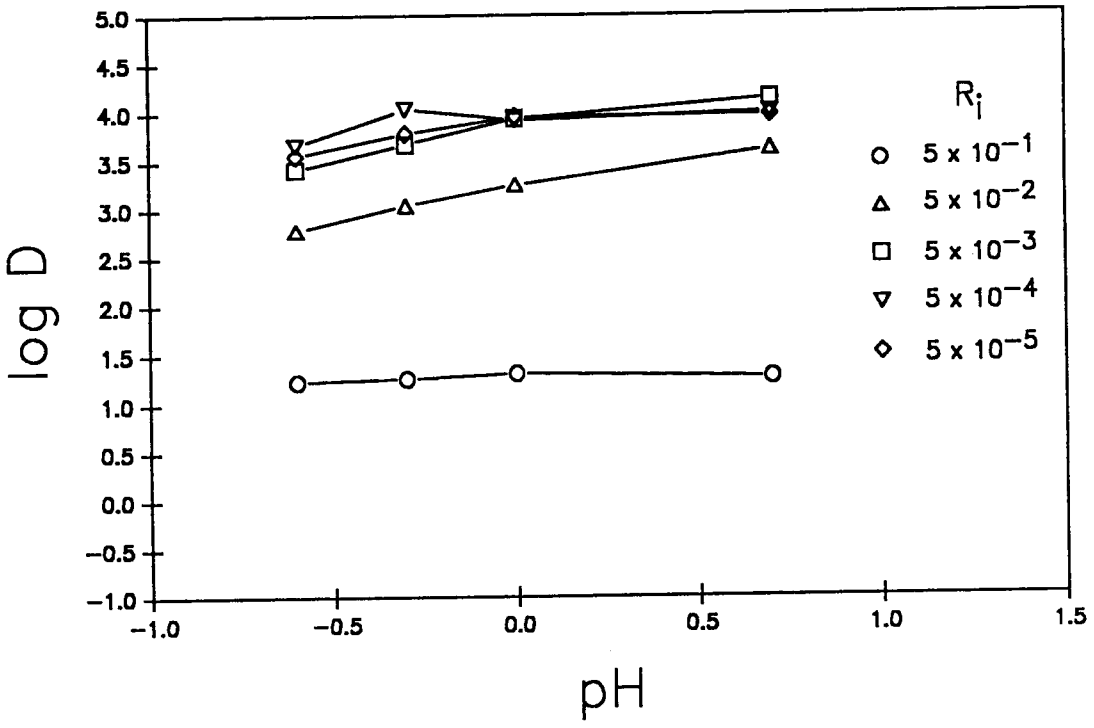

Figure 93. R_i dependence of Fe extraction by the 2% cross-linked gel phosphinic resin at constant 4M nitrate background.

Table 61

Comparison of Fe, Hg and Mn Extraction by the Phosphinic Resin from 4M and 0.01M HNO_3 at Varying R_i's

$[HNO_3]$	Metal	% Absorbed / log D	
		$R_i = 1.0$	$R_i = 5 \times 10^{-4}$
4M	Fe	11.99/0.56	99.52/3.71
	Hg	7.35/0.30	99.31/3.56
	Mn	4.77/0.09	8.22/0.36
0.01M	Fe	8.90/0.40	99.97/4.94
	Hg	99.65/3.88	99.59/3.80
	Mn	29.60/1.03	99.81/4.12

(coordination in 4M HNO_3 versus a mix of ion exchange and coordination in 0.01M HNO_3).

The log D/pH correlations for Hg extraction by the 2% cross-linked phosphinic resin are presented in Figure 94 for R_i's ranging from 0.50 to 5 X 10^{-5}. The following overall dependence of log D on R_i was observed: 0.50 << 5 X 10^{-2} ~ 5 X 10^{-5} < 5 X 10^{-3} ~ 5 X 10^{-4}. The decreased absorption at an R_i of 5 X 10^{-5} suggests that metal ion reduction by the phosphinic resin does not occur at very dilute solution conditions. Examination of Table 61 shows a loading effect in the extraction of Hg by the phosphinic from 4M HNO_3. For example, only 7.35% of Hg was absorbed at an R_i of 1.0 compared to 99.31% at an R_i of 5 X 10^{-4}. In contrast, no loading effect was observed in 0.01M HNO_3: 99.65% was absorbed at an R_i of 1.0 versus 99.59% at 5 X 10^{-4}. The reduction of mercuric ions by the phosphinic resin provides for the high levels of extraction from 0.01M HNO_3. As discussed previously, an increase in solution pH favors metal ion reduction by the resin as governed by the Nernst equation. The pH dependence of the resin's redox component was also indicated by the observation of mercury metal in the vial after extraction at an R_i of 1.0 from 0.01M HNO_3. No reduced metal was visible in the sample containing 4M HNO_3.

Ag complexation by the 2% gel phosphinic resin was found to exhibit a loading effect at an R_i of 0.50 only in the lowest pH solutions as indicated in Figure 95. Unlike the Hg results, a decline in Ag extraction was not observed for the most dilute metal ion concentrations. This finding may indicate that Ag is not being reduced by the phosphinic under the pH conditions of this study. A dependence

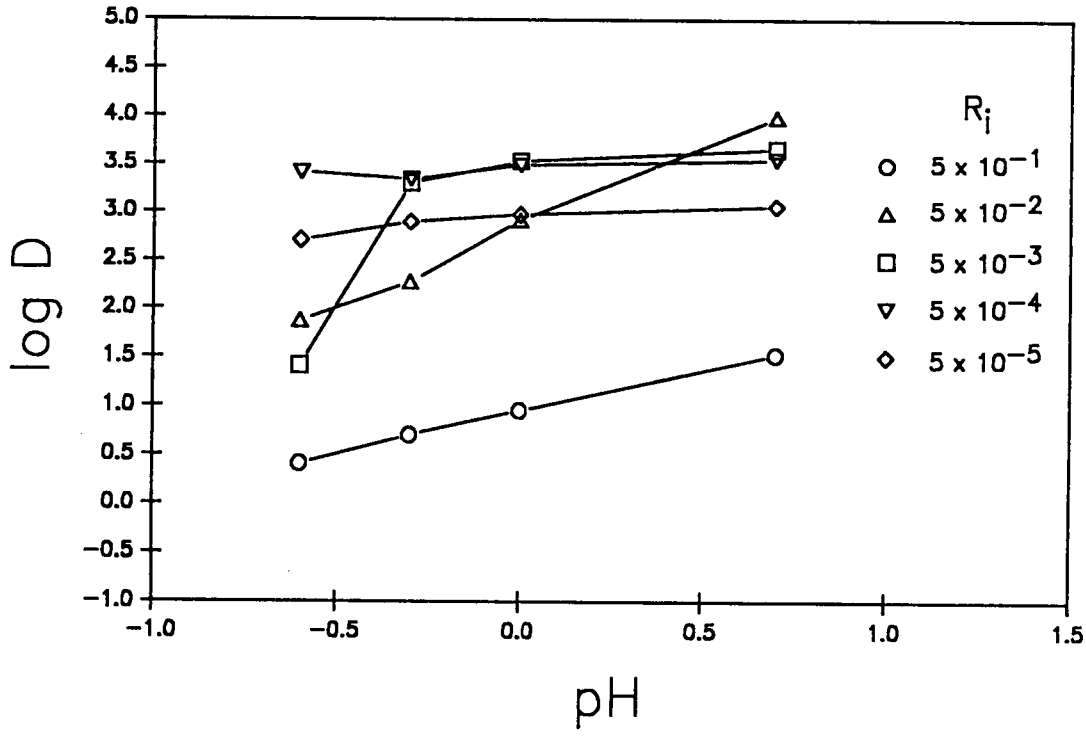

Figure 94. R_i dependence of Hg extraction by the 2% cross-linked gel phosphinic resin at constant 4M nitrate background.

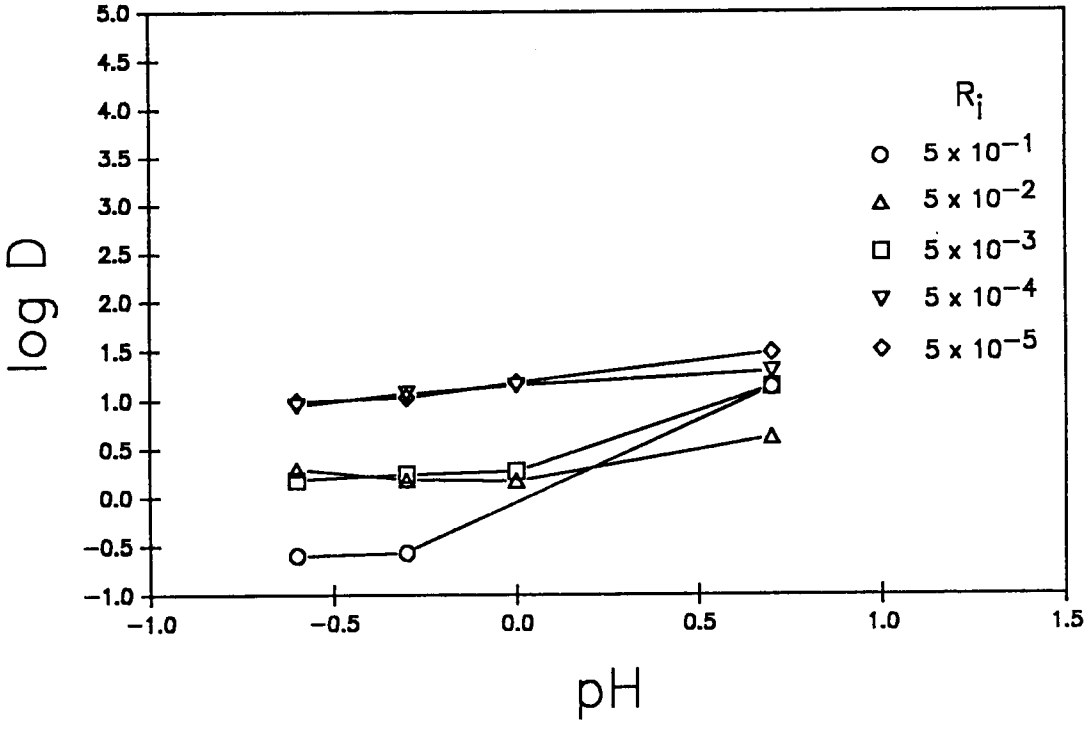

Figure 95. R_i dependence of Ag extraction by the 2% cross-linked gel phosphinic resin at constant 4M nitrate background.

of the redox component on the metal ion concentration is expected due to the stoichiometric requirements of the reduction reaction: the probability that two silver ions come into close enough proximity to the P-H bond for the transfer of two electrons would likely be diminished at very dilute metal ion concentrations.

Table 62 presents the data for Ag extraction at an R_i of 1.0 from background solutions of 4M and 0.01M HNO_3. As with Hg, these results also point to the pH dependence of the phosphinic's redox reaction: at an R_i of 1.0, the phosphinic resin absorbed only 1.41% of the Ag ions from a solution of 4M HNO_3 as opposed to 88.08% from 0.01M HNO_3. Considerably higher levels of Ag than Mn were absorbed from 0.01M HNO_3, further indication that the redox reaction accounts for the elevated levels of Ag extracted from high pH solutions.

As shown in Figure 96, no loading effect was apparent for Mn extraction by the phosphinic resin over the pH range of -0.60 to 0.70. These results reflect the low propensity of the phosphinic resin to coordinate Mn at any metal ion concentration. The data in Table 61, however, indicate a significant loading effect in the higher pH background solution (log D of 1.03 at an R_i of 1.0 compared to 3.80 at 5×10^{-4}). In contrast to the results in low pH solutions where complexation must occur by coordination, significant levels of Mn can be extracted by ion exchange in 0.01M HNO_3, thus resulting in loading effects at high R_i's.

Figures 97-100 present the log D/pH correlations for Fe, Hg, Ag and Mn extraction at R_i's of 0.5 to 5×10^{-5} by the 2% gel phosphonic resin. As with the phosphinic, loading effects were apparent for Fe

Table 62

Extraction of Fe, Hg, Mn and Ag by Phosphinic and Phosphonic Resins at an R_i of 1.0

Resin	Metal	4M HNO_3			0.01M HNO_3		
		% Abs	log D	mequiv/g	% Abs	log D	mequiv/g
phosphinic	Fe	11.99	0.56	0.64	8.90	0.40	0.46
	Hg	7.35	0.30	0.37	99.65[a]	3.88	5.32
	Ag	1.41	-0.44	0.07	88.08	2.27	4.49
	Mn	4.77	0.09	0.24	29.60	1.03	1.51
phosphonic	Fe	51.35	1.37	2.31	16.38	0.64	0.73
	Hg	43.41	1.22	1.90	97.99[a]	3.04	4.45
	Ag	10.08	0.38	0.43	35.43	1.08	1.57
	Mn	4.29	-0.02	0.18	23.44	0.83	1.04

[a] Solution pH of 1.34 (0.045M HNO_3) required to dissolve $Hg(NO_3)_2$ salt.

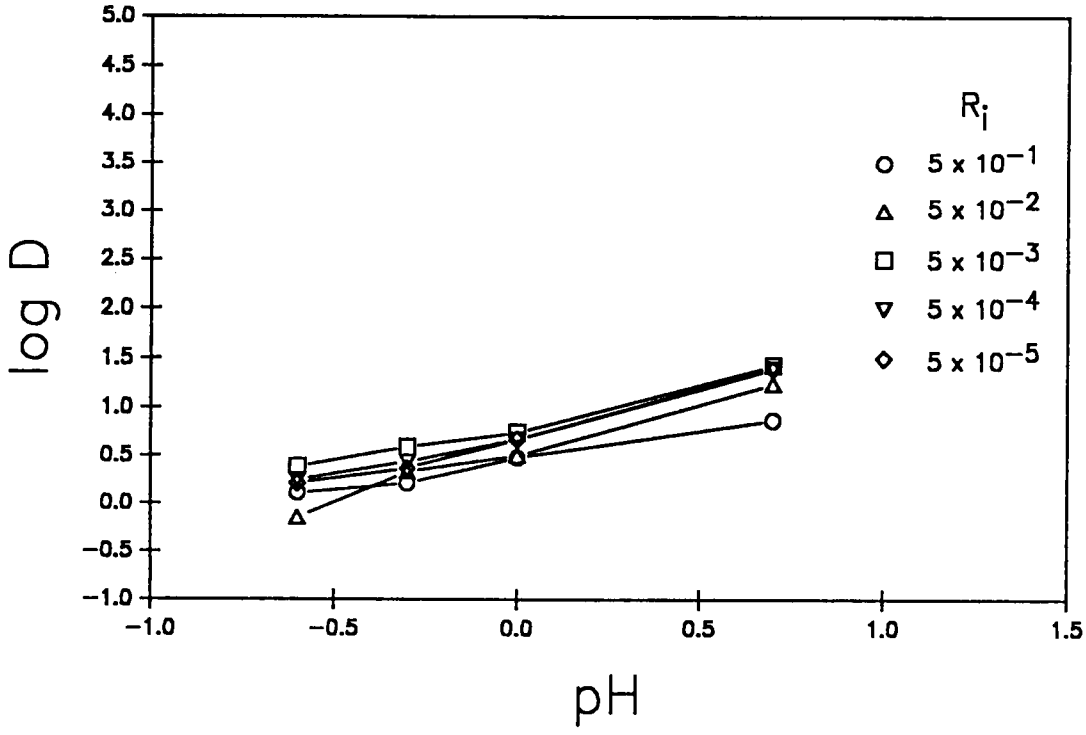

Figure 96. R_i dependence of Mn extraction by the 2% cross-linked gel phosphinic resin at constant 4M nitrate background.

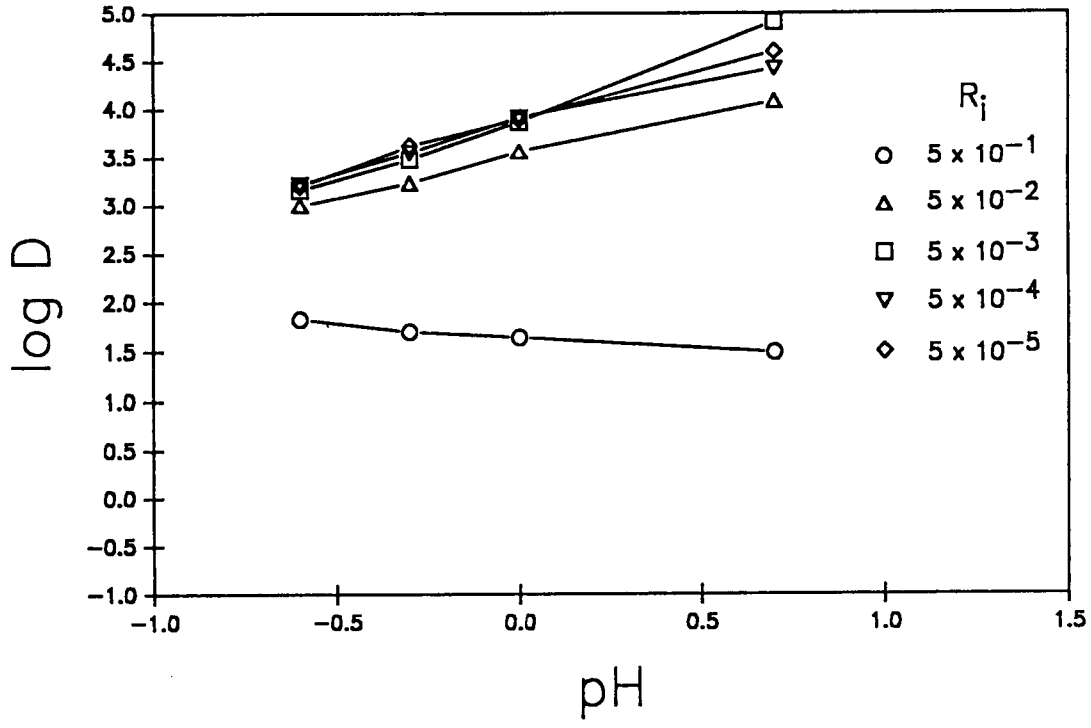

Figure 97. R_i dependence of Fe extraction by the 2% cross-linked gel phosphonic resin at constant 4M nitrate background.

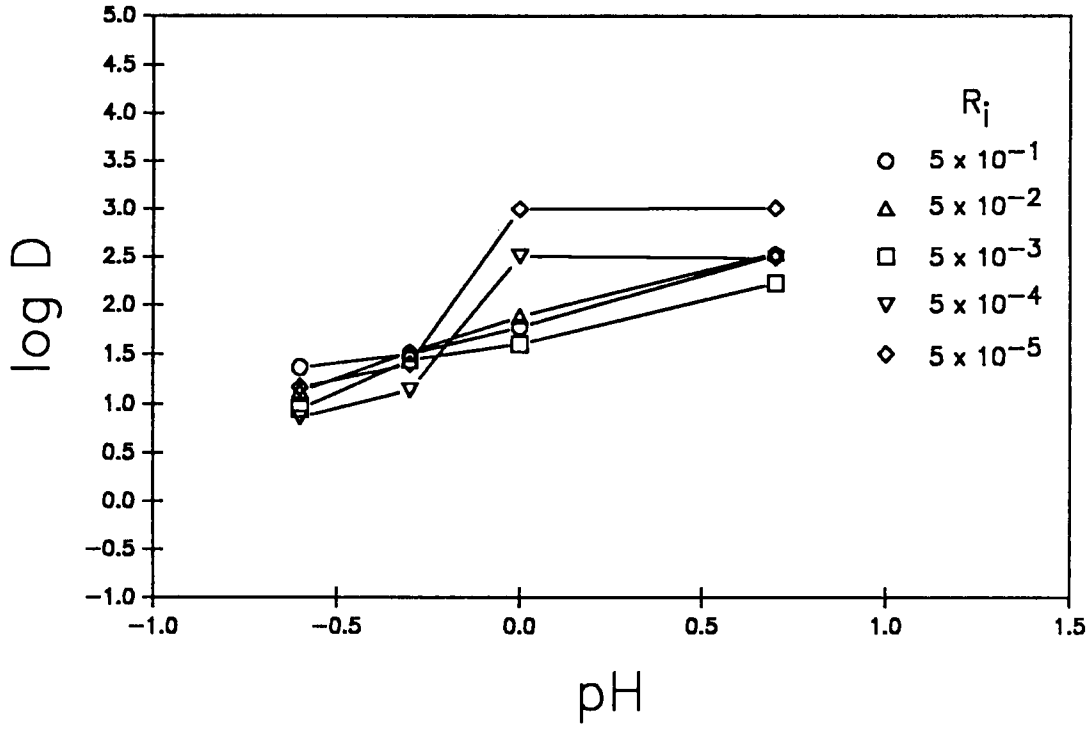

Figure 98. R_i dependence of Hg extraction by the 2% cross-linked gel phosphonic resin at constant 4M nitrate background.

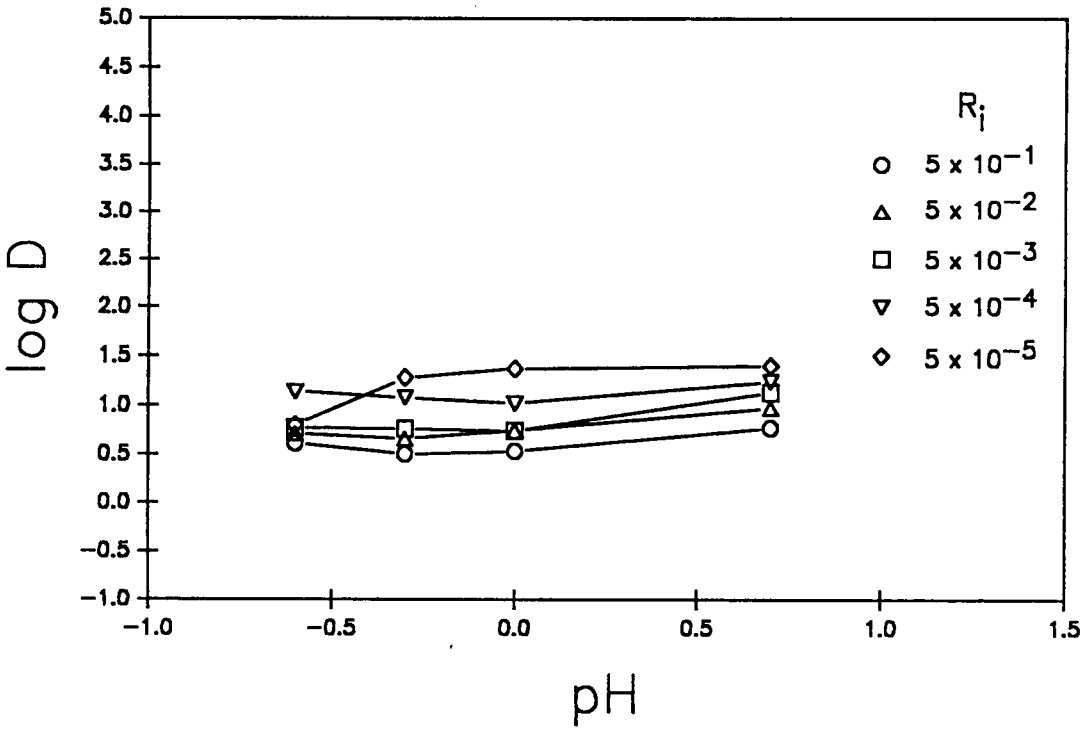

Figure 99. R_i dependence of Ag extraction by the 2% cross-linked gel phosphonic resin at constant 4M nitrate background.

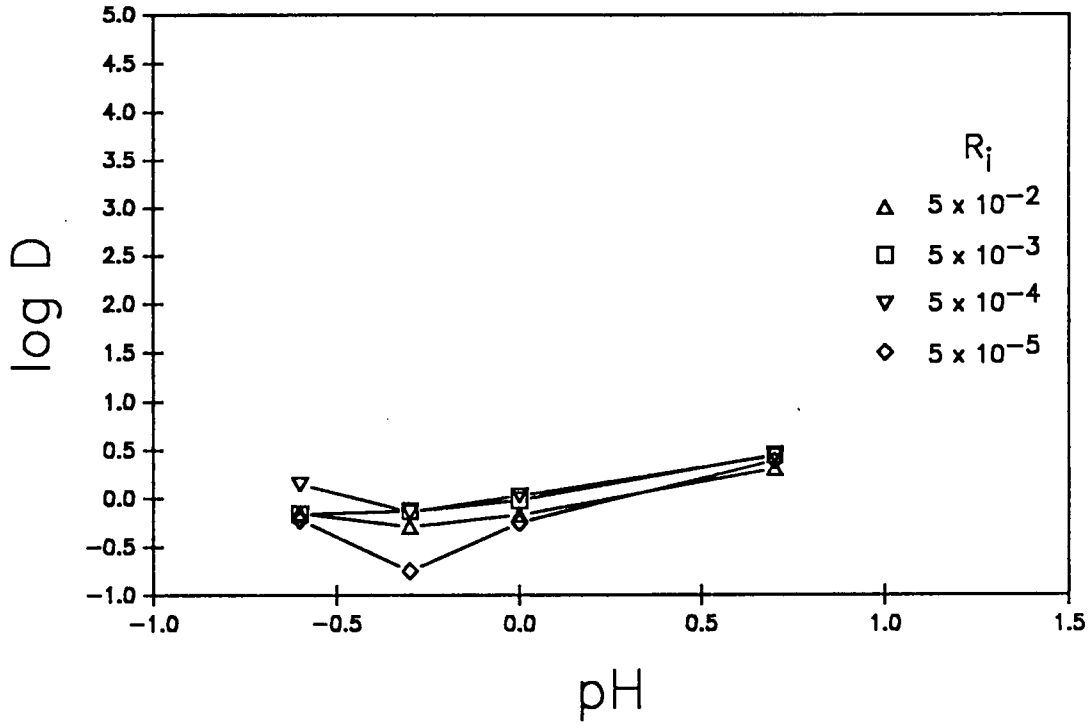

Figure 100. R_i dependence of Mn extraction by the 2% cross-linked gel phosphonic resin at constant 4M nitrate background.

absorption at an R_i of 0.5 and were not observed in the complexation of Mn. However, loading effects were less evident for the phosphonic in the extraction of Hg and Ag.

In Table 62 (page 318), the complexation of Fe, Hg, Ag and Mn is compared for background solutions of 4M and 0.01M HNO_3 at an R_i of 1.0. The phosphonic resin has a greater affinity for Fe in 4M HNO_3 (log D 1.37) than in 0.01M HNO_3 (log D 0.64). These findings indicate that the coordination of the neutral ferric nitrate salt by the phosphoryl oxygen is preferred over ion exchange of the ferric ion by the acidic hydrogen of the phosphonic resin. This behavior was also observed with the phosphinic resin, although to a lesser degree (log D of 0.56 in 4M HNO_3 vs. 0.40 in 0.01M HNO_3). Complexation of Hg, Ag and Mn was higher by both resins in 0.01M HNO_3 than in 4M HNO_3, suggesting a greater affinity for ion exchange of these metals than for coordination. Comparing the Hg results for the two resins shows the phosphonic to be a stronger coordinator of Hg in 4M HNO_3 than the phosphinic; in 0.01M HNO_3, however, extraction of Hg by the phosphinic resin was slightly higher due to its reduction of mercuric ions. The Ag results in 4M HNO_3 also indicate the superior coordinative ability of the phosphonic resin for Ag. In 0.01M HNO_3, the phosphinic resin is clearly superior to the phosphonic, however, owing to the reduction of Ag ions to the corresponding metal. The Mn results for the two resins are similar at both HNO_3 concentrations, suggesting that neither resin coordinates the hard Mn ion in highly acidic solution and that both have similar ion-exchange affinities for Mn in 0.01M HNO_3.

The results in Table 62 (page 318) also point to the importance of solution conditions in determining the metal ion selectivity series for DMBP's. For example, the metal ion affinity displayed by the phosphinic resin at an R_i of 1.0 changed from Fe > Hg > Mn > Ag in 4M HNO_3 to Hg > Ag > Mn > Fe in 0.01M HNO_3. At an R_i of 5 X 10^{-4}, a preference for Fe and Hg over Mn was observed in 4M HNO_3, whereas in 0.01M HNO_3 the three metals were extracted to the same level. Additionally, the affinity series displayed by the phosphonic resin at an R_i of 1.0 changed from Fe > Hg > Ag > Mn in 4M HNO_3 to Hg > Ag > Mn > Fe in 0.01M HNO_3.

Figures 101-108 give the R_i study results for 10% cross-linked gel and MR phosphinic resins. Overall, similar results were obtained for the 2% and 10% cross-linked resins. The 10% gel resin, however, exhibited a loading effect at a much lower R_i (5 X 10^{-3}) in the extraction of Fe than the 2% gel resin. This result may be related to decreased metal ion accessibility of the more tightly cross-linked gel network. In contrast to the results with the other gel resins, the log D values for Fe extraction by the 10% MR phosphinic decreased with the R_i in the following order: 5 X 10^{-3} > 5 X 10^{-4} > 5 X 10^{-5}. In comparing the % absorbed values, however, little variation was apparent for the three R_i values: 99.05% at 5 X 10^{-5}, 99.77% at 5 X 10^{-4} and 99.95% at 5 X 10^{-3}. These results illustrate that small differences in % absorbed lead to large variations in log D when very high levels of metal are extracted by the resin.

The results of the R_i study on the liquid extractant DEHP are shown in Figures 109 and 110 for Fe and Hg extraction, respectively. No significant differences in % absorbed were observed over the R_i range of

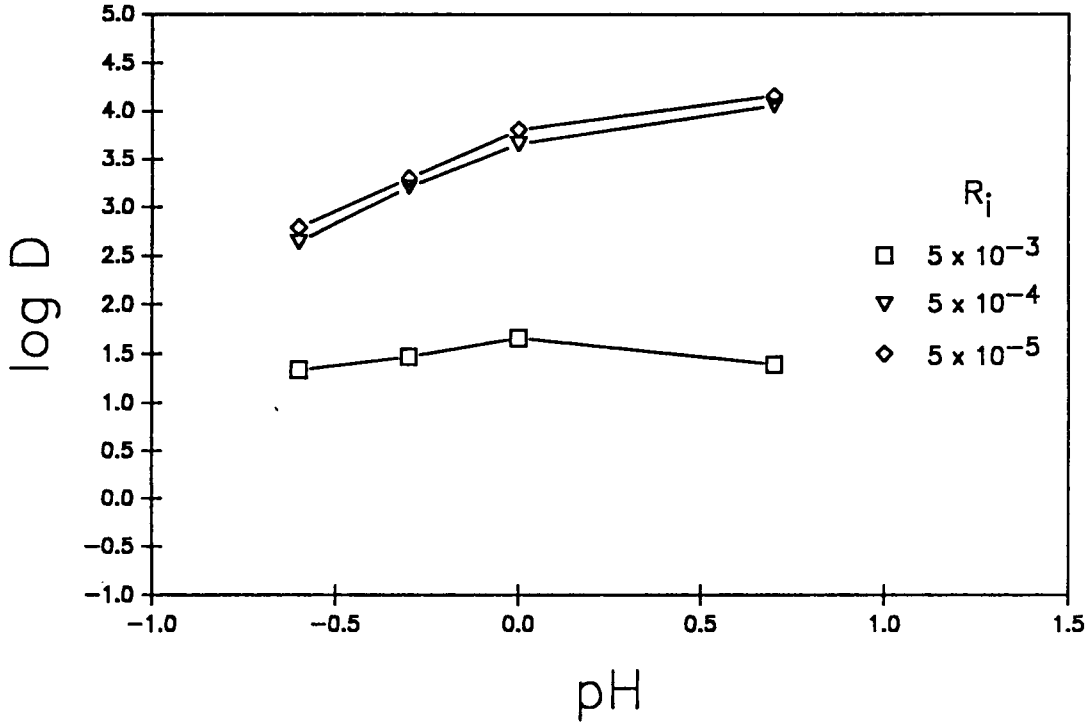

Figure 101. R_i dependence of Fe extraction by the 10% cross-linked gel phosphinic resin at constant 4M nitrate background.

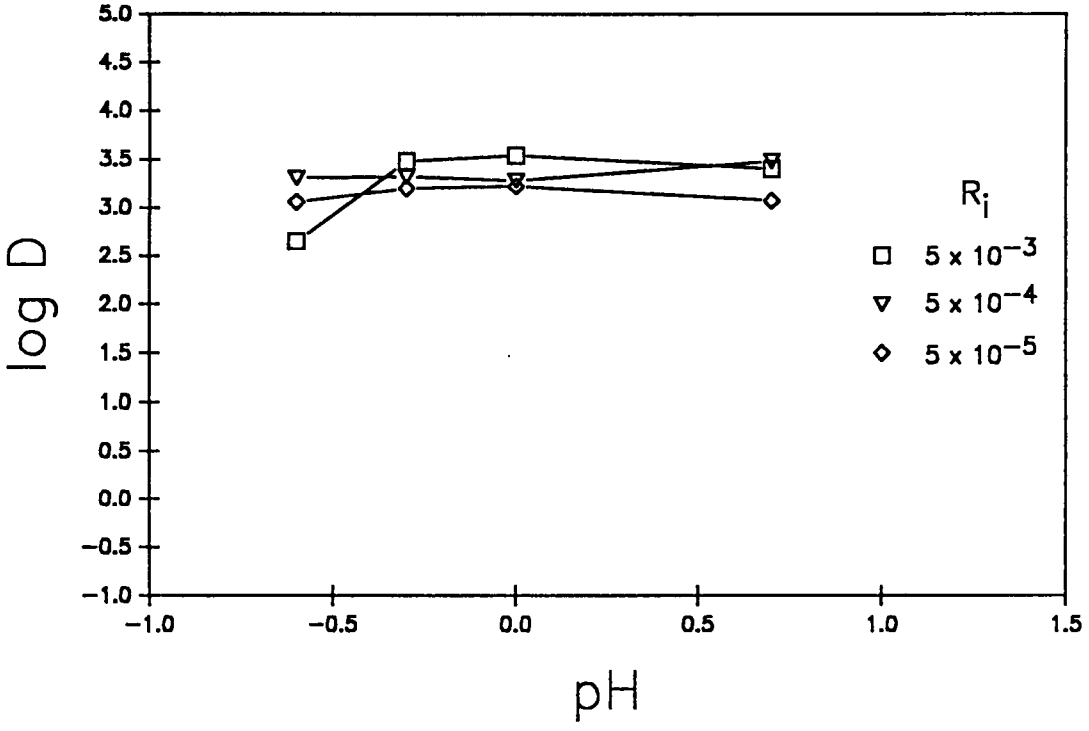

Figure 102. R_i dependence of Hg extraction by the 10% cross-linked gel phosphinic resin at constant 4M nitrate background.

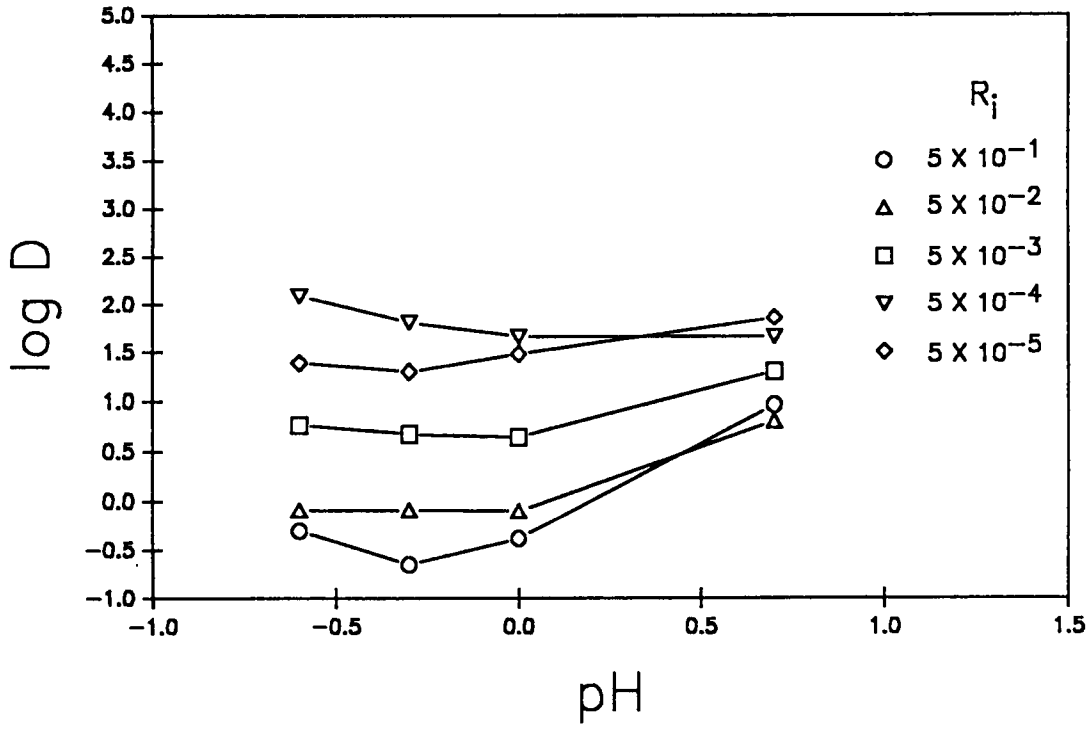

Figure 103. R_i dependence of Ag extraction by the 10% cross-linked gel phosphinic resin at constant 4M nitrate background.

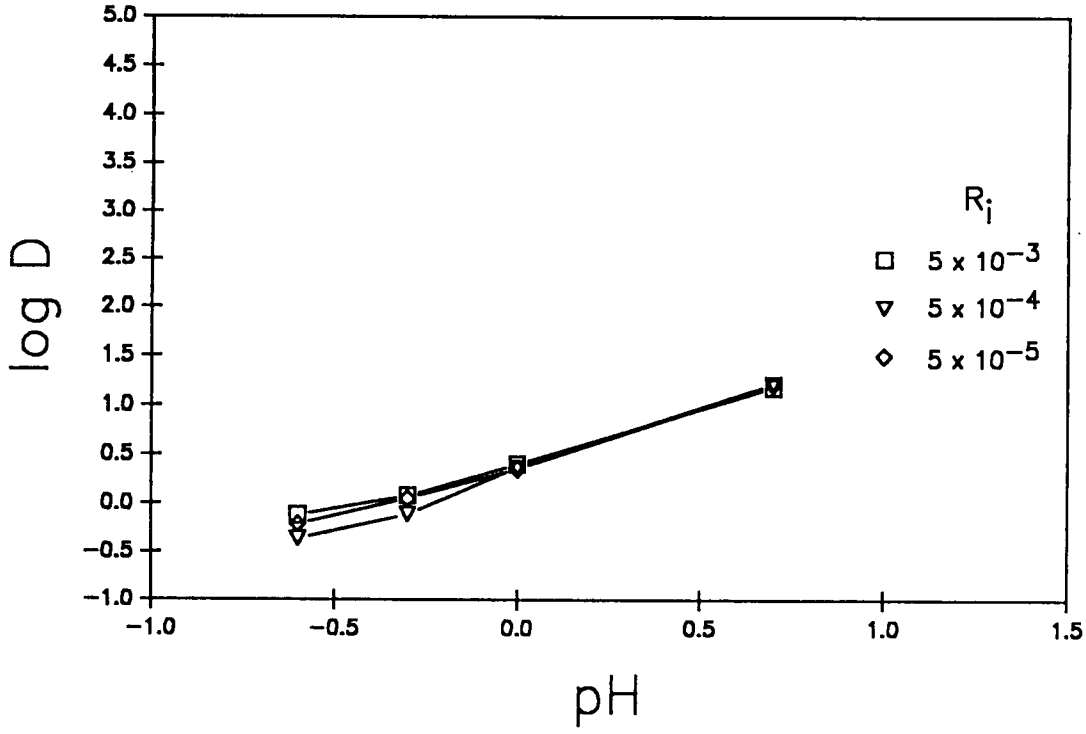

Figure 104. R_i dependence of Mn extraction by the 10% cross-linked gel phosphinic resin at constant 4M nitrate background.

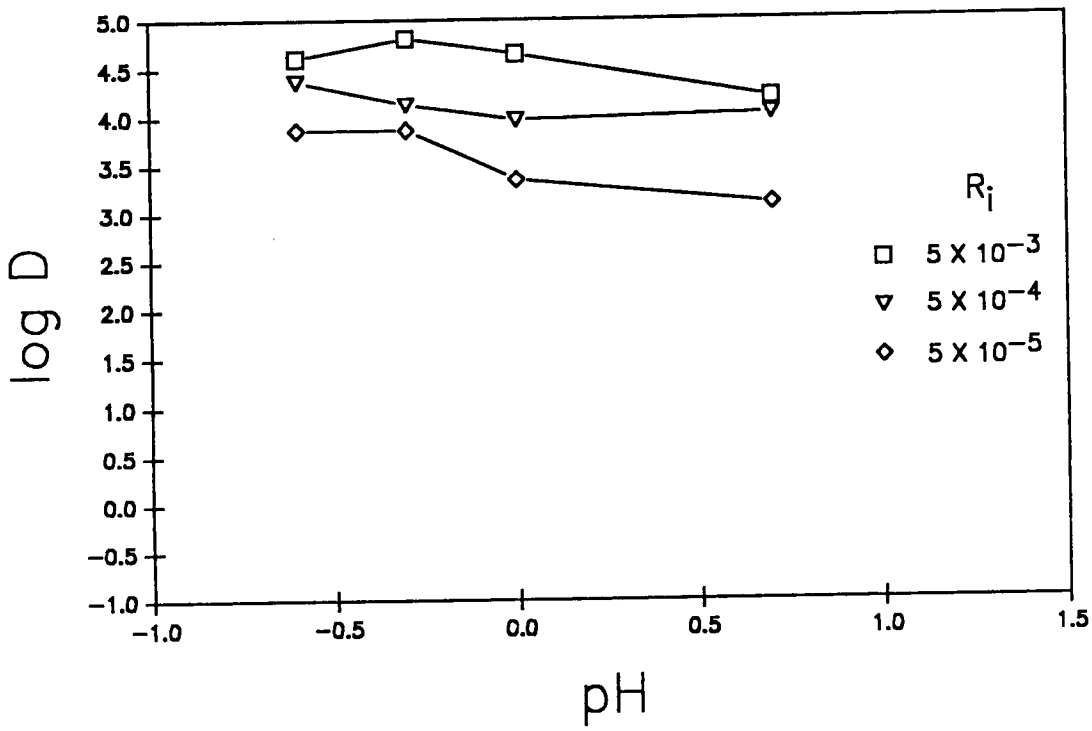

Figure 105. R_i dependence of Fe extraction by the 10% cross-linked MR phosphinic resin at constant 4M nitrate background.

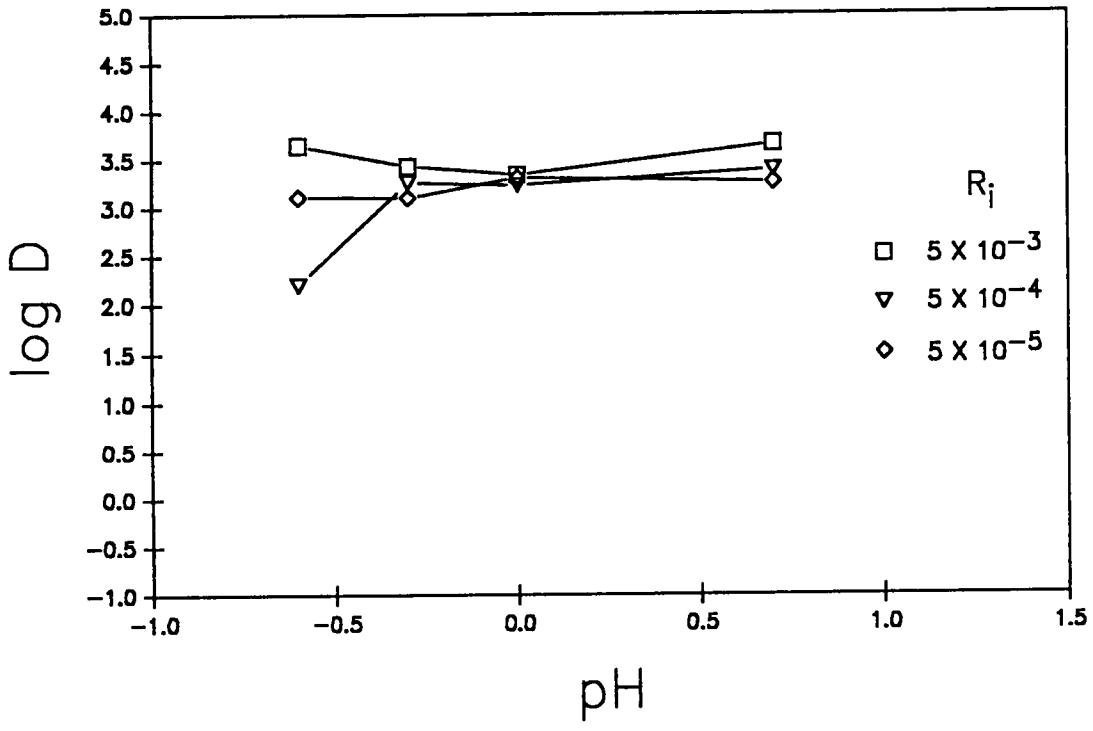

Figure 106. R_i dependence of Hg extraction by the 10% cross-linked MR phosphinic resin at constant 4M nitrate background.

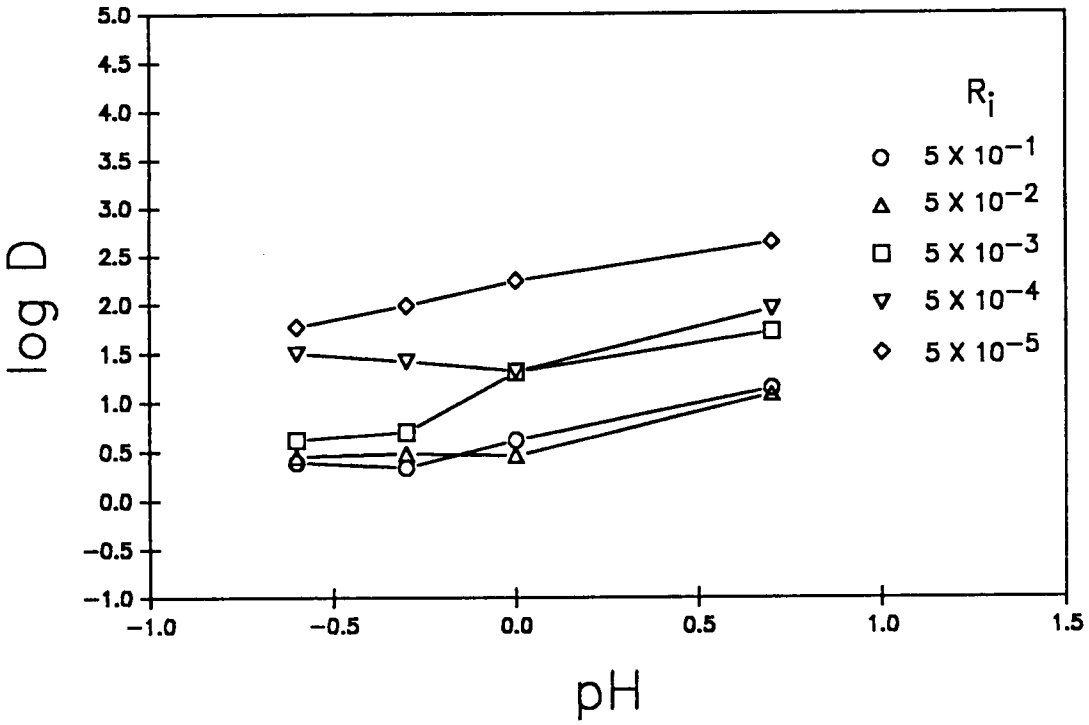

Figure 107. R_i dependence of Ag extraction by the 10% cross-linked MR phosphinic resin at constant 4M nitrate background.

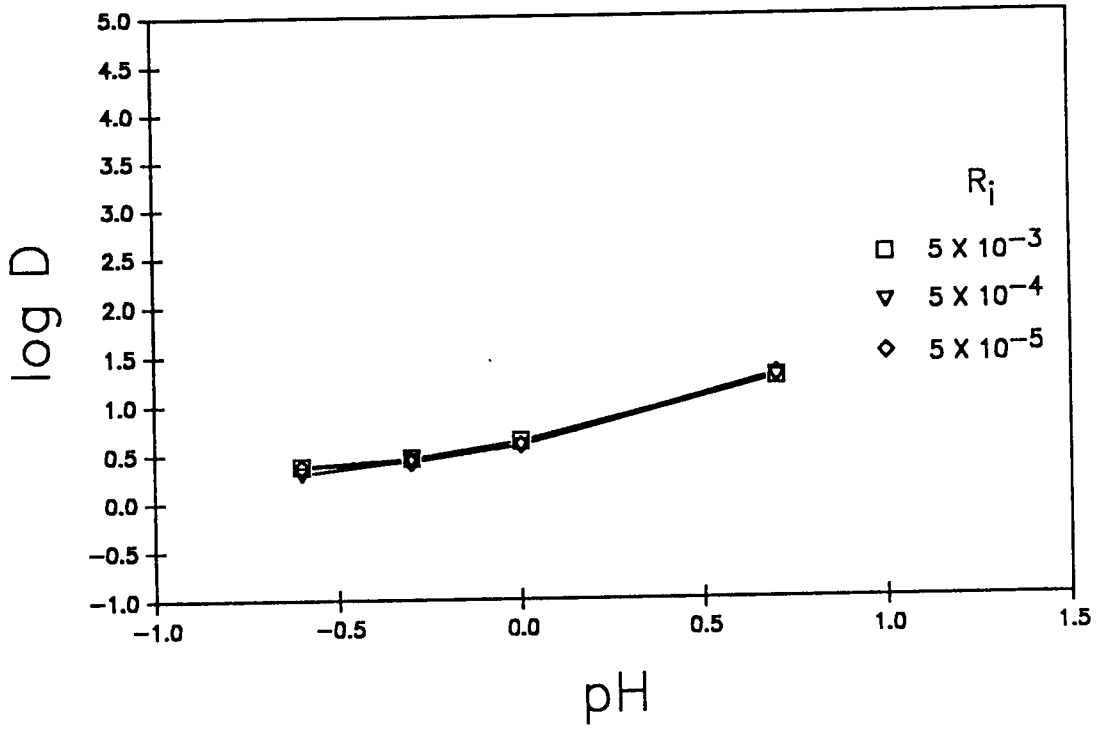

Figure 108. R_i dependence of Mn extraction by the 10% cross-linked MR phosphinic resin at constant 4M nitrate background.

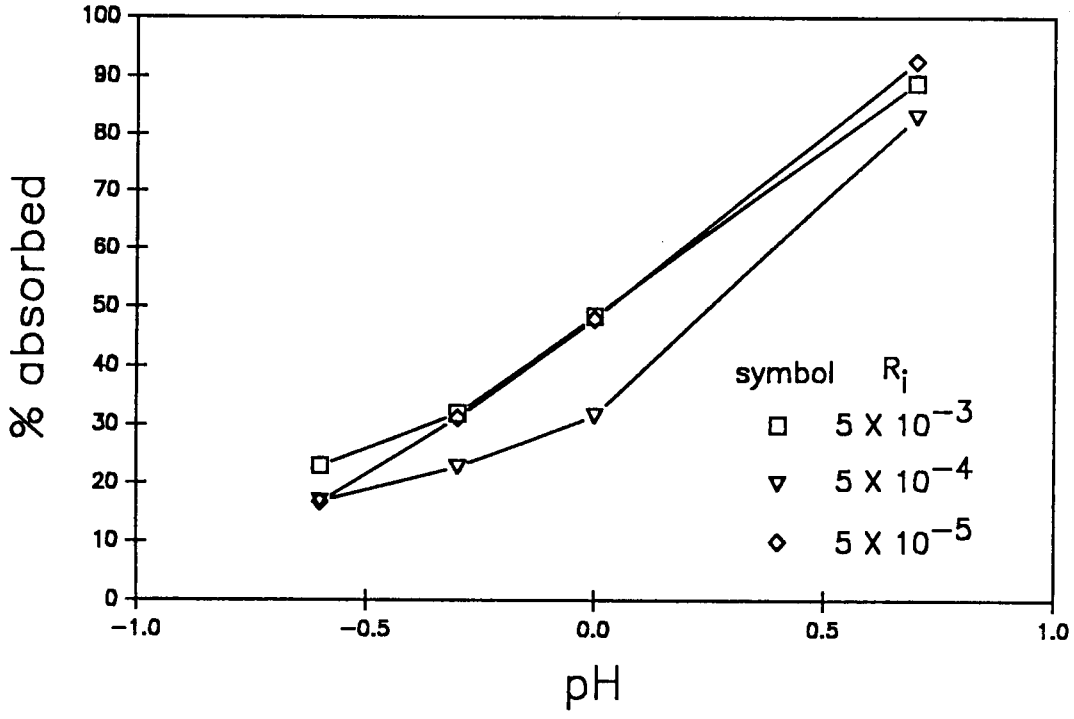

Figure 109. R_i dependence of Fe extraction by DEHP at constant 4M nitrate background.

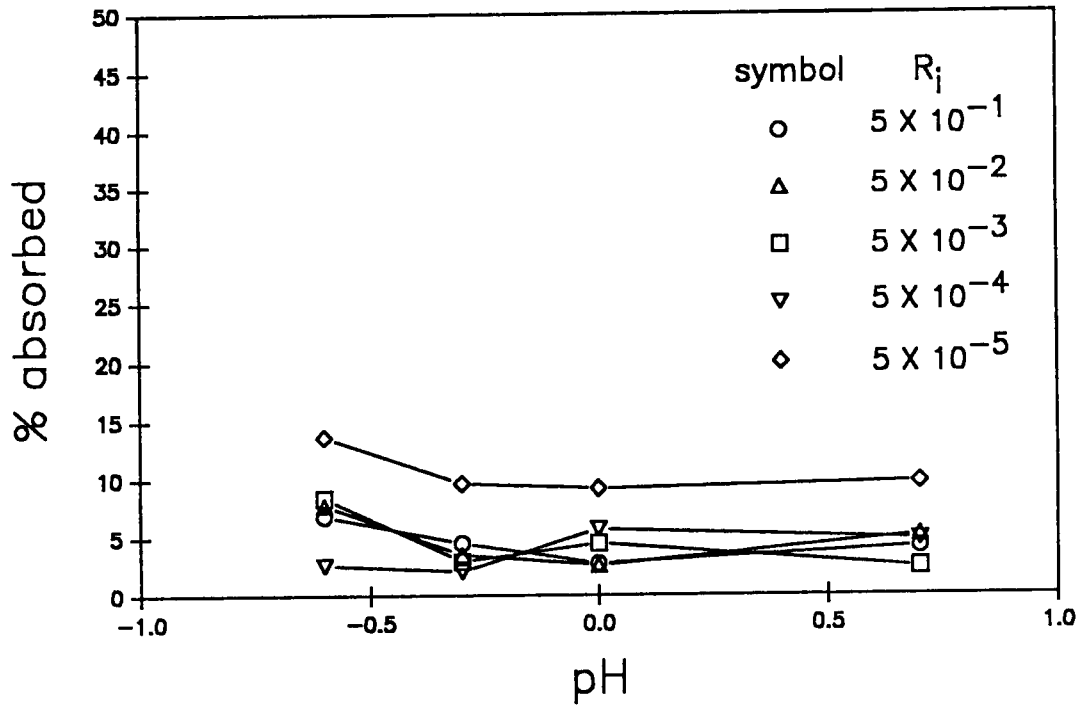

Figure 110. R_i dependence of Hg extraction by DEHP at constant 4M nitrate background.

5×10^{-3} to 5×10^{-5} for Fe extraction. Furthermore, in contrast to the phosphinic resin results, no loading effects were apparent for the liquid extractant at R_i's ranging from 0.5 to 5×10^{-5}, although slightly greater levels of extraction were obtained at 5×10^{-5} than at higher loading ratios.

The influence of the background sodium nitrate concentration on the extraction of Mn and Ag was examined at R_i levels ranging from 1.0 to 5×10^{-5}. The extractions were performed from solutions of 4M, 2M and 0M $NaNO_3$ at a pH of 3.5. The results of the study are given as plots of log D versus R_i in Figure 111 for Mn and Figure 112 for Ag. By affecting the form of the extracting species in solution, the background nitrate concentration may in turn influence the extraction results. For example, at low concentrations of the target metal ion and high background nitrate concentrations, the neutral metal nitrate is likely the predominant species in solution. Thus metal extraction would be expected to increase under conditions which favor coordination of the neutral salt (i.e. low pH). On the other hand, at higher metal nitrate concentrations, more charged species may be present in solution. In this case, extraction would be expected to increase under ion-exchanging conditions (i.e. high pH). The results in Figures 111 and 112 indicate that the decreases in extraction due to the loading effect occur at approximately the same R_i ($\sim 5 \times 10^{-2}$) for all background solutions, suggesting that loading behavior is independent of the solution nitrate concentration.

The results for both Mn and Ag indicate higher degrees of absorption in the absence of $NaNO_3$ for all R_i's, although the effect was

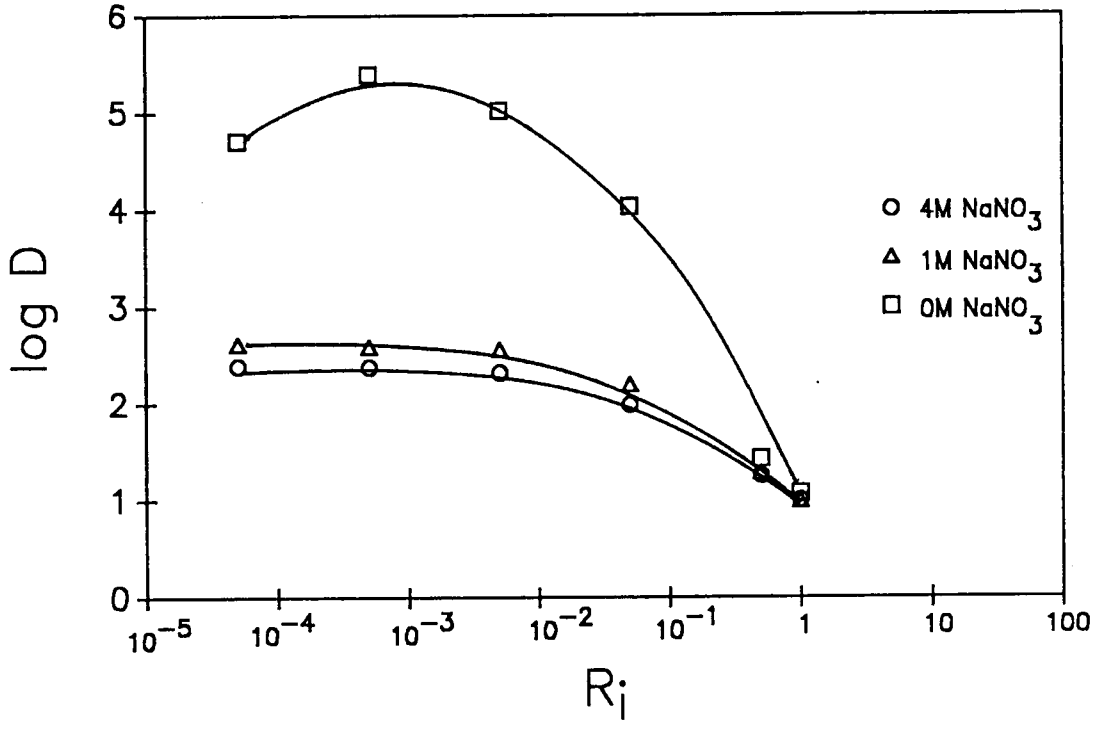

Figure 111. R_i dependence of Mn extraction by the phosphinic resin determined from solutions of varying nitrate concentration.

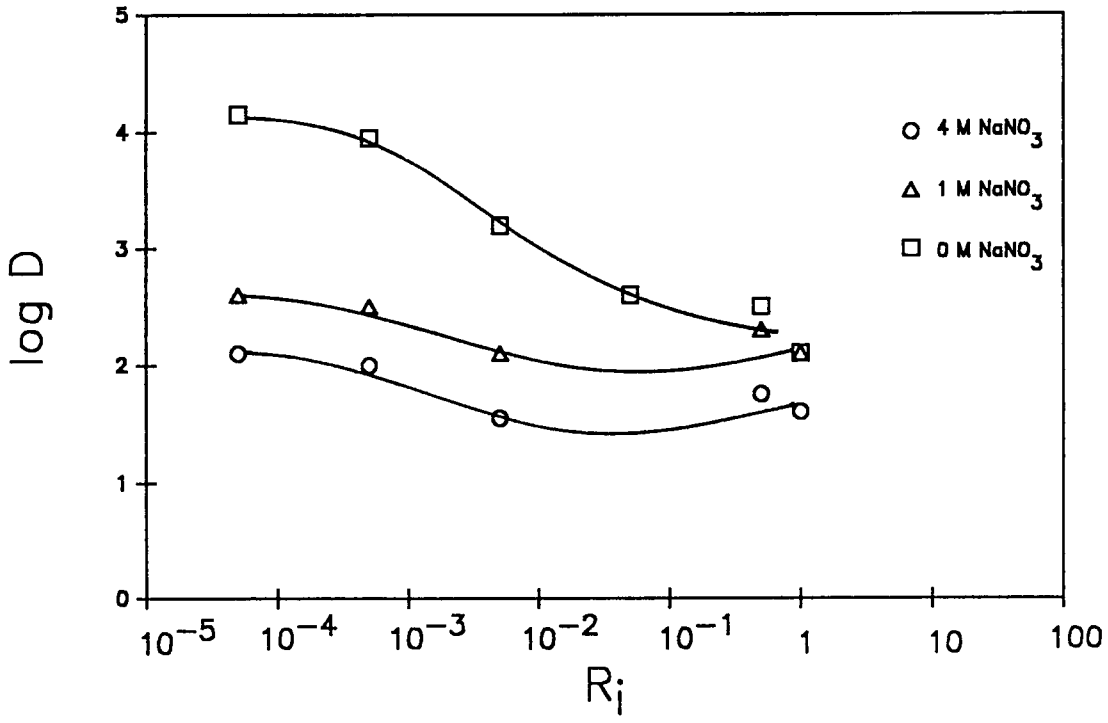

Figure 112. R_i dependence of Ag extraction by the phosphinic resin determined from solutions of varying nitrate concentration.

not as dramatic with Ag extraction as with Mn. Diminished Mn extraction in the sodium-containing solutions results from the competing ion-exchange reaction with sodium ions. The reduction of Ag ions also decreased in the presence of excess $NaNO_3$ due to sodium ions occupying the ion-exchange sites.

As predicted by stiochiometric considerations, comparison of the Mn and Ag results in Figures 111 and 112 provides evidence that Ag^+ reduction does not occur with the phosphinic resin at low metal ion concentrations. The extraction results in the absence of $NaNO_3$ show that at R_i values greater than 0.5, higher levels of Mn were extracted than Ag, suggesting that the phosphinic's recognition mechanism is inoperative at dilute solution conditions. Thus, at low R_i values, both metals are extracted through ion-exchange from pH 3.5 solutions, and therefore, the divalent Mn^{2+} is preferred over the monovalent Ag^+.

CHAPTER V

CONCLUSIONS

A new category of polymers termed dual mechanism bifunctional polymers (DMBP's) has been developed for use as highly specific metal ion complexing agents. These polymers contain two groups on the same polymer backbone each of which functions by a different mechanism. The access mechanism allows for metal ion entry into the polymer matrix by ion-exchanging with the metal ion and the recognition mechanism provides for specificity in the extraction through either reduction or coordination of the metal ion. Class I ion-exchange/redox polymers were synthesized to contain phosphinic acid ligands which were capable of ion-exchange through the acidic hydrogen and reduction of certain metal ions via the P-H bond. The Class I phosphinic resin was found to have a higher affinity for metal ions such as Hg^{2+} with favorable potentials for reduction by the P-H bond than for non-reducible ions such as Zn^{2+}. The Class II ion-exchange/coordination polymers were prepared to contain an acidic phosphorus group for ion-exchange and a phosphoryl oxygen or tertiary amine group for coordination. A series of Class II polymers were synthesized containing different substituents attached to phosphorus in order to vary the degree of softness and polarizabilty of the phosphoryl oxygen coordinating ligand. Extraction studies with these resins suggested that variation in the phosphoryl oxygen polarizibility resulted in different metal ion ligating abilities of the polymers. These findings indicate that, given a multicomponent ionic

solution, a polymer can be tailored to selectively complex targeted metal ions in the solution by adjusting the hard/soft character and polarizability of the phosphoryl oxygen coordinating ligand.

CHAPTER VI

EXPERIMENTAL

Copolymer Synthesis

A suspension polymerization technique was employed to prepare the divinylbenzene cross-linked polystyrene and poly(vinylbenzyl chloride) beads. The polymerization apparatus consisted of a three-neck round-bottom flask equipped with a condenser, thermometer and an overhead stirrer with a double-paddle stir shaft. Oxygen was excluded from the system by a nitrogen purge which was continued throughout the polymerization. The aqueous phase was composed of 0.96 g gelatin dissolved in 100.1 g H_2O at 50 °C, 11.90 g poly(diallyldimethylammonium chloride) (Calgon Corp.), 6.33 g boric acid and 216.5 g H_2O. The pH of the aqueous phase was then adjusted to 10.5 by the addition of 50% NaOH. After adding the aqueous phase to the reaction flask, the stir motor was adjusted to the appropriate speed to obtain the desired bead size (e.g. 250 rpm gave predominantly -20+40 mesh sizes). For the preparation of a 2% cross-linked gel polymer, the organic phase consisted of 286.7 g styrene (Aldrich Chemical Company) or vinylbenzyl chloride (Dow Chemical Company), 10.83 g divinylbenzene (Dow; contained 44.6% ethylstyrene as impurity) and 3.00 g benzoyl peroxide initiator. The aqueous and organic phases were mixed for 2 min and then allowed to separate for 1 min (repeated three times). The polymerization mixture was then heated to 80 °C over a 2-h period and held at this temperature for 10 h. To ensure complete polymerization, the reaction mixture was heated for an

additional 2 h at 100 °C. After cooling to room temperature, the copolymer beads were washed with pH 4 water (adjusted with HCl) and then distilled water. The beads were dried at room temperature and then sieved using a U.S. Standard Screen Series. The poly(vinylbenzyl chloride) beads required soxhleting in toluene to remove unreacted vinylbenzyl chloride and/or divinylbenzene from the polymer pores.

To obtain macroreticular (MR) polymers, half of the monomer mixture was replaced with a phase extender. For example, a 5% cross-linked MR polymer was prepared using the aqueous phase described above and an organic phase composed of 134.95 g styrene or vinylbenzyl chloride, 13.55 g divinylbenzene, 150 g 4-methyl-2-pentanol (Aldrich) and 1.5 g benzoyl peroxide. The 2-h hold at 100 °C employed in the gel synthesis was replaced for the MR beads by a 6-h steam distillation to remove the alcohol.

Phosphinic Acid Resin Synthesis

Cross-linked polystyrene gel beads (10 g) were placed in a 250-mL round-bottom flask equipped with a condenser, thermometer and overhead stirrer. The gel copolymer was swelled for 1 h in 80 mL PCl_3 (Aldrich). For 10 g of macroreticular beads, 130 mL PCl_3 was required for complete swelling. In the preparation of a fully functionalized phosphinic resin, 0.77 mole $AlCl_3$ (Aldrich) was added per mole of copolymer. The reaction mixture was heated to reflux (76 °C) over 1 h and this temperature was maintained for 4 h. Lower levels of functionalization were obtained using reaction temperatures of -78 °C to 50 °C. After cooling to room temperature, the reaction mixture was quenched by

addition to ice water saturated with NaCl. The functionalized beads were isolated and washed with water until a neutral pH was obtained. Conditioning of the resin was carried out in a glass fritted funnel by successive 1-h elutions of 1 L water, 4 wt% NaOH, water, 4 wt% HCl and water. The resins used in radiotracer experiments were further purified by soxhleting in water for 17 h followed by two complete reconditioning cycles. The resin was analyzed for its total acid, primary acid and phosphorus capacities.

Phosphinic Resin Oxidation Using Hydrogen Peroxide

A 500-mL reaction flask outfitted with an overhead stirrer, condenser and thermometer was charged with phosphinic resin (10 g dry weight) and 20% H_2O_2 (300 mL). The mixture was stirred for 1 h and then heated to reflux over a 4-h period. This temperature was maintained for 1 h after which the reaction mixture was allowed to cool to room temperature. The beads were washed with water followed by conditioning and characterization as specified for the phosphinic resin.

Phosphonic Acid Resin Synthesis

The functionalization apparatus used to prepare the phosphonic resin was identical to that for the phosphinic. Cross-linked poly(VBC) beads (10 g) were swollen for 1 h in 80 mL PCl_3, followed by the addition of 10.48 g $AlCl_3$ (1.2 mole $AlCl_3$/mole of copolymer). The reaction mixture was heated to reflux (76 °C) over a period of 1 h and then held at reflux for 4 h. After cooling the mixture to room temperature, hydrolysis was carried out by either of two methods. In

Method I, the contents of the round-bottom were poured into ice water saturated with NaCl. In Method II, the excess PCl_3 was removed and the beads were washed three times with 200-mL portions of dioxane. Hydrolysis was accomplished by the dropwise addition of 70% aqueous dioxane. After hydrolysis, the phosphonic resin was washed with water and conditioned as described for the phosphinic. Following conditioning, the resin was soxhleted in water for 17 h and then reconditioned through two complete cycles. The phosphorus and acid capacities were then determined.

Mixed Ester, Monoester and Diester Resin Synthesis

As in the phosphonic resin synthesis, 10 g of poly(VBC) beads were swollen in 80 mL PCl_3 for 1 h in a 250-mL flask equipped with an overhead stirrer, condenser and thermometer. The $AlCl_3$ catalyst (10.48 g; 1.2 mole/mole copolymer) was added and the reaction mixture heated to 76 °C over 1 h. After a 4-h hold at 76 °C, the reaction was allowed to cool to room temperature and the beads were washed free of PCl_3 using five to six 200-mL portions of toluene. After washing was complete, 50 mL of toluene was added to the beads to allow for fluidity of the reaction mixture. At this time the flask was equipped with an addition funnel through which the quench solution was added. For the preparation of mixed ester resins, the quench solution consisted of pyridine and aqueous ethanol in equimolar amounts. The ethanol to water ratio varied according to the desired degree of esterification, For example, an 8:1 mole ratio of ethanol to water produced a resin with 84.8% esterification while a 2:1 ratio gave 25.3% esterification. Enough

aqueous ethanol was added to contact the resin with a total of 0.7 moles of ethanol plus water. To avoid a rapid rise in the reaction temperature, the quench solution was added slowly over a 2-3 h period and the reaction flask was immersed in an ice bath. The addition rate was adjusted to maintain the temperature at ≤ 10 °C. After the addition was complete, the reaction mixture was stirred for 1 h while the temperature was held at 0-5 °C. To ensure that solvolysis was complete, the first solution was siphoned off and a second quench solution added to the resin. The was allowed to stir with the resin for 17 h as the reaction temperature was slowly increased to room temperature. After removing the second quench solution, the resin was washed four times with 200 mL 95% ethanol and eight times with 200 mL 50% ethanol. The resin was then placed in a fritted funnel and conditioned with successive elutions (1 L/h) of water, 4 wt% NaOH, water, 4 wt% HCl and water. The resin was characterized by NaOH titration (17-h stir and titration curve) and phosphorus elemental analysis.

The monoester resin was prepared in the same manner as the mixed ester with the following exceptions. The quench solution was composed of equimolar amounts of absolute ethanol (0.7 mole/10 g copolymer) and pyridine. The second ethanol quench was heated to reflux (89 °C) for 16 h. Following washing in ethanol and conditioning, the monoester resin was soxhleted in water for 17 h and then reconditioned two times. Analysis was carried as with the mixed ester resin.

The diethyl ester resin was synthesized as described above except under milder functionalization conditions using $FeCl_3$ as the Friedel-Crafts catalyst thus allowing for a less exothermic ethanolysis

reaction. The quench solution consisted of 32.25 g anhydrous ethanol (0.7 mole/10 g copolymer) and 32.25 g toluene. The dimethyl, di-*n*-propyl and di-*n*-butyl ester resins were prepared in the same manner from the corresponding alcohols. Both *n*-propanol and *n*-butanol were freshly distilled before use. To increase the degree of esterification by excluding atmospheric moisture, a nitrogen sweep was employed during the quench reaction. Additionally, the quench solution was added at a slower rate than for the mixed ester and monoester resins. After washing in alcohol, conditioning, soxhleting and reconditioning two times, the diester resins were analyzed by phosphorus elemental and 17-h NaOH titration.

Amine Resin Synthesis

All aminations were performed in three-neck round-bottom flasks equipped with overhead stirrers, condensers and thermometers. For low-boiling amines, cold-finger condensers were used to avoid loss of amine during the reaction. In the preparation of the dimethylamine resin, a mixture of 10 g poly(VBC) beads, 210 mL 25 wt% dimethylamine (Aldrich) and 3.4 g 50 wt% NaOH was refluxed (52 °C) for 7 h. The diethylamine resin was synthesized by refluxing (55 °C) 10 g poly(VBC) beads in 210 mL diethylamine (Aldrich) and 3.4 g 50 wt% NaOH for 6 h. An 8-h reflux of 10 g poly(VBC) beads in 210 ml 70 wt% ethylamine (Aldrich) and 3.4 g 50 wt% NaOH produced the ethylamine resin. Di-*n*-propyl resins were obtained by refluxing (98 °C) 10 g poly(VBC) beads in 150 mL di-*n*-propyl amine (Aldrich) and 3.4 g 50 wt% NaOH for 8 h. The di-*n*-butylamine resin was synthesized by refluxing (91 °C) 10 g poly(VBC) beads, 150 mL

80% dioxane and 150 mL di-*n*-butylamine (Aldrich) for 47 h. After allowing to cool to room temperature, the aminated beads were washed with water, collected and placed in a fritted funnel. Conditioning was then carried out by passing 1 L of the following through the resin bead over a period of 1 h: water, 4 wt% NaOH, water, 4 wt% HCl and water. For the di-*n*-butylamine resin, the conditioning sequence was preceded by a 1-h elution with 1 L of 95% ethanol. The resins were analyzed for total anion exchange capacity, salt splitting anion exchange capacity and chlorine capacity.

Amine/Ester Resin Synthesis

A partially functionalized diethyl ester resin was obtained as described above except using 0.77 mole $FeCl_3$ catalyst/mole copolymer. The bifunctional dimethylamine/ester, diethylamine/ester and ethylamine/ester resins were prepared from the diethyl ester resin (19 g dry weight) by the procedure described in the previous section for the monofunctional amine resins. The di-*n*-propyl/ester resin was obtained by refluxing (55 °C) partially functionalized diethyl ester resin (6 g dry weight) in 100 g di-*n*-propylamine, 100 g H_2O and 100 mL absolute ethanol for 24 h. After amination, the beads were cooled, washed with water and conditioned over 1 h with 1 L each of water, 4 wt% NaOH, water, 4 wt% HCl and water. The acid, phosphorus, chlorine and total anion exchange capacities were then determined.

Dimethylamine/Phosphonic Resin Synthesis

A partially functionalized phosphonic resin was prepared as previously described except using a 40 °C reaction temperature and 0.77 mole $AlCl_3$ catalyst/mole copolymer. The phosphonic resin was converted to the sodium salt form by elution with 1 L 4 wt% NaOH over a 1-h period. Amination of the sodium salt of the phosphonic resin (10 g dry weight) was performed by the same procedure as for the monofunctional dimethylamine resin. Conditioning and characterization of the amine phosphonic was carried out as specified for the amine/ester resins.

Thiol and Thiol Phosphonic Synthesis

A three-neck round-bottom flask equipped with overhead stirrer, condenser and thermometer was charged with 10 g poly(VBC) beads and 140 mL ethylene dichloride. After allowing the beads to swell for 1 h, the ethylene dichloride was siphoned off and replaced with ethanol (95%, 160 ml) and thiourea (9.62 g). The mixture was heated to reflux (73 °C) over 1 h and held at reflux for 24 h. The resin can be isolated at this point to give an isothiouronium salt. After cooling to room temperature, the liquid was decanted from the beads and 300 mL 10% NaOH was added. Following a 24-h reflux period, the reaction mixture was cooled to room temperature and the solution was removed from the beads. The beads were washed with water and then conditioned by elution (1 L/h) with water, 4 wt% NaOH, water, 4 wt% HCl and water. The resin was analyzed for any remaining chlorine by elemental analysis.

The synthesis of the thiol phosphonic resin was carried out according to the above procedure except using a partially functionalized

phosphonic resin (substituted to 67% by reaction with 0.77 mole $AlCl_3$/mole copolymer at 40 °C). Unlike the poly(VBC) beads, however, the phosphonic resin did not require pre-swelling in ethylene dichloride. To the partially substituted phosphonic resin (10 g dry weight) were added 5 g thiourea and 81 mL 95% ethanol. Following the reflux period, the liquid was decanted from the beads and 210 mL of 10% NaOH was added. After refluxing for 24 h, the beads were washed with water, conditioned and analyzed as described for the thiol resin.

Determination of % Solids

The resin was aspirated for 5 min at 720 mm Hg. A weighed sample of the suction-dried resin (approximately 1 g) was dried at 110 °C for 16 h to remove all water from the resin pores. After drying was complete, the sample was reweighed and the % solids calculated according to the equation

$$\% \text{ solids} = \frac{\text{sample weight of oven-dried resin}}{\text{sample weight of suction-dried resin}} \times 100\%$$

Determination of Resin Acid Capacity

A sample of suction-dried resin (approximately 0.5-1.0 g dry weight) was placed in a 250-mL ground glass Erlenmeyer flask and stirred for 17 h with 200 mL standard 0.1N NaOH in 5 wt% NaCl. A 50-mL aliquot was then removed and titrated with 0.15N H_2SO_4 using a phenolphthalein indicator. The acid capacity (in units of mequiv/g) was calculated as follows:

$$\text{acid capacity} = \frac{(\text{vol NaOH})(\text{N NaOH}) - 4(\text{vol } H_2SO_4)(\text{N } H_2SO_4)}{\text{g dry resin}}$$

The NaOH solution was standardized against primary standard potassium hydrogen phthalate and was then used to determine the concentration of the sulfuric acid solution.

The acid capacity of samples with low aqueous reagent accessibility was determined using a standard solution of KOH in 81% aqueous dioxane. The titration was performed exactly as described above for aqueous NaOH.

Determination of Acid Capacity by Titration Curve

A sample of suction-dried resin (approximately 0.5 g dry weight) was placed in a beaker with 50 mL H_2O and titrated with hourly 1-ml additions of standard 0.1N NaOH. The solution pH was determined after each 1-h equilibration period using a Corning Model 150 pH meter. For some resins, the titration was carried out using sodium ethoxide as the titrant instead of NaOH. The sodium ethoxide solution was prepared by dissolving 3.45 g sodium metal in 1 L absolute ethanol and was standardized against primary standard potassium hydrogen phthalate. The resin was eluted for 1 h with 500 mL absolute ethanol before titration. The resin was then placed in 50 mL 95% ethanol and titrated as described above.

Phosphorus Elemental Analysis[117]

Oven-dried resin (20 mg) was placed in a 125-mL Erlenmeyer flask

with 10 mL 72% $HClO_4$ and 5 mL concentrated HNO_3. The mixture was heated until the beads were digested and the solution became clear. After cooling to room temperature, the solution was diluted to 100 mL with water. To a 5-mL aliquot of this solution was added (in the following order) 3.5 mL 72% $HClO_4$, 4.5 mL freshly prepared amidol reagent (1 g recrystallized 2,4-diaminophenol dihydrochloride (Aldrich), 10 g Na_2SO_3, 2.7 g concentrated H_2SO_4 and 90 g H_20) and 3.5 mL ammonium molybdate solution (4.4 g in 50 mL H_20). After dilution to 50 mL with water, the solution was allowed to develop for 30 min. A blank solution containing all reagents except the phosphorus solution was prepared and used to zero the spectrometer. The absorbance of the solution was measured at 700 nm on a Bausch and Lomb Spectronic 21. The amount of phosphorus present in the sample was determined from a Beer's Law plot (slope = 131.70 mL/mg) using a series of K_2HPO_4 standards. The phosphorus capacity was calculated (in units of mequiv/g) from the following equation:

$$\text{phosphorus capacity} = \frac{(\text{Absorbance})(1000\ \text{mL})}{(\text{g resin})(30.974\ \text{mg/mequiv})(131.7\ \text{mL/mg})}$$

Chlorine Elemental Analysis

Sodium metal (0.5 g) and xylene (3 mL) were placed in a 15- x 160-mm Pyrex test tube. The tube was clamped to a ring stand and the sodium melted using a Bunsen Burner. A second test tube, also clamped to a ring stand, was charged with 0.3 g of oven-dried resin, 2 g sodium metal and 1 mL xylene. The two test tubes were connected with a U-shaped

glass transfer tube equipped with a rubber stopper at one end. One end of the transfer tube was immersed into the molten sodium of the first test tube and the end with the stopper was tightly connected to the second test tube. While continuing to heat the first test tube, the sodium in the second test tube was slowly melted using a second Bunsen Burner. After the sodium was melted, the second test tube was heated strongly for 2-4 min to decompose the beads. The chlorine gas produced by sodium fusion of the resin passed through the transfer tube and was bubbled through the molten sodium of the first test tube. Both tubes were heated strongly for 15 min. After cooling to room temperature, the two test tubes and transfer tube were broken into a 250-mL beaker containing 100 mL methanol. The methanol was evaporated and the resulting solid was dissolved with water. The solution was quantitatively transferred with filtering into a 250-mL volumetric flask. A 50-mL aliquot of this solution was acidified with concentrated HNO_3 to a methyl orange endpoint (red) and was then neutralized with 0.3M NaOH to a yellow endpoint. A Mohr titration was employed to determine the amount of chloride in the sample using standard 0.05M $AgNO_3$ (8.494 g dissolved in 1 L distilled water) as the titrant and 5 wt% $K_2Cr_2O_4$ (2 mL) as the indicator. The chlorine capacity (in mequiv/g) was calculated as follows:

$$\text{chlorine capacity} = \frac{5(\text{vol } AgNO_3)(\text{N } AgNO_3)}{\text{g resin}}$$

When nitrogen was present in the sample, the fusion solution was boiled

for 15 min after acidification to remove CN^- which was found to interfere with the Mohr titration.

Determination of Primary Acid Capacity by Iodine Oxidation[118]

Iodine oxidation analysis involved three steps: (1) oxidation of the phosphinic resin's P-H bonds with KI_3 solution, (2) reduction of the excess I_2 with sodium thiosulfate solution and (3) back titration of the excess sodium thiosulfate with KI_3 solution. A 0.2N KI_3 solution was prepared by dissolving 25.4 g iodine and 80 g potassium iodide in 1 L H_2O. The sodium thiosulfate solution (0.1N) consisted of 25 g Na_2S_2O3 and 0.2 g Na_2CO_3 (as a preservative) in 1 L H_2O and was standardized against primary standard KIO_3 using a starch indicator. The concentration of the KI_3 solution was determined using the standard sodium thiosulfate solution.

The oxidation was carried out by placing 0.5 g (dry weight) of suction-dried resin into a 250-mL brown bottle with 50 mL KI_3 solution and 2 mL pyridine. After shaking for 22 h, 50 mL of 0.1N sodium thiosulfate solution was added. The sample was shaken until the thiosulfate had reacted with the iodine absorbed in the resin, as indicated by the beads becoming clear. If the reaction required longer than 1.5 h, 5 mL of toluene was added and the sample was shaken for 30 min to facilitate removal of iodine from the resin pores. The entire sample was titrated for the remaining thiosulfate with the KI_3 solution using starch as the indicator (blue endpoint). The resin's primary acid capacity (in mequiv/g) was calculated according to the following equation:

$$1° \text{ acid capacity} = \frac{(\text{vol } KI_3)(N\ KI_3) - (\text{vol } Na_2S_2O_3)(N\ Na_2S_2O_3)}{2(\text{g dry resin})}$$

Determination of Primary Acid Capacity by Metal Ion Oxidation

The phosphinic resin's primary acid capacity was also quantified by oxidation of the P-H bond using Ag^+ and Hg^{2+} as oxidizing agents. A sample of suction-dried resin (1-2 g dry weight) was placed in a 250-mL bottle with 100 mL water and a fourfold excess (based on the resin's phosphorus capacity) of $AgNO_3$ or $Hg(NO_3)_2$. For example, to a 1-g sample of resin having a phosphorus capacity of 5 mequiv/g, 3.4 g $AgNO_3$ or 3.2 g $Hg(NO_3)_2$ was added. After shaking for 17 h, the resin was poured into a glass fritted funnel. The resin was eluted (1 L/2 h) with HNO_3 (4M for Ag oxidation and 8M for Hg oxidation) and then with water until the pH of the effluent was neutral. The total acid capacity of the oxidized resin was determined using the procedure described above (17 h stir with excess NaOH). The increase in acid capacity after oxidation represented the resin's primary acid capacity.

Attempted Determination of Primary Acid Capacity by Chromic Acid Oxidation

A 0.1M solution of potassium dichromate was prepared by dissolving 58.8368 g primary standard $K_2Cr_2O_7$ (dried 2 h at 150 °C) and 600 mL H_2SO_4 in 2 L H_2O. Ferrous ammonium sulfate solution (0.1M) was obtained by diluting 19.81 g $Fe(NH_4)_2(SO_4)_2 \cdot 6H_2O$ and 50 mL 3M H_2SO_4 to 500 mL with water. This solution was standardized against the dichromate solution by potentiometric titration using a Corning Model 130 pH meter equipped

with a platinum electrode and a silver-silver chloride reference electrode. Resin oxidation was performed by placing suction-dried phosphinic resin (0.5 g dry weight) in a 50 mL ground glass Erlenmeyer flask with 25 mL 0.1M dichromate solution. The mixture was stirred for 12 h, after which time a 5-mL aliquot of the solution was removed and titrated with 0.1M ferrous ammonium sulfate solution as described above. The primary acid capacity (in mequiv/g) was calculated to be:

$$1° \text{ acid capacity} = \frac{3(\text{vol } Cr_2O_7^{2-})(\text{M } Cr_2O_7^{2-}) - 2.5(\text{vol } Fe^{2+})(\text{M } Fe^{2+})}{\text{g dry resin}}$$

It must be noted that this procedure gave much higher primary acid capacities than with iodine and metal ion oxidation techniques, an indication that the dichromate oxidizing agent was too strong for the selective oxidation of the P-H bonds.

Determination of Nitric Acid Complexing Ability of Phosphoryl Oxygen

A sample of suction-dried resin containing four milliequivalents of phosphorus sites was shaken for 17 h with 10 mL of standard 1.0M HNO_3. For the liquid extractants, 12 mL of extractant solution (in toluene) of the appropriate concentration to give four milliequivalents of phosphorus sites was shaken for 15 h with 10 mL of 1.0M HNO_3. An aliquot of the aqueous phase was removed from the resin or organic solution and titrated with standard 0.1M NaOH. The amount of H^+ absorbed by the liquid extractant or resin was given by:

$$\text{mequiv } H^+ \text{ abs/g extractant} = \frac{\text{mequiv } H^+_{\text{initial}} - \text{mequiv } H^+_{\text{final}}}{\text{g dry resin or extractant}}$$

Determination of Total Anion Exchange Capacity (TAEC)

A suction-dried sample (5-10 g dry weight) of mono-or bifunctional amine resin in the protonated form with the chloride counterion was placed in a glass fritted funnel. The chloride counterion was exchanged for the nitrate anion by elution with 1 L 4 wt% $NaNO_3$ over a period of 1 h. The effluent was collected in a 1 L volumetric flask and a 100-mL aliquot was titrated for chloride using the Mohr titration as described for the chlorine elemental analysis. The TAEC (in units of mequiv/g) was calculated by the following equation:

$$\text{TAEC} = \frac{10(\text{vol } AgNO_3)(\text{N } AgNO_3)}{\text{g dry resin}}$$

Determination of Salt Splitting Anion Exchange Capacity (SSAC)

The mono- or bifunctional amine resin (5-10 g dry weight) in the chloride form was converted to the free amine by elution with 1 L 4 wt% NaOH over 1 h. After washing with 1 L water, 1 L 4 wt% $NaNO_3$ was passed through the resin over a 1-h period allowing for exchange of the hydroxide counterion of the quaternary amine groups with the nitrate anion. The eluant was collected in a 1 L volumetric flask and was titrated for hydroxide ion using 0.1N H_2SO_4. The SSAC (units of mequiv/g) was calculated to be

$$\text{SSAC} = \frac{10(\text{vol } H_2SO_4)(\text{N } H_2SO_4)}{\text{g dry resin}}$$

Copper Extraction Studies

Suction-dried resin containing one milliequivalent of active sites (based on P capacity for phosphorus resins, tot(OH) for the sulfonic resin and P capacity plus TAEC for the amine phosphonic resin) was placed in a 125-mL bottle with 100 mL of 1 X 10^{-3}N $Cu(NO_3)_2$ (R_i = 0.1). Copper nitrate solutions were prepared by dissolving 0.12 g $Cu(NO_3)_2 \cdot 2.5$ H_2O in 1 L H_2O and also in 1 L of the following background solutions: 5 X 10^{-3}M $NaNO_3$, 4M $NaNO_3$, 0.2M HNO_3/3.8M $NaNO_3$ and 2M HNO_3/2M $NaNO_3$. The copper solution and resin were shaken for 17 h. The concentration of Cu was determined before and after resin contact by titration with 1 X 10^{-3}M EDTA with murexide as the indicator.[119] The % of Cu^{2+} absorbed by the resin from the solution was calculated to be

$$\%\text{ absorbed} = \frac{[Cu^{2+}]_i - [Cu^{2+}]_f}{[Cu^{2+}]_i} \quad (100\%)$$

The EDTA solution was standardized against a zinc solution (1 g zinc metal dissolved in 6M HNO_3 and diluted to 1 L with water) using the murexide indicator.

Hg and Ag Extraction Studies by Titrimetric Analysis

Extraction studies with Hg^{2+} and Ag^{+} were carried out by shaking (17 h) suction-dried resin containing one milliequivalent of active

sites with 100 mL $Hg(NO_3)_2$ or $AgNO_3$ solution of the appropriate concentration to give the selected R_i. The metal ion solutions were prepared to contain the desired background levels of $NaNO_3$ and HNO_3. A Volhard titration[120] was employed to determine the Ag and Hg concentrations before and after equilibration with the resin. An aliquot of the metal solution was titrated to a brick-red endpoint using NH_4SCN solution as the titrant and 5 mL of ferric ammonium sulfate solution (10 g of the dodecahydrate dissolved in 100 mL 6M HNO_3) as the indicator. The concentration of the NH_4SCN solution was determined by titration of a standard 0.05M $AgNO_3$ solution. The % absorbed values were calculated exactly as for Cu.

Lanthanide and Actinide Extraction Studies

The extraction of lanthanide and actinide ions was studied by contacting a sample of suction-dried resin containing 1 milliequivalent of active sites with 5 mL of 4M-0.2M HNO_3 (alone or in the presence enough $NaNO_3$ to maintain a constant 4M nitrate background) and a radiotracer level of $^{152-154}Eu$. ^{230}Th, ^{233}U, ^{241}Am or ^{239}Pu. After a 17-h equilibration period on a reciprocating Eberbach shaker, a 1-mL aliquot of the radioactive solution was removed. For the α-emitting isotopes (all except Eu), the 1-mL aliquot was added to 10 mL scintillating fluid and counted on a liquid scintillation counter. The Eu isotope was a γ-emitter and was counted in a NaI-TlI well-type scintillation counter equipped with a multichannel analyzer. Each sample was counted for two 1-min periods. A blank solution was prepared containing only the background solution and the radioactive spike. The amount of metal

absorbed by the resin was determined by the difference in counts per minute (cpm) of the blank and the solution after contact with the resin. For the α-emitting isotopes, a different blank was prepared for each background solution because the amount of quenching in the sample was dependent on the concentration of HNO_3 and $NaNO_3$. For example, the same spike level of ^{241}Am had a count rate per minute 118,000 in 2M HNO_3/2M $NaNO_3$ compared to 123,000 in 0.2M HNO_3/3.8M $NaNO_3$. Because the count rate of the γ-emitting isotope was independent of the background solution composition, only one blank solution was prepared from one representative background solution. The following peaks were counted for each radioisotope: 0.123-1.4 MeV, Eu; 4.69 MeV, Th; 4.82 MeV, U; 5.57 MeV, Am; and 5.16 MeV, Pu. The % metal absorbed by the resin was calculated as follows:

$$\% \text{ absorbed} = \frac{cpm_i - cpm_f}{cpm_i} \quad (100\%)$$

The distribution coefficient (D), defined as the ratio of metal in the resin phase per gram of resin to the metal in the aqueous phase per milliliter of solution, was calculated according to the equation

$$D = \frac{5(cpm_i - cpm_f)}{(cpm_f)(g \text{ dry resin})} \quad .$$

Transition Metal Ion Extraction Studies by the Radiotracer Technique

The transition metal ion solutions ranging in concentration from

10^{-2} to 10^{-5}N were obtained by a 1:10 dilution of stock metal nitrate solutions with stock background solutions to give varying concentrations of HNO_3 (4M-10^{-4}M) and $NaNO_3$ (0M-3.9999M). The stock metal nitrate solutions were prepared by dissolving the appropriate amount of the metal salt and enough concentrated HNO_3 to obtain a pH of 1.5 to 1.7 (to prevent metal ion hydrolysis) in water purified by passage through a mixed-bed ion-exchange column followed by double distillation from $KnMO_4$. The stock background solutions (also prepared using purified water) were of the appropriate concentrations to yield the desired levels of HNO_3 and $NaNO_3$ after 9:10 dilution. For example, a solution containing 1 X 10^{-5}N $Hg(NO_3)_2$, 1M HNO_3 and 3M $NaNO_3$ was obtained by dilution of a 10 mL aliquot of 1 X 10^{-4}N $Hg(NO_3)_2$ (pH 1.5) to 100 mL with 1.11M HNO_3/3.33M $NaNO_3$ stock background solution. The $NaNO_3$ used in solutions containing $AgNO_3$ was purified to remove chloride impurity and thus prevent the precipitation of AgCl. Recrystallization was accomplished by dissolving with heat 52 g reagent grade $NaNO_3$ in 1500 mL of 95% methanol. The solution was then cooled to affect crystallization. The $NaNO_3$ crystals were collected and washed with absolute ethanol. The ethanol was removed by means of rotary evaporation.

Solutions of transition metal ions greater than 1 X 10^{-2}N were obtained by dissolving the appropriate amounts of metal nitrate, sodium nitrate and nitric acid in purified water to give the desired final concentrations. The concentrations of Hg, Ag, Fe and Mn solutions prepared in this manner were verified by titrimetry. The previously described Volhard method was employed to titrate Ag and Hg. EDTA

titrations[119] were used to determine the concentrations of Fe (Variamine Blue B indicator) and Mn (Erio T indicator).

The transition metal ion extractions were performed by shaking suction-dried resin (containing one milliequivalent of ligand sites), 5 mL of metal solution prepared as described above and a radioactive spike (10 - 100 μL of approximately 10^{-8}M metal nitrate) for 17 h on an Eberbach reciprocating shaker. A 1-mL aliquot of the solution was removed and counted as described above for Eu using a NaI-Tl well-type gamma scintillation counter equipped with a multichannel analyzer. The following peaks were counted for each radiotracer (all γ emitters): 0.279 MeV, ^{203}Hg; 1.097-1.289 MeV, ^{59}Fe; 1.173-1.332 MeV, ^{60}Co; 0.835 MeV, ^{54}Mn; 1.114 MeV, ^{65}Zn; and 0.656-0.885 MeV, ^{110m}Ag. The amount of metal absorbed by the resin was determined by comparison of the sample counts to those of a blank. The calculation of % absorbed and D was the same as described for the lanthanides and actinides. Scatter in the results may be caused by counting resin fines in the 1-mL aliquot. The resins were thus carefully sieved to remove the fines before carrying out the extraction. If resin attrition occurred during the shaking process, the fines were removed by centrifugation of the solution before counting.

Metal Ion Extraction Studies Using Liquid Extractants

An organic phase was prepared by dissolving the extractant in toluene to give the desired concentration (usually 0.2M). The aqueous phase consisted of the metal nitrate (present at levels of 1 X 10^{-5}N to 1 X 10^{-1}N) in varying concentrations of HNO_3 and $NaNO_3$ (to yield a 4M

nitrate background) and a radioactive spike of the target metal ion. Extraction were performed by placing 5 mL of each phase in a 20-mL scintillation vial and shaking for 17 h. The count rate per minute (cpm) of a 1-mL aliquot of each phase was measured using a gamma-scintillation counter described previously. The background count rate was measured for a 10-min period and subtracted from both the sample and blank count rates. The % metal absorbed by the extractant was determined by comparison of the aqueous phase counts to those of a blank as described by the following equation:

$$\% \text{ absorbed} = \frac{cpm_{blank} - cpm_{aqueous}}{cpm_{aqueous}} \quad (100\%)$$

The distribution coefficient was calculated as the ratio of metal in the organic phase divided by that in the aqueous phase:

$$D = \frac{cpm_{organic}}{cpm_{aqueous}}$$

The material balance for the system was determined by comparing the blank counts to the sum of the counts in the organic and aqueous phases after extraction. A lower total count rate in the aqueous and organic phases than in the blank indicated that the extraction results were in error due to loss of metal to a third phase.

The extractants were obtained from the following sources and used without further purification: 2,4,4-trimethylpentyl phosphinic acid

(Cyanex 272), gift of the American Cyanamid Company; di-2-ethylhexyl phosphoric acid (DEHP), Aldrich; tri-octylphosphine oxide (TOPO), Eastman Chemical Company; tri-*n*-butyl phosphate (TBP), Eastman; and dicyclohexyl phosphinic acid (DCHPA), gift from the Oak Ridge National Laboratory (in house preparation[121]). The extractant purity was determined for the extractants (except TBP) by potentiometric titration in 95% ethanol using standard sodium ethoxide an the titrant. The following results were obtained: Cyanex 272, 88.9% purity; TOPO, 99.6%; DEHP, 93.2% and DCHPA, 91.6%. Some extractants were also examined by phosphorus elemental analysis to give the following % purity results: Cyanex 272, 95.6%; DEHP, 96.0%; and DCHPA, 96.4%. The melting range of DCHPA was determined to be 141-142 °C (141.0-141.5 °C reported[122]). The proton NMR spectrum of DCHPA (recorded on a Nicolet 200 MHz instrument on 0.01 mole fraction of extractant in CCl_4) showed a multiplet at δ 1.5-2.0 ppm (22 H) and a singlet at δ 12.36 ppm (1 H), in accord with the reported chemical shift of δ 12.37 ppm for the hydroxyl proton.[123]

LIST OF REFERENCES

1. *Separation and Purification: Critical Needs and Opportunities*; Committee on Separation Science and Technology. Board on Chemical Sciences and Technology. Commission on Physical Sciences, Mathematics and Resources. National Research Council. National Academy Press: Washington, D.C. 1987.

2. Ritcey, G.M.; Ashbrook, A.W. *Solvent Extraction: Principles and Applications to Process Metallurgy, Part I*; Elsevier: Amsterdam, 1984.

3. Murthy, T.K.S.; Koppiker, K.S.; Gupta, G.K. In *Recent Developments in Separation Science*; Li, N.N.; Navratil, J.D., Eds.; CRC Press: Boca Raton, 1986; Vol. 8, Chapter 1.

4. Marcus, Y.;Kertes. A.S. *Ion Exchange and Solvent Extraction of Metal Complexes*; Wiley Interscience: London, 1969.

5. Mason, G.W.; Lewey, S.; Peppard, D.F. *J. Inorg. Nucl. Chem.* **1964**, *26*, 2271.

6. Cook, L.F.; W.W. Szmokaluk *Proc. Int. Solvent Extr. Conf.* **1971**, *1*, 451.

7. Sato, T. Takeda, T. *J. Inorg. Nucl. Chem.* **1970**, *32*, 3387.

8. Rigg, T. Garner, J.O. *J. Inorg. Nucl. Chem.* **1967**, *29*, 2019.

9. Kolarik, Z.; Pankova, H. *J. Inorg. Nucl. Chem.* **1966**, *28*, 2325.

10. Brown, C.G.; Sherrington, L.G. *J. Chem. Tech. Biotechnol.* **1979**, *29*, 193.

11. Sekine, T.; Hasegawa, Y. *Solvent Extraction Chemistry: Fundamentals and Applications*; Marcel Dekker: New York, 1984.

12. Ashbrook, A.W. *Coord. Chem. Rev.* **1975**, *16*, 285.

13. Kordosky, G.A.; Olafson, S.M.; Lewis, R.G.; Deffner, V.L.; House, J.E. *Sep. Sci. Tech.* **1987**, *22*, 215.

14. Petrow, H.G.; Sohn, B.; Allen, R.J. *Anal. Chem.*, **1961**, *33*, 1301.

15. El-Yamani, I.S.; Farah, M.Y.; Abd El-Aleim, F.A. *Talanta*, **1978**, *25*, 523.

16. Miller, J.D.; Mooiman, M.B. *Sep. Sci. Technol.* **1984**, *19*, 895.

17. McKay, H.A.C. In *Science and Technology of Tributyl Phosphate*; Schulz, W.W.; Navratil, J.D., Eds.; CRC Press: Boca Raton, 1984; Vol. 1, Chapter 1.

18. Peppard, D.F.; Driscoll, W.J.; Sironen, R.J.; McCarty, S. *J. Inorg. Nucl. Chem.* **1957**, *4-5*, 326.

19. Thornhill, P.G.; Wigstol, E.; Van Weert, G. *J. Metals* **1971**, *23*, 13.

20. Sinegibova, O.A.; Yagodin, G.A. *At. Energy Rev.* **1966**, *4*, 93.

21. Gagliardi, E.; Woess, H.P. *Anal. Chim. Acta.* **1969**, *48*, 107.

22. *Handbook of Solvent Extraction*; Lo, T.C.; Baird, M.H.I.; Hanson, C., Eds.; John Wiley and Sons: New York, 1983.

23. De, A.K.; Khopkar, S.M.; Chalmers, R.A. *Solvent Extraction of Metals*; Van Nostrand Reinhold: London, 1970.

24. Ritcey, G.M. *Sep. Sci. Technol.* **1983**, 18, 1617.

25. Lewis, C.J. In *Recent Developments in Separation Science*; Li, N.N., Ed.; CRC Press: Boca Raton, 1972; Vol. 2, pp. 47-57.

26. Tavarides, L.L.; Bae, J.H.; Lee, C.K. *Sep. Sci. Technol.* **1987**, 22, 581-617.

27. Walsh. D.J.; Crosby, P.; Dalton, R.F. *Polymer* **1983**, 24, 423-427.

28. Flett, D.S.; Pearson, D. *Chem. and Ind.*, **1975**, 639-645.

29. Dorfner, K. *Ion Exchangers: Properties and Applications*; Ann Arbor Science: Ann Arbor, Michigan, 1972.

30. Miller, W.S.; Mindler, A.B. In *Recent Developments in Separation Science*; Li, N.N., Ed.; CRC Press: Boca Raton, 1977; Vol. 3, Part A, pp. 151-169.

31. Adams, B.A.; Holmes, E.L. *J. Soc. Chem. Ind.* **1935**, *54*, 1T.

32. D'Alelio, G.F. U.S. Patent 2 340 111, 1944.

33. D'Alelio, G.F. U.S. Patent 2 366 007, 1944.

34. Helfferich, F. *Ion Exchange*; McGraw Hill: New York, 1962.

35. U.S. Patent 2 591 573, 1953.

36. Streat, M.; Naden, D. In *Ion Exchange and Sorption Processes in Metallurgy*; Streat, M.; Naden, D., Eds. Critical Reports on Applied Chemistry, Vol. 19; John Wiley and Sons: Chicester, 1987, Chapter 1.

37. Kunin, R. *Ion Exchange Resins*; John Wiley and Sons: New York, 1950.

38. Kunin, R. McGarvey, F.X. U.S. Patent 2 578 938, 1951.

39. McGarvey, F.X.; Kunin, R. In *Ion Exchange Technology*; Nachod, F.C.; Schubert, J., Eds.; Academic Press: New York, 1956, Chapter 11.

40. Ancillotti, F.; Mauri, M.M.; Pescarollo, E. *J. Catal.* **1977**, *46*, 49.

41. Ford, W.T., Ed. *Polymeric Reagents and Catalysts*; American Chemical Society: Washington, D.C., 1986.

42. Helfferich, F. In *Advances in Chromatography*; Giddings, J.C.; Keller, R.A., Eds.; Marcel Dekker: New York, 1965; Vol. 1, Chapter 1.

43. Walton, H.F.; Navratil, J.D. in *Recent Developments in Separation Science*; Li, N.N., Ed.; CRC Press: Boca Raton, 1981; Vol. 6, Chapter 5.

44. Morrison, W.S. In *Ion Exchange Technology*; Nachod, F.C.; Schubert, J., Eds.; Academic Press: New York, 1956, Chapter 13.

45. Gerstner, F. In *Ion Exchange Technology*; Nachod, F.C.; Schubert, J., Eds.; Academic Press: New York, 1956, Chapter 14.

46. Tompkins, E.R.; Khym, J.X.; Cohn, W.E. *J. Am. Chem. Soc.* **1947**, *69*, 2769.

47. Diamond, R.M.; Whitney, D.C. in *Ion Exchange*; Marinsky, J.A., Ed.; Marcel Dekker: New York, 1966; Vol. 1, Chapter 8.

48. Boyd, G.E.; Vaslow, F.; Lindenbaum, S. *J. Phys. Chem.* **1964**, 68, 590.

49. Bauman, W.C. In *Ion Exchange: Theory and Application*; Nachod, F.C., Ed.; Academic Press: New York, 1949; pp. 45-75.

50. Warshawsky, A. *Angew. Makromol. Chem.* **1982**, *109/110*, 171.

51. Myasoedova, G.V.; Savvin, S.B. *Crit. Rev. Anal. Chem.* **1986**, *17*, 1.

52. Sahni, S.K.; Reedijk, J. *Coord. Chem. Rev.*, **1984**, 1.

53. Warshawsky, A. In *Ion Exchange and Sorption Processes in Hydrometallurgy*; Streat, M.; Naden, D., Eds.; Critical Reports on Applied Chemistry, Vol. 19; John Wiley and Sons: Chichester, 1987, Chapter 4.

54. Grinstead, R.R. *J. Met.* **1979**, 13.

55. Mykytiuk, A.P.; Russell, D.S.; Sturgeon, R.E. *Anal. Chem.* **1980**, *52*, 1281.

56. Slovak, Z.; Slovakova, S.; Smrz, M. *Anal. Chim. Acta.* **1975**, *75*, 127.

57. Warshawsky, A.; Deshe, A.; Rossey, G.; Patchornik, A. *Reactive Polymers* **1984**, *2*, 301.

58. Flett, D.S. *Trans. Inst. Min. Metal.* **1974**, *83*, C30.

59. Phillips, R.J.; Fritz, J.S. *Anal. Chem.* **1978**, *50*, 1504.

60. Warshawsky, A.; Kahana, N. *J. Am. Chem. Soc.* **1982**, *104*, 2663.

61. Koster, G.; Schmuckler, G. *Anal. Chim. Acta.* **1967**, *38*, 179.

62. Kadlec, V.; Matejka, Z. *J. Appl. Chem. Biotechnol.* **1973**, *23*, 41.

63. Kennedy, J.; Lane, E.S.; Robinson, B.K. *J. Appl. Chem.* **1958**, *8*, 459.

64. Kennedy, J.; Davies, R.V.; Small, H.; Robinson, B.K. *J. Appl. Chem.* **1959**, *9*, 32.

65. Kennedy, J.; Wheeler, V.J. *Anal. Chim. Acta.* **1959**, *20*, 412.

66. Walsh, E.N.; Beck, T.M.; Toy, A.D.F. *J. Am. Chem. Soc.* **1956**, *78*, 4455.

67. Bartulin, J.; Cardenas, J.; Maturana, H. *Hydrometallurgy* **1982**, *8*, 137.

68. Marhol, M.; Beranova, H.; Cheng, K.L. *J. Radioanal. Chem.* **1974**, *21*, 177.

69. *Duolite Ion-Exchange Manual*; Chemical Process Co.: Redwood City, CA, 1960.

70. Egawa, H.; Nonaka, T.; Ikari, M. *J. Appl. Poly. Sci.* **1984**, *29*, 2045.

71. Selzer, R.B.; Howery, D.G. *Macromolecules* **1986**, *19*, 2673.

72. Helfferich, F. In *Ion Exchange*; Marinsky, J.A., Ed.; Marcel Dekker: New York, 1966; Vol.1, Chapter 2.

73. Janauer, G.E.; Gibbons, R.E., Jr.; Bernier, W.E. In *Ion Exchange and Solvent Extraction*; Marinsky, J.A.; Marcus, Y., Eds.; Marcel Dekker: New York, 1985; Vol. 9, Chapter 2.

74. Alexandratos, S.D. *Sep. Purif. Meth.* **1988**, *17*, 67.

75. Alexandratos, S.D.; Wilson, D.L. *Macromolecules* **1986**, *19*, 280.

76. Alexandratos, S.D.; Quillen D.R.; McDowell, W.J. *Sep. Sci. Tech.* **1987**, *22*, 983.

77. Alexandratos, S.D.; Quillen, D.R.; Bates, M.E. *Macromolecules* **1987**, *20*, 1191.

78. Pearson, R.G. *Chemistry in Britain* **1967**, *3*, 103.

79. Pearson, R.G. *Science* **1966**, *151*, 172.

80. Alexandratos, S.D.; Bates, M.E. *Macromolecules* **1988**, *21*, 2905.

81. Alexandratos, S.D.; Strand, M.A.; Quillen, D.R.; Walder, A.J. *Macromolecules* **1985**, *18*, 829.

82. Kosolapoff, G.M.; Huber, W.F. *J. Am. Chem. Soc.* **1947**, *69*, 2020.

83. Frank, A.W. *J. Org. Chem.* **1959**, *24*, 966.

84. *Handbook of Chemistry and Physics*, 62nd ed.; Weast, R.C., Ed.; CRC Press: Boca Raton, 1981; D-133.

85. Skoog, D.A.; West, D.M. *Fundamentals of Analytical Chemistry*, 2nd ed.; Holt, Rinehart, and Winston: New York, 1963, p. 446.

86. Alexandratos, S.D.; Wilson, D.L.; Strand, M.A.; Quillen, D.R.; Walder, A.J.; McDowell, W.J. *Macromolecules* **1985**, *18*, 835.

87. Kennedy, J.; Burford, F.A.; Sammes, P.G. *J. Inorg. Nucl. Chem.* **1960**, *14*, 114.

88. Clay, J.P. *J. Org. Chem.* **1951**, *16*, 892.

89. Kinnear, A.M.; Perren, E.A. *J. Chem. Soc.* **1952**, 3437.

90. Pepper, K.W.; Paisley, H.M.; Young M.A. *J. Chem. Soc.* **1953**, 4097.

91. *Handbook of Chemistry and Physics*, 62nd ed.; Weast, R.C., Ed.; CRC Press: Boca Raton, 1981; D-139.

92. Mathur, J.N. *Solv. Extr. Ion Exch.* **1983**, *1*, 349.

93. Kolarik, Z.; Puzic, R.G., Maksimovic, Z..B. *J. Inorg. Nucl. Chem.* **1969**, *31*, 2485.

94. Bates, M.E. Masters Thesis, University of Tennessee, Mar. 1988.

95. Liang, G., The University of Tennessee, personal communication, May 1989.

96. Farrall, M.J.; Frechet, J.M.J. *J. Org. Chem.* **1976**, *41*, 3877.

97. Frechet, J.M.J.; de Smet, M.D.; Farrall, M.J. *Polymer*, **1979**, *20*, 675.

98. Nieustad, T.J.; Kieboom, A.P.G.; Breijer, A.J., van der Linden, J.; van Bekkum, H. *Rec. Trav. Chim. Pays-Bas* **1976**, *95*, 225.

99. Crampton, M.R. In *The Chemistry of the Thiol Group, Part I*; Patai, S., Ed.; John Wiley and Sons: New York, 1974, Chapter 8, p. 398.

100. Weaver, B. In *Ion Exchange and Solvent Extraction*; Marinsky, J.A.; Marcus, Y., Eds.; Marcel Dekker: New York, 1974; Vol. 6, Chapter 4.

101. Peppard, D.F.; Mason, G.W. *Nucl. Sci. Eng.* **1963**, *16*, 382.

102. Cotton, F.A.; Wilkinson, G.W. *Advanced Inorganic Chemistry*; Third Ed.; Interscience: New York, 1972; p 1110.

103. Peppard, D.F.; Mason, G.W.; Andrejasich, C.M. *J. Inorg. Nucl Chem.* **1965**, *27*, 697.

104. Durst, R.A. In *Ion-Selective Electrodes in Analytical Chemistry*; Freiser, H., Ed.; Plenum Press:New York, 1980, Chapter 5.

105. Coleman, C.F. *Atomic Energy Rev.* **1964**, *2*, 3.

106. Horwitz, E.P.; Bloomquist, C.A.A.; Sauro, L.J.; Henderson, D.J. *J. Inorg. Nucl. Chem.* **1966**, *28*, 2313.

107. Alexandratos, S.D.; Wilson, D.L.; Kaiser, P.T.; McDowell, W.J. *Reactive Polymers*, **1987**, *5*, 23.

108. Sandell, E.B. *Colorimetric Determination of Traces of Metals*, 3rd ed.; Interscience: New York, 1959.

109. Willard, H.H.; Merritt, L.L., Jr.; Dean, J.A.; Settle, F.A., Jr. *Instrumental Methods of Analysis*, 6th ed.; D. Van Nostrand: New York, 1981; p. 1001.

110. Slavin, W. *Atomic Absorption Spectroscopy*; Interscience: New York, 1968.

111. Carswell, D.J. *Introduction to Nuclear Chemistry*; Elsevier: Amsterdam, 1967; p. 251

112. Huheey, J.H. *Inorganic Chemistry*, 3rd ed.; Harper and Row: New York, 1983; p. 295.

113. Solomons, T.W.G. *Organic Chemistry*, 2nd ed.; John Wiley and Sons: New York, 1980; p. 811.

114. Pearson, R.G. *J. Am. Chem. Soc.* **1963**, *85*, 3533.

115. Nishide, H.; Izushi, T.; Arai, H.; Yoshioka, N.; Tsuchida, E. *J. Macromol. Sci.-Chem.* **1987**, *A24*, 343.

116. Siddell, T.H. *J. Inorg. Nucl. Chem.* **1960**, *13*, 151.

117. Arcus, C.L.; Matthews, R.J.S. *J. Chem. Soc.* **1956**, Part IV, 4207.

118. Blake, C.A.; Brown , K.B.; Coleman, C.F. Report 1964; Oak Ridge National Laboratory: Oak Ridge, TN, 1955.

119. Schwarzenbach, G.; Flaschka, H.; H.M.N.H. Irving, translator *Complexometric Titrations*, 2nd ed. in English; Meuthen: London, 1969.

120. Skoog, D.A; West, D.M. *Analytical Chemistry*, 3rd ed.; Saunders: Philadelphia, 1980; p 581.

121. Brown, K.B. Oak Ridge National Laboratory, 1952.

122. Stiles, A.R.; Rust, F.F.; Vaughan, W.E. *J. Am. Chem. Soc.* **1952** *74*, 3282.

123. Ferraro, J.R.; Peppard, D.F. *J. Phys. Chem.* **1963**, *67*, 2639.

124. Galeazzi, L. Italian Patent 1 002 121, 1976.

APPENDIX

CHLOROMETHYLATION OF POLYSTYRENE

Chloromethylation of sytrene/DVB copolymers to yield poly (vinylbenzyl chloride) was investigated as an alternative to the copolymerization of vinylbenzyl chloride and divinylbenzene. The introduction of chloromethyl groups onto cross-linked polystyrene beads was accomplished by the reaction shown in Figure 113.[124]

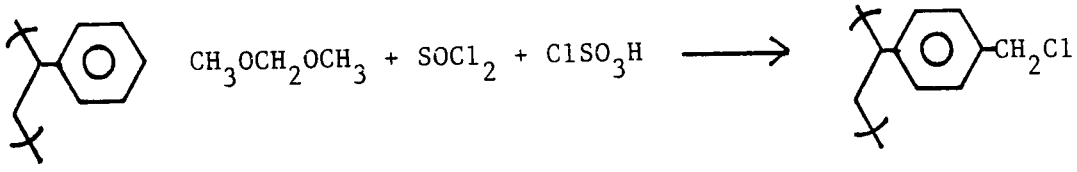

Figure 113. Chloromethylation of polystyrene.

The influence of the ratio of methylal to thionyl chloride on the degree of chloromethylation was examined. The reaction was carried out using 10 g of 2% cross-linked polystyrene gel beads and the following molar ratios of methylal to thionyl chloride: 0.4/0.4, 0.8/0.4, 0.6/0.6 and 0.8/0.6. The beads were first swelled for 1 h in methylal. The reaction mixture was then cooled to 15 °C and the thionyl chloride was added in a dropwise manner over a period of 30 min. The chlorosulfonic acid catalyst (15 mL) was then added over a 1-h period. The reaction mixture was heated to reflux and maintained at this temperature for 6 h. After cooling to room temperature, the reaction flask was immersed in an ice bath. The remaining thionyl chloride and chlorosulfonic acid were

decomposed by the slow addition of 40 mL methanol followed by 60 mL of 50% methanol. The beads were washed in the reaction flask with water and 95% ethanol and then transferred to a glass fritted funnel. Following elution with 500 mL 95% ethanol, a sample of beads was removed and dried for 16 h at 110 °C. A chlorine elemental analysis was performed on the dried sample.

Table 63 presents the chlorine elemental analysis results for the four sets of reactions carried out at varying methylal/thionyl chloride ratios. The theoretical chlorine capacity for the complete monosubstitution of all styrene rings of the 2% cross-linked resin is 6.32 mequiv/g. The Cl capacities for the beads synthesized at ratios of methylal to thionyl chloride of 0.4/0.4 and 0.6/0.6 exceed that predicted for monofunctional substitution. These results suggest that the chloromethylation reaction proceeded slightly beyond monosubstitution at equimolar methylal/thionyl chloride ratios. A slight excess of methylal over thionyl chloride (0.8/0.6) appears to favor complete monosubstitution of the styrene rings as shown by the close agreement of the observed and theoretical Cl capacities. A large excess of methylal over thionyl chloride (0.8/0.4), however, resulted in only 54% substitution of the styrene rings.

Table 63

Results of Chlorine Elemental Analysis
of Chloromethylated Resins

mole methylal/mole thionyl chloride[a]	tot(Cl)[b]	% rxn[c]
0.4/0.4	6.90	109%
0.8/0.4	3.39	54%
0.6/0.6	6.50	103%
0.8/0.6	6.27	99%

[a] Per 10 g 2% crosslinked polystyrene beads.
[b] Units of mequiv/g.
[c] Based on complete monosubstitution of all styrene rings.

VITA

Donna Rice Quillen was born in Kingsport, Tennessee on June 11, 1962. She attended elementary schools in that city and graduated from Lynn View High School in June 1980. She received the Bachelor of Science degree in Chemistry from the University of Tennessee in June 1984. In September 1984 she accepted a teaching and research assistantship from the Chemistry Department at the University of Tennessee and began study toward the Ph.D. degree in Polymer Chemistry. The degree was awarded in December 1989.

The author is a member of the American Chemical Society and Phi Beta Kappa. She will be employed by the Tennessee Eastman Company in Kingsport, Tennessee following graduation.